UNIVERSITY OF LIVERPOOL

MicroRNAs in gastric and oesophageal cancer-associated myofibroblasts

Thesis submitted in accordance with the requirements of the University of Liverpool for the degree of Doctor of Philosophy by

Liyi Wang

April 2013

Abstract

MicroRNAs (miRNAs) are small RNAs of ~22 nucleotides in length that regulate gene expression post-transcriptionally. MicroRNAs regulate many biological processes, and may contribute to cancer initiation and progression. In the normal gastrointestinal mucosa, myofibroblasts are involved in wound healing, and in tumours, they play a role in cancer progression. The present study aimed to determine the miRNA expression profiles in different populations of myofibroblasts from gastric and oesophageal tissues, namely, cancer-associated myofibroblasts (CAMs), adjacent non-tumour tissue myofibroblasts (ATMs) and normal tissue myofibroblasts (NTMs), and to investigate the processes that are influenced by differential miRNA abundance in different myofibroblast populations. In addition, miRNA profiling of a putative myofibroblast precursor cell type, mesenchymal stromal cells (MSCs), was studied.

Global miRNA expression profiling of a panel of previously characterised gastric and oesophageal myofibroblasts was determined using locked nucleic acid (LNA) miRNA arrays. The microarray data for hsa-miR-29b, hsa-miR-181d, hsa-miR-214 and hsa-miR-424 were validated by quantitative RT-PCR. Using unsupervised miRNA datasets, principal component analysis (PCA) segregated gastric and oesophageal NTMs, and CAMs from gastric and oesophageal carcinomas. Analysis of global miRNA expression showed distinct profile of MSCs in comparison to gastric and oesophageal NTMs. Hierarchical clustering analysis of miRNAs exhibiting significantly different abundance revealed distinct clusters between CAMs and ATMs, CAMs and NTMs and between ATMs and NTMs.

In 12 paired samples of gastric CAMs and their corresponding ATMs, 12 miRNAs were significantly different with hsa-miR-181d being the most up-regulated miRNA in CAMs. Using already validated targets of 10 of these

miRNAs, an analysis using MetaCore® indicated that the regulation of cell cycle progression and Wnt signalling were differentially affected. In a comparison of each CAM and its corresponding ATM, Wnt signalling was the only process that was significantly targeted by miRNAs that were different in abundance, in all 12 pairs.

Using previously determined gene expression data, pairwise analysis of 20 transcripts associated with Wnt signalling showed a significant increase in WNT5A and TGFB2 mRNAs in CAMs compared to their ATMs. Additionally, Western blot analysis showed increased expression of Wnt-5a in CAMs. The results of migration and EdU incorporation assays indicated that Wnt-5a induced the migration and proliferation of both CAMs and ATMs. The abundance of hsa-miR-181d was significantly increased in CAMs by Wnt-5a. Migration of AGS (gastric cancer) cells was stimulated by Wnt-5a and was inhibited in the presence of TIMP-3, a validated target of the miR-181 family. After hsa-miR-181d knockdown, the migration and proliferation of CAMs were significantly decreased, and stimulation with Wnt-5a reversed the migratory inhibition of hsa-miR-181d knockdown CAMs. Conditioned medium from hsa-miR-181d knockdown CAMs inhibited the migration of AGS cells.

The findings suggest that differential miRNA abundance is a feature of normal myofibroblasts from the stomach and oesophagus, and myofibroblasts from normal and cancer tissues. One consequence is increased Wnt-5a in gastric CAMs that is implicated in the regulation of cell migration, in health and disease, at least partly through modulation of hsa-miR-181d.

Table of Contents

Acknowledgements

Foremost, I would like to express my special thanks to Prof Andrea Varro and Prof Graham Dockray for putting ideas during discussion, and for writing and completion of this thesis. I am grateful to people who provided help during the research project, especially Prof Rod Dimaline, Dr Islay Steele, Dr Lucille Rainbow, Dr Jithesh Puthen and members in the research group. I would like to thank the Wellcome Trust for funding the research project in this thesis. I would like to acknowledge the help from Exiqon microRNA Services, and thank tutors from the English Language Centre for their help in thesis writing. Finally, I want to thank my family for their ongoing support and patience.

List of symbols, abbreviations or other

Abbreviation	Meaning
AC-ATMs	Myofibroblasts from tissue adjacent to oesophageal adenocarcinoma
AC-CAMs	CAMs from oesophageal adenocarcinoma
ACh	Acetylcholine
ADAMs	A disintegrin and metalloproteinases
ADAMTS	ADAMs with thrombospondin motifs
ANOVA	Analysis of variance
APC	Adenomatous polyposis coli
ATMs	Adjacent non-tumour tissue myofibroblasts
ATM-CM	Conditioned medium from ATMs
ATP	Adenosine triphosphate
BCL2	B-cell CLL/lymphoma 2
BSA	Bovine serum albumin
Ca^{2+}	Calcium ions
cagA	cytotoxin-associated gene A
CCK-2	Cholecystokinin-2
CAMs	Cancer-associated myofibroblasts
CAM-CM	Conditioned medium from CAMs
CAMKII	Calcium/calmodulin-dependent protein kinase II
cAMP	cyclic AMP
CD	clusters of differentiation molecules
CDH1	Cadherin 1, type 1, E-cadherin (epithelial)
cDNA	complementary DNA
CDX2	Caudal type homeobox 2
CK1α	Casein kinase 1-alpha

CM	Conditioned medium
COX1	Cyclooxygenase-1
COX2	Cyclooxygenase-2
CTNNB1	Catenin (cadherin-associated protein), beta 1, 88kDa
DAPI	4',6-diamidino-2-phenylindole
dChip	DNA-chip analyzer
DCLK1	Doublecortin-like kinase 1
DHH	Desert hedgehog
DGCR8	DiGeorge syndrome critical region gene 8
DMEM	Dulbecco modified Eagle's medium
DNA	Deoxyribonucleic acid
DNMT	DNA methyltransferase
ECM	Extracellular matrix
ECL	Enhanced chemiluminescence
ECL cells	Enterochromaffin-like cells
EDTA	Ethylenediaminetetraacetic acid
EdU	5-ethynyl-2'-deoxyuridine
e.g.	For example
EGF	Epidermal growth factor
EMT	Epithelial-to-mesenchymal transition
EPCs	Endothelial progenitor cells
EZH2	Enhancer of zeste homolog 2
FBS	Fetal bovine serum
FDR	False discovery rate
FGF	Fibroblast growth factor
FITC	Fluorescein
FZD	Frizzled family receptor

GAPDH	Glyceraldehyde-3-phosphate dehydrogenase
GATA6	GATA binding protein 6
GFP	Green fluorescent protein
GLI1	GLI family zinc finger 1
GRP	Gastrin-releasing peptide
GSK3β	Glycogen synthase kinase 3-beta
H_2-receptor	Histamine H_2 receptor
H	hour
HBEGF	Heparin-binding EGF-like growth factor
HEPES	N-2-hydroxyethylpiperazine-N'-2-ethanesulfonic acid
HES1	Hairy and enhancer of split 1
HGF	Hepatocyte growth factor
H^+/K^+-ATPase	gastric acid secreting pump (i.e. proton pump)
HLA-DR	Major histocompatibility complex, class II, DR
H. pylori	*Helicobacter pylori*
i.e.	In other words
IGF	Insulin-like growth factor
IGFBP3	Insulin-like growth factor binding protein-3
IGFBP5	Insulin-like growth factor binding protein-5
IHH	Indian hedgehog
JNK	Jun N-terminal kinase
KEGG	Kyoto Encyclopedia of Genes and Genomes
KGF	Keratinocyte growth factor
KRAS	v-Ki-ras2 Kirsten rat sarcoma viral oncogene homolog
LGR5	Leucine-rich repeat containing G protein-coupled receptor 5
LOWESS	Locally weighted scatterplot smoothing
ΔLMR	Difference in $\log_2$ median ratio

LNA	Locked nucleic acid
LOH	Loss of heterozygosity
LRP5/6	Low density lipoprotein receptor-related protein 5 or 6
MCGS	Mesenchymal stem cell growth supplement
MHC	Class II Major histocompatibility complex
min	Minute
MIP1α	Macrophage inflammatory protein 1-alpha
miRNAs	microRNAs
MMP	Matrix metalloproteinase
mRNA	Messenger ribonucleic acid
MSCs	Mesenchymal stromal cells
MSCBM	Mesenchymal stem cell basal medium
NFAT	Nuclear factor of activated T-cells
NF-$_K$β	Nuclear factor-kappa B
NHE	Na^+/H^+ exchanger
NICD	Notch intracellular domain
NLK	Nemo-like kinase
NSAIDs	Non-steroidal anti-inflammatory drugs
nt	nucleotides
NTMs	Normal tissue myofibroblasts
PAI	Plasminogen activator inhibitor
PAGE	Polyacrylamide gel electrophoresis
PBS	Phosphate-buffered saline
PCA	Principal component analysis
PCP	Planar cell polarity
PCR	Polymerase chain reaction
PKC	Protein kinase C

PN1	Protease nexin-1
Pre-miRNAs	Precursor miRNAs
Pri-miRNAs	Primary miRNAs
PTCH1	Patched 1
REG1A	Regenerating protein-1α
RIN	RNA integrity number
RIPA	Radioimmunoprecipitation assay
RISC	RNA-induced silencing complex
RNA	Ribonucleic acid
ROR2	Receptor tyrosine kinase-like orphan receptor 2
RT-PCR	Reverse transcription polymerase chain reaction
RYK	Receptor-like tyrosine kinase
SATB2	SATB homeobox 2
SC-ATMs	Myofibroblasts from tissue adjacent to oesophageal squamous cell carcinoma
SC-CAMs	CAMs from oesophageal squamous cell carcinoma
SDS	Sodium dodecyl sulphate
SHH	Sonic hedgehog
α-SMA	Alpha-smooth muscle actin
SMO	Smoothened, frizzled family receptor
SNPs	Single-nucleotide polymorphisms
SST	Somatostatin
TARBP	Trans-activation response RNA binding protein
TβR-I	TGFβ type I receptor
TβR-II	TGFβ type II receptor
TBST	0.1% Tween-20 in Tris buffer saline
TCF/LEF	T-cell factor/lymphoid enhancer factor

TEMED	N,N,N,N-tetramethylethylene-diamine
TGFβ	Transforming growth factor-beta
TGFβ3	Transforming growth factor-beta 3
TGFBI	Transforming growth factor, beta-induced
TIMP	Tissue inhibitor of metalloproteinase
TLRs	Toll-like receptors
TP53	Tumour protein p53
tPA	Tissue-type plasminogen activator
Tris base	Tris(hydroxymethyl)aminomethane
uPA	Urokinase-type plasminogen activator
uPAR	Urokinase plasminogen activator receptor
3'UTRs	3' untranslated regions
VEGF	Vascular endothelial growth factor
WNT	Wingless-type MMTV integration site family

CHAPTER ONE

Introduction

1.1 Overview

The double helix structure of deoxyribose nucleic acid (DNA), which was held together by pyrimidine and purine bases through hydrogen bonding, was first described by Watson and Crick in 1953 [1]. Not long after, a concept emerged that the genetic information was transferring from DNA to messenger ribonucleic acid (mRNA), which served as a template for protein synthesis, and this idea became known as the "central dogma of molecular biology" [2]. Subsequently, the idea has been revised as more complex mechanisms emerged in eukaryotes for processing genetic information [3]. For example, the existence of reverse transcriptase, which converts mRNA to complementary DNA (cDNA), the presence of non-coding sequences in the genome, the mechanisms of epigenetics that alter transcriptional activity, and post-transcriptional gene regulation such as alternative pre-messenger RNA splicing have all been described [3]. Despite many controversies, the central dogma remains relevant today as it provides a basic framework for understanding the mechanisms of controlling gene expression and protein synthesis [3].

Recent advances in genomic research have included the human genome project, which indicates an approximately 20,000 protein-coding genes account for only about 1% of the entire human genome [4]. The remaining transcripts are non-coding RNAs, some of which are involved in the translational machinery (e.g. ribosomal RNAs, transfer RNAs) and some are involved in splicing (e.g. small nucleolar RNAs) [5]. A group of small non-coding RNAs called microRNAs (miRNAs), which were first discovered in *Caenorhabditis elegans* in 1993,

function to regulate gene expression post-transcriptionally either by inducing translational repression or by mRNA degradation, or both [6]. Currently, more than 2000 human mature miRNA sequences are deposited in the miRBase (release 19; August 2012). It is predicted that up to 60% of protein-coding genes are targets of miRNAs, thus indicating the importance of miRNAs in regulating post-transcriptional gene activity, and also influencing biological processes [7].

The present thesis focuses on the regulation of gene expression by miRNAs in cancer and in particular, gastric carcinoma, oesophageal squamous cell carcinoma and oesophageal adenocarcinoma. According to cancer mortality statistics (2010), oesophageal and stomach cancers are in the top ten most common causes of cancer death in the United Kingdom. In addition, there is a high incidence of gastric and oesophageal adenocarcinomas in other European countries and developing countries [8, 9]. So far, studies have largely focused on malignant epithelial cells, but recent research suggests the involvement of the tumour microenvironment in malignant progression as well as in mediating therapeutic resistance [10]. It is known that tumour cell growth, invasion and metastasis can be modulated by miRNAs in stromal cells [11] but in general, the latter are poorly understood. The present study focuses on miRNAs in cancer-associated myofibroblasts (CAMs), which are an abundant cell type in both gastric and oesophageal tumour stromata and may provide a novel therapeutic strategy for cancer treatment.

1.2 The upper gastrointestinal tract

The upper gastrointestinal tract, which consists of the salivary glands, oesophagus, stomach and the small intestine, functions to aid food digestion and nutrient absorption [12]. The oesophagus is a tubular organ that transports food and fluids to the stomach. The oesophagus also consists of upper and lower oesophageal sphincters so as to prevent the reflux of gastric juice [13]. In addition, the stomach is an endocrine and exocrine organ that aids food digestion through the secretion of gastric juice, which contains hydrochloric acid and digestive enzymes [14]. The five regions of the stomach are: a) the cardia, which is near to the gastroesophageal junction; b) the fundus, which is the upper portion near to the oesophagus; c) the body or the corpus, which is the intermediate region; d) the pyloric antrum, which is the lower portion of the stomach, and e) the pyloric sphincter, which separates between the stomach and duodenum of the small intestine [15].

1.2.1 Pathophysiology of oesophageal mucosa

The oesophageal mucosa, consisting of non-keratinised squamous epithelium, contains submucosal mucous glands that secrete protective factors such as mucin and bicarbonate ions so that diffusion of hydrogen ions into the mucosa, and auto-proteolytic digestion by pepsin are prevented [16]. Gastroesophageal reflux is a common condition in which there is recurrent regurgitation of acidic gastric juice into the distal oesophagus, resulting in reflux oesophagitis [17]. Subsequent genetic mutations of epithelial cells can cause either benign oxyntocardia metaplasia or intestinal metaplasia, which may progress to Barrett's oesophagus

[18]. Barrett's oesophagus is characterised by an acquired metaplastic change from squamous epithelium to an intestinal phenotype with goblet cell differentiation [19]. In addition to acid, the reflux of bile acids from the duodenum through the stomach and into the oesophagus may also contribute to the development of Barrett's oesophagus. This is due to the inhibition of Notch signalling (Chapter 1.5.3) and an increased expression of caudal type homeobox 2 (CDX2), a marker for intestinal epithelial differentiation [20].

Oesophageal cancers are commonly classified into two histological sub-types: squamous cell carcinoma and adenocarcinoma [21]. Cigarette smoking and alcohol consumption are risk factors for the development of oesophageal squamous cell carcinoma [21] while Barrett's oesophagus is a risk factor for the development of dysplasia and oesophageal adenocarcinoma [19].

1.2.2 Gastric acid regulation and mucosal defence mechanisms

Tubular gastric glands in the gastric mucosa consist of mucous neck cells, other secreting cells, proliferating cells and enteroendocrine cells [22]. Gastric glands in the fundus and corpus regions are populated by histamine-secreting enterochromaffin-like (ECL) cells, acid-secreting parietal cells and peptic/chief cells that release pepsinogen, whereas glands in the antrum are populated by gastrin-secreting G cells [15, 23].

The antral hormone, gastrin, was discovered in 1905 by John Edkins and subsequently, it has been characterised as a peptide hormone which stimulates gastric acid secretion [24]. Other acid secretagogues such as acetylcholine (ACh)

and histamine are associated with gastric acid secretion too [25]. The regulation of gastric acid secretion at the cellular level is shown in Figure 1.1. Gastrin binds to cholecystokinin-2 (CCK-2) receptors, previously known as gastrin/CCK-B receptors that are expressed by ECL cells, and induces histamine synthesis and secretion [26]. When histamine binds to its H_2-receptor on the surface of parietal cells, there is an increase in cyclic adenosine monophosphate (cAMP) and intracellular calcium ions (Ca^{2+}) with subsequent activation of protein kinase C (PKC) [27]. Protein kinases phosphorylate intracellular proteins, leading to the fusion of acid secreting pump (H^+/K^+-ATPase) vesicles to the plasma membrane of parietal cells, allowing the secretion of a hydrogen ion in exchange for a potassium ion by utilising one adenosine triphosphate (ATP) molecule [25].

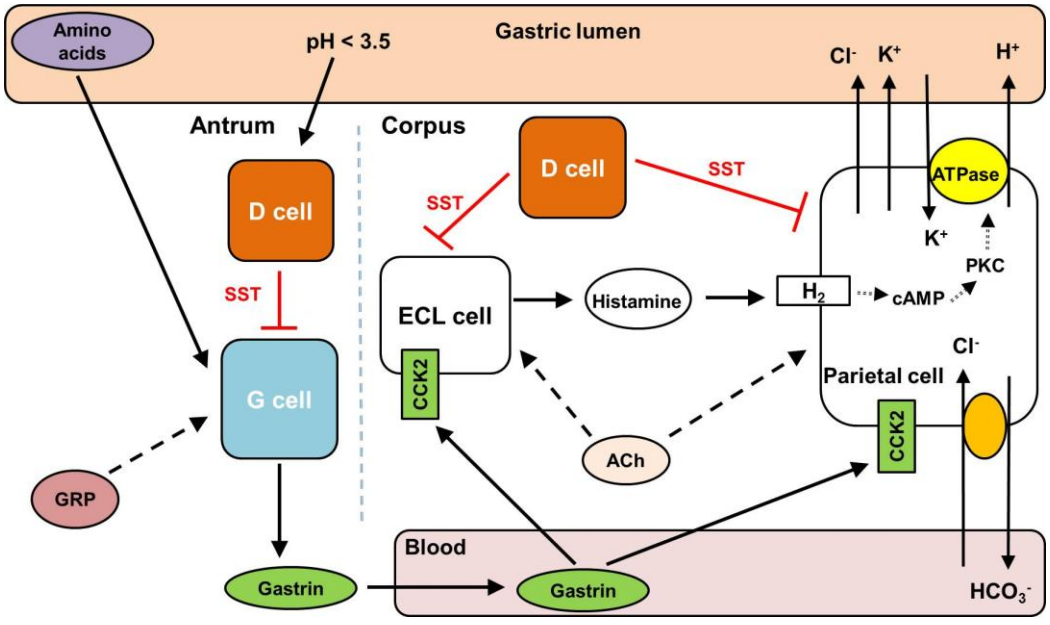

Figure 1.1 A schematic representation of the regulation of gastric acid secretion. Amino acids from the gastric lumen and gastrin-releasing peptide (GRP) from the nervous system stimulate G cells to release gastrin which binds to CCK-2 receptors on the surface of ECL and parietal cells. In ECL cells, there is an increased biosynthesis and secretion of histamine. The binding of histamine to its H_2-receptor on the surface of a parietal cell activates PKC and subsequently, the acid secreting pump (H^+/K^+-ATPase). ACh from the nervous system can induce acid secretion in parietal cells. The secretion of somatostatin (SST) from antral and corpus D cells inhibits the signalling mechanisms of acid secretion.

The role of a mucus bicarbonate barrier is to protect the gastric mucosa against hydrochloric acid and luminal pepsin. Pepsin belongs to a family of active proteases and is released when pepsinogen from peptic/chief cells is cleaved by gastric acid [28]. To maintain a neutral pH microenvironment at the cell surface, the secretion of bicarbonate ions from surface gastric epithelial cells inhibits the diffusion of hydrogen ions into the mucosa through the process of neutralisation [28]. Additionally, mucus from mucous cells serves as a physical barrier against the proteolytic activity of pepsin, and to inhibit the diffusion of hydrogen ions [28]. Furthermore, the secretion of acid from parietal cells causes bicarbonate ions to be released and diffused into the lumen of capillary blood vessels, leading to an alkaline tide, and may contribute to acid neutralisation at the epithelial cell surface [29].

Subsequent secretion of gastric acid reduces luminal pH and at pH below 3.5, D cells in the gastric antrum secrete somatostatin (SST), which inhibits G cells through paracrine signalling [22]. Additionally, when stimulated by neurohumoral factors such as noradrenaline, vasoactive intestinal polypeptide, calcitonin gene-related peptide and cholecystokinin, corpus D cells secrete SST to inhibit the functions of parietal and ECL cells [22]

1.2.3 Pathology of gastric epithelium

Chronic *Helicobacter pylori* (*H. pylori*) infection and the use of non-steroidal anti-inflammatory drugs (NSAIDs) and aspirin are risk factors for the development of peptic ulcer disease [30, 31]. Peptic ulcer disease, which is described as mucosal defects of at least 0.5 cm in diameter that penetrate through the muscularis

mucosa, can be classified into duodenal ulcers or gastric ulcers [32]. Additionally, there is a significant increase in peptic ulcers in NSAID users with *H. pylori* infection compared to those NSAID users without *H. pylori* infection [33].

Chronic *H. pylori* infection causes gastritis in which SST concentrations are reduced, resulting in increased gastrin secretion [34]. Gastritis can be classified into antral-predominant gastritis or corpus atrophic gastritis. Antral gastritis is associated with increased gastrin-stimulated acid secretion that results in the development of duodenal ulcers [35]. Prolonged gastrin stimulation or hypergastrinaemia causes mucosal hyperplasia through increased expression of growth factors including regenerating protein-1α (REG1A) and heparin-binding EGF-like growth factor (HBEGF) by ECL and parietal cells, respectively [36, 37].

Conversely, corpus gastritis has been linked to the development of gastric ulcers and is associated with impaired acid secretion such as inhibition of parietal cell function [38]. A decrease in acid secretion leads to an increased secretion of gastrin, which stimulates epithelial cell proliferation [39]. Continuous epithelial cell proliferation and inflammation induce gastric gland loss and atrophy in the antrum and subsequently, intestinal metaplasia, which is a precursor lesion of intestinal-type gastric adenocarcinoma [40, 41]. Atrophy is described as loss of glandular tissue due to continuous mucosal injury [38].

About 3% of *H. pylori* positive individuals subsequently develop gastric carcinoma [42] while the risk for patients with gastric ulcer to develop gastric carcinoma is 2-fold increase [43]. The pathogenicity of *H. pylori* is attributed to strains containing cagA (cytotoxin-associated gene A) gene that has been associated with the development of gastric cancer [44]. Also, it has been found

that *H. pylori* infection induces spermine oxidase in gastric epithelial cells, resulting in cell apoptosis and the production of hydrogen peroxide that causes DNA damage [45]. Furthermore, a sub-population of gastric epithelial cells is found to exhibit apoptosis resistance and DNA damage, thus increasing the risk for malignant transformation of normal epithelial cells [45].

In addition, there is evidence suggesting a contribution of chronic *H. pylori* infection to autoimmune atrophic gastritis such as pernicious anaemia [46]. Pernicious anaemia causes vitamin B12 deficiency and is characterised by atrophy of the corpus glands, and detection of serum antibodies against the H^+/K^+-ATPase of parietal cells and secreted intrinsic factor [46, 47]. Moreover, population studies have indicated an increased risk of gastric carcinoma and gastric carcinoid tumours in patients with pernicious anaemia [48].

1.3 The maintenance of tissue organisation in the upper gastrointestinal tract

The integrity of the upper gastrointestinal tract epithelium is partly maintained by epithelial stem cells that divide asymmetrically to produce two daughter stem cells; one of which continues to self-renew while the other generates a population of progenitor cells, which proliferates and differentiates into various epithelial lineages [49]. Evidence suggests a single gastric stem cell, on average, is located in the isthmus region of each gland unit [50]. In addition, oesophageal stem cells are thought to reside in the basal compartment of the squamous epithelium while stem cells from the small intestine are located at the base of the crypt [51].

The stem cell niche, which consists of extracellular matrix (ECM) and mesenchymal cells (e.g. subepithelial myofibroblasts), is thought to provide an optimal microenvironment to maintain progenitor cell survival, and to regulate epithelial cell functions through mesenchymal-epithelial interactions [52]. In mucosal injury, myofibroblasts and bone marrow derived mesenchymal stromal cells (MSCs) also contribute to wound healing [49].

1.3.1 Epithelial progenitor cells

The maintenance of tissue architecture depends on the rates of cell proliferation, differentiation and apoptosis. In the gastric glands, there is a bi-directional migration of progenitor cells, also known as transit amplifying cells, from the isthmus or neck region towards the superficial epithelium to become mucous cells, and towards the gland base region to differentiate into parietal and peptic/chief cells [53]. As the cells differentiate, they lose their replicative capacity and undergo apoptosis eventually with an average turnover period of 3, 54 and 194 days for gastric pit, parietal and peptic/chief cells, respectively [53]. Furthermore, the turnover period in gastric epithelial cells is altered during pathological conditions (e.g. chronic *H. pylori* infection during gastric carcinogenesis) [54].

Studies have identified gastric progenitor cell markers such as the expression of doublecortin-like kinase 1 (DCLK1) in the isthmus region of corpus glands, and the expression of villin transgene in some base regions of antral glands [50]. Villin-positive cells have been shown to have multi-lineage potential after interferon stimulation [55]. Additionally, leucine-rich repeat containing G protein-

coupled receptor 5 (LGR5), which is a well-known biomarker for intestinal stem cells, is expressed in the base region of antral glands [56].

In cancer, stem cells or progenitor cells may transform into malignant cells due to the acquisition of mutations. This gives rise to cancer stem cells or termed cancer-propagating cells, which are defined as a population of self-renewal cells within the tumour that initiate and sustain malignant growth [57]. Furthermore, recent work points to the ability of these cells to seed new tumours and to spawn non-cancer stem cell populations that lack the tumour-initiating ability [58]. Cancer stem cells are generally associated with aggressive tumours and poor prognosis [59]. For example, CD44 molecule, which is a transmembrane glycoprotein, is shown to be a biomarker for gastric cancer stem cells, and has been associated with an increase in resistance to chemotherapy-induced cell death [60].

1.3.2 Mesenchymal stromal cells

Unlike adult tissue stem cells, MSCs are heterogeneous, non-hematopoietic and reside in the niche of perivascular tissues (e.g. bone marrow and adipose tissue) [61]. They are described as plastic-adherent fibroblast-like cells that exhibit multipotent differentiation capacity *in vitro* [62]. According to the International Society for Cellular Therapy, MSCs are positive for human clusters of differentiation (CD) molecules, namely, CD105, CD73 and CD90, and negative for CD45, CD34, CD14, CD19 and HLA-DR surface molecules [63].

The roles of MSCs include the regulation of immune response and maintenance of tissue homeostasis. Previous studies have demonstrated the effects of MSCs on

suppressing the proliferation of T cells [64], and reducing the proliferation and cytotoxicity of natural killer cells [65], thus suggesting immunosuppressive properties in MSCs. During wound healing, MSCs migrate to the injury site and differentiate into myofibroblasts and endothelial cells [61]. Moreover, MSCs exhibit chemotactic activity. For example, MSCs secrete vascular endothelial growth factor (VEGF) and macrophage inflammatory protein 1-alpha (MIP1α) to recruit endothelial cells and macrophages, respectively [66].

1.3.3 Myofibroblasts

Myofibroblasts are relatively rare in most normal tissues but in response to injury, local fibroblasts transdifferentiate into myofibroblasts, also known as "activated fibroblasts", to facilitate wound healing through deposition of ECM proteins and secretion of growth factors and cytokines [67]. During wound healing, myofibroblasts may also originate from pericytes and bone marrow MSCs [67]. In contrast to other tissues, there is a population of residual myofibroblasts, which regulates epithelial cell functions in the gastrointestinal tract [68].

Myofibroblasts are characterised by positive staining for alpha smooth muscle actin (α-SMA) and vimentin, and negative staining for desmin [69]. Moreover, fibronectin, which is involved in cell adhesion and migration, has been detected on the myofibroblast surface [69]. In human cultured gastric and colonic myofibroblasts, the expression of cyclooxygenase-1 (COX1) and cyclooxygenase-2 (COX2), involved in prostaglandin synthesis [70, 71], may contribute to the maintenance of glandular architecture and mucosal protection [72]. During inflammation, gastric myofibroblasts exhibit increased rates of cell migration and

proliferation [73]. Additionally, a previous study has shown that gastric myofibroblasts express Na^+/H^+ exchanger (NHE) isoforms and that NHE1 plays a role in regulating migration and proliferation of gastric myofibroblasts [74].

Myofibroblasts regulate the migration and proliferation of epithelial cells physiologically. In superficial mucosal injury, colonic myofibroblasts secrete transforming growth factor-beta 3 (TGF-β3), which induces rapid epithelial cell migration across the wound layer in a process called restitution, so as to maintain the integrity of the epithelium [75]. Furthermore, TGF-β3 enhances transepithelial resistance as a previous study has demonstrated the inhibition of secretagogue-induced chloride secretion from epithelial cells [76]. In addition, growth factors that are secreted by myofibroblasts such as hepatocyte growth factor (HGF) [77] and keratinocyte growth factor (KGF) [78] have been associated with increased proliferation of the gastrointestinal tract epithelial cells.

There is also a role for myofibroblasts in mucosal immunology. Intestinal myofibroblasts have been associated with innate immune responses through regulation and expression of toll-like receptors (TLRs) [79]. When stimulated with bacterial lipopolysaccharide or lipoteichoic acid, the expression of TLR-2, TLR-3, TLR-4, TLR-6 and TLR-7 in intestinal myofibroblasts is increased, leading to the secretion of pro-inflammatory cytokines and chemotactic factors that recruit immune cells to sites of inflammation [79]. Furthermore, the expression of class II major histocompatibility complex (MHC) molecules in colonic myofibroblasts has been found, suggesting these cells function as antigen-presenting cells which activate CD4-positive T-cells during activation of adaptive immunity [80].

1.4 Extracellular matrix homeostasis

In addition to cytokine secretion, myofibroblasts deposit ECM proteins (e.g. collagens, laminins, fibronectin) and secrete ECM-degrading proteases which regulate ECM turnover [81]. The ECM helps to maintain tissue architecture and homeostasis and normally, it serves as a barrier to tumour growth and metastasis [82]. The ECM consists of fibrous proteins (e.g. collagens) embedded in a visco-elastic gel of glycoproteins (e.g. fibronectin), proteoglycans (e.g. decorin) and glycosaminoglycans (i.e. hyaluronan) [83]. The maintenance of ECM homeostasis involves regulation by proteases and their inhibitors. These proteases are classified into metalloproteinases; mainly the matrix metalloproteinases (MMPs), serine proteases such as urokinase-like plasminogen activator (uPA) and tissue-type plasminogen activator (tPA), and cysteine proteases such as collagen-degrading cathepsins [84].

1.4.1 Matrix metalloproteinases

The MMPs, which belong to a family of zinc-dependent endopeptidases, are involved in physiological processes (e.g. embryonic development, wound healing) and cancer progression [85]. A total of 28 human MMPs has been identified, and they are classified into five main categories according to their substrate specificity, primary structures, and cellular localization, namely, the matrilysins (e.g. MMP7), collagenases (e.g. MMP1), stromelysins (e.g. MMP3), gelatinases (e.g. MMP2), and the membrane-type MMPs (e.g. MMP14) [86]. Other members of the metalloproteases include a disintegrin and metalloproteinases (ADAMs),

which are transmembrane proteins, and ADAMs with thrombospondin motifs (ADAMTS), which are secreted and bound to ECM proteins [84].

The MMPs are synthesised as inactive zymogens (i.e. pro-MMPs) and mostly they become activated after proteolytic cleavage in the extracellular environment [87]. The activity of MMPs is low in the normal state, and is induced in response to external stimulus. For example, proinflammatory cytokines stimulate the secretion of MMP1, MMP2 and MMP3 in colonic myofibroblasts [88, 89]. In intestinal and gastric myofibroblasts, the expression of MMP1, MMP2 and MMP3 has also been identified, suggesting the importance of these MMPs [73, 90]. Substrates for MMP1 such as perlecan and insulin-like growth factor binding protein-3 (IGFBP3) have been shown to increase the bioavailability of fibroblast growth factor (FGF) and insulin-like growth factor (IGF), respectively [91]. Additionally, studies have shown the proteolytic activation of transforming growth factor-beta (TGF-β) by MMP2, and the cleavage of E-cadherin by MMP3 [87].

Matrilysin (i.e. MMP7), which is predominantly expressed in epithelium, is implicated in regulating myofibroblast function [73]. In the stomach, secreted MMP7 cleaves insulin-like growth factor binding protein-5 (IGFBP5) and subsequently releases IGF-II, which induces the proliferation and migration of gastric myofibroblasts [92]. Other substrates of MMP7 that mediate cell apoptosis and migration are membrane surface proteins, such as Fas ligand, E-cadherin and fibronectin [87].

1.4.2 Tissue inhibitors of metalloproteinases

Tissue inhibitors of metalloproteinases (TIMPs) are negative regulators of MMPs, ADAMs and ADAMTS [93]. In tissue fluids, α2-macroglobulin, which is a plasma protein, serves as an important MMP inhibitor [87]. Nonetheless, other functions of TIMPs that have been studied include activation of pro-MMPs (e.g. pro-MMP2, pro-MMP9), inhibition of angiogenesis, and induction of cell proliferation and migration [93].

The TIMP family consists of 4 members (i.e. TIMP1, TIMP2, TIMP3 and TIMP4) and they exhibit differential expression patterns and different affinities for various MMPs [82]. For example, previous studies using mouse tissues have shown that TIMP3 expression is abundant in the kidney, lung and brain [94] while TIMP4 expression is abundant in the heart, brain, ovary and skeletal muscle [95]. In addition, *H. pylori* infection in human gastric tissue has been found to increase the abundance of TIMP1, TIMP3 and TIMP4 in glandular epithelial cells, and the abundance of TIMP3 in myofibroblast-like cells [96].

Studies have shown that TIMP1 is a poor inhibitor for membrane type MMPs, such as MMP14, MMP16 and MMP24 [93]. Unlike other TIMPs, TIMP3 has low solubility, binds to the heparan sulphate proteoglycans within the ECM, and inhibits several members of ADAMs (e.g. ADAM10, ADAM17) and ADAMTS (e.g. ADAMTS4, ADAMTS5) [87].

1.4.3 Plasminogen activator-plasmin system

uPA and tPA are serine proteases that generate plasmin from plasminogen [97]. Both uPA and tPA are inhibited by plasminogen activator inhibitor-1 (PAI1) and protease nexin-1 (PN1) while plasmin is effectively inhibited by α2-antiplasmin [97].

Binding of uPA to its receptor (i.e. uPAR) converts plasminogen into plasmin, which is involved in degradation of ECM proteins and activation of several MMPs [84]. Conversely, receptor bound tPA converts plasminogen into plasmin that is involved in fibrinolysis and thrombolysis [97]. Increased expression of uPA and uPAR has been reported in subepithelial cells of *H. pylori* positive gastric corpus tissue, and this may influence the proliferation of epithelial cells through activation of HGF [97, 98].

1.5 Gastrointestinal tract signalling pathways

Myofibroblasts are believed to be a key mesenchymal cell type that maintains the integrity of epithelium [99]. Signalling pathways that are implicated in the maintenance of epithelial structure and function include: 1) Transforming growth factor-β/bone morphogenetic protein signalling, 2) Hedgehog signalling, 3) Notch signalling, 4) Wnt signalling and 5) growth factor signalling (e.g. hepatocyte growth factor, HGF, keratinocyte growth factor, KGF, insulin-like growth factor, IGF and epidermal growth factor, EGF) [99, 100].

1.5.1 Transforming growth factor-β/bone morphogenetic protein signalling

The TGF-β or bone morphogenetic protein (BMP) signalling pathway normally inhibits the proliferation of epithelial cells, and induces myofibroblast differentiation and activation [101]. Members of the TGF-β superfamily include BMPs, activins and TGF-β isoforms 1, 2 and 3 encoded from three separate genes [101]. In the gastric mucosa, TGF-β3 expression is found in parietal, peptic/chief and mucous cells while TGF-β1 and TGF-β2 expression are mainly expressed in parietal and peptic/chief cells, respectively [102]. Upon binding by a ligand, serine/threonine kinase TGF-β type II receptor (TβR-II) activates TGF-β type I receptor (TβR-I), leading to phosphorylation of receptor-regulated Smads (e.g. Smad2 and Smad3) [101]. Phosphorylated Smad proteins form a heteromeric complex with common-partner Smads, known as Smad4 in mammals, and then the complex translocates into the nucleus to activate gene transcription [101]. In advanced stages of gastric carcinoma, TGF-β becomes an oncogene and activation of TGF-β signalling increases the expression of phosphorylated Smad2, which is associated with diffuse-type gastric cancer metastasis, and correlated with poor survival [103].

1.5.2 Hedgehog signalling

In the gastrointestinal tract, hedgehog signalling is implicated in anti-inflammatory responses and is involved in regulating homeostasis and differentiation of progenitor cells [104, 105]. Studies have also implicated the role of hedgehog signalling in developmental patterning of the gastrointestinal tract and lung tissues [106]. The hedgehog family ligands, namely, sonic hedgehog

(SHH), indian hedgehog (IHH) and desert hedgehog (DHH), exhibit the same affinity for patched family receptors, PTCH1 and PTCH2 [107]. Upon binding of hedgehog ligand to a PTCH receptor, the inhibition of smoothened (SMO) by the receptor was released [108]. This results in stabilisation and nuclear localisation of the Gli family of transcriptional factors (e.g. GLI1, GLI2 and GLI3), which activate the transcription of target genes such as PTCH1 and GLI1 [104].

The expression of SHH mRNA has been found in the gastric fundus, small intestinal and colonic crypts, but not in the oesophagus and gastric antrum [104]. Additionally, it was found that parietal cells express SHH and PTCH1, whereas peptic/chief cells in the gland base region express only PTCH1 [109, 110]. The expression of SHH in parietal cells is stimulated by gastrin and in turn, SHH induces the expression of H^+/K^+-ATPase in parietal cells, suggesting a positive correlation of hedgehog signalling with gastric acid secretion [111].

1.5.3 Notch signalling

Progenitor cell populations in the gastrointestinal tract is regulated by Notch signalling, which can be classified into canonical and non-canonical signalling pathways [112]. Canonical Notch signalling pathway has been shown to induce the proliferation and inhibit the differentiation of progenitor cells in the isthmus region of gastric glands, basal layer of oesophageal epithelium and in the colonic crypt base region [112, 113].

Notch family receptors (i.e. NOTCH1, NOTCH2, NOTCH3 and NOTCH4) and ligands (i.e. Jagged 1 and 2, Delta-like 1, 3 and 4) are single-pass transmembrane

proteins [114]. In the canonical Notch signalling pathway, a Notch ligand expressed on neighbouring cells binds to the extracellular domain of the Notch receptor, resulting in the cleavage of the extracellular domain that is mediated by ADAM type metalloproteases [114]. The extracellular domain is then internalised into ligand-expressing cells by endocytosis and is degraded by lysosomes while the Notch intracellular domain (NICD) is cleaved by γ-secretase [114]. After cleavage, the NICD translocates into the nucleus and forms a transcriptional complex with the CSL family of DNA binding factors and mastermind-like family coactivators, resulting in the transcriptional activation of genes such as hairy and enhancer of split 1 (HES1) [112].

1.5.4 Wnt signalling

Physiologically, the Wnt signalling pathway is essential for regulation of epithelial lineage differentiation from progenitor cells and for regulation of progenitor cell proliferation [115]. In the human genome, a total of 19 WNT genes have been identified, and they belong to a family of cysteine-rich secreted glycoproteins which can activate two different pathways, known as canonical and non-canonical Wnt signalling pathways [116]. Activation of Wnt signalling is transduced by the Frizzled (FZD) family of receptors including ten mammalian receptors that have been identified [117]. When Wnt proteins bind to FZD receptors, there are 3 main signalling pathways that are transduced: a) the canonical Wnt/β-catenin pathway, b) the non-canonical Wnt/Ca^{2+} pathway and c) the non-canonical planar cell polarity (PCP) pathway [117] (Figure 1.2).

In the canonical Wnt/β-catenin signalling pathway, the β-catenin cascade is induced when Wnt proteins (e.g. Wnt-1, Wnt-3a) bind to FZD receptors in the presence of low density lipoprotein receptor-related protein 5 or 6 (LRP5/6) co-receptors [116]. In the absence of Wnt activation, β-catenin is bound to a complex, which consists of adenomatous polyposis coli (APC), axin, glycogen synthase kinase 3-beta (GSK3β) and casein kinase 1-alpha (CK1α), and is phosphorylated and subsequently ubiquitinated, resulting in rapid degradation of β-catenin by the proteasome [115]. Alternatively, β-catenin may be bound to cadherin at the plasma membrane [118]. Upon binding of Wnt protein to the FZD receptor, the kinase activity of GSK3β and CK1α is inhibited, preventing the phosphorylation and degradation of β-catenin. Subsequently, unphosphorylated β-catenin accumulates in the cytosol and translocates into the nucleus, where it acts as a co-factor for T-cell factor/lymphocyte enhancer factor (TCF/LEF) transcriptional activation [116]. Recently, Clevers suggests that β-catenin is phosphorylated in the presence of Wnt activation but the subsequent ubiquitination of phosphorylated β-catenin is inhibited [119]. Eventually, the β-catenin-APC complex becomes saturated with phosphorylated β-catenin, causing newly synthesised β-catenin to accumulate in the cytosol and then translocate into the nucleus [119].

Activation of the non-canonical Wnt signalling pathway normally occurs when Wnt proteins (e.g. Wnt-4, Wnt-5a, Wnt-11) bind to FZD receptors in the presence of receptor tyrosine kinase-like orphan receptor 2 (ROR2) and receptor-like tyrosine kinase (RYK) co-receptors [116]. Studies have shown that Wnt-5a activates mainly non-canonical Wnt signalling pathways but under certain circumstances, Wnt-5a can activate the canonical Wnt/β-catenin signalling

pathway [120]. In the non-canonical Wnt/Ca^{2+} signalling pathway, Ca^{2+}/calmodulin-dependent protein kinase II (CAMKII) is activated by an influx of Ca^{2+} ions, resulting in nemo-like kinase (NLK) activation that leads to the phosphorylation of TCF/LEF and subsequently, inhibits the β-catenin-TCF/LEF complex to interact with DNA promoter site for transcriptional activation [121]. Additionally, the Wnt/Ca^{2+} signalling pathway activates PKC and calcineurin, which causes the dephosphorylation and nuclear localisation of nuclear factor of activated T cells (NFAT) [122]. The other non-canonical PCP pathway is involved in the regulation of cell polarisation within the plane of epithelial cell sheet, and has been shown to activate cytoskeletal regulators such JUN N-terminal kinase (JNK) [122].

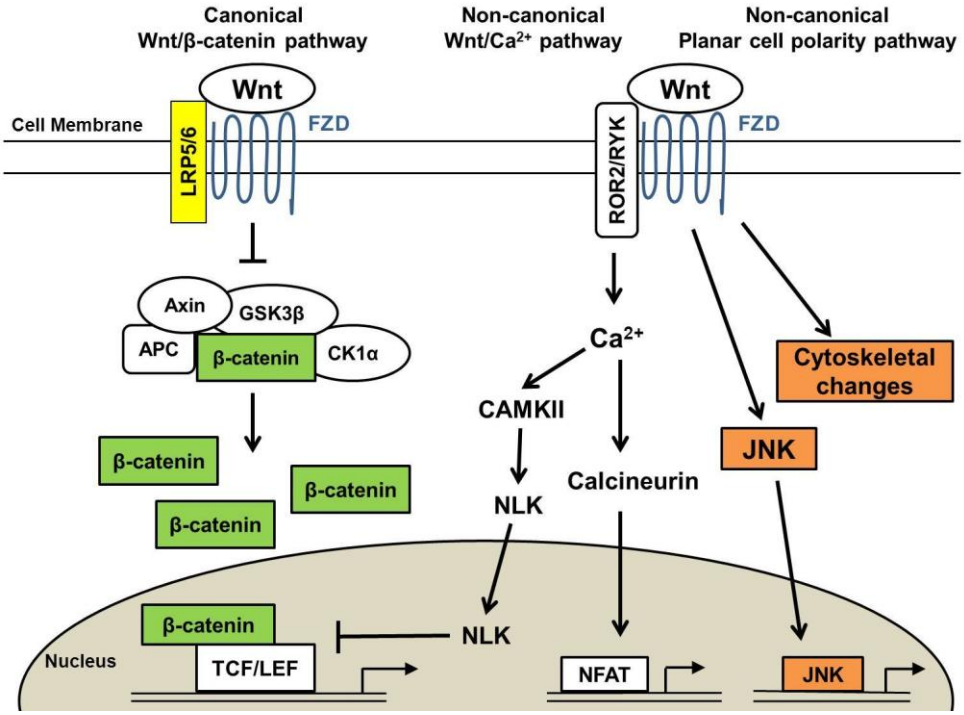

Figure 1.2 A schematic representation of Wnt signal transduction pathways. Binding of Wnt proteins to FZD receptors in the presence of LRP5/6 coreceptors activates the canonical Wnt signalling pathway in which β-catenin is stabilised in the cytosol and then translocates into the nucleus to activate the transcription of Wnt-responsive genes. The non-canonical Ca^{2+}-dependent Wnt signalling pathway activates NLK via phosphorylation by CAMKII and stimulates NFAT-dependent transcription. The other non-canonical Wnt pathway activates JNK and induces cytoskeletal reorganisation.

The expression of Wnt-2, Wnt-4, Wnt-5a and Wnt-5b has been reported in murine intestinal myofibroblasts [123] and human colonic myofibroblasts [124]. Furthermore, the expression of FZD1, FZD4, FZD5, FZD6, FZD7 and LRP6 has been found in crypt epithelial cells and colonic myofibroblasts [124, 125]. This distribution suggests that the secretion of Wnt proteins by mesenchymal cells activates the Wnt pathways through autocrine and paracrine signalling, implicating mesenchymal-epithelial interactions [123].

1.6 The biology of cancer

Abnormal secretion of growth factors and cytokines, and deregulation of signalling pathways have been linked to neoplastic development [126]. Moreover, it is well established that genetic alterations (e.g. gene mutations) result in malignant transformation, and that transformed cells exhibit different phenotypes from normal cells in terms of promoting tumour growth and progression (Figure 1.3) [127]. More recently, the discovery of miRNAs, which function as post-transcriptional gene regulators, has been shown to influence carcinogenesis, and this provides an additional insight on the mechanisms that alter cancer cell behaviour, including proliferative and metastatic potential effects (Chapter 1.7).

Metastasis is the ability of tumour cells to invade the surrounding tissue, disseminate into the bloodstream and induce neoplastic potential at the distant site [128]. This was first described by Paget in 1889 when he proposed the "seed and soil" hypothesis of metastasis, in which malignant tumour cells ('seed') preferentially grow at a particular organ site or microenvironment ('soil') [128, 129]. About a hundred years later, Dvorak described tumours as "wounds that fail

to heal", indicating there are similarities between tumour stromal inflammatory response and wound healing [130]. Indeed, chronic inflammation is linked to many types of malignant tumour, including chronic *H. pylori* infection-associated gastric carcinoma and Barrett's induced oesophageal adenocarcinoma [131], and this clearly indicates the involvement of the microenvironment in cancer initiation and progression (Chapter 1.8).

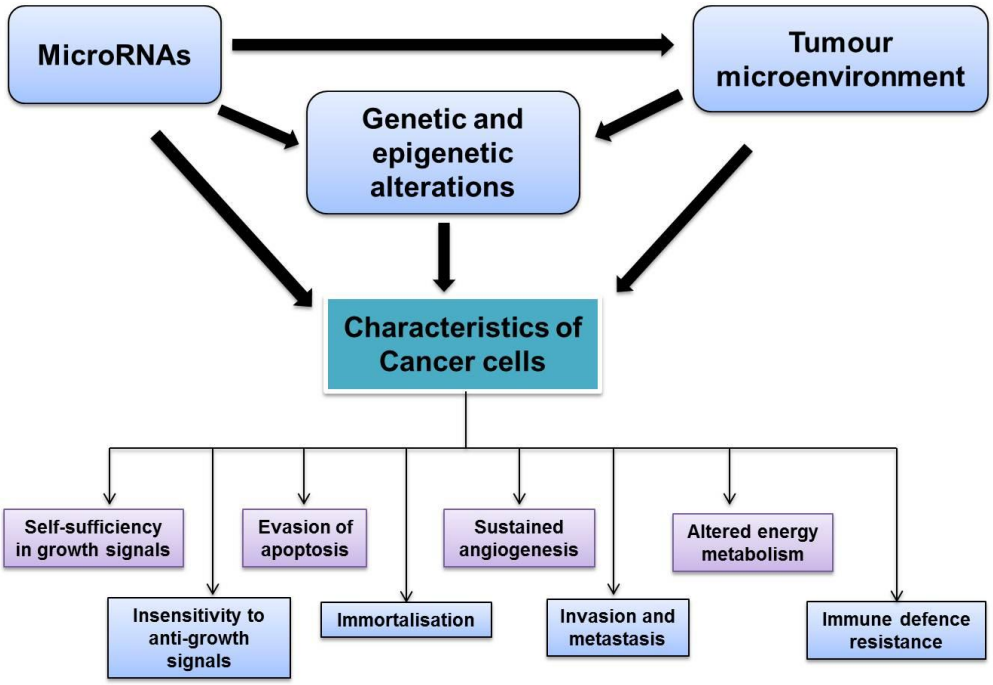

Figure 1.3 Hallmarks of cancer cells in tumour growth and progression. Cancer cells exhibit characteristics that promote malignancy. Genetic changes and epigenetic regulation have been commonly found in cancer cells while stromal-tumour interactions have been implicated in cancer progression. Recent research has focused on miRNAs that influence cancer cell behaviour and also miRNAs in stromal cells of the tumour microenvironment. The molecular interactions that promote cancer cell growth, invasion and metastasis could potentially be used for novel therapeutic strategies.

1.6.1 Hallmarks of cancer

Six hallmark capabilities of cancer cells that dictate tumour growth and malignancy are originally proposed by Hanahan and Weinberg: a) self-sufficiency in growth signals; cancer cells release mitogenic signals so they reduce their dependence on exogenous growth stimulation, b) insensitivity to anti-growth factors; cancer cells evade anti-proliferative actions of tumour suppressor genes, c) evasion of apoptosis; cancer cells are resistant to apoptosis through deregulation of pro and anti-apoptotic proteins of the BCL2 family or by loss of tumour suppressor gene functions, d) immortalisation; cancer cells acquire unlimited proliferative potential, e) sustained angiogenesis; an 'angiogenic switch' is continuously activated that results in vasculature formation to support tumour growth and f) invasion-metastasis activation; the loss of ECM components and cell-cell adhesion molecules (e.g. E-cadherin) allow the cells to invade adjacent tissue and move to a distant site [132]. Subsequently, two additional hallmark capabilities have emerged from recent research development: g) cancer cells reprogram their energy metabolism to glycolysis for increased survival and effective proliferation, also known as the Warburg effect [133] and lastly, h) cancer cells acquire the ability to resist immunological destruction by lymphocytes, macrophages and natural killer cells [127].

Nonetheless, Hanahan and Weinberg stress the involvement of genetic and epigenetic alterations in cancer cells, and the tumour microenvironment in contributing to the acquisition of hallmark capabilities. Tumour stromal cells play a role in promoting tumour angiogenesis, cancer cell growth and invasion through ECM remodelling, and secretion of cytokines and growth factors that activate cancer cell signalling pathways [134].

1.6.2 Genetic mutations

Genetic mutations, which refer to the permanent, heritable change in nucleotide sequences, are already reported in many tumours and they occur in more than 1% of all genes in the human genome, mostly functioning as oncogenes, tumour suppressor or DNA mismatch repair genes [135]. Loss-of-function of tumour suppressor genes occurs when both copies of the gene are mutated, known as the "two-hit hypothesis" of tumour suppression [136], and this was originally identified by Knudson in 1971. He proposed that two mutational events in the retinoblastoma gene were required for the development of hereditary and sporadic retinoblastoma [137]. Hereditary retinoblastoma usually occurred at a younger age because the first mutation is inherited and tumour forms when the second mutation is acquired. In a similar manner, inactivation of E-cadherin (CDH1) gene in gastric cancer cells is the result of two genetic hits, suggesting the function of tumour suppressor genes in mediating cancer cell invasion and metastasis [138].

Subsequently, the discovery of specific genetic alterations in colorectal carcinoma, by Fearson and Vogelstein, has provided a useful model to illustrate multi-hit events in carcinogenesis [139]. In this case, mutations on chromosome 5q containing APC in normal colon cells induce the formation of adenomatous polyp, and subsequent oncogenic mutation of v-Ki-ras2 Kirsten rat sarcoma viral oncogene homolog (KRAS) on chromosome 12p results in dysplasia [136, 139]. Furthermore, loss of chromosome 18q, point mutation on one allele of TP53 and allele loss of chromosome 17p that contains TP53 induce the development of colon carcinoma [139].

1.6.3 Genetic instability

In addition to genetic mutation, genetic instability such as chromosomal instability and microsatellite instability is well characterised in tumours. Chromosomal instability, which has been detected in 84% of gastrointestinal tumours, is defined as chromosomal abnormalities including aneuploidy and loss of heterozygosity (LOH) [140]. Aneuploidy is described as variations in genomic copy number and is correlated with the expression of oncogenes and tumour suppressor genes [141]. Additionally, aneuploidy has been associated with lymph node metastasis and histological subtypes of gastric adenocarcinomas [141]. In addition, the second genetic hit that inactivates tumour suppressor genes is known as LOH [140]. For example, LOH of TP53 tumour suppressor gene is associated with early stage of gastric carcinogenesis. Furthermore, microsatellite instability has been reported in 25% to 50% of sporadic gastric cancer and is usually caused by mutational or epigenetic inactivation of mismatch repair genes [142]. Microsatellite instability is defined as high frequency of replication errors that result in deletions or insertions of nucleotides within the microsatellite region [140].

1.6.4 Epigenetic alterations

Changes in epigenetic modifications to DNA molecules and histone proteins contribute to cancer initiation and progression, and have been recognised in drug development for epigenetic therapy [143]. Epigenetics, which are defined as heritable and reversible modifications of chromatin structure without altering the DNA sequence, are important regulators of gene expression [144]. The main mechanisms involved are DNA methylation and covalent modifications of

histones. DNA methylation is the addition of a methyl group to cytosines in CpG dinucleotides and is catalysed by DNA methyltransferases such as DNMT1, DNMT3A and DNMT3B [144].

High frequency of GC content and CpG dinucleotides, termed CpG islands, are present in the promoter region of about 50% of all genes [145]. Abnormal DNA methylation of CpG islands in the promoter regions is linked to the silencing of tumour suppressor genes such as CDH gene in gastric carcinoma [146]. There is increased DNA methylation in *H. pylori* infected gastric epithelial cells, suggesting the contribution of DNA methylation in chronic inflammation [147]. Additionally, a more recent study using *Helicobacter*-infected mice has indicated a decrease in global DNA methylation in gastric epithelial cells and stromal myofibroblasts during the early phase of dysplasia, prior to gastric carcinogenesis [148]. Furthermore, stromal myofibroblasts from gastric cancer has been associated with global DNA hypomethylation [149]. Taken all these findings, targeting DNA methylation for epigenetic therapy may be fundamental to prevent *Helicobacter*-associated gastric cancer initiation and progression.

1.7 MicroRNAs

MicroRNAs (miRNAs) are small non-coding RNAs of 18 to 25 nucleotides in length that regulate post-transcriptional gene expression. In the gastrointestinal tract, miRNAs play a role in developmental and physiological processes [150] such as intestinal epithelial cell differentiation and maintenance of intestinal barrier function [151]. Additionally, altered miRNA expression in gastric and oesophageal carcinomas, and pre-neoplastic tissues, has been identified [152, 153]

and these deregulated miRNAs may contribute to chromosomal instability, epigenetic changes and altered transcriptional regulation [154]. Moreover, it has been suggested that about 50% of human miRNAs are located in chromosomal regions that are frequently altered in human cancers (e.g. LOH, fragile sites) [155]. During the development of gastrointestinal tumours, there is increasing evidence to suggest the role of up and down-regulated miRNAs as oncogenes and tumour suppressor genes, respectively [154].

1.7.1 MicroRNA expression and function

MicroRNAs regulate gene expression by inducing translational repression or degradation of mRNAs through perfect or partial complementary binding of the 5'end of mature miRNAs to the 3' untranslated regions (UTRs) of the mRNA targets, known as the "seed" region (6 to 8 nucleotides) [156]. However, recent work suggests that miRNAs may bind to sites in the 5'UTR and within the coding region of mRNAs [153]. It is estimated that miRNAs represent 1% of the human genes [157], and they are commonly located within introns or in between protein-coding genes [153]. Additionally, miRNAs are classified into sequence families based on similarity of their seed sequence and overall nucleotide sequence [7]. The mechanism of miRNA biogenesis and function is described in Figure 1.4. Briefly, primary miRNAs (pri-miRNAs) are produced when miRNA genes are transcribed by RNA polymerase II or excised as an intron from mRNA transcripts. Then, pri-miRNAs are cleaved by Drosha enzyme and its binding partner, DiGeorge syndrome critical region gene 8 (DGCR8) to form precursor miRNAs (pre-miRNAs) [153]. Pre-miRNAs, which have a stem loop hairpin structure, are

transported into the cytoplasm by exportin 5. In the cytoplasm, pre-miRNAs are cleaved by Dicer and its binding partner, trans-activation response RNA binding protein (TARBP), to produce short RNA duplexes of 19 to 24 nucleotides in length [7]. After unwinding, one of the miRNA strands is rapidly degraded while the other mature miRNA is incorporated into the RNA-induced silencing complex (RISC) [153]. The mature miRNA guides the RISC to the 3'UTR binding site of a mRNA target, resulting in inhibition of mRNA translation or degradation of mRNA that depends on the degree of complementarity of the base-pairing sequence [158].

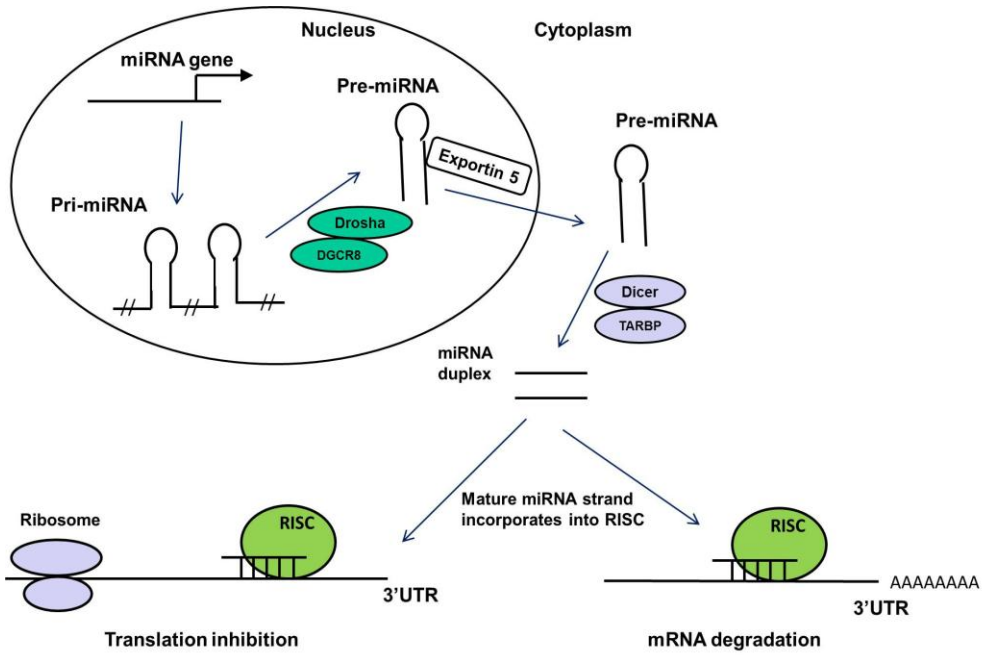

Figure 1.4 Biosynthesis and functions of miRNAs. A pri-miRNA is transcribed from a miRNA gene and is cleaved by Drosha to produce pre-miRNAs. A pre-miRNA is exported into the cytoplasm that is mediated by exportin 5. In the cytoplasm, pre-miRNA is cleaved by Dicer to give a miRNA duplex. After unwinding, the mature miRNA strand incorporates into the RISC and guides the complex to the site of 3'UTR of a mRNA target. The miRNA-complex induces either translational repression or mRNA degradation.

1.7.2 Altered miRNA expression in gastric and oesophageal cancers

MicroRNA expression profiling of tumour samples has been used to identify histological tumour subtypes and to classify poorly differentiated tumours [159]. For example, distinct miRNA profiles between squamous cell carcinoma and adenocarcinoma of the oesophagus [160]. Altered expression of miRNAs has been shown to regulate the expression of mRNA targets that contribute to cancer progression [153]. Differential expression of miRNAs in gastric and oesophageal cancer tissues was identified using microarray or polymerase chain reaction (PCR)-based approach. For example, increased expression of miR-21 which is found in gastric carcinoma [161], oesophageal squamous cell carcinoma and oesophageal adenocarcinoma [160], down-regulates the expression of tumour suppressor, leading to tumour growth and invasion [150]. Additionally, decreased expression of miR-143 and miR-145 are commonly found in the gastrointestinal tract tumours (e.g. gastric carcinoma, oesophageal squamous cell carcinoma, oesophageal adenocarcinoma, colon carcinoma) and are associated with cancer cell growth and decreased sensitivity to chemotherapeutic treatment [153, 162]. On the other hand, the role of miRNAs in cancer progression may depend on the cellular context. For example, miR-192 and miR-215 are found to be up-regulated in gastric carcinomas compared to non-neoplastic tissues [163], but are down-regulated in colon carcinoma [164].

1.7.3 Epigenetics in miRNAs

It is recognised that epigenetics (i.e. DNA methylation and histone modifications) regulate gene expression (Chapter 1.6.4). In addition, epigenetic alterations play a role in the regulation of miRNA expression that may result in abnormal activation of oncogenes and silencing of tumour suppressor genes during cancer development and metastasis [165, 166]. A model, using DNMT1 and DNMT3B double knockout colon cancer cells, has shown that DNA methylation regulates approximately 10% of miRNA expression [167]. It is suggested that the expression of miRNAs is regulated: a) directly; through DNA methylation at CpG islands on the promoter region of miRNA genes and b) indirectly; through DNA methylation that affects the expression of transcription factors, which in turn, regulate miRNA gene transcription [167].

In gastric cancer, down-regulated miRNAs such as miR-10b, miR-181c, miR-34b and up-regulated miRNAs such as miR-196b have been directly associated with DNA methylation [153]. Moreover, a recent study has shown that cagA of *H. pylori* indirectly induces the expression of DNMT3B, which in turn decreases the expression of *let*-7, and subsequently activates the oncogenic KRAS pathway for gastric carcinogenesis [168]. These may, therefore, indicate a role of DNA methylation in gastric cancer initiation and progression.

Dysregulation of the epigenetic machinery by miRNAs (also termed epi-miRNAs) has also been implicated in carcinogenesis. For example, in lung cancer cells, down-regulation of miR-29 family members (i.e. miR-29a, miR-29b and miR-29c) induces methylation-silencing of tumour suppressor genes through increased expression of miR-29 targets, DNMT3A and DNMT3B [169]. Another study

reveals genomic loss of the miR-101 gene in prostate cancer cells, resulting in the overexpression of enhancer of zeste homolog 2 (EZH2), which is a histone methyltransferase [169].

1.8 Tumour microenvironment

The tumour microenvironment consists of ECM, vasculature, soluble paracrine factors and non-malignant stromal cells, such as cancer-associated myofibroblasts (CAMs), inflammatory cells, endothelial cells, pericytes and bone marrow derived stromal cells [170]. In gastrointestinal tumours, stromal cells constitute 60% to 90% of the tumour mass with CAMs being an important stromal cell type in tumour progression [171]. The abundance of gastric CAMs is positively correlated with tumour size and lymph node metastasis in gastric carcinoma [172]. Additionally, inflammatory cells (e.g. lymphocytes, macrophages, dendritic cells) are involved in tumour malignancy and suppression of anti-tumour immune response [173]. Endothelial cells and pericytes, also known as perivascular cells or mural cells, coordinate to maintain the normal physiology of vasculature, and also contribute to tumour angiogenesis and metastasis [174].

Distinct profiles of gene expression and proteome in cancer stromal cells from microdissected tissues of colorectal and bladder carcinomas, respectively, have been demonstrated [175, 176]. In addition, miRNA regulated gene expression in stromal cells and its influence on tumour progression has been reported. Some studies have suggested genetic alterations in the tumour stroma such as loss of TP53 gene in prostate cancer stromal cells [177]. However, there is no evidence to suggest this applies to all other cancers.

1.8.1 Cancer-associated myofibroblasts

Cross-talk between CAMs and epithelial cancer cells, termed stromal-epithelial interactions, promotes cancer cell growth and induces malignant transformation [134]. Myofibroblasts, including CAMs, are generally characterised by the presence of mesenchymal surface markers, α-SMA and vimentin, and the absence of cytokeratin, smoothelin and CD31 [178]. Immunochemistry of α-SMA has been commonly used to identify CAMs, which are an abundant stromal cell type in epithelial tumours. A recent proteomic study has demonstrated differential expression of secreted proteins in gastric CAMs compared to their adjacent non-tumour myofibroblasts (ATMs), and one of these proteins, transforming growth factor, beta-induced (TGFBI), is decreased in CAMs and may be associated with lymph node metastasis [179].

The tumour-promoting properties in myofibroblasts from cancers have been studied widely and the term, cancer-associated fibroblasts, is often used. It is recognised that cancer-associated fibroblasts contain a higher number of myofibroblasts, which contribute to tumour progression, compared to normal fibroblast population [180]. For example, HGF secreted by cancer-associated fibroblasts is involved in oesophageal squamous carcinoma cell invasion [181]. In oesophageal squamous cell carcinoma, paracrine TGF-β signalling from carcinoma cells induces a myofibroblast phenotype in cancer-associated fibroblasts that results in the secretion of vascular endothelial growth factor (VEGF), which promote tumour angiogenesis by inducing endothelial cell migration and proliferation [182].

It has been suggested that CAM population is heterogeneous as studies have demonstrated their origins from: a) resident fibroblasts, b) bone marrow derived MSCs, c) epithelial cells through epithelial-mesenchymal transition (EMT), d) endothelial cells through endothelial-mesenchymal transition and e) pericytes by transdifferentiation [183]. Moreover, a recent study has shown the transformation of adipose tissue derived MSCs that is induced by ovarian cancer-derived exosomes [184].

Post-transcriptional gene regulation by miRNAs in cancer-associated fibroblasts has been studied in various cancers. In endometrial cancer, decreased expression of miR-31 and miR-148a in cancer-associated fibroblasts induces the expression of SATB homeobox 2 (SATB2) and WNT10B, respectively, resulting in increased migration and invasion of cancer cells [185, 186]. In addition, decreased miR-320 expression in stromal fibroblasts of breast cancer regulates the secretome expression in fibroblasts, which in turn, results in tumour growth and invasion [187]. A more recent study has determined miRNA expression profiles in fibroblasts from breast cancer and non-neoplastic fibroblasts, and revealed the signalling pathways associated with target genes of differentially expressed miRNAs [188]. Other analyses include up-regulation of miR-16 and miR-320 in bladder cancer-associated fibroblasts compared to normal bladder fibroblasts [189].

1.8.2 Bone marrow derived mesenchymal stromal cells

Studies using murine models have shown that bone marrow derived MSCs differentiate into CAMs, contributing to tumour growth and progression [190, 191]. It is estimated that 20% to 25% of CAMs in the tumour stroma are derived from the bone marrow, and they exhibit increased expression of cytokines (e.g. Wnt-5a) [192, 193], implicating the contribution of deregulated signalling pathways in carcinogenesis. In addition, differentiation of MSCs into endothelial progenitor cells (EPCs) induces tumour angiogenesis [194] and increased levels of EPCs in the systemic circulation of cancer patients have been detected [195]. MSCs also exhibits anti-immune effect on tumours through suppression of T cells cytotoxicity [196].

1.9 Aims and objectives

The interaction between stromal and tumour cells contributes to malignancy [197], and it is recognised that CAMs, inflammatory cells, endothelial cells and bone marrow derived stromal cells are all involved in promoting tumour growth, angiogenesis and invasion (Figure 1.5).

Myofibroblasts are physiologically important for maintaining tissue homeostasis and for wound healing [68]. However, the transformation of myofibroblasts to CAMs is not clearly understood even though a contribution of cancer cells that induce the distinct phenotype of CAMs has been suggested [198]. Results from the research group have revealed differential expression of mRNA transcripts and secretory proteins in CAMs of gastric and oesophageal carcinomas compared to

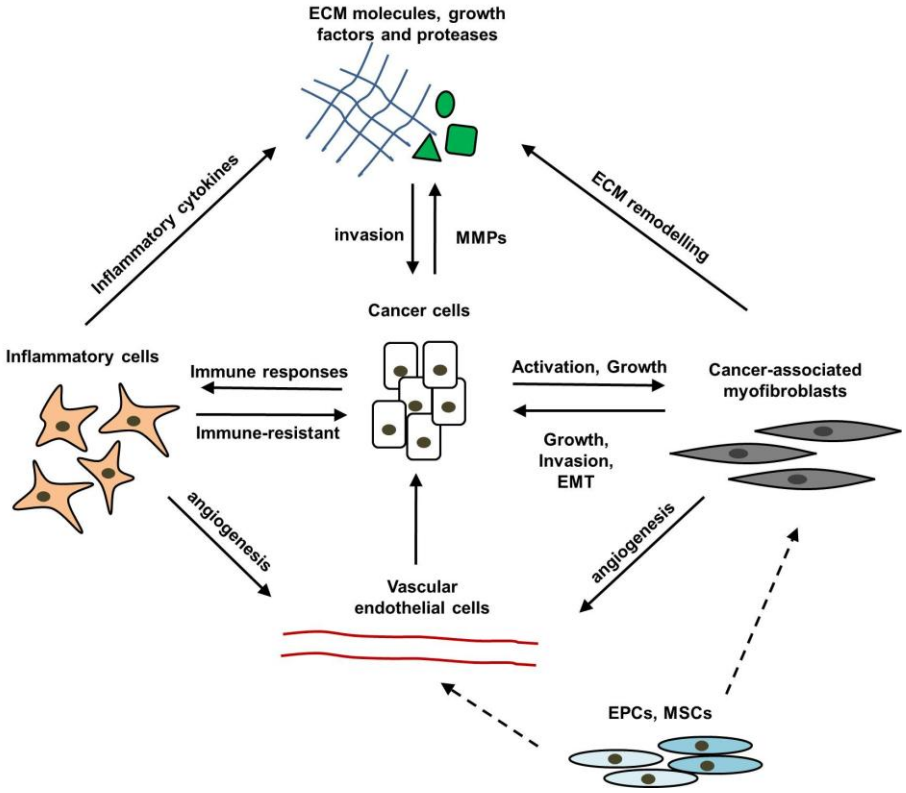

Figure 1.5 Role in cancer growth and progression by the tumour microenvironment. Cancer-associated myofibroblasts, inflammatory cells, endothelial cells, MSCs and ECM constitute the microenvironment that surrounds cancer cells. Interactions between cancer cells and the tumour microenvironment contribute to tumour growth, invasion and metastasis. CAMs, a major component of the microenvironment in many epithelial tumours, secrete cytokines and proteases to induce tumour angiogenesis, EMT, cancer cell growth and invasion. Bone marrow derived MSCs and EPCs may differentiate into CAMs and endothelial cells, respectively.

corresponding ATMs. In addition, it has been shown that there is global DNA hypomethylation in gastric CAMs [149, 193].

Over the last 10 years, miRNA research has become a hot topic in cancer biology. For example, miRNA expression profiling has revealed differential miRNA expression in tumour tissues as well as in serum samples from gastric and oesophageal cancer patients [153]. Nevertheless, the studies of miRNAs in CAMs are still limited. Therefore, the present study aimed to identify the expression of miRNAs that distinguish different populations of myofibroblasts (Figure 1.6) and

to determine the contribution of miRNAs of remodelling the microenvironment of the upper gastrointestinal tract cancers.

The specific objectives for this study were:

1.9.1 To determine the miRNA expression signatures of gastric and oesophageal myofibroblasts, and bone marrow derived MSCs.

1.9.2 To identify miRNA regulatory networks in gastric and oesophageal myofibroblasts.

1.9.3 To investigate the role of canonical and non-canonical Wnt signalling pathways in gastric myofibroblasts and cancer cells.

1.9.4 To demonstrate the biological significance of hsa-miR-181d in gastric CAMs.

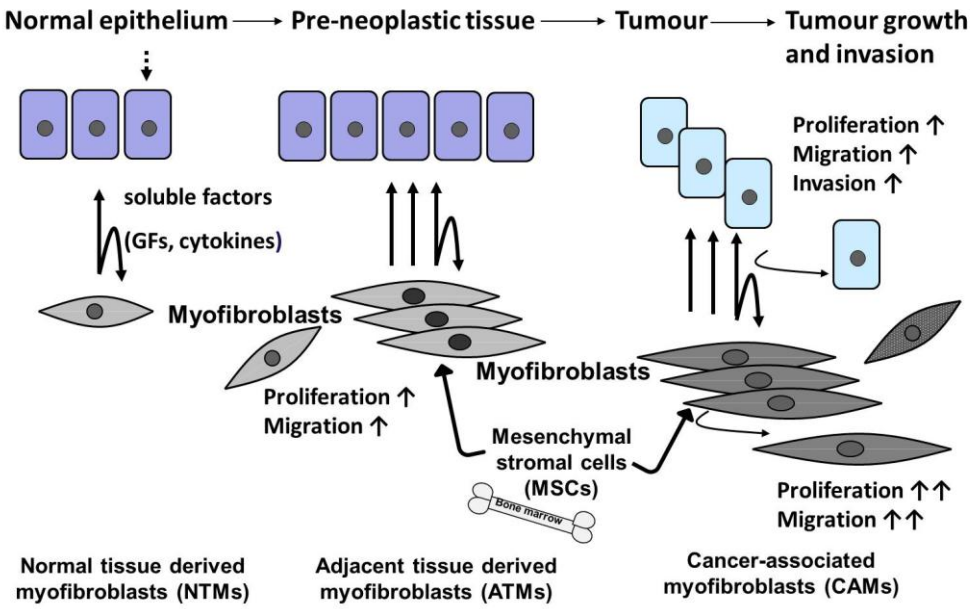

Figure 1.6 Epithelial-stromal interactions in carcinogenesis and cancer progression. In normal mucosa, myofibroblasts (NTMs) are involved in regulating epithelial cell function and in tissue repair via inflammation response. Chronic inflammation induces genetic alterations in epithelial cells that lead to cancer development. Myofibroblasts of pre-neoplastic tissue (ATMs) undergo epigenetic changes and acquire the phenotype of CAMs. Paracrine signalling between cancer cells and CAMs results in cancer cell growth and invasion. Bone marrow derived MSCs play a role in contributing to myofibroblast population.

CHAPTER TWO

Materials and methods

2.1 Materials

Dulbecco modified Eagle's medium (DMEM), 0.25% trypsin-EDTA solution, penicillin-streptomycin (100 U/ml), MEM non-essential amino acid solution 100X, antibiotic-antimycotic Solution, Tween 20 for electrophoresis, N,N,N,N-tetramethylethylene-diamine (TEMED), sodium dodecyl sulphate (SDS) and 10X Tris buffered saline were purchased from Sigma-Aldrich (Poole, UK). The miRNeasy Mini kit, Plasmid Maxi kit, and Cignal TCF/LEF Reporter (luciferase) construct were purchased from Qiagen (Crawley, UK). Phosphate-buffered saline 10X, pH 7.4 (PBS) was obtained from Life Technologies (Paisley, UK) and 10X RIPA lysis buffer was from Merck Millipore (Billerica, MA, USA). Phosphatase inhibitor, cocktail set II and protease inhibitor, cocktail set III were purchased from Calbiochem (La Jolla, CA, USA). Fetal bovine serum (FBS) and the human dermal fibroblast Nucleofector kit were obtained from Lonza (Basel, Switzerland). Prestained protein ladder was obtained from Fermentas (Glen Burnie, MD, USA). Hybond-ECL nitrocellulose membrane was obtained from GE Healthcare Life Sciences (Little Chalfont, UK). Formaldehyde (16% solution microfiltered) was obtained from Agar Scientific (Stansted, UK). Biocoat control inserts (24 well-plate, 0.8 micron) and Falcon 4-well culture slides were obtained from BD (Franklin Lakes, NJ, USA). Protease-free bovine serum albumin (BSA) and normal donkey serum were obtained from Jackson Immuno Research Laboratories (West Grove, PA, USA). Vectashield mounting medium for fluorescence with and without DAPI were purchased from Vector Laboratories (Peterborough, UK). Microscope slides were obtained from Thermo Scientific Gerhard Menzel (Braunschweig, Germany) and cover slips were obtained from Scientific Laboratory Supplies (Hessle, UK). Microscope cover glass (13 mm in

diameter) was obtained from VMR (Darmstadt, Germany). The Click-iT EdU Alexa Fluor 488 Imaging kit was purchased from Invitrogen (Paisley, UK). ImmunStar WesterC kit was purchased from BioRad (Hemel Hempstead, UK). TransFast transfection reagent and Dual-Luciferase Reporter Assay System were obtained from Promega (Southampton, UK). CombiMag was purchased from OZ Biosciences (Marseille, France). Acrylamide (30%) stock solution was obtained from Severn Biotech Ltd (Kidderminster, UK). Tris base was obtained from VWR International BVBA (Leuven, Belgium) and methanol was obtained from Fisher Scientific (Loughborough, UK). All other chemicals were obtained from Sigma-Aldrich.

2.2 Recombinant proteins and antibodies

Monoclonal rat anti-Wnt-5a and recombinant human IGF-II, Wnt-3a, Wnt-5a and TIMP-3 were purchased from R&D Systems (Abingdon, UK). Monoclonal mouse anti-β-catenin was obtained from Cell Signaling Technology (Danvers, MA, USA). Polyclonal rabbit anti-TIMP-3 (C-terminus) was obtained from Merck Millipore (Billerica, MA, USA). Mouse antibody to glyceraldehyde-3-phosphate dehydrogenase (GAPDH) was purchased from Biodesign Int (Memphis, TN, USA). Fluorescein (FITC)-conjugated AffiniPure donkey anti-mouse antibody was obtained from Jackson Immuno Research Laboratories. Goat anti-mouse, and rabbit anti-rat conjugated to horseradish peroxidase were purchased from Sigma-Aldrich. Goat anti-rabbit conjugated to horseradish peroxidase was purchased from Thermo Scientific Pierce Antibodies (Rockford, IL, USA).

2.3 Patients' tissue specimens and ethical approval

Myofibroblasts prepared from the upper gastrointestinal tract tumours and adjacent tissues, at least 5 cm away from the tumour margin, were obtained from the Department of Surgery, University of Szeged, Szeged, Hungary (Tables 2.3.1, 2.3.2) [73]. Normal tissue myofibroblasts were prepared from 6 deceased transplant donors. Written and informed consent from patients had been obtained. Ethics approval was obtained from the Human Investigation Review Board, University of Szeged. Both normal and tumour tissues were confirmed by histopathology [179]. The TNM Classification of Malignant Tumour was applied according to Union for International Cancer Control (www.uicc.org).

2.4 Cell culture

Myofibroblasts were cultured in DMEM supplemented with 10% FBS, 1% penicillin-streptomycin (100 U/ml), 1% MEM non-essential amino acid solution 100X and 1% antibiotic-antimycotic solution. Gastric carcinoma cells, AGS (American Type Culture Collection, Manassas, VA, USA) and MKN45 (RIKEN, Ibaraki, Japan), were cultured in DMEM supplemented with 10% FBS and 1% penicillin-streptomycin (100 U/ml). Cells were incubated in a humidified atmosphere at 37^{o}C and 5% CO_2. Medium was replaced every two days and cells were split at 90% confluence using 0.25% trypsin-EDTA solution. Human MSCs isolated from bone marrow aspirates of healthy donors (Table 2.3.3) were obtained from Lonza (Basel, Switzerland) and PromoCell GmbH (Heidelberg, Germany). Cells were cultured in mesenchymal stem cell basal medium (MSCBM) supplemented with 10% mesenchymal stem cell growth supplement

(MCGS), 2% L-Glutamine and 0.1% GA-1000. Medium was changed every 3 days and cells were split at 90% confluence.

2.5 Total RNA extraction and small RNA quantification

Total RNA was extracted from myofibroblasts and MSCs using the miRNeasy Mini kit according to the manufacturer's protocol. Total RNA concentration, ratios of A260/A280 (i.e. absorbance at 260 nm and 280 nm) and A260/A230 (i.e. absorbance at 260 nm and 230 nm) were determined using a NanoDrop 2000/2000c Spectrophotometer (Thermo Scientific, Camberley, UK). Concentration of total RNA was expressed in µg/µl. The A260/A280 ratio indicates the presence of protein contamination while the A260/A230 ratio indicates the contamination with organic compounds such as phenol; values of ~2.0 and ~1.4, respectively, were considered acceptable for subsequent applications (i.e. microarray). The protocol for small RNA enrichment was provided by the Ambion mirVana miRNA isolation kit (Life Technologies, Paisley, UK). Small RNA and miRNA concentrations in total RNA or enriched samples were assessed using an Agilent 2100 Bioanalyzer with a small RNA kit (Agilent Technologies, Wokingham, UK), and this was performed by Dr Lucille Rainbow.

No.	Patient	Age	Gender	Survival (months)	TNM Staging	Location	Lauren Classification	Adjacent Tissue
1	Sz42	72	M	>47	pT1N0M0	antrum corpus border	medullar (non-Lauren)	intestinal metaplasia, atrophy
2	Sz45	82	M	3	pT4N2M0	antrum	intestinal	intestinal metaplasia, chronic gastritis
3	Sz190	65	F	5	pT4N4M1	antrum corpus border	mixed	chronic gastritis
4	Sz192	49	F	22	pT3N1M0	antrum corpus border	diffuse	chronic gastritis
5	Sz194	76	M	25	pT1N0M0	antrum	intestinal	intestinal metaplasia, chronic gastritis
6	Sz198	77	M	>38	pT2aN0M0	antrum	intestinal	intestinal metaplasia, chronic gastritis
7	Sz268	76	M	15	pT4N2M0	antrum	intestinal	intestinal metaplasia, atrophy, chronic gastritis
8	Sz271	72	M	>34	pT3N1M0	corpus	mixed	chronic gastritis
9	Sz294	84	F	>31	pT3N0M0	antrum corpus border	intestinal	chronic gastritis
10	Sz305	59	F	17	pT3N2M0	antrum and corpus	diffuse	chronic gastritis
11	Sz308	51	M	9	pT1N3M0	antrum corpus border	mixed	chronic gastritis
12	Sz389	67	M	>30	pT3N1M0	antrum	intestinal	chronic gastritis
13	Sz187	39	F	31	pT4N2M0	antrum corpus border	intestinal	no adjacent tissue
14	Sz197	54	M	>45	pT2aN0M0	antrum corpus border	diffuse	no adjacent tissue
15	Sz196	67	M	NA	NA	corpus	NA	NA
16	Sz241	44	F	NA	NA	corpus and antrum	NA	NA
17	Sz246	45	M	NA	NA	corpus and antrum	NA	NA
18	Sz261	52	F	NA	NA	corpus and antrum	NA	NA
19	Sz279	60	M	NA	NA	antrum	NA	NA
20	Sz334	52	F	NA	NA	corpus and antrum	NA	NA
21	Sz351	41	M	NA	NA	corpus and antrum	NA	NA

Table 2.3.1 Characteristics of patients and tissue histology from which gastric myofibroblasts were generated. Identification number, age, gender, post-operative survival (>; alive at the time of submission), TNM staging (p refers to stage given by pathologic examination of a surgical specimen, T describes tumour size, N describes regional lymph node involvement and M describes distant metastasis), tumour location, tumour classification and pathology assessment of adjacent non-tumour tissue of patients 1 to 14 from which gastric CAMs and ATMs were generated. Identification number, age and gender of patients 15 to 21 from which gastric NTMs were generated from normal corpus and antrum tissues.

No.	Patient	Age	Gender	Survival (months)	TNM Staging	Location	Classification	Adjacent Tissue
1	Sz173	72	M	18	pT3N1M0	oesophagus	Barrett adenocarcinoma	Barrett's
2	Sz193	64	M	19	pT2N3M0	cardia	Barrett adenocarcinoma	Barrett's
3	Sz282	70	F	>25	pT3N1M1	cardia	Barrett adenocarcinoma	Barrett's
4	Sz306	56	M	34	pT3N1M0	oesophagus	squamous carcinoma	CIM, PAM (cardia)
5	Sz360	52	M	31	pT3N1M0	oesophagus	squamous carcinoma	normal
6	Sz373	49	M	35	pT2N1M0	oesophagus	squamous carcinoma	GERD
7	Sz467	69	M	14	pT3N1M0	oesophagus	squamous carcinoma	PAM (cardia)
8	Sz241	44	F	NA	NA	oesophagus	NA	NA
9	Sz246	45	M	NA	NA	oesophagus	NA	NA
10	Sz261	52	F	NA	NA	oesophagus	NA	NA
11	Sz279	60	M	NA	NA	oesophagus	NA	NA
12	Sz334	52	F	NA	NA	oesophagus	NA	NA
13	Sz351	41	M	NA	NA	oesophagus	NA	NA

Table 2.3.2 Characteristics of patients and tissue histology from which oesophageal myofibroblasts were generated. Identification number, age, gender, post-operative survival (>; alive at the time of submission), TNM staging (p refers to stage given by pathologic examination of a surgical specimen, T describes tumour size, N describes regional lymph node involvement and M describes distant metastasis), tumour location, tumour classification and pathology assessment of adjacent non-tumour tissue of patients 1 to 7 from which oesophageal CAMs and ATMs were generated. Identification number, age, gender and tissue location of patients 8 to 13 from which oesophageal NTMs were generated.

No.	Donor	Age	Gender	Tissue location	Distributor
1	HMSC-7F3914	21	M	Bone marrow	Lonza
2	HMSC-7F3674	22	F	Bone marrow	Lonza
3	HMSC-7F3753	43	M	Bone marrow	Lonza
4	HMSC-7F3458	36	M	Bone marrow	Lonza
5	HMSC-GF4393	19	M	Bone marrow	Lonza
6	HMSC-PromoCell	64	M	Bone marrow	PromoCell GmbH

Table 2.3.3 Characteristics of six donors from which bone marrow MSCs were obtained. Identification number, age, gender and tissue of six donors from which MSCs were obtained either from Lonza or PromoCell. HMSC represents human mesenchymal stromal cells.

2.6 MicroRNA array profiling

Analysis of total RNA quality and miRNA microarray procedures were performed by "Exiqon Services" (Vedbaek, Denmark). The quality of total RNA was verified by an Agilent 2100 Bioanalyzer with RNA 6000 LapChip kit. A RNA Integrity Number (RIN) indicates integrity of ribosomal peaks and a value greater than 7.0 is considered to indicate a good RNA quality. Total RNA from samples and references were labelled with Hy3™ and Hy5™ fluorescent labels, respectively, using the miRCURY™ LNA Array power labelling kit (Exiqon), according to the procedure described by the manufacturer. A reference sample contained all samples from the same tissue type (i.e. bone marrow, gastric and oesophageal tissues). The Hy3™-labelled samples and a Hy5™-labelled reference RNA sample were mixed pairwise and hybridised to the miRCURY™ LNA Array version 5th Generation (Exiqon), which contains capture probes targeting all miRNAs for human, mouse or rat registered in the miRBase version 14.0 at the Sanger Institute. The hybridisation was performed by using a Tecan HS 4800 hybridisation station (Grodig, Austria) according to the miRCURY™ LNA array manual. After hybridisation, the microarray slides were scanned and stored in an ozone free environment (i.e. ozone level below 2.0 ppb) in order to prevent potential bleaching of the fluorescent dyes. The miRCURY™ LNA array slides were scanned using an Agilent G2565BA Microarray Scanner System (Agilent Technologies, Santa Clara, CA, USA), and image analysis was carried out using the ImaGene 8.0 software (BioDiscovery, Hawthorne, CA, USA). The quantified signals were background corrected (i.e. Normexp with offset value 10) [199] and normalised using the global locally weighted scatterplot smoothing (LOWESS) regression algorithm.

2.7 Data and bioinformatic analysis

Log base 2 of transformed median Hy3/Hy5 ratios were calculated using median signals on capture probe replicates, and the average $\log_2$ median ratios across samples were obtained from Exiqon. The difference in $\log_2$ median ratio (ΔLMR) between sample groups were calculated and subjected to Student t-tests (two-tailed) or ANOVA to find miRNAs that varied significantly, at $p < 0.05$ (Bonferroni-corrected where applicable) across sample groups. The fold-difference is equivalent to 2^ΔLMR. The miRNA data resource was assessed at miRBase (www.mirbase.org) [200]. Principal component analysis (PCA) and hierarchical clustering analysis on miRNA datasets were performed using DNA-Chip Analyzer (dChip) software (www.dchip.org) [201]. Targets of miRNAs that have been validated by experiments were obtained from TarBase [202], miRecords [203] and MetaCore® (GeneGO, St Joseph, MI, USA) databases. Network enrichment analysis of miRNA targets was performed using MetaCore® software. Statistically significant networks were identified, at $p < 0.05$ (FDR 5%). Predicted targets of hsa-miR-181d were retrieved from TargetScan Release 5.1 [204] using a context score below -0.2 for high efficacy targets [205]. Gene expression profiles of gastric myofibroblasts, previously carried out using GeneChip Human Genome U133 Plus 2.0 Array (Affymetrix, High Wycombe, UK) (Appendix 2.1), were used to determine the abundance of transcripts that are targets of hsa-miR-181d and encoded proteins associated with Wnt signalling.

2.8 MicroRNA real-time quantitative reverse transcription PCR analysis

MicroRNA reverse transcription polymerase chain reaction (RT-PCR) analysis was used to verify the miRNA array data and was performed by "Exiqon Services" (Vedbaek, Denmark). For the latter, 50 ng total RNA was reverse transcribed in 10 µl reactions using the miRCURY LNA™ Universal RT microRNA PCR, polyadenylation and cDNA synthesis kit (Exiqon); each sample was processed in triplicate. cDNA was diluted 100 times and 4 µl was used in 10 µl PCR reactions according to the protocol for miRCURY LNA™ Universal RT microRNA PCR. Each miRNA was assayed once by RT-PCR using triplicate per cDNA. The amplification was performed in a LightCycler® 480 Real-Time PCR System (Roche, Basel, Switzerland) in 384-well plates.

MicroRNA real-time RT-PCR analysis was also carried out in-house as part of this project, and made used of total RNA extracted using the Ambion mirVana miRNA Isolation kit (Life Technologies). RNA concentration was determined and 2 µg RNA per sample was reverse transcribed. RT-PCR was carried out using a 7500 real time PCR system (Applied Biosystems, Warrington, UK) and the All-in-One miRNA qRT-PCR Detection kit (GeneCopoeia, Rockville, MD, USA) according to the manufacturer's protocol. Briefly, Poly A polymerase was added to extend the 3' end of miRNAs, and at the same time, an Oligo-dT Adaptor primer reverse transcribed the poly-A miRNAs. The reverse transcribed miRNAs (i.e. cDNA) was diluted at 1:50, and 2 µl was used in 20 µl PCR reactions. Each sample was carried out in triplicate. Mature sequences for miRNA primers were:

5’-AACAUUCAUUGUUGUCGGUGGGU for hsa-miR-181d (MIMAT0002821), 5’-UAGCACCAUUUGAAAUCAGUGUU for hsa-miR-29b (MIMAT0000100), 5’-ACAGCAGGCACAGACAGGCAGU for hsa-miR-214 (MIMAT0000271), 5’-CAGCAGCAAUUCAUGUUUUGAA for hsa-miR-424 (MIMAT0001341) and 5’-UCCCUGAGACCCUUUAACCUGUGA for hsa-miR-125a-5p (MIMAT0000443).

2.9 Data pre-processing

The LightCycler® 480 software was used to determine the Cp value, and to generate amplification and melting curves by Exiqon. LinRegPCR (11.5) software was used to determine the amplification efficiency. The average amplification efficiency was used to correct raw Cp values. Reference miRNAs were analysed for stability using the SLqPCR algorithm which is similar to geNorm, and a selection of the most stable reference miRNAs, namely, hsa-miR-125a-5p, hsa-miR-24 and hsa-miR-22 were used to normalize all measurements on a well-to-well basis.

For in-house analysis, SDS v1.4 software was used to determine the Ct value and product melting curve. The abundance of hsa-miR-181d, hsa-miR-214 or hsa-miR-424 was normalised to hsa-miR-125a-5p abundance in the same sample. Relative miRNA expression was performed using the $2^{-\Delta\Delta Ct}$ method [206].

2.10 MicroRNA knockdown and overexpression

Knockdown of hsa-miR-181d expression was carried out using the miArrest miRNA inhibitor expression clone (GeneCopoeia). Overexpression of hsa-miR-181d was carried out using the miExpress precursor miRNA expression clone of hsa-miR-181d (GeneCopoeia).

2.11 Plasmid amplification and transient nucleofection

The hsa-miR-181d inhibitor and precursor hsa-miR-181d expression clones were amplified and purified by using the Plasmid Maxi kit prior to transfection using an Amaxa Nucleofector and the human dermal fibroblast Nucleofector kit. Briefly, harvested cells (500,000 cells per nucleofection) were centrifuged at 200 g for 10 min (4^{o}C). The cell pellet per nucleofection sample was resuspended in 100 µl human dermal fibroblast Nucleofector solution, and added with 3 µg DNA plasmid. The sample was transferred to an Amaxa certified cuvette and Nucleofector program U-23 was selected. After nucleofection, 500 µl pre-warmed supplemented DMEM was added to the sample and it was placed in a culture flask or 6-well plate containing supplemented DMEM. Cells were incubated in a humidified atmosphere at 37^{o}C and 5% CO_2 for 24 h before replacing with a fresh medium. Cells were used for further studies after 48 h post-transfection.

2.12 SDS-polyacrylamide gel electrophoresis and Western blot analysis

Gastric myofibroblasts or carcinoma cells were washed twice using PBS and lysed using 100 µl RIPA lysis buffer containing 1% protease inhibitor and 1% phosphatase inhibitor. Cell lysates were sonicated for 5 min, kept in ice for 30 min, and then centrifuged for 3 min at 12,000 g (4^{o}C). Supernatants were collected and stored at -80^{o}C until required. Protein quantification was carried out using the Pierce BCA Protein Assay kit (Thermo Scientific). The 10% resolving gel consisted of 8.25 ml acrylamide, 10 ml distilled water, 6.25 ml 1.5 M Tris-HCl pH 8.8, 0.25 ml 10% (w/v) SDS, 0.125 ml 10% ammonium persulphate and 0.01 ml TEMED. The 4% stacking gel consisted of 1.3 ml acrylamide, 6.1 ml distilled water, 2.5 ml 0.5 M Tris-HCl pH 6.8, 0.1 ml 10% (w/v) SDS, 0.05 ml 10% ammonium persulphate and 0.01 ml TEMED. 5X Running buffer (pH 8.3) consisted of 25 mM Tris base, 192 mM glycine and 0.1% SDS. Protein samples (60 µg) and 5 µl prestained protein ladder were loaded and resolved in gels by running buffer at 100 V for 110 min. After SDS-PAGE, resolving gels were soaked in transfer buffer, which contained glycine, Tris base and methanol, for 5 min and transfer of proteins from gels to nitrocellulose membranes was carried out at 100 V for 1 h. Membranes were washed 3 times for 10 min using 0.1% Tween-20 in Tris buffered saline (TBST), and incubated in blocking buffer (i.e. 5% non-fat milk in TBST) for 1 h. Membranes were incubated overnight with TIMP-3 or Wnt-5a antibody diluted in blocking buffer at 4^{o}C. Next day, membranes were washed 3 times for 10 min using TBST, and incubated in blocking buffer containing goat anti-rabbit or rabbit anti-rat conjugated to horseradish peroxidase for 1 h at room temperature. After 1 h, membranes were washed 3 times for 10 min by using TBST, and incubated with peroxide solution and luminol solution

(1:1) for 5 min. Membranes were exposed and proteins were detected using a ChemiDoc XRS+ with ImageLab software (BioRad). Membranes were re-probed with mouse monoclonal anti-GAPDH. Relative expression levels were determined by ImageLab software, and normalised to the corresponding GAPDH level.

2.13 Immunocytochemistry

Gastric myofibroblasts (60,000 cells per well) and MKN45 cells (80,000 cells per well) were seeded on 4-well culture slides and incubated overnight in supplemented DMEM. Gastric myofibroblasts and MKN45 cells were serum-starved for 24 h and 48 h, respectively and stimulated with 1 µg/ml human recombinant Wnt-3a or Wnt-5a in serum-free DMEM for 60 min. Cells were washed twice using PBS and fixed using 4% paraformaldehyde for 10 min at room temperature. The fixative was removed and cells were washed three times using PBS for 5 min. Fixed cells were covered with ice-cold 100% methanol and incubated at -20^{o}C for 5 min. Cells were then washed using PBS for 5 min and incubated with 5% normal donkey serum in PBS with 0.3% Triton X-100 for 30 min. After that, cells were incubated with β-catenin mouse monoclonal antibody (1:200 dilutions) overnight at 4^{o}C and protected from light. Primary antibody was aspirated and cells were washed sequentially using 0.14 M NaCl, 0.5 M NaCl and again 0.14 M NaCl for 5 min each. Cells were incubated with FITC-conjugated donkey anti-mouse antibody diluted in 10 mM HEPES (pH 7.5) for 1 h at room temperature and protected from light. Cells were washed three times using PBS for 10 min and applied with mounting medium for fluorescence containing DAPI.

Cover slips were placed on top of the slides, and the edges were sealed with nail polish. Three independent experiments were performed.

2.14 Assay of proliferating cells using EdU incorporation

Procedures were adapted using the protocol for Click-iT EdU Imaging kit. Gastric myofibroblasts, AGS and MKN45 cells (10,000 cells per well) were seeded and incubated overnight in supplemented DMEM followed by serum starvation for 24 h and 48 h, respectively. Gastric myofibroblasts, AGS and MKN45 cells were incubated in conditioned medium (CM) or serum-free DMEM containing 1 µg/ml recombinant Wnt-3a or Wnt-5a for 24 h, and in the meantime, they were incubated with 10 µM 5-ethynyl-2'-deoxyuridine (EdU) for 24 h and 2 h, respectively. After 24 h incubation, cells were washed twice using PBS and fixed using 4% paraformaldehyde for 30 min at room temperature. The fixative was removed and cells were washed twice using 3% BSA in PBS. Cells were permeabilised using 0.5% Triton X-100 in PBS for 20 min at room temperature and then washed twice using 3% BSA in PBS. Cells per well were incubated with 500 µl Click-iT reaction cocktail, which was prepared according to the manufacturer's protocol, on a shaker for 30 min at room temperature and protected from light. The reaction cocktail was removed and cells were washed using 3% BSA in PBS followed by PBS. For DNA staining, cells were incubated in Hoechst 33342 (2 µg/ml) for 30 min at room temperature and protected from light. Cells were washed twice using PBS and applied with mounting medium for fluorescence without DAPI. Cover slips were placed on the upper surface of the

slides, and the edges were sealed with nail polish. Each experiment was performed in triplicate.

2.15 Microscopy

A Zeiss AxioCam HRM fluorescence microscope (Carl Zeiss, Welwyn Garden City, UK) on 40x objective lens was used to determine the total number of cell nuclei at 10 different fields using the UV (blue) channel. EdU positive nuclei and β-catenin immunofluorescence were identified using the FITC (green) channel. The proportion of proliferating cells was determined by taking the total number of EdU positive nuclei divided by the total number of cell nuclei and expressed as a percentage. The proportion of cells containing nuclear β-catenin was determined by taking the total number of cells with nuclear localisation of β-catenin divided by the total number of cell nuclei and expressed as a percentage.

2.16 Migration assay

The migration of gastric myofibroblasts and AGS cells was studied using 8 μm pore Biocoat control inserts on 24 well-plates. Cells were harvested after incubation with 0.25% trypsin-EDTA Solution for 4 to 8 min, and neutralised with DMEM containing 1% FBS. Cell counts were performed using a haemocytometer. Cell suspensions were diluted in serum-free DMEM such that 500 μl DMEM in each upper chamber contained 10,000 cells. 750 μl CM or serum-free DMEM containing 1 μg/ml recombinant Wnt-3a or Wnt-5a was added to each of the bottom chambers. Cells were incubated for 16 h, and migrated cells were stained

on the lower surface of the membranes using the Reastain Quick-Diff kit (Reagena, Takojantie, Finland). Membranes were removed and placed on microscope slides with immersion oil (Sigma-Aldrich) underneath and covered with cover slips. Cells were visualised and counted from 5 different fields using 10x objective lens and a Zeiss Axiovert25 Microscope. Each experiment was performed in triplicate.

2.17 Magnetofection and luciferase assays

Gastric myofibroblasts (100,000 cells per well) were seeded on 6-well plates and incubated overnight in supplemented DMEM. Transfection solution was prepared according to the manufacturer's protocol, and consisted of 1 µg Cignal TCF/LEF Reporter (luciferase) construct, 6 µl TransFast transfection reagent and 2 µl CombiMag in 500 µl serum-free DMEM. Medium was removed and myofibroblasts were incubated with the transfection solution on a magnetic plate for 20 min at room temperature. The transfection solution was removed and replaced with pre-warmed supplemented DMEM. Myofibroblasts were incubated in a humidified atmosphere at 37^{o}C and 5% CO_2 for 24 h. Myofibroblasts were washed twice using serum-free DMEM and incubated with 1 µg/ml recombinant Wnt-3a or Wnt-5a diluted in serum-free DMEM for 8 h. Myofibroblasts were washed once using PBS and lysed using 500 µl passive lysis buffer on a shaker for 15 min at room temperature. Luciferase assay buffer II and Stop & Glo Reagent were prepared according to the manufacturer's protocol. Activities of firefly luciferase and Renilla luciferase were measured by Dual Luciferase assay using a Lumat LB 9507 tube luminometer (Berthold Technologies, Bad Wildbad,

Germany). Firefly luciferase activity is driven by the promoter of interest and Renilla luciferase activity is the internal control. Data was presented as a ratio of firefly luciferase to Renilla luciferase values. Each experiment was performed in triplicate.

2.18 Statistics

Results were presented as mean ± standard error of the mean. Comparisons were made using Student's t-test or analysis of variance (ANOVA), where appropriate, and were considered significant, at $p < 0.05$.

CHAPTER THREE

MicroRNA expression profiling of myofibroblasts and mesenchymal stromal cells

3.1 Introduction

This work focuses on a group of myofibroblasts that have been generated from gastric and oesophageal cancers, adjacent non-tumour tissues, and normal tissues of the stomach and oesophagus. These cultured primary myofibroblasts have also been studied in detail. Gastric myofibroblasts have been characterised by staining positive for vimentin and α-SMA. They have been shown to express MMP1, MMP2, MMP3 and MMP9, and all TIMP1 to TIMP4 [73]. In addition, gastric myofibroblasts exhibit increased proliferation and migration in response to epithelial-derived MMP7 by activating IGF-II [73]. Furthermore, a recent study has indicated increased rates of proliferation and migration in gastric CAMs compared to ATMs or NTMs [179]. Using methylation-sensitive SNP array analysis, it was found that there is hypomethylation of genomic DNA in gastric CAMs compared to normal myofibroblasts [149]. Microarray and proteomic analyses have also indicated transcriptomes (Steele and Varro, preliminary data) and secretomes [179] of gastric CAMs are significantly different from corresponding ATMs.

In addition, functional characterisation of oesophageal myofibroblasts has been studied recently. For example, there is an increased rate of proliferation in oesophageal CAMs compared to corresponding ATMs and NTMs. Moreover, conditioned medium from oesophageal CAMs increases migration and proliferation of oesophageal cancer cell lines (Kumar and Varro, personal communication).

Changes in miRNA expression have been described in gastric and oesophageal tumours and their pre-neoplastic tissues [153]. Additionally, a recent study using

microdissected tissues has indicated increased expression of oncogenic miRNAs in colorectal cancer stromal tissue compared to normal stromal tissue [207], suggesting there may be altered miRNA expression in myofibroblasts, which are abundant in the tumour stroma. However, the miRNA expression profiles of myofibroblasts from gastric and oesophageal cancers and their counterparts from non-tumour tissues have yet to be determined.

The aims for the work described in this chapter were:

3.1.1 To determine the miRNA expression profiles of upper gastrointestinal tract myofibroblasts and their putative precursors (i.e. bone marrow MSCs).

3.1.2 To characterise differentially abundant miRNAs in myofibroblasts from different pathological conditions.

3.1.3 To compare myofibroblasts and MSCs by applying PCA and hierarchical clustering analysis to global and differential miRNA expression profiles.

3.2 Methods

Gastric and oesophageal myofibroblasts had previously been generated from human tissue specimens, namely, CAMs, ATMs and NTMs [179] (Chapter 2.3). Total RNA of myofibroblasts and MSCs was analysed for RNA concentration, RNA purity and RIN (Appendix 3.2.1). Examples of total RNA profiles which were verified by Agilent 2100 Bioanalyzer are illustrated in Appendix 3.2.2. Small RNA and miRNA concentrations (Appendix 3.2.3), the integrity of small RNAs (6 to 150 nucleotides) (Appendix 3.2.4) and minimal miRNA degradation after six months storage (Appendix 3.2.5) [208] were determined in selected samples. An increase in miRNA concentration in enriched RNA samples (Appendix 3.2.6) was demonstrated using the Ambion mirVana miRNA Isolation Kit.

MicroRNA expression profiling was determined by using locked nucleic acid (LNA) microarrays and the Hy5-reference and Hy3-sample labelling method (Chapter 2.6). Spike-in controls were used to assess the quality of the data from MSCs (Appendix 3.2.7), gastric myofibroblasts (Appendix 3.2.8) and oesophageal myofibroblasts (Appendix 3.2.9). To validate the microarray data, quantitative RT-PCR analysis was performed on specific miRNAs using the LNA Universal RT microRNA PCR or All-in-One miRNA qRT-PCR Detection kit. A single Hy3 channel analysis of miRNA abundance was used to compare arrays from different type of tissues. Dual channel analysis of miRNA abundance was determined using the ratio intensity of Hy3 to Hy5 (i.e. internal control) and was used for inter-array comparisons of the same tissue type. Hierarchical clustering analysis and PCA were performed using dChip software. MicroRNAs that exhibited difference in abundance by $\geq$ 20% or 40%, at $p < 0.05$, were considered significant.

3.3 Results

3.3.1 Global miRNA expression profiles in myofibroblasts and MSCs

Using dual channel analysis (i.e. Hy3 and Hy5), an average of 28%, 25% and 27% of the microarray probes were detected in MSCs (n =6), gastric NTMs (n =12) and oesophageal NTMs (n =6), respectively. From the analysis, it was found that 317, 276 and 300 mature human miRNAs were expressed in all MSCs, all gastric NTMs and all oesophageal NTMs, respectively (Table 3.3.1). When miRNA detection in at least 80% of the samples was taken into account, the number of detected miRNAs in MSCs, gastric NTMs and oesophageal NTMs corresponded to 342, 295 and 320 mature human miRNAs, respectively. Full lists of expressed miRNAs are presented in the appendices: MSCs (Appendix 3.3.1), gastric corpus NTMs (Appendix 3.3.2a), gastric antral NTMs (Appendix 3.3.2b) and oesophageal NTMs (Appendix 3.3.3).

In contrast, a single Hy3 channel analysis of miRNA abundance in all MSCs and all NTMs was used to compare samples from different type of tissues. Using this method, 246, 255 and 248 miRNAs were detected in at least 80% of MSCs, gastric NTMs and oesophageal NTMs, respectively. Of these, 218 miRNAs were expressed in MSCs, gastric and oeosphageal NTMs while 17 miRNAs were expressed in both gastric and oesophageal NTMs, but not in MSCs (Figure 3.3.1). Furthermore, there were small numbers of miRNAs that were detected specifically in MSCs (13 miRNAs), gastric NTMs (11 miRNAs) and oesophageal NTMs (7 miRNAs).

Cell type	Number of common miRNAs	
	100% of samples	>80% of samples
MSC (n = 6)	317	342
Gastric corpus NTM (n = 6)	278	298
Gastric antral NTM (n = 6)	291	301
Gastric NTM (n = 12)	276	295
Oesophageal NTM (n = 6)	300	320

Table 3.3.1 Numbers of miRNAs expressed in at least 80% of MSCs, gastric NTMs or oesophageal NTMs using dual channel microarray analysis.

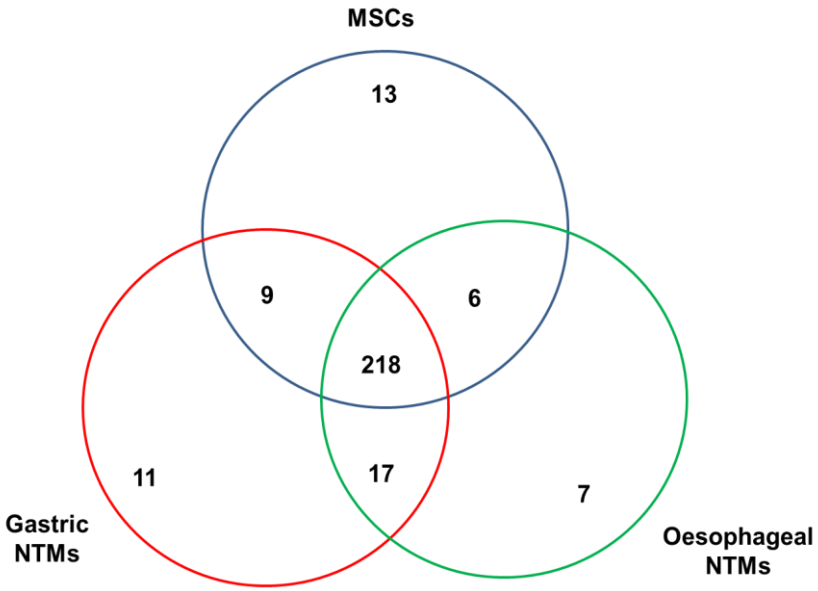

Figure 3.3.1 Numbers of miRNAs expressed in at least 80% of all MSCs, all gastric NTMs and all oesophageal NTMs using a single Hy3 channel microarray analysis.

3.3.2 Validation of miRNA expression using quantitative RT-PCR

To validate the microarray data, RT-PCR analysis was used to measure the abundance of hsa-miR-29b, hsa-miR-214 and hsa-miR-424. These miRNAs were selected because they were highly expressed in all MSCs, gastric and oesophageal myofibroblasts, but also exhibited differential expression in cancer (as described later).

Consistent with the microarray data, RT-PCR analysis showed that the abundance of hsa-miR-29b was significantly (ANOVA $p < 0.001$, compared to MSCs) increased in gastric CAMs, ATMs and NTMs (Figure 3.3.2A). When comparing each myofibroblast sample to the mean of MSCs, a similar trend was obtained, with relative abundance of hsa-miR-29b greater than 1.0 in most of the gastric samples (Figure 3.3.2B). A scatter plot indicated a positive correlation (correlation coefficient = 0.901) between microarray and PCR analyses (Figure 3.3.2C).

On the other hand, both microarray and RT-PCR analyses showed the abundance of hsa-miR-214 was significantly (ANOVA $p < 0.001$, compared to MSCs) decreased in all oesophageal CAMs, ATMs and NTMs (Figure 3.3.3A). When each oesophageal sample was compared to the mean of MSCs, the relative abundance of hsa-miR-214 was less than 1.0 in all oesophageal samples (Figure 3.3.3B). Again, a significant correlation (correlation coefficient = 0.685) between microarray and PCR analyses was found (Figure 3.3.3C).

A

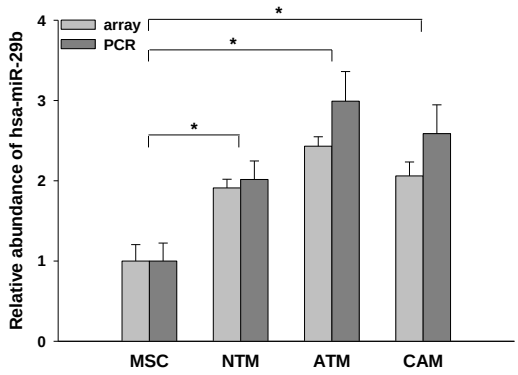

B

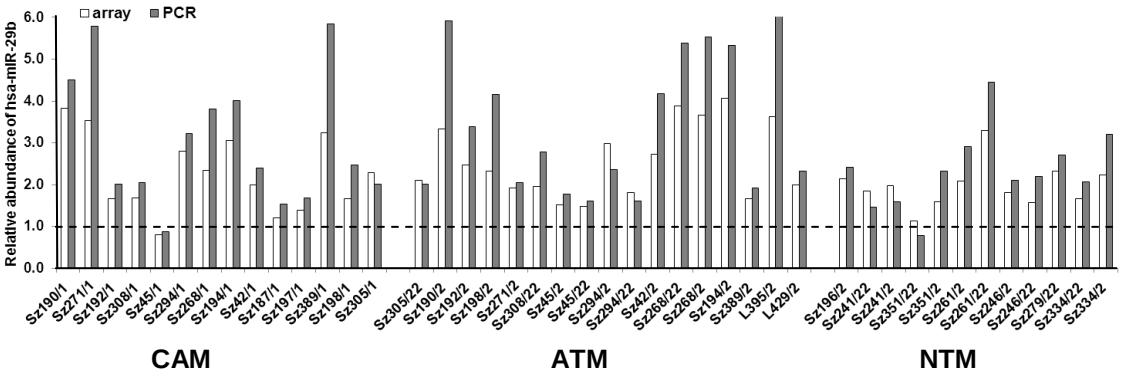

C

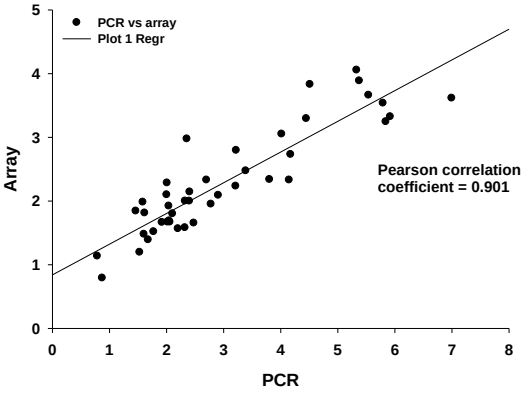

Figure 3.3.2 Validation of hsa-miR-29b abundance in gastric myofibroblasts compared to MSCs. (A) The abundance of hsa-miR-29b in gastric CAMs, ATMs and NTMs was determined by array and RT-PCR analyses (ANOVA $p < 0.001$, compared to MSCs). Values represent the mean of all relevant samples. (B) The abundance of hsa-miR-29b in each gastric CAM, ATM or NTM compared to MSCs (n=6, mean abundance = 1.0) was determined by array and RT-PCR analyses. (C) A scatter plot of PCR versus array (n = 43) reveals a Pearson correlation coefficient of 0.901 at $p < 0.05$. (*$p < 0.05$)

A

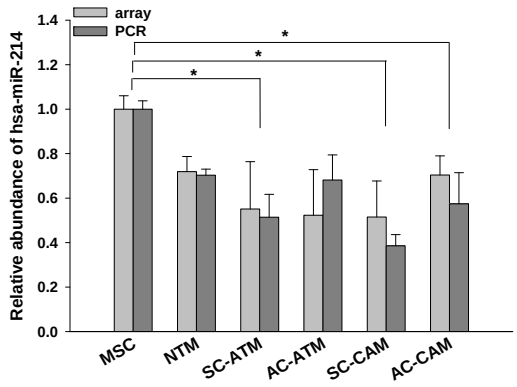

B

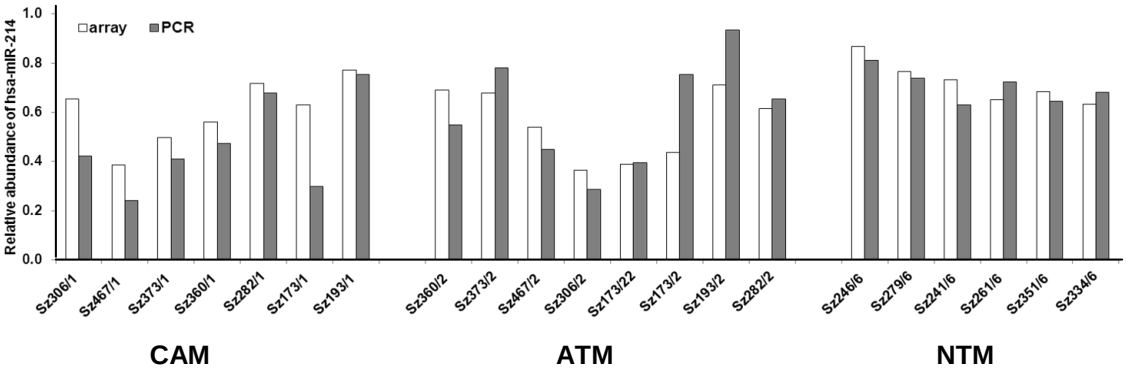

C

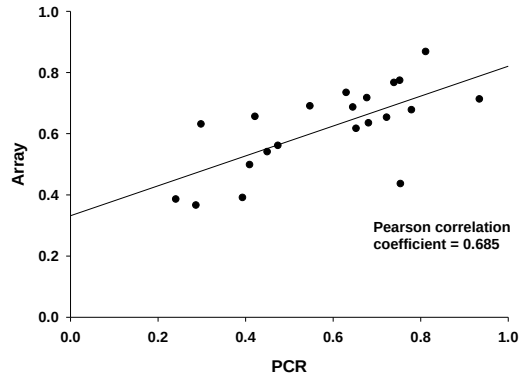

Figure 3.3.3 Validation of hsa-miR-214 abundance in oesophageal myofibroblasts compared to MSCs. (A) The abundance of hsa-miR-214 in oesophageal SC-CAMs, AC-CAMs, SC-ATMs, AC-ATMs and NTMs was determined by array and RT-PCR analyses (ANOVA $p < 0.001$, compared to MSCs). Values represent the mean of all relevant samples. (B) The abundance of hsa-miR-214 in each oesophageal CAM, ATM or NTM compared to MSCs (n=6, mean abundance = 1.0) was determined by array and RT-PCR analyses. (C) A scatter plot of PCR versus array (n = 21) reveals a Pearson correlation coefficient of 0.685 at $p < 0.05$. (*$p < 0.05$)

In the third example, the abundance of hsa-miR-424 was significantly (ANOVA $p < 0.05$, compared to NTMs) decreased in gastric CAMs and ATMs by using microarray and RT-PCR analyses (Figure 3.3.4A). When comparing each sample of CAM and ATM to the mean of NTMs, the relative abundance of hsa-miR-424 was less than 1.0 with just 4 exceptions, namely, Sz42/1, Sz45/1, Sz42/2 and Sz305/22 (Figure 3.3.4B). A scatter plot indicated a positive correlation (correlation coefficient = 0.926) between microarray and PCR analyses (Figure 3.3.4C).

3.3.3 Unsupervised clustering analysis of global miRNA expression

To determine the relations of MSCs, gastric and oesophageal myofibroblasts, single Hy3 channel data of miRNA abundance were analysed by PCA and hierarchical clustering analysis. Distinct clusters of MSCs (n = 6), gastric NTMs (n = 12) and oesophageal NTMs (n = 6) were obtained by PCA (Figure 3.3.5A). When hierarchical clustering analysis was performed on the same set of samples, it was found that gastric NTMs were grouped into one cluster while MSCs and oesophageal NTMs were in the other distinct cluster (Figure 3.3.5B).

The same methodology was then extended to the analysis of MSCs and CAMs from gastric and oesophageal carcinomas. In Figure 3.3.6A, the PCA shows distinct clusters of MSCs (n = 6), gastric CAMs (n = 14), oesophageal squamous cell carcinoma derived CAMs (SC-CAMs, n = 4) and oesophageal adenocarcinoma derived CAMs (AC-CAMs, n = 3). It was noted that SC-CAMs and AC-CAMs were closely associated even though they were clustered separately. When hierarchical clustering analysis was performed, gastric CAMs

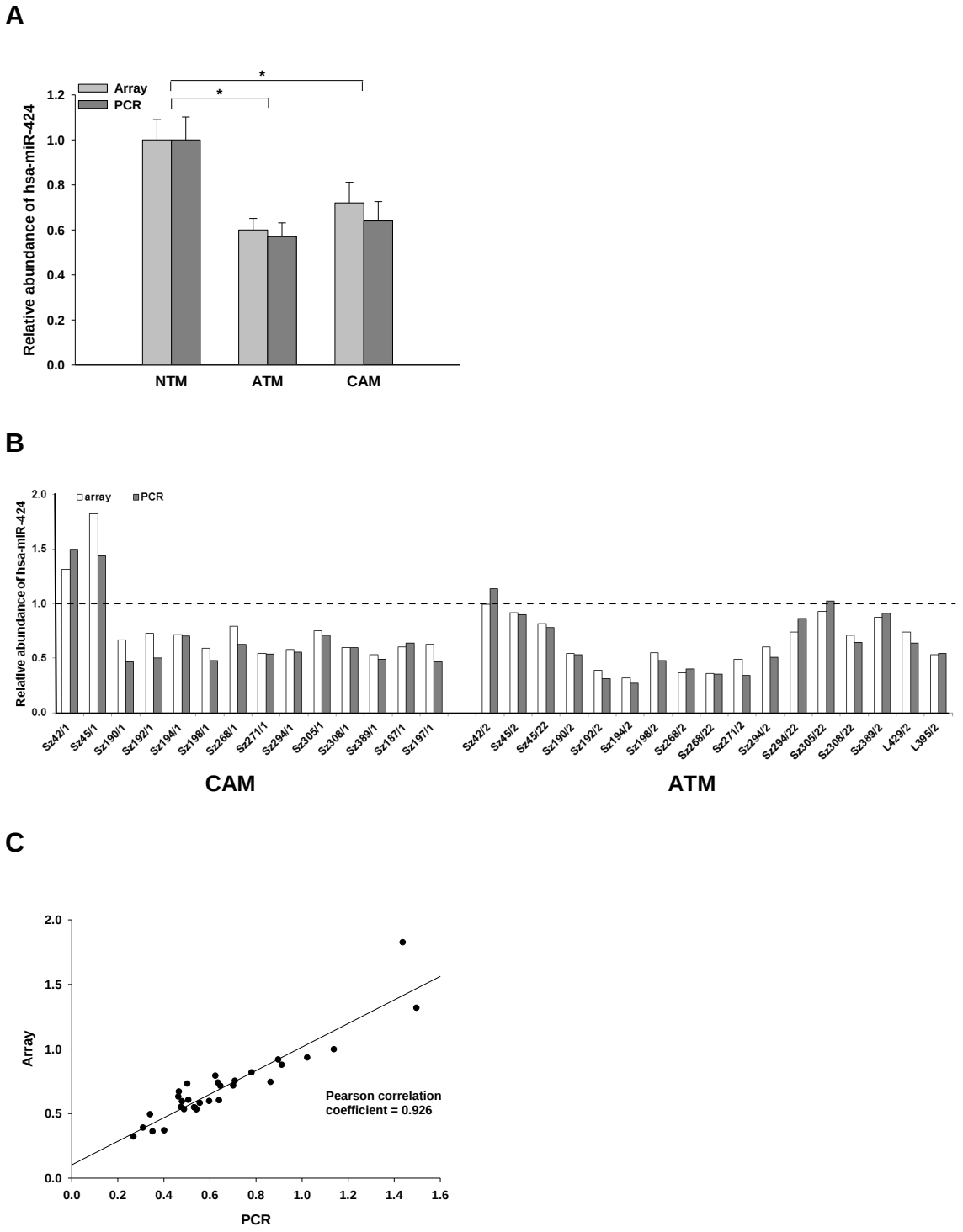

Figure 3.3.4 Validation of hsa-miR-424 abundance in gastric CAMs and ATMs compared to NTMs. (A) The abundance of hsa-miR-424 in gastric CAMs and ATMs was determined by array and RT-PCR analyses (ANOVA $p < 0.05$, compared to NTMs). Values represent the mean of all relevant samples. (B) The abundance of hsa-miR-424 in each gastric CAM or ATM compared to NTMs (n=12, mean abundance = 1.0) was determined by array and RT-PCR analyses. (C) A scatter plot of PCR versus array (n = 31) reveals a Pearson correlation coefficient of 0.926 at $p < 0.05$. (*$p < 0.05$)

A

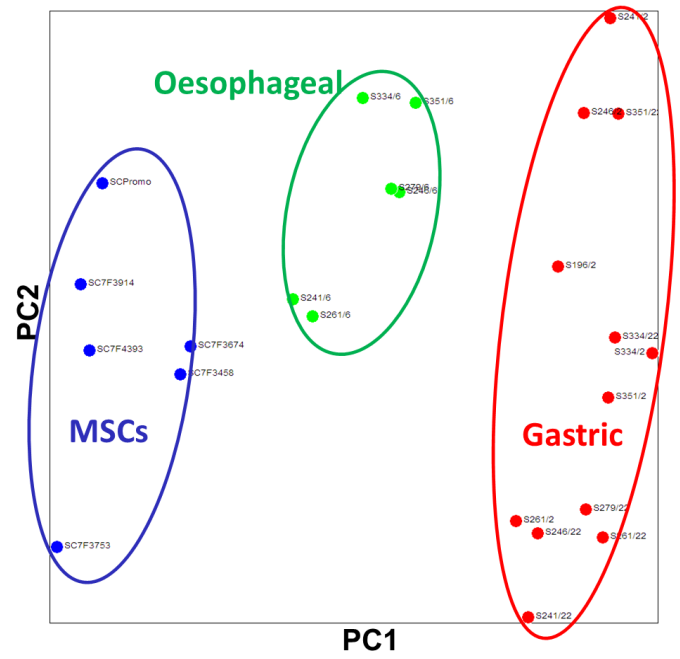

B

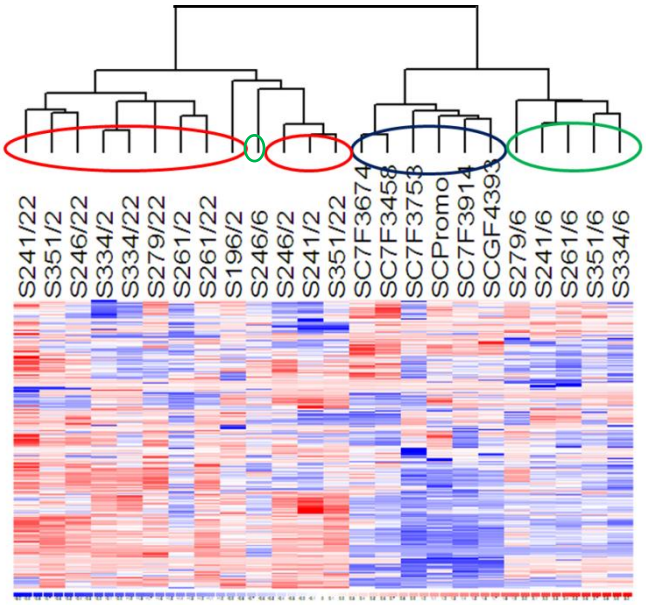

Figure 3.3.5 Distinct global miRNA expression profiles of MSCs and NTMs. (A) Separate clusters of MSCs (blue), oesophageal NTMs (green) and gastric NTMs (red) were determined by PCA. (B) The heat map of gastric NTMs (red), MSCs (blue) and oesophageal NTMs (green) on global miRNA expression. The colour scale below illustrates the relative expression level of a miRNA across all samples: red - expression level above mean; blue - expression level below mean.

A

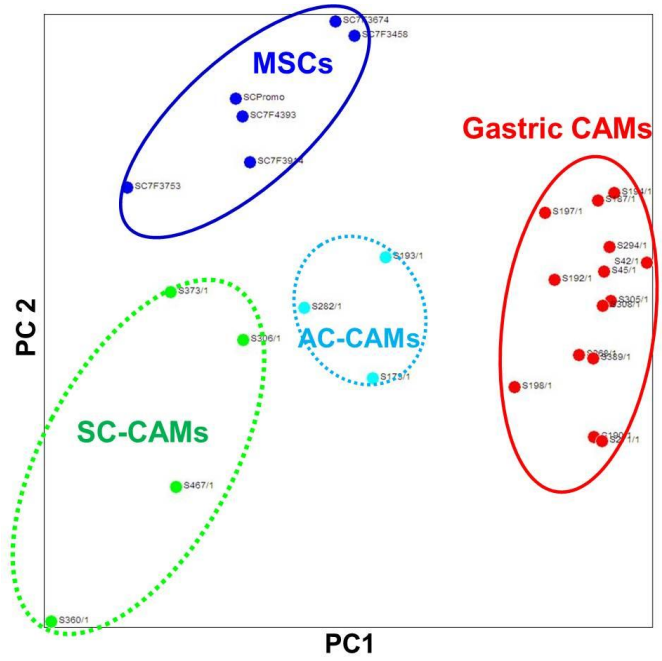

B

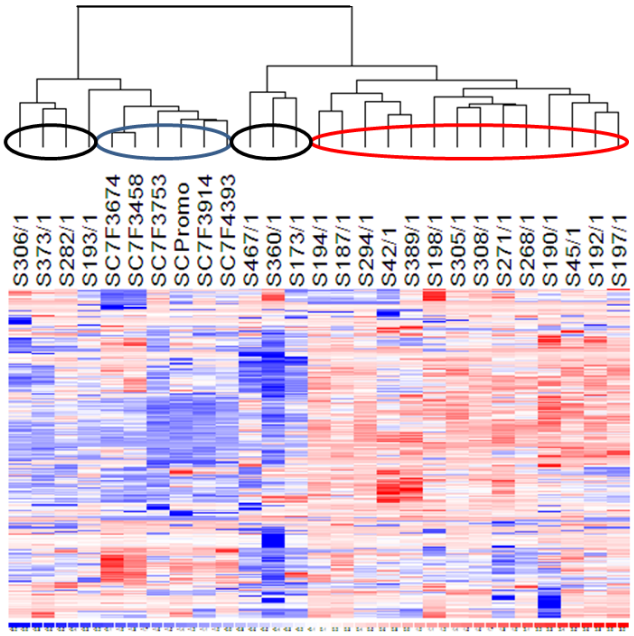

Figure 3.3.6 Distinct global miRNA expression profiles of MSCs, gastric and oesophageal CAMs. (A) Separate clusters of MSCs (blue), gastric CAMs (red), oesophageal SC-CAMs (green) and oesophageal AC-CAMs (light blue) were determined by PCA. (B) The heat map of MSCs (blue), oesophageal CAMs (black) and gastric CAMs (red) on global miRNA expression. The colour scale below illustrates the relative expression level of a miRNA across all samples: red - expression level above mean; blue - expression level below mean.

and MSCs were in two separate clusters, whereas oesophageal CAMs were found in both clusters (Figure 3.3.6B).

3.3.4 Frequency distribution of miRNA abundance in MSCs and myofibroblasts

After analysing global miRNA profiles of MSCs and myofibroblasts, the next step was to identify miRNAs that distinguish different populations. Using miRNA abundance from single Hy3 channel data, the frequency of altered miRNA abundance between two populations was plotted into histograms followed by the identification of those miRNAs that exhibited significant difference in abundance. When gastric NTMs were compared to oesophageal NTMs, the frequency of miRNA abundance followed a normal distribution, but a distinct group of 19 miRNAs, which exhibited a difference in abundance by $\geq 40\%$, were significantly different ($p < 0.001$) (Figure 3.3.7A).

When comparing the frequency distribution of miRNA abundance in MSCs relative to gastric NTMs, there were 48 miRNAs that were significantly different in abundance ($p < 0.001$) (Figure 3.3.7B). In addition, there were 9 miRNAs that were significantly different ($p < 0.001$) when MSCs were compared to oesophageal NTMs (Figure 3.3.7C). When miRNA abundance in gastric CAMs was compared to SC-CAMs, a distinct group of 38 miRNAs were significantly up-regulated ($p < 0.001$) (Figure 3.3.7D). The comparison of gastric CAMs and AC-CAMs showed a slight positively skewed distribution, with 13 miRNAs that were significantly up-regulated ($p < 0.001$) in gastric CAMs (Figure 3.3.7E).

Full lists of significantly different miRNAs and their relative abundance from the above comparisons are presented in the appendices: gastric NTMs compared to oesophageal NTMs (Appendix 3.3.4); MSCs compared to gastric NTMs (Appendix 3.3.5); MSCs compared to oesophageal NTMs (Appendix 3.3.6); gastric CAMs compared to SC-CAMs (Appendix 3.3.7) and gastric CAMs compared to AC-CAMs (Appendix 3.3.8).

3.3.5 Differentially abundant miRNAs in myofibroblasts from gastric carcinoma, adjacent non-tumour and normal gastric tissues

The data presented so far indicates myofibroblasts from different tissue microenvironments exhibit distinct miRNA profiles. This analysis was then extended to a comparison of miRNA abundance in gastric CAMs, ATMs and NTMs. Using dual channel microarray analysis, a total of 286 miRNAs was detected in at least 80% of all CAMs, all ATMs and all NTMs (Figure 3.3.8). The number of miRNAs which were detected specifically in gastric CAMs, ATMs and NTMs were 0, 5 and 1, respectively.

The frequency of miRNA abundance in 12 gastric CAMs compared to their corresponding ATMs followed a normal distribution (Figure 3.3.9A). A relatively small subset of 12 miRNAs exhibited a significant (paired t-test, $p < 0.05$) difference in abundance by $\geq 20\%$ (Table 3.3.2A). The less stringent criterion compared to the previous 40% cut-off was applied due to lower overall variation between CAM and ATM because they were from the same individual, and unlike previously, inter-individual variation was not relevant. The relative

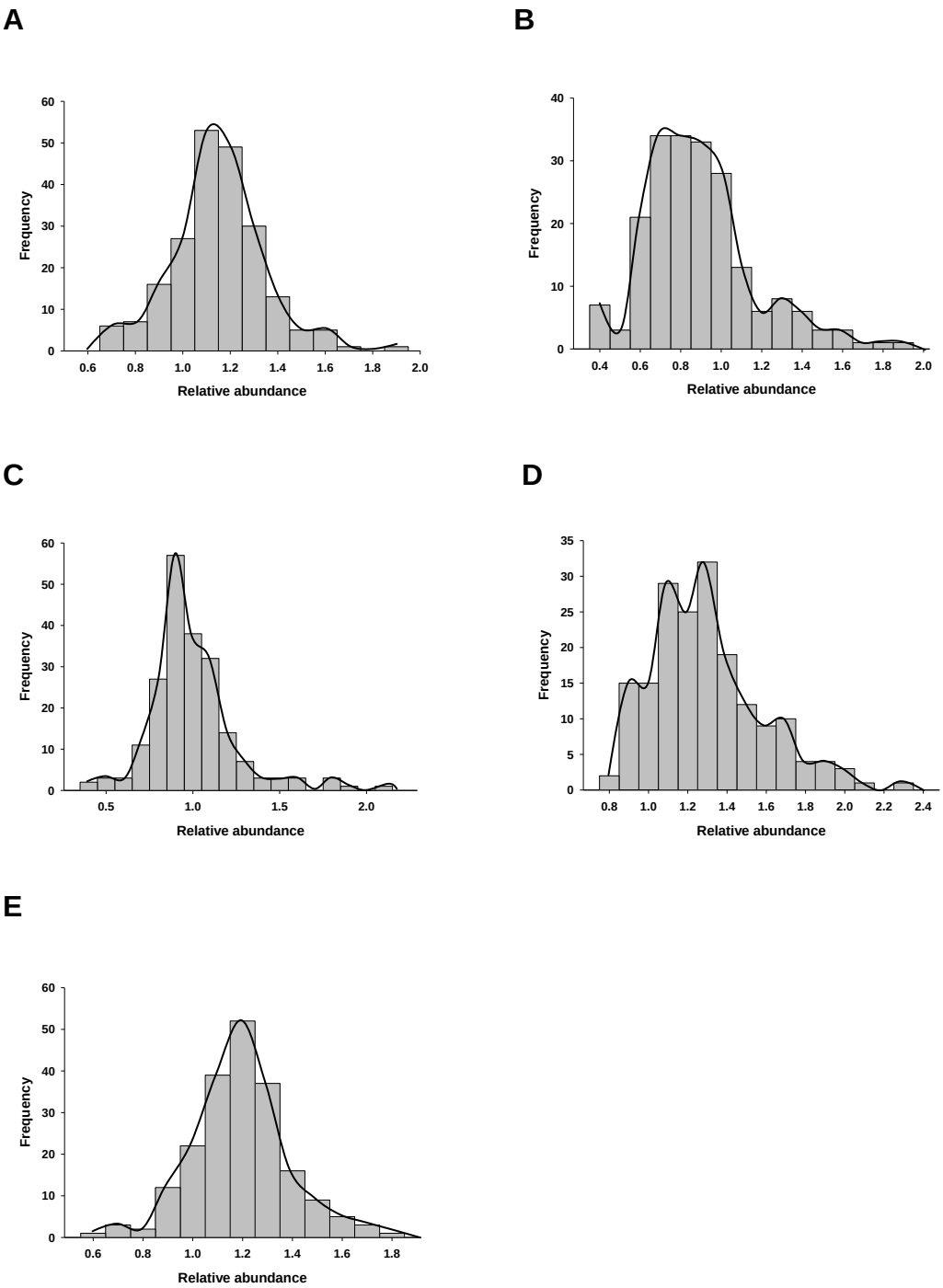

Figure 3.3.7 Using single channel microarray analysis, the frequency distribution of miRNA relative abundance in (A) gastric NTMs compared to oesophageal NTMs; there were 19 differentially abundant miRNAs (≥ 1.4-fold, $p < 0.001$), (B) MSCs compared to gastric NTMs; there were 48 differentially abundant miRNAs (≥ 1.4-fold, $p < 0.001$), (C) MSCs compared to oesophageal NTMs; there were 9 differentially abundant miRNAs (≥ 1.4-fold, $p < 0.001$), (D) gastric CAMs compared to SC-CAMs; there were 38 differentially abundant miRNAs (≥ 1.4-fold, $p < 0.001$) and in (E) gastric CAMs compared to AC-CAMs; there were 13 differentially abundant miRNAs (≥ 1.4-fold, $p < 0.001$).

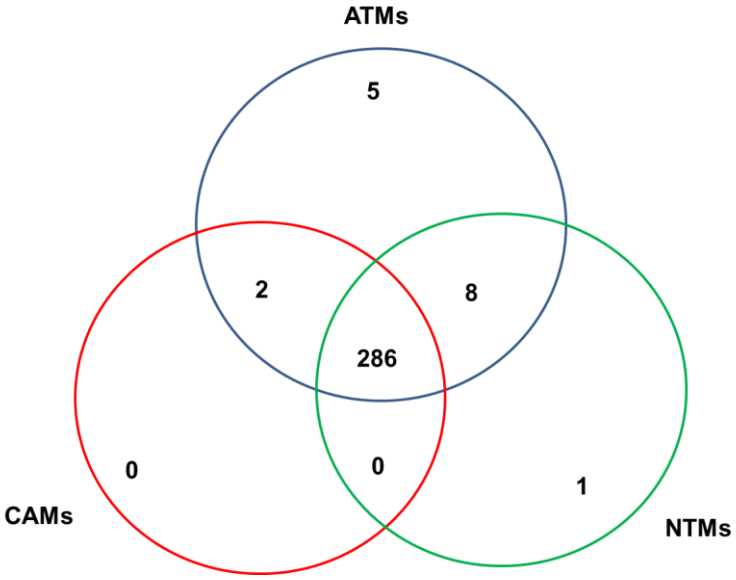

Figure 3.3.8 Numbers of miRNAs that were expressed in at least 80% of gastric NTMs (n = 12), ATMs (n = 17) and CAMs (n = 14) by using dual channel microarray analysis.

abundance of 10 of these miRNAs, which were available in MetaCore® database and were found in all 12 pairs of gastric CAMs and ATMs, are presented in the appendix (3.3.9).

Next, comparisons of miRNA abundance in CAMs and ATMs with NTMs were analysed so as to identify miRNAs that may be altered in the stroma during the early stage of gastric carcinogenesis. The frequency distribution of miRNA abundance in gastric CAMs compared to NTMs showed tails at both sides (Figure 3.3.9B), with 23 miRNAs exhibiting a significant ($p < 0.05$) difference in abundance by $\geq 40\%$ (Table 3.3.2B). Of these miRNAs, 13 miRNAs were down-regulated while 10 miRNAs were up-regulated. When gastric ATMs were compared to NTMs, the frequency of miRNA abundance followed a normal distribution (Figure 3.3.9C), with 16 miRNAs that were significantly different ($p < 0.05$) (Appendix 3.3.10).

3.3.6 Validation of miRNA abundance in gastric CAM comparisons

Pairwise analysis of 12 gastric CAMs compared to their corresponding ATMs showed that hsa-miR-181d exhibited the highest mean difference in abundance (Figure 3.3.10A). Relative abundances of hsa-miR-181d in CAMs of Sz190, Sz192 and Sz268 compared to their respective ATMs were 2.5, 1.5 and 1.1, respectively, and validation using quantitative RT-PCR indicated values of 1.8, 2.3 and 0.9, respectively (Figure 3.3.10B). In addition, both microarray and RT-PCR analyses showed decreased abundance of hsa-miR-214 and hsa-miR-424 in CAMs of Sz192, Sz268 and Sz389, when compared to Sz246 (NTMs) (Figures 3.3.10C, 3.3.10D).

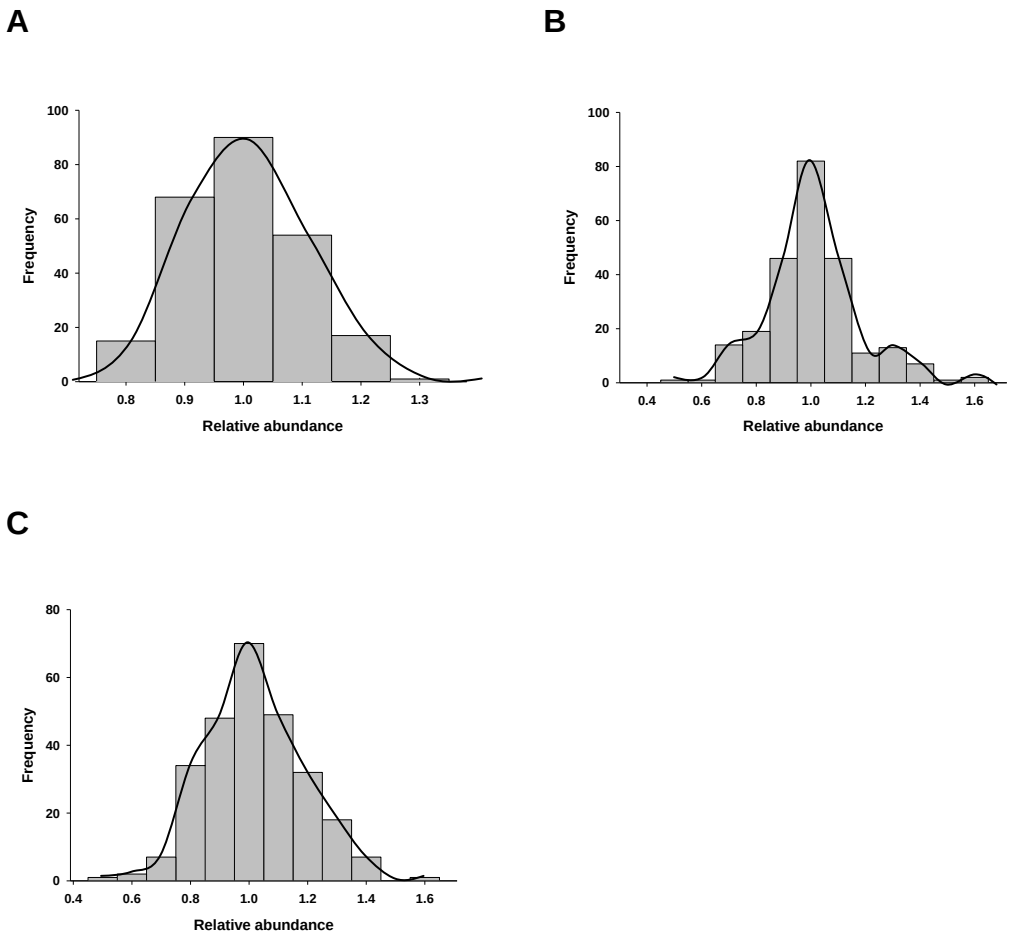

Figure 3.3.9 Using dual channel microarray analysis, the frequency distribution of miRNA relative abundance in (A) gastric CAMs compared to ATMs; there were 12 differentially abundant miRNAs (≥ 1.2-fold, $p < 0.05$), (B) gastric CAMs compared to NTMs; there were 23 differentially abundant miRNAs (≥ 1.4-fold, $p < 0.05$) and in (C) gastric ATMs compared to NTMs; there were 16 differentially abundant miRNAs (≥ 1.4-fold, $p < 0.05$).

No.	Probe Id	Annotation	Relative abundance	p-value
1	46561	hsa-miRPlus-E1168	-1.32	3.34E-02
2	146076	hsa-miR-483-3p	-1.16	2.85E-02
3	145901	hsa-miR-494	-1.16	2.53E-02
4	145740	hsa-miR-625*	-1.16	2.50E-02
5	19582	hsa-miR-106b	1.17	2.57E-02
6	30687	hsa-miR-93	1.18	3.22E-02
7	10936	hsa-miR-130b	1.19	3.91E-02
8	11053	hsa-miR-32	1.20	6.83E-03
9	27720	hsa-miR-15a	1.21	3.96E-02
10	17280	hsa-miR-15b	1.21	3.20E-02
11	13143	hsa-miR-301a	1.21	3.60E-02
12	145636	hsa-miR-181d	1.24	2.71E-02

Table 3.3.2A Relative abundance of significantly different miRNAs in pairwise analysis of gastric CAMs compared to ATMs, at $p < 0.05$ (paired t-test).

No.	Probe Id	Annotation	Relative abundance	p-value
1	146016	hsa-miR-1978	-2.13	9.22E-04
2	145725	hsa-miR-518b	-1.59	1.70E-03
3	146076	hsa-miR-483-3p	-1.52	8.93E-03
4	46749	hsa-miRPlus-E1033	-1.52	6.58E-03
5	42679	hsa-miR-642	-1.49	4.33E-04
6	42641	hsa-miR-145	-1.45	4.43E-02
7	42806	hsa-miR-886-3p	-1.43	1.03E-02
8	46630	hsa-miRPlus-F1064	-1.41	1.09E-03
9	11014	hsa-miR-214	-1.39	5.49E-03
10	42965	hsa-miR-424	-1.39	2.19E-02
11	42513	hsa-miR-300	-1.37	9.86E-04
12	17354	hsa-miR-637	-1.37	4.64E-02
13	46733	hsa-miRPlus-E1117	-1.35	3.08E-03
14	46739	hsa-miR-1308	1.35	6.55E-04
15	46328	hsa-miR-1274b	1.36	8.92E-05
16	21526	hsa-miRPlus-E1031	1.36	2.55E-02
17	46537	hsa-miRPlus-E1038	1.37	2.13E-04
18	10977	hsa-miR-183	1.38	3.35E-02
19	46698	hsa-miR-1280	1.40	9.68E-05
20	42825	hsa-miR-888*	1.42	2.65E-05
21	46732	hsa-miR-1264	1.44	4.18E-05
22	46292	hsa-miR-1274a	1.45	2.33E-03
23	145978	hsa-miRPlus-E1258	1.59	1.47E-04

Table 3.3.2B Relative abundance of significantly different miRNAs in gastric CAMs compared to NTMs, at $p < 0.05$.

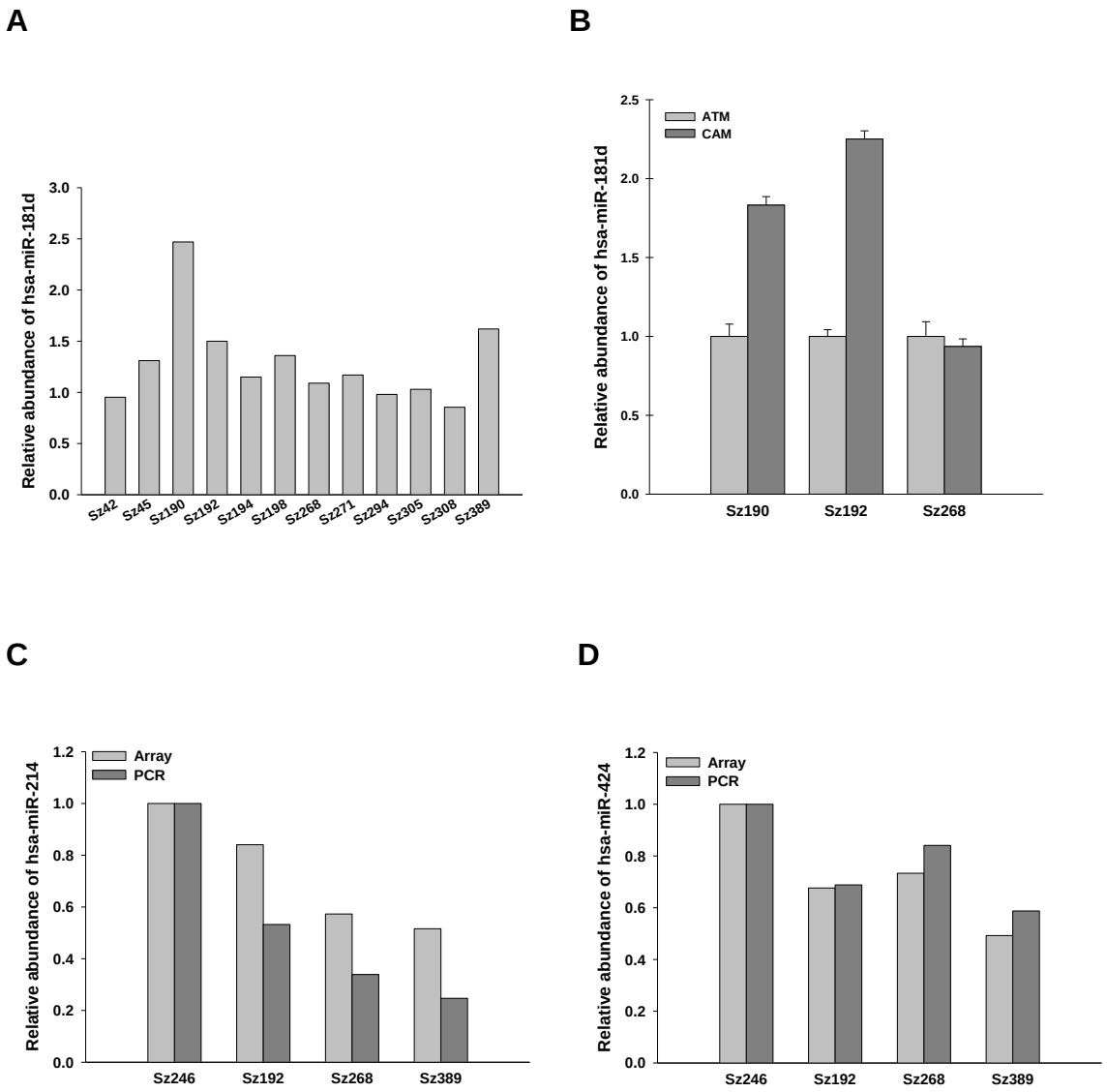

Figure 3.3.10 Abundances of hsa-miR-181d, hsa-miR-214 and hsa-miR-424 in single samples of gastric CAMs compared to ATMs or NTMs were determined by microarray and RT-PCR analyses. (A) The abundance of hsa-miR-181d in individual paired samples of gastric CAMs compared to corresponding ATMs from 12 patients was determined by microarray analysis. (B) An increase in hsa-miR-181d abundance in CAMs of Sz190 and Sz192 compared to corresponding ATMs was confirmed by using RT-PCR. No abundance difference was found in CAMs of Sz268 compared to corresponding ATMs. (C) When compared to Sz246 (NTMs; abundance = 1.0), the abundance of hsa-miR-214 was decreased in CAMs of Sz192, Sz268 and Sz389. (D) When compared to Sz246 (NTMs, abundance = 1.0), the abundance of hsa-miR-424 was decreased in CAMs of Sz192, Sz268 and Sz389.

3.3.7 Differentially abundant miRNAs in myofibroblasts from oesophageal squamous cell carcinoma, adjacent non-tumour and normal oesophageal tissues

The miRNA data analysis of gastric myofibroblasts as described above was then extended to oesophageal myofibroblasts. When SC-CAMs was compared to their adjacent non-tumour tissue derived myofibroblasts (SC-ATMs), the frequency of miRNA abundance showed a positively skewed distribution (Figure 3.3.11A), with 16 miRNAs that were significantly (paired t-test, $p < 0.05$) different between two groups (Appendix 3.3.11). In a comparison of each SC-CAM and corresponding SC-ATM, the relative abundance of 14 of these miRNAs, which were available in MetaCore® database, is indicated in the appendix (3.3.12).

When SC-CAMs were compared to oesophageal NTMs, the frequency of miRNA abundance followed a normal distribution with a small peak at the positive tail (Figure 3.3.11B) and with 18 miRNAs that exhibited significant ($p < 0.05$) difference in abundance (Appendix 3.3.13). Additionally, when SC-ATMs were compared to NTMs, the frequency distribution of miRNA abundance was positively skewed (Figure 3.3.11C), with a total of 26 miRNAs that were significantly ($p < 0.05$) different (Appendix 3.3.14).

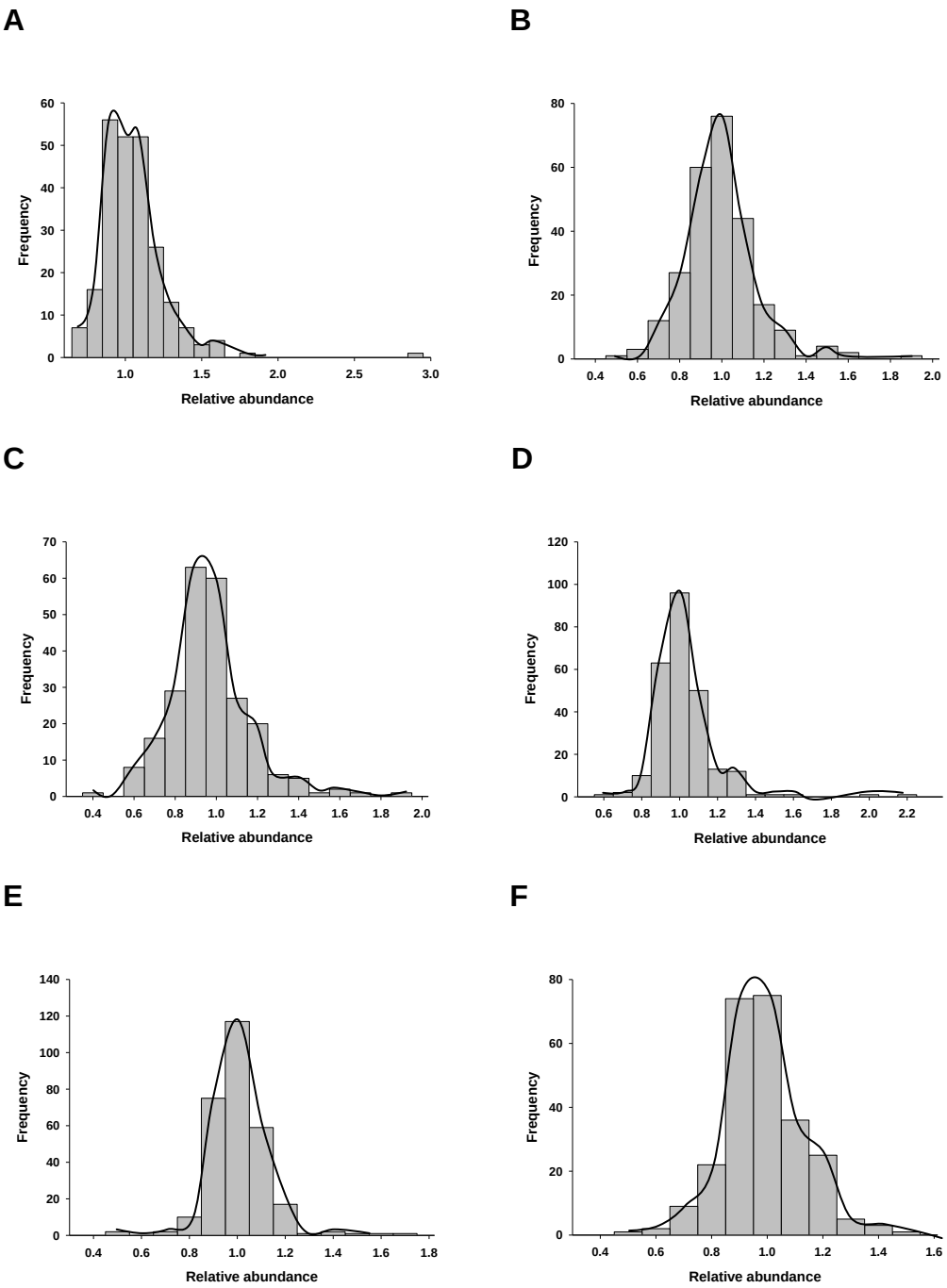

Figure 3.3.11 Using dual channel microarray analysis, the frequency distribution of miRNA relative abundance in (A) SC-CAMs compared to SC-ATMs; there were 16 differentially abundant miRNAs (≥ 1.2-fold, $p < 0.05$), (B) SC-CAMs compared to NTMs; there were 18 differentially abundant miRNAs (≥ 1.4-fold, $p < 0.05$), (C) SC-ATMs compared to NTMs; there were 26 differentially abundant miRNAs (≥ 1.4-fold, $p < 0.05$), (D) AC-CAMs compared to AC-ATMs; there were 5 differentially abundant miRNAs (≥ 1.2 fold, $p < 0.05$), (E) AC-CAMs compared to NTMs; there were 9 differentially abundant miRNAs (≥ 1.2 fold, $p < 0.05$) and in (F) AC-ATMs compared to NTMs; there were 10 differentially abundant miRNAs (≥ 1.4 fold, $p < 0.05$).

3.3.8 Differentially abundant miRNAs in myofibroblasts from oesophageal adenocarcinoma, adjacent non-tumour and normal oesophageal tissues

The comparison of AC-CAMs with adjacent tissue derived myofibroblasts (AC-ATMs) showed the frequency distribution of miRNA abundance was positively skewed (Figure 3.3.11D), with only 5 miRNAs that were significantly different (paired t-test, $p < 0.05$) (Appendix 3.3.15). In a comparison of each AC-CAM and corresponding AC-ATM, the relative abundance of 4 of these miRNAs that were found in MetaCore® is indicated in the appendix (3.3.16).

The frequency of miRNA abundance in AC-CAMs compared to NTMs followed a normal distribution (Figure 3.3.11E). There were 9 miRNAs that exhibited a significant ($p < 0.05$) difference in abundance by ≥ 20% (Appendix 3.3.17). When AC-ATMs were compared to NTMs, the frequency of miRNA abundance showed a slight positively skewed distribution (Figure 3.3.11F), with a group of 10 miRNAs that exhibited a significant difference in abundance by ≥ 40% (Appendix 3.3.18).

3.3.9 Hierarchical clustering analysis of differentially abundant miRNAs

After the identification of differential miRNA abundance in myofibroblasts from cancer, adjacent non-tumour and normal tissues, hierarchical clustering analysis was performed to determine whether these miRNA expression profiles could distinguish myofibroblasts from different types of tissue. Heat maps of differentially abundant miRNAs did not distinguish between gastric CAMs and

ATMs (Figure 3.3.12A), but gastric CAMs (86%) and ATMs (76%) were segregated from NTMs (Figures 3.3.12B, 3.3.12C).

When hierarchical clustering analysis was performed using differential miRNA abundance in oesophageal myofibroblasts, there were distinct clusters between SC-CAMs and SC-ATMs (Figure 3.3.13A), SC-CAMs and NTMs (Figure 3.3.13B), and between SC-ATMs and NTMs (Figure 3.3.13C). Heat maps of differential miRNA abundance, however, could not clearly segregate AC-CAMs from AC-ATMs (Figure 3.3.14A). Distinct clusters between AC-CAMs and NTMs (Figure 3.3.14B), and AC-ATMs and NTMs (Figure 3.3.14C) were shown.

A

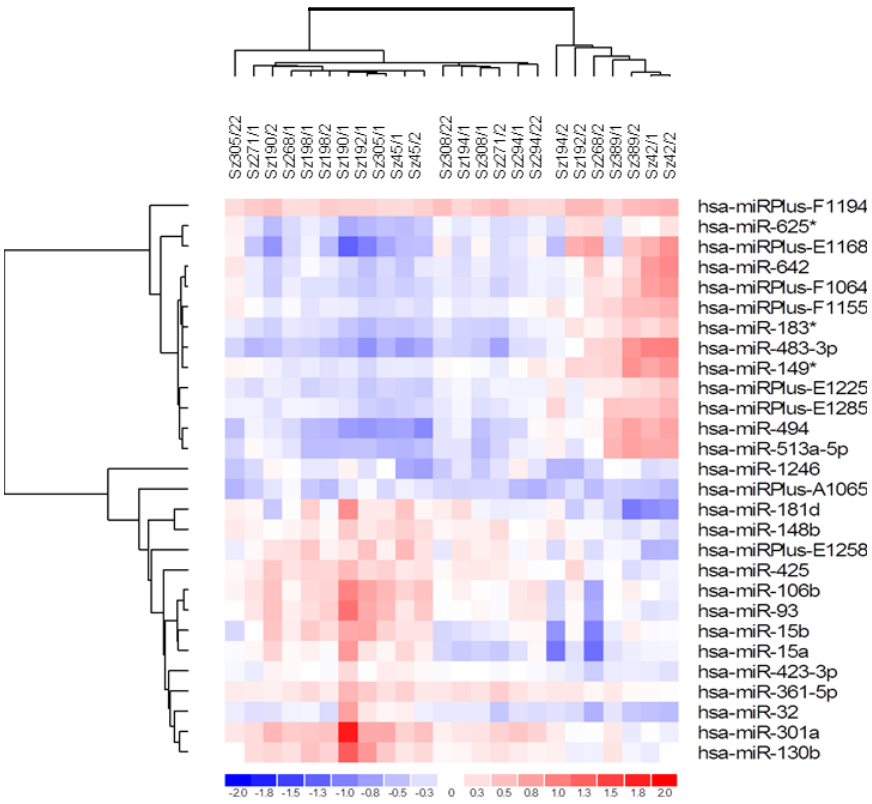
Sz305/22
Sz271/1
Sz190/2
Sz268/1
Sz198/1
Sz196/2
Sz190/1
Sz192/1
Sz305/1
Sz45/1
Sz45/2
Sz308/22
Sz194/1
Sz308/1
Sz271/2
Sz294/1
Sz294/22
Sz194/2
Sz192/2
Sz268/2
Sz389/1
Sz389/2
Sz42/1
Sz42/2
hsa-miRPlus-F1194
hsa-miR-625*
hsa-miRPlus-E1168
hsa-miR-642
hsa-miRPlus-F1064
hsa-miRPlus-F1155
hsa-miR-183*
hsa-miR-483-3p
hsa-miR-149*
hsa-miRPlus-E1225
hsa-miRPlus-E1285
hsa-miR-494
hsa-miR-513a-5p
hsa-miR-1246
hsa-miRPlus-A1065
hsa-miR-181d
hsa-miR-148b
hsa-miRPlus-E1258
hsa-miR-425
hsa-miR-106b
hsa-miR-93
hsa-miR-15b
hsa-miR-15a
hsa-miR-423-3p
hsa-miR-361-5p
hsa-miR-32
hsa-miR-301a
hsa-miR-130b
-2.0 -1.8 -1.5 -1.3 -1.0 -0.8 -0.5 -0.3 0 0.3 0.5 0.8 1.0 1.3 1.5 1.8 2.0

B

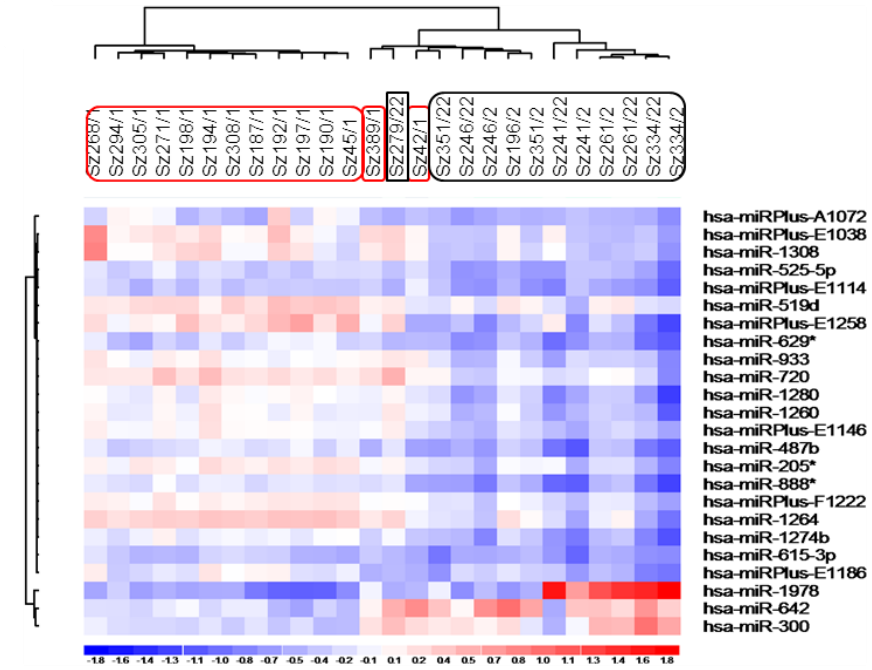
SZ268/1
Sz294/1
Sz305/1
Sz271/1
Sz198/1
Sz194/1
Sz308/1
Sz187/1
Sz192/1
Sz197/1
Sz190/1
Sz45/1
Sz389/1
SZ279/22
Sz42/1
Sz351/22
Sz246/22
Sz246/2
Sz196/2
Sz351/2
Sz241/22
Sz241/2
Sz261/22
Sz334/22
Sz334/2
hsa-miRPlus-A1072
hsa-miRPlus-E1038
hsa-miR-1308
hsa-miR-525-5p
hsa-miRPlus-E1114
hsa-miR-519d
hsa-miRPlus-E1258
hsa-miR-629*
hsa-miR-933
hsa-miR-720
hsa-miR-1280
hsa-miR-1260
hsa-miRPlus-E1146
hsa-miR-487b
hsa-miR-205*
hsa-miR-888*
hsa-miRPlus-F1222
hsa-miR-1264
hsa-miR-1274b
hsa-miR-615-3p
hsa-miRPlus-E1186
hsa-miR-1978
hsa-miR-642
hsa-miR-300
-1.8 -1.6 -1.4 -1.3 -1.1 -1.0 -0.8 -0.7 -0.5 -0.4 -0.2 -0.1 0.1 0.2 0.4 0.5 0.7 0.8 1.0 1.1 1.3 1.4 1.6 1.8

C

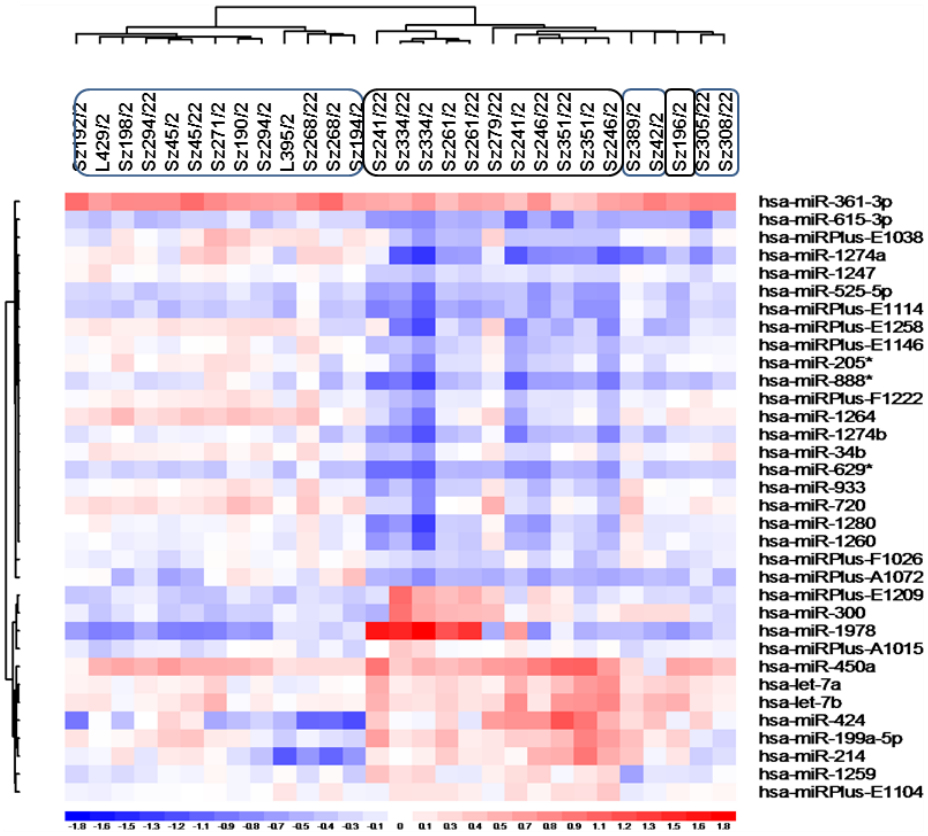

Figure 3.3.12 Two-way hierarchical clustering analysis of significantly different miRNAs in gastric myofibroblasts. (A) The heat map of differential miRNA abundance ($p < 0.05$) in pairwise analysis of gastric CAMs and ATMs. (B) The heat map of differential miRNA abundance ($p < 0.001$) shows segregation of 86% CAMs (red; n = 14) from NTMs (black; n = 12). (C) The heat map of differential miRNA abundance ($p < 0.001$) shows segregation of 76% ATMs (blue; n = 17) from NTMs (black; n = 12). Clusters of differentially abundant miRNAs are shown on the left. The colour scale below illustrates the relative abundance of a miRNA across all samples: red - abundance above mean; blue - abundance below mean.

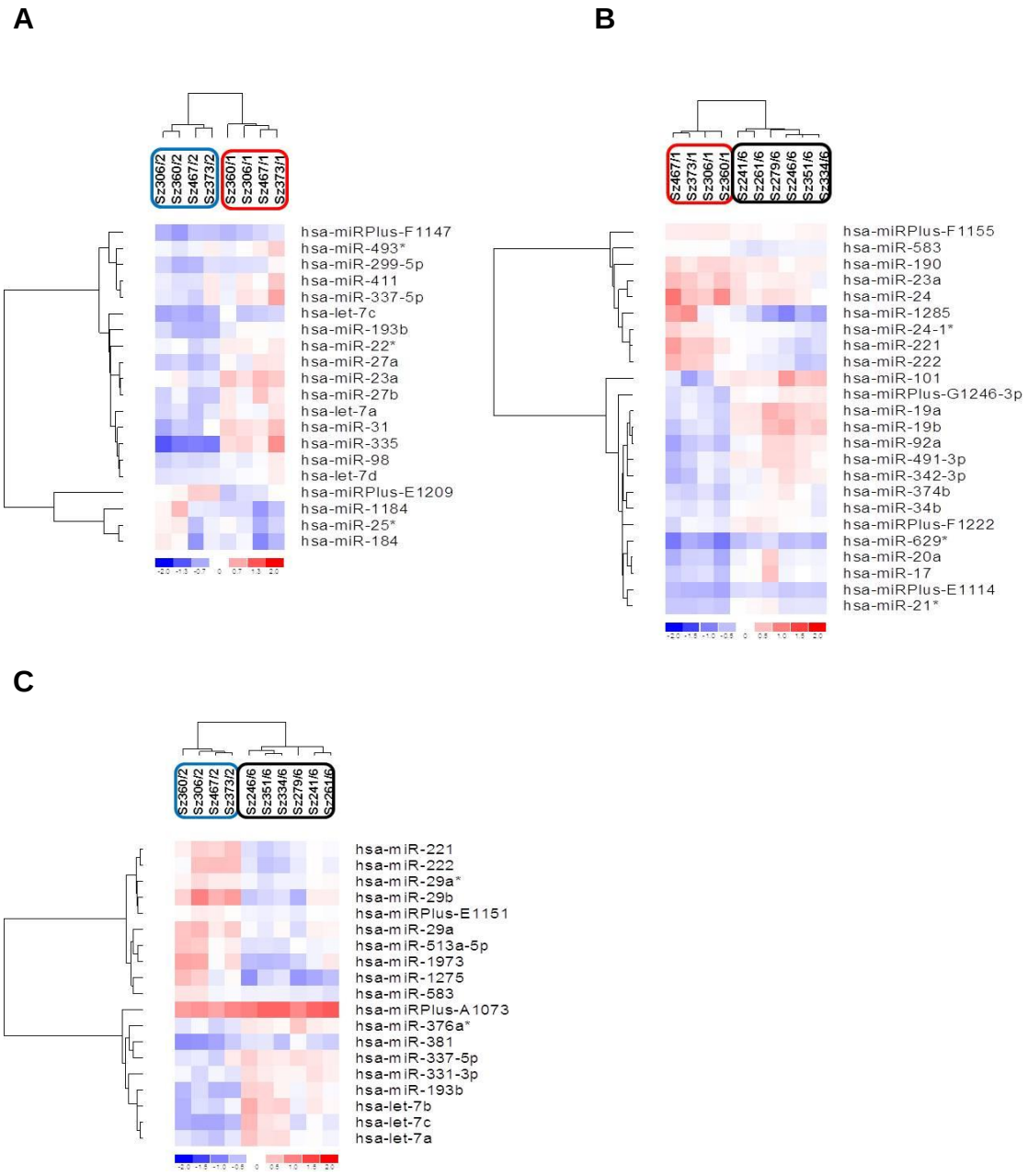

Figure 3.3.13 Two-way hierarchical clustering analysis of significantly different miRNAs in osophageal SC-CAMs, SC-ATMs and NTMs. (A) The heat map of differential miRNA abundance ($p < 0.05$) in pairwise analysis of SC-CAMs (red) and SC-ATMs (blue). (B) The heat map of differential miRNA abundance ($p < 0.01$) shows segregation of SC-CAMs (red) from NTMs (black). (C) The heat map of differential miRNA abundance ($p < 0.01$) shows segregation of SC-ATMs (blue) from NTMs (black). Clusters of differentially abundant miRNAs are shown on the left. The colour scale below illustrates the relative abundance of a miRNA across all samples: red - abundance above mean; blue - abundance below mean.

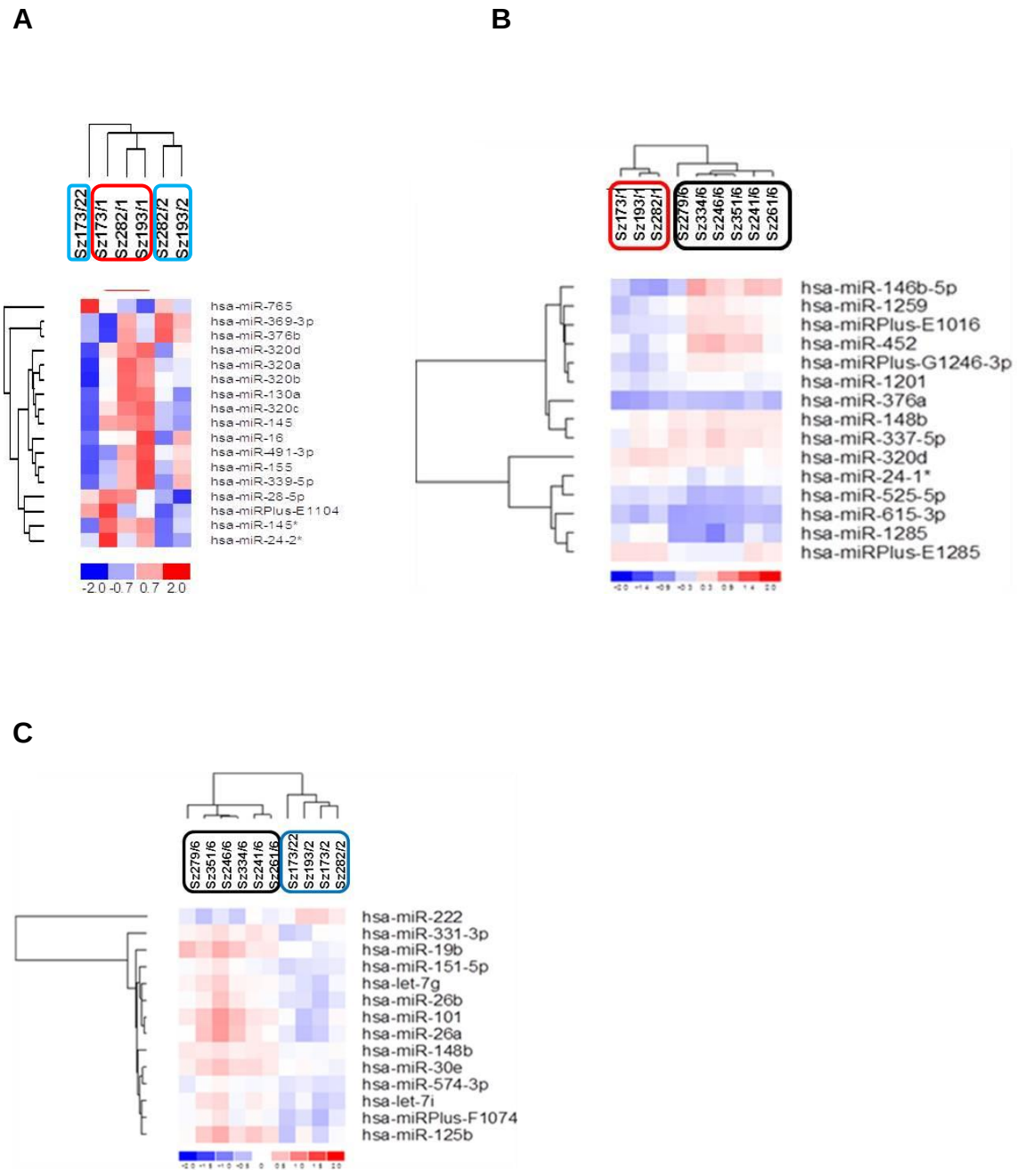

Figure 3.3.14 Two-way hierarchical clustering analysis of significantly different miRNAs in osophageal AC-CAMs, AC-ATMs and NTMs. (A) The heat map of differential miRNA abundance ($p < 0.05$) in pairwise analysis of AC-CAMs (red) and AC-ATMs (blue). (B) The heat map of differential miRNA abundance ($p < 0.05$) shows segregation of AC-CAMs (red) from NTMs (black). (C) The heat map of differential miRNA abundance ($p < 0.01$) shows segregation of AC-ATMs (blue) from NTMs (black). Clusters of differentially abundant miRNAs are shown on the left. The colour scale below illustrates the relative abundance of a miRNA across all samples: red - abundance above mean; blue - abundance below mean.

3.4 Discussion

MicroRNAs are recognised as important regulators of gene expression. However, the study of miRNAs in stromal cells is currently limited. In this chapter, the results showed that: (a) myofibroblasts from different tissue microenvironments exhibit distinct global miRNA expression profiles, (b) miRNA expression of MSCs is distinct from NTMs and that (c) differentially abundant miRNAs distinguish different populations of myofibroblasts. Using pairwise comparison in gastric CAMs and ATMs, miRNA analysis identified 12 miRNAs that were significantly different in abundance, suggesting these miRNAs may contribute to the myofibroblast phenotype during gastric carcinogenesis and progression. Moreover, the comparison of gastric CAMs and NTMs identified a set of 23 differentially abundant miRNAs that may be involved in stromal-induced tumour progression. Additionally, the comparison of gastric ATMs and NTMs revealed a set of 16 miRNAs whose abundance may be altered by chronic inflammation (e.g. *H. pylori* induced inflammation). Although there is a low sample size of oesophageal myofibroblasts, a similar approach has been applied to these samples. Lastly, the microarray data for a set of 4 miRNAs, namely, hsa-miR-181d, hsa-miR-29b, hsa-miR-214 and hsa-miR-424, were validated by quantitative RT-PCR.

The present study used LNA miRNA arrays to determine miRNA expression profiles in MSCs and myofibroblasts. MicroRNA detection may be subjected to poor specificity and low sensitivity (i.e. hybridisation efficiency) due to short nucleotide length and sequence homology in miRNAs, [209]. The development of chemically modified probes, such as LNA-modified oligonucleotides, aims to overcome these problems. Indeed, LNA probes have been used successfully in

applications such as northern blotting [210], *in-situ* hybridization [211], microarray [212] and RT-PCR analysis [213]. Moreover, a comparison of quantitative miRNA expression between LNA microarray and next-generation sequencing indicates there is a higher sensitivity and better correlation between microarray data and RNA content [214].

Besides mature miRNA sequences, there were miRPLUS and miR* sequences on the LNA miRNA array which was used for the present study. A total of 308 miRPLUS sequences from the array were not found in miRBase and MetaCore® databases, but these were considered potentially as functional miRNA sequences. In addition, miR* sequences were thought to be non-functional and in low abundance [200]. It has been suggested that when miRNA duplexes unwind, the mature miRNA strand is incorporated into the RISC while the other strand containing miR* sequence is degraded [215]. As a result, most miRNA studies have focused on the dominant form of miRNA sequences.

The latest version of Exiqon LNA miRNA array contains only 25 miRPLUS sequences, suggesting many miRPLUS sequences have been validated and deposited in miRBase database. In addition, mature miRNA and miR* sequences in miRBase have been renamed as miRNA sequences from the 5' or 3' arms, and one of the two is the miRNA that is predominantly expressed. These amendments suggest rapidly increasing knowledge of miRNAs over the past few years that are attributable to advances in miRNA research tools and increased interest in miRNA research. Despite shortfalls at the time of performing microarray analysis, the results from this study have, nevertheless, characterised miRNA expression profiles previously unknown in MSCs and myofibroblasts.

For miRNA expression analysis, miRNAs that exhibited difference in abundance between group comparisons at $p < 0.05$ across samples were considered significant in the present study. A fold-difference of at least 1.2 or 1.4 was applied to identify differential abundant miRNAs that were distinctly different between group comparisons. The Bonferroni Test was attempted to prevent false positive results, but comparisons between different populations of myofibroblasts failed in this testing. This may not be unexpected, especially in paired samples of myofibroblasts that exhibit genetic similarity.

Hierarchical clustering analysis and PCA are common tools for analysing expression data. Hierarchical clustering analysis classifies samples according to similarities in their expression profiles, and segregates samples into two main clusters followed by sub-clusters. On the other hand, PCA, which can produce two or more clusters, is a mathematical method that contains principal components with the highest variance across samples. Using global miRNA expression profiles, hierarchical clustering analysis revealed an association of MSCs with oesophageal NTMs, but not gastric NTMs, whereas PCA indicated distinct clusters of MSCs, gastric and oesophageal NTMs.

MicroRNAs are involved in many biological processes, and their functions may vary depending on cell types. There are currently no miRNA studies that compare stromal cells from different type of tissues. The present analysis of miRNA abundance identified significant up-regulation of hsa-miR-138-1*, hsa-miR-320d, hsa-miR-301a and hsa-miR-101 in gastric NTMs compared to oesophageal NTMs. Hsa-miR-320d is a member of the miR-320 family which has been found to induce apoptosis in cardiomyocytes [216]. In addition, hsa-miR-301a and hsa-miR-101 are involved in the regulation of immune response in T cells and

macrophages, respectively [217, 218]. The role of these significantly different miRNAs in NTMs has not been determined, but the results suggest myofibroblasts in different tissue microenvironments exhibit different properties that may determine epithelial function in the stomach and oesophagus.

There is emerging evidence indicating that MSCs are a source of myofibroblasts in the tissue stroma during inflammation, wound healing and cancer progression [193, 219]. However, the role of miRNAs in myofibroblast differentiation has not been addressed. When MSCs were compared to gastric and oesophageal NTMs, it was found that hsa-miR-29c was significantly decreased while hsa-miR-140-3p and hsa-miR-15a were significantly increased. The expression of miR-29 and miR-140 has been linked to Wnt signalling in osteoblasts [220] and chondrocytes [221], respectively.

When MSCs were compared to gastric NTMs, hsa-miR-125b was identified as top up-regulated miRNA. Additionally, it was found that hsa-miR-34a was significantly down-regulated in MSCs compared to oesophageal NTMs. Studies have shown that hsa-miR-125b is highly abundant in mouse embryonic stem cells and progenitor cells, and that it is involved in the inhibition of myeloid cell differentiation [222] and cardiomyocyte differentiation [223]. Furthermore, hsa-miR-34a has been shown to induce neuronal differentiation [224, 225], and is associated with the suppression of canonical Wnt signalling [215]. These significantly different miRNAs in MSCs are, therefore, presumably involved in regulating cell differentiation and determining cell fate.

The present study also identified up-regulation of several miRNAs (e.g. hsa-miR-933, hsa-miR-491-3p, hsa-miR-551b, hsa-miR-30d) when gastric CAMs were

compared to CAMs from both subtypes of oesophageal cancer. Hsa-miR-30d has been identified as an oncogene (i.e. oncomiR) that correlated with poor survival in ovarian cancer patients [226]. Additionally, it has been shown that hsa-miR-491-3p functions as a tumour suppressor in colorectal cancer cells by inducing cell apoptosis [227]. However, the role of these miRNAs in stromal cells needs to be investigated.

In reviewing this field, Aprelikova noted cancer-associated fibroblasts from endometrial cancer exhibited differential miRNA expression (e.g. miR-31), and these miRNAs might be important in tumour biology [11]. Using hierarchical clustering analysis, differentially abundant miRNAs in group comparisons could potentially distinguish between CAMs and ATMs, CAMs and NTMs, and between ATMs from NTMs. However, gastric CAMs and ATMs are not clearly distinguished between each other even though gastric CAMs and ATMs are functionally different.

When gastric CAMs were compared to their corresponding ATMs, there were 12 miRNAs that exhibited significant difference in abundance. Hsa-miR-181d was then selected as the miRNA of interest because it exhibited the highest difference in abundance between CAMs and ATMs. Using PCR analysis, validation of hsa-miR-181d was performed in 3 paired samples of gastric CAMs and ATMs. Importantly, up-regulation of miR-181b has been found in cancer-associated fibroblasts of endometrial cancer but no further studies have been carried out [11]. Hsa-miR-181d belongs to the miR-181 family which consists of three other members (i.e. hsa-miR-181a, hsa-miR-181b and hsa-miR-181c). The members exhibit a common seed region and their sequences differ from one another by one nucleotide [228]. Increased expression of miR-181 in hepatocellular cancer stem

cells has been associated with cell migration and invasion [229]. Additionally, an increase in miR-181a expression is correlated with increased sensitivity to foreign antigens in immature T cells, thus implicating the role of miR-181a in regulating adaptive immune response [230].

In the following chapter 4, the regulatory role of differentially abundant miRNAs in different populations of myofibroblasts is investigated.

CHAPTER FOUR

MicroRNA targets and regulatory networks

4.1 Introduction

Many primary studies of miRNAs focus on determining miRNA targets and their biological roles. To help to identify miRNA targets, several computational algorithms (e.g. TargetScan, PicTar, miRanda) have been developed to predict targets. However, predicted targets can differ between programs and the rate of false positives has been shown to be more than 30% [231, 232]. As a result, experimental evidence for identifying true targets of a particular miRNA is essential [233].

Recent developments suggest that a large number of transcripts may be regulated by each miRNA and that the same transcript can be regulated by multiple miRNAs [232, 234]. An integrated analysis of miRNA and gene expression profiles can be used to identify biological processes that are regulated by co-expressed miRNAs. The advantage of this approach is the ability to identify putative downstream mRNA targets by using an inverse correlation with altered miRNA expression [235]. However, this approach could not detect miRNA targets, whose abundance is unchanged at the transcript level but is regulated at the translational level.

An example of recent work relating to miRNAs in stromal cells is studies in prostate cancer-associated fibroblasts, which exhibit decreased expression of miR-15a and miR-16, leading to activation of FGF signalling pathway and increased cancer cell proliferation and migration [236]. In the previous chapter, comparisons between different populations of myofibroblasts, which were generated from tumour, adjacent non-tumour or normal tissues, have identified a set of miRNAs that exhibit significant differences in abundance. To predict the biological functions that are associated with these miRNAs, a network enrichment analysis

was performed using targets of miRNAs that are expressed in myofibroblasts and that have been validated experimentally as targets of a specific miRNA.

The aims for the work described in this chapter were:

4.1.1 To identify targets of miRNAs that exhibited significant differences in abundance in gastric and oesophageal myofibroblasts.

4.1.2 To analyse the abundance of hsa-miR-181d targets in gastric myofibroblasts.

4.1.3 To identify significant networks that are enriched with targets of differentially abundant miRNAs in gastric and oesophageal myofibroblasts.

4.2 Methods

Targets of differentially abundant miRNAs that were previously validated by direct experimental studies, termed here validated targets, were obtained from MetaCore®, TarBase [202] and miRecords [203]. Targets of miR* sequences and a small number of newly identified miRNAs were excluded as work on these miRNAs is too limited. Predicted targets of hsa-miR-181d were obtained from TargetScan 5.1 [204]. The term "network" is used here to describe the extended interactions of proteins that are involved in a particular biological mechanism. Differential analysis of the connectivity of miRNA targets, and other interacting proteins, in a particular functional category, was performed using network enrichment by MetaCore®. Networks that were enriched were considered significant, at $p < 0.05$ (FDR 5%).

Microarray gene expression profiling of myofibroblasts was previously performed in the Liverpool Genome Facility using GeneChip Human Genome U133 Plus 2.0 Arrays (Affymetrix, High Wycombe, UK). The mRNA abundance of putative targets of hsa-miR-181d, TIMP3, NLK and GATA binding protein 6 (GATA6) was analysed. The expression of TIMP3 was determined in gastric myofibroblasts using quantitative RT-PCR (Appendix 2.1) and Western blotting (Chapter 2.12).

4.3 Results

4.3.1 Validated targets of miRNAs that exhibited significant differences in abundance in gastric and oesophageal myofibroblasts

To predict the functional role of miRNAs that distinguish different populations of myofibroblasts, validated targets and chromosomal locations of differentially abundant miRNAs were determined. These miRNAs in gastric and oesophageal myofibroblasts had been determined previously in chapter 3. Using the database from MetaCore®, and occasionally miRecords and TarBase, target genes of significantly different miRNAs in gastric CAMs compared to ATMs (Table 4.3.1), gastric CAMs compared to NTMs (Table 4.3.2), and gastric ATMs compared to NTMs (Table 4.3.3) were identified.

In oesophageal myofibroblasts, target genes of differentially abundant miRNAs in oesophageal SC-CAMs compared to SC-ATMs (Table 4.3.4), oesophageal SC-CAMs compared to NTMs (Table 4.3.5), and oesophageal SC-ATMs compared to NTMs (Table 4.3.6) were identified. Similarly, target genes of differentially abundant miRNAs were identified in AC-CAMs compared to AC-ATMs (Table 4.3.7), AC-CAMs compared to NTMs (Table 4.3.8), and AC-ATMs compared to NTMs (Table 4.3.9). Validated targets of miRNAs that are listed in all these tables were subsequently used in the network analysis.

No.	Probe Id	Annotation	Relative abundance	p-value	Chromosomal location	Target genes
1	145740	hsa-miR-625*	-1.17	2.50E-02		
2	145901	hsa-miR-494	-1.17	2.53E-02	14q32.31	CDK6, PTEN, FGFR2, LIF, BIRC5, CAMK2D
3	146076	hsa-miR-483-3p	-1.17	2.85E-02	11p15.5	PUMA, CTNNB1, ASH2L, SOCS3
4	19582	hsa-miR-106b	1.17	2.57E-02	7q22.1	VEGFA, ITCH, CDKN1A, E2F1, APP, PCAF, MAPK14, TGFBR2, NCOA3, STAT3
5	30687	hsa-miR-93	1.18	3.22E-02	7q22.1	CDKN1A, E2F1, VEGFA, ESR1, ITGB8, P53DINP1A, MICA, SP1, TGFBR2
6	10936	hsa-miR-130b	1.19	3.91E-02	22	RUNX3, P53DINP1A, PPARG, CSF1
7	11053	hsa-miR-32	1.20	6.83E-03	9q31.3	FXR1, E2F1, PCAF, BCL2L11
8	13143	hsa-miR-301a	1.21	3.60E-02	19q32	ESR1, MOX2, SERPINE1, PUMA, PTEN, FOXF2
9	27720	hsa-miR-15a	1.21	3.96E-02	13q14.2	BCL2, CCND1, CADM1, VEGFA, BMI1, MYB, DMTF1, WNT3A, CSE1L, FGFR1, IGF1R, MCM5, AKT3, MYB, CDC25A, CDK4, CHEK1
10	17280	hsa-miR-15b	1.21	3.20E-02	3q25.33	BCL2, RECK, CCNE1, MKK4, MAP2K4
11	145636	hsa-miR-181d	1.24	2.71E-02	19p13.13	NLK, CDX2, GATA6, BCL2, TIMP3, VSNL1, TCL1A, PLAG1, KRAS, IL2, GRIA2, CYLD, CDKN1B, AICDA, NOTCH4, RASSF1A, CDKN1B, PROX1, KPNA4

Table 4.3.1 Relative abundance, chromosomal location and validated targets of differentially abundant miRNAs in pairwise analysis of gastric CAMs compared to ATMs. No data available at the time of analysis is indicated by shading in grey.

No.	Probe Id	Annotation	Relative abundance	p-value	Chromosomal location	Target genes
1	146016	hsa-miR-1978	-2.13	9.22E-04		
2	145725	hsa-miR-518b	-1.59	1.70E-03	19q13.42	
3	146076	hsa-miR-483-3p	-1.51	8.93E-03	11p15.5	PUMA
4	42679	hsa-miR-642	-1.50	4.33E-04	19q13.32	
5	42641	hsa-miR-145	-1.44	4.43E-02	5q32	IGF1R, PARP8, IRS1, MYC, CBFB, RTKN, KRT7, FSCN1, MUC1, PPP3CA, CLINT1, MMP11, SOX2, STAT1, KLF4, ESR1, CCNA2, ICAD, CLINT1, HOXA9, OCT4, FSCN1
6	42806	hsa-miR-886-3p	-1.43	1.03E-02		
7	42965	hsa-miR-424	-1.38	2.19E-02	Xq26.3	PLAG1, NFIA, FGFR1, MAP2K1, CCNE1, CCND1, CCNF, CDK6, MKLP1, CDC25A, CHEK1, CCND3, CDC14A, ATF6A, WEE1, ANLN, MYB, SIAH1
8	11014	hsa-miR-214	-1.38	5.49E-03	1q24.3	PTEN, MAPK8, MAP2K3, POU4F2, EZH2
9	42513	hsa-miR-300	-1.37	9.86E-04	14q32.31	
10	17354	hsa-miR-637	-1.37	4.64E-02	19p13.3	
11	11022	hsa-miR-221	1.17	2.13E-02	Xp11.3	KIT, CDKN1C, CDKN1B, ESR1, BMF, BIM, DDIT4, ICAM1, DDIT4, BNIP3L, TNFA, REDD1, MDM2, ESR1, TIMP3, PUMA, FOXO3A, FOS, CDK11B
12	42724	hsa-miR-34b	1.18	2.89E-03	11q23.1	CREB1, TCL1A, MYC, NOTCH4/2/1, SFRS2, CDK6, MYB, BCL2, HGFR, HMGA2, CCNE2
13	46739	hsa-miR-1308	1.35	6.55E-04		
14	46328	hsa-miR-1274b	1.36	8.92E-05	19	
15	10977	hsa-miR-183	1.38	3.35E-02	7q32.2	BTRC, FOXO1, KIF2A, VIL2, SLC1A1
16	46698	hsa-miR-1280	1.40	9.68E-05	3	
17	42825	hsa-miR-888*	1.42	2.65E-05		
18	46732	hsa-miR-1264	1.44	4.18E-05	X	
19	46292	hsa-miR-1274a	1.45	2.33E-03	5	

Table 4.3.2 Relative abundance, chromosomal location and validated targets of differentially abundant miRNAs in gastric CAMs compared to NTMs. No data available at the time of analysis is indicated by shading in grey.

No.	Probe Id	Annotation	Relative abundance	p-value	Chromosomal location	Target genes
1	146016	hsa-miR-1978	-1.98	7.78E-04		
2	42965	hsa-miR-424	-1.66	6.02E-04	Xq26.3	PLAG1, NFIA, FGFR1, MAP2K1, CCNE1, CCND1, CCNF, CDK6, MKLP1, CDC25A, CHEK1, CCND3, CDC14A, ATF6A, WEE1, ANLN, MYB, SIAH1
3	42641	hsa-miR-145	-1.58	1.48E-02	5q32	IGF1R, PARP8, IRS1, MYC, CBFB, RTKN, KRT7, FSCN1, MUC1, PPP3CA, CLINT1, MMP11, SOX2, STAT1, KLF4, ESR1, CCNA2, ICAD, CLINT1, HOXA9, OCT4, FSCN1
4	11014	hsa-miR-214	-1.48	5.82E-04	1q24.3	PTEN, MAPK8, MAP2K3, POU4F2, EZH2
5	145725	hsa-miR-518b	-1.47	3.98E-03	19q13.42	
6	42679	hsa-miR-642	-1.36	3.38E-03	19q13.32	
7	11030	hsa-miR-26a	-1.36	1.03E-03	3p22.2	SERBP1, SMAD1, PLAG1, TGFBR2, EZH2, CSK3B, CPEB2/3/4, PTEN, IL6, HMGA2, IFNB, CCNE2, GDAP1, PGR
8	42513	hsa-miR-300	-1.36	5.46E-04	14q32.31	
9	46732	hsa-miR-1264	1.38	6.95E-05	X	
10	46698	hsa-miR-1280	1.40	2.38E-05	3	
11	42825	hsa-miR-888*	1.42	2.79E-05		
12	46292	hsa-miR-1274a	1.61	1.94E-04	5	

Table 4.3.3 Relative abundance, chromosomal location and validated targets of differentially abundant miRNAs in gastric ATMs compared to NTMs. No data available at the time of analysis is indicated by shading in grey.

No.	Probe Id	Annotation	Relative abundance	p-value	Chromosomal location	Target genes
1	46258	hsa-miR-1184	-1.45	2.37E-02	X	
2	145801	hsa-miR-184	-1.20	3.20E-02	15q25.1	NFAT1, AKT2
3	17482	hsa-miR-411	1.16	1.66E-02	14q32.31	
4	11038	hsa-miR-299-5p	1.19	2.24E-02	14q32.31	SPP1, OPN, VEGFA, ESR1, AR
5	11182	hsa-miR-98	1.22	8.20E-03	Xp11.22	FUS1, HMGA2, SOCS4, TUSC2, E2F2, MYC, CISH, EZH2, TP53
6	145820	hsa-let-7c	1.27	3.45E-02	21q21.1	HMGA2, MYC, TGFBR1, TRIM71, KRT19, BCL2L1
7	146011	hsa-let-7a	1.29	8.99E-04	9q22.32	LIN28, HMGA2, KRAS, RAVER2, NF2, ITGB3, NRAS, TRIM71, CASP3, DICER1, PRDM1, EIF2C4, HRAS, E2F2, HOXA9, CCND2, MYC, UHRF2, KRAS1P, KBRAS2, DICER, IL13
8	17944	hsa-miR-337-5p	1.30	2.68E-02	14q32.2	
9	10987	hsa-miR-193b	1.37	5.92E-03	16p13.12	PLAU, ETS1, CCND1, ESR1
10	46483	hsa-miR-27a	1.40	2.38E-02	19p13.13	SP1, PHB, RUNX1, FOXO1, FADD, PEX7, RXRA, APC, GCA, EDAR, SOCS6, SPRY2, AML1, FKHR, BAG2
11	42744	hsa-miR-23a	1.40	2.56E-02	19p13.13	GLSK, IL6RA, ES1, HMGA2
12	145944	hsa-miR-27b	1.42	4.81E-02	9q22.32	NOTCH1, MMP13, PPARG, ST14, CYP1B1, RXRA, C/EBPalpha, A2BAR, EYA4, EDNRA
13	11052	hsa-miR-31	1.62	4.48E-03	9p21.3	MMP16, ITGA5, FIH1, RDX, FZD3, FGF10, FOXP3, MPRIP, RHOA, SELE, KRT17, KRT16, LATS2, KSR2, E2F6, DICER, PPP2R2A, BMPR2, DLX3, DKK1, DACT3
14	11065	hsa-miR-335	2.87	3.68E-03	7q32.2	SOX4, MERTK, PTPRN2, RUNX2, SP1, DKK1, IGF1R, ESR1, SOD2, ID4

Table 4.3.4 Relative abundance, chromosomal location and validated targets of differentially abundant miRNAs in pairwise analysis of oesophageal SC-CAMs compared to SC-ATMs. No data available at the time of analysis is indicated by shading in grey.

No.	Probe Id	Annotation	Relative abundance	p-value	Chromosomal location	Target genes
1	10998	hsa-miR-19b	-1.61	2.25E-04	13q31.3	ESR1, SOCS1, FMR1, PTEN
2	31026	hsa-miR-101	-1.59	8.03E-03	1p31.3	MYCN, MCL1, ICOS, EZH2, PTGS2, ATM, MTOR, ATXN1, COX2, MAGI2, DNAPK
3	145693	hsa-miR-92a	-1.55	3.60E-04	13q31.3	ITGA5, BMPRII, GAM
4	10997	hsa-miR-19a	-1.50	3.28E-04	13q31.3	PTEN, THBS1, ESR1, BIM, CCND1, BMPRII, ERBB4, NR4A2, PP2A, DOCK5, PRMT5, NURRI, SOCS1, ATXN, AMPK
5	42708	hsa-miR-99a	-1.46	3.97E-02	21q21.1	IGF1R, RPTOR, MTOR, RAVER2, FGFR3
6	42703	hsa-miR-490-3p	-1.44	1.02E-02	7q33	
7	145845	hsa-miR-20a	-1.41	3.74E-03	13q31.3	VEGFA, E2F1, BCL2, E2F3, CCND1, RUNX1, IL8, BIM, BMPRII, MEF2D, MAP3K12, JAK1, MICA, HLF, LRF, CCNE2, BMPR2, AIB1, APP, GAM, RB1, RASA2, PTENP1, PCAF, MAPK14, CDKN1A
8	17927	hsa-miR-491-3p	-1.40	8.91E-04	9p21.3	BCL2L1
9	46801	hsa-miR-106a	-1.38	1.31E-02	Xq26.2	RB1, CCKN1A, MYLIP, HIPK3, ARID4B, APP
10	32884	hsa-miR-342-3p	-1.36	5.75E-03	14q32.2	
	11023	hsa-miR-222	1.46	4.01E-03	Xp11.3	CDKN1B, KIT, CDKN1C, ESR1, BIM, SOD2, MMP1, FOS, PPP2R2A, ICAM1, PUMA, TIMP3, PTEN, FOXO3A,
11	17506	hsa-miR-24	1.47	4.53E-03	9q22.32	DND1, CCNA2, CDK4, BRCA1, AURKB, CDC2, FEN1, CDK1, MYC, ALK4, AE1, NOTCH1, NIPK, MAP2K4, HNF4A, FURIN, FAF1, E2F2, MKK4, DHFR, MAPK14, CDKN2A
12	146086	hsa-miR-30a	1.51	4.72E-02	6q13	NOTCH1, LIN28, ITGA2, BDNF, BECN1, KRT7, TNRC6A
13	11022	hsa-miR-221	1.54	9.86E-04	Xp11.3	KIT, CDKN1C, CDKN1B, ESR1, BMF, BIM, DDIT4, ICAM1, DDIT4, BNIP3L, TNFA, REDD1, MDM2, ESR1, TIMP3, PUMA, FOXO3A, FOS, CDK11B
14	145852	hsa-miR-210	1.60	2.67E-02	11p15.5	MNT, CASP8AP2, TCF7L2, SDHD, NDUFA4, RAD52, PTP1B, HOXA9, HOXA1, FGFRL1, E2F3, EFNA3, COX10, ALK4, ISCU
15	13140	hsa-miR-138	1.62	1.88E-02	3p21.32	KRT, EID1, TERT, ROCK2, RIMS2, APT1, EFNB3, PHRET1, RHOC,
16	145981	hsa-miR-1285	1.93	5.40E-03	7q21-q22	TP53, TGM2

Table 4.3.5 Relative abundance, chromosomal location and validated targets of differentially abundant miRNAs in oesophageal SC-CAMs compared to NTMs. No data available at the time of analysis is indicated by shading in grey.

No.	Probe Id	Annotation	Relative abundance	p-value	Chromosomal location	Target genes
1	42965	hsa-miR-424	-1.72	2.18E-02	Xq26.3	ANLN, ATF6, CDC14A, CCND3, CCND1, CDC25A, CHEK1, CCNE1, VEGFR2, FGFR1, SIAH1, MKLP1, PLAG1, TARBP2, VEGFA, NFIA, CDK6, WEE1
2	42708	hsa-miR-99a	-1.66	2.98E-02	21q21.1	IGF1R, RPTOR, MTOR, RAVER2, FGFR3,
3	145820	hsa-let-7c	-1.63	2.32E-03	21q21.1	HMGA2, MYC, TGFBR1, TRIM71, KRT19, BCL2L1
4	10306	hsa-miR-146b-5p	-1.60	1.55E-02	10q24.32	CARD10, IL8, IL6, EGFR, ESR1, CEGP1, MMP16, PSMC6, SMAD4
5	31026	hsa-miR-101	-1.58	2.54E-02	1p31.3	APP, ATXN1, ATM, EED, EZH2, ICOS, MAGI2, MCL1, ABCA1, MTOR, ABCC5, PTGS2, STMN1, RAB5A, ATG4D, NKCC1
6	10987	hsa-miR-193b	-1.55	5.03E-04	16p13.12	CCND1, ETS1, ESR1, AKR1C2, SHMT2, YWHAZ, ETO, MCL1, STARD7, PLAU
7	11052	hsa-miR-31	-1.51	1.82E-02	9p21.3	MMP16, ITGA5, FIH1, RDX, FZD3, FGF10, FOXP3, MPRIP, RHOA, SELE, KRT17, KRT16, LATS2, KSR2, E2F6, DICER, PPP2R2A, BMPR2, DLX3, DKK1, DACT3
8	46320	hsa-miR-31*	-1.50	1.54E-02		
9	11030	hsa-miR-26a	-1.48	3.46E-02	3p22.2	CPEB3, GSK3B, GDAP1, IL6, EZH2, MTDH, IFNB1, BDNF, CDK6, CCNE1, PHF6, HMGA2, RLI
10	17749	hsa-let-7b	-1.48	7.93E-03	22q13.31	KRT, CDK6, CDC25A, BCL7A, LIN28, CCND1, HMGA2, TLX, CISH, IMP1, IFNB, KRT19
11	5740	hsa-miR-21	-1.43	3.52E-02	17q23.1	BCL7A, APAF1, ZNF75, DOCK9, ZADH2, UBE2D3, TIMP3, THRB, SMAD7, SP1, SPG20, SPRY2, TGFBR2, PDCD4, PTEN, TP73L, PPIF, BMPR2, TP53BP2, TIAM1, SREBF1, RECK, RHOB, PPARA, PACE4, OLR1, NUSAP1, NT3, MSH2, MEF2C, MAN1, LRRC57, MATN2, GRHL3, HMGN2, ICAM1, IL1B, PLAT, IP10, IL12A, DOCK4, DOCK5, DOCK7, DICER, CDC25A, CCL1, ALX1, ANKRD46, AIM1L, JAG1, WNT1, SPRY2, ANP32A, LRRFIP1, SMARCA4

12	30787	hsa-miR-125b	-1.41	2.24E-02	11q24.1	AP1M1, BAK1, BCL2, BMF, BMPR1B, JUN, MYC, CBX7, CBFB, CCR5, CDC25C, TP53, ZAC1, PPP2CA, PRKRA, E2F3, ETS1, FGFR2, IL2RB, IL10RA, PRDM1, IFNG, IRF4, VDR, TDG, STAT3, PUMA, PSMB7, PSMB8
13	10998	hsa-miR-19b	-1.41	3.23E-02	13q31.3	TLR2, PTEN, TGFBR2, NDF1, MYCN, DKK3, BCL2L11
14	145647	hsa-miR-584	-1.39	2.76E-02	5q32	ITLN1
15	146011	hsa-let-7a	-1.36	5.91E-03	9q22.32	LIN28, HMGA2, KRAS, RAVER2, NF2, ITGB3, NRAS, TRIM71, CASP3, DICER1, PRDM1, EIF2C4, HRAS, E2F2, HOXA9, CCND2, MYC, UHRF2, KRAS1P, KBRAS2, DICER, IL13
16	145832	hsa-miR-381	-1.35	5.69E-03	14q32.31	BDNF, ESR1
17	29379	hsa-miR-452	-1.35	3.75E-02	Xq28	WNT5A
18	11039	hsa-miR-29a	1.36	2.68E-03	7q32.3	CDK6, PIK3R1, CXXC6, DNMT3A, DNMT3B, DKK1, COL3A1, CDC42, CD276, BCL2, BACE1, ZFP36, SFRP2, PMP22, RAN, GLUL, INSIG1, MCL1, SPARC, KREMEN2
19	146001	hsa-miR-1977	1.36	2.17E-02		
20	11022	hsa-miR-221	1.41	7.99E-04	Xp11.3	ETS1, ESR1, DICER, CDKN1B, BMF, KIT, ARHI, MDM2, APAF1, REDD1, PUMA, TIMP3, PTEN, FOXO3A, PTPRM, PIK3R1, TRPS1, THRB, CDKN1C
21	11041	hsa-miR-29c	1.44	3.16E-02	1q32.2	LAMG1, DNMT3A, DNMT3B, COL3A1, COL4A1, COL15A1, TDG, FUSIP1, COL1A1, COL1A2, COL4A2, PIK3R1, CDC42, FBN, SPARC, PIK3R1, MMP2
22	11023	hsa-miR-222	1.50	3.09E-03	Xp11.3	MMP1, SOD2, HOXA4, FOXO3A, ETS1, ESR1, DICER, CDK4, KIT, ARHI, APAF1, PAK1, CDKN1B, SNTB1, PPP2R2A, TIMP3, PTEN, PUMA, CDKN1C, CXCL12, STAT5A, TRPS1
23	146165	hsa-miR-1973	1.65	7.62E-03	3	
24	46620	hsa-miR-1275	1.70	3.15E-03	6	
25	11040	hsa-miR-29b	1.87	1.30E-03	7q32.3	BMP1, ADAM12, NKIRAS2, MCL1, ID1, COL1A1, COL5A3, COL4A2, EOMES, DNMT3A, MMP2, BACE1, YY1, CDK6, VAMP3, HDAC4, DUSP2, ACVR2A, SP1, RHOBTB1, PUMA, BCL2L11, CDC42, TBX21, RAX, PIK3R1, IFNG, IP30

Table 4.3.6 Relative abundance, chromosomal location and validated targets of differentially abundant miRNAs in oesophageal SC-ATMs compared to NTMs. No data available at the time of analysis is indicated by shading in grey.

No.	Probe Id	Annotation	Relative abundance	p-value	Chromosomal location	Target genes
1	27533	hsa-miR-320a	1.15	2.29E-02	8p21.3	MCL1, TAC1, HSPB6, MMP9, ETS2, BIRC5, CD71
2	46324	hsa-miR-320b	1.16	2.73E-02	1	
3	10967	hsa-miR-16	1.19	7.88E-03	13q14.2	BLC2, ARL2, TPPP3, RARS, FGF2, CCND1, RTN4, AXIN2
4	31867	hsa-miR-145*	1.34	3.59E-02		
5	42641	hsa-miR-145	1.82	1.90E-02	5q32	ACE1, CBFB, PPP3CA, CLINT1, IFNB1, BNIP3, STAT1, CFTR, DAB2, MUC1, MMP11, PAI1, SOX9, SOX2, KLF4, OCT4

Table 4.3.7 Relative abundance, chromosomal location and validated targets of differentially abundant miRNAs in pairwise analysis of oesophageal AC-CAMs compared to AC-ATMs. No data available at the time of analysis is indicated by shading in grey.

No.	Probe Id	Annotation	Relative abundance	p-value	Chromosomal location	Target genes
1	10306	hsa-miR-146b-5p	-1.86	8.18E-03	10q24.32	EGFR, IL8, IL6, ESR1, SMAD4, PSMC6, MMP16
2	29379	hsa-miR-452	-1.39	2.39E-02	Xq28	WNT5A
3	145981	hsa-miR-1285	1.44	2.31E-02	7q21-q22	TP53, TGM2

Table 4.3.8 Relative abundance, chromosomal location and validated targets of differentially abundant miRNAs in oesophageal AC-CAMs compared to NTMs. No data available at the time of analysis is indicated by shading in grey.

No.	Probe Id	Annotation	Relative abundance	p-value	Chromosomal location	Target genes
1	42965	hsa-miR-424	-1.69	2.18E-02	Xq26.3	ANLN, ATF6, CDC14A, CCND3, CCND1, CDC25A, CHEK1, CCNE1, VEGFR2, FGFR1, SIAH1, MKLP1, PLAG1, TARBP2, VEGFA, NFIA, CDK6, WEE1
2	11030	hsa-miR-26a	-1.50	8.78E-03	3p22.2	CPEB3, GSK3B, GDAP1, IL6, EZH2, MTDH, IFNB1, BDNF, CDK6, CCNE1, PHF6, HMGA2, RLI
3	31026	hsa-miR-101	-1.48	7.17E-03	1p31.3	APP, ATXN1, ATM, EED, EZH2, ICOS, MAGI2, MCL1, ABCA1, MTOR, ABCC5, PTGS2, STMN1, RAB5A, ATG4D, NKCC1
4	42708	hsa-miR-99a	-1.47	4.44E-02	21q21.1	FRAP1, SMARCA5, SMARCD1, IGF1R, FGFR3, RPTOR
5	10306	hsa-miR-146b-5p	-1.44	2.87E-02	10q24.32	CARD10, IL8, IL6, EGFR, ESR1, CEGP1, MMP16, PSMC6, SMAD4
6	30787	hsa-miR-125b	-1.44	6.62E-03	11q24.1	AP1M1, BAK1, BCL2, BMF, BMPR1B, JUN, MYC, CBX7, CBFB, CCR5, CDC25C, TP53, ZAC1, PPP2CA, PRKRA, E2F3, ETS1, FGFR2, IL2RB, IL10RA, PRDM1, IFNG, IRF4, VDR, TDG, STAT3, PUMA, PSMB7, PSMB8
7	27217	hsa-miR-34a	-1.35	1.21E-02	1p36.22	WNT1, WNT3, LRP6, LEF1, CTNNB1, VCL, ULBP2, YY1, LDHA, MTA2, AXL, SYT1, STX1A, BIRC5, MSI1, MYT1, AXIN2, MEK1, MET, MAD2B, E2F3, MAD2L2, CDK4, FOXP1, CDC25A, AGBL5, AF9, ACSM3, CCND1, BCL2
8	146200	hsa-miR-1974	1.35	2.14E-02		
9	11040	hsa-miR-29b	1.38	3.73E-02	7q32.3	BMP1, ADAM12, NKIRAS2, MCL1, ID1, COL1A1, COL5A3, COL4A2, EOMES, DNMT3A, MMP2, BACE1, YY1, CDK6, VAMP3, HDAC4, DUSP2, ACVR2A, SP1, RHOBTB1, PUMA, BCL2L11, CDC42, TBX21, RAX, PIK3R1, IFNG, IP30
10	46292	hsa-miR-1274a	1.50	4.33E-02		

Table 4.3.9 Relative abundance, chromosomal location and validated targets of differentially abundant miRNAs in oesophageal AC-ATMs compared to oesophageal NTMs. No data available at the time of analysis is indicated by shading in grey.

4.3.2 Integrated analysis of hsa-miR-181d targets and their mRNA abundance in gastric myofibroblasts

In chapter 3, hsa-miR-181d was identified as the most up-regulated miRNA in gastric CAMs by using pairwise analysis of miRNA abundance in 12 gastric CAMs and their corresponding ATMs. Here, validated targets of the miR-181 family, including TIMP3, NLK and GATA6, were identified and briefly described in Table 4.3.10. Using the existing microarray gene expression data, the mRNA abundance of TIMP3 (Figure 4.3.1A), NLK (Figure 4.3.1B) and GATA6 (Figure 4.3.1C) in each gastric CAM compared to corresponding ATM from 12 patients was analysed. The analysis showed that the mRNA abundance of TIMP3 was decreased in several paired samples of gastric CAMs and ATMs, including Sz190 and Sz192. Paired samples from Sz190 and Sz192 were selected for more detailed studies because increased hsa-miR-181d abundance in each gastric CAM compared to corresponding ATM had already been validated by quantitative RT-PCR (Chapter 3.3.6). Further analysis using RT-PCR confirmed decreased abundance of TIMP3 mRNA in CAMs of Sz190 and Sz192 compared to respective ATMs (Figure 4.3.2A). In addition, Western blot analysis of TIMP-3 showed that the intensity of bands at 24 kDa and 15 kDa was reduced in CAMs compared to corresponding ATMs in these two paired samples (Figure 4.3.2B).

The above description demonstrated the association of hsa-miR-181d and TIMP3 expression in gastric myofibroblasts. As TIMP-3 is an ECM protein that inhibits the activity of MMPs, it was suggested that targets of hsa-miR-181d regulate extracellular interactions. To test this hypothesis, enriched network analysis of predicted hsa-miR-181d targets was performed. Firstly, target genes of

No.	Gene Symbol	Name	Biological significance	References
1	AICDA	activation-induced cytidine deaminase	Down-regulated miR-181b is involved in B cell malignant transformation.	[237]
2	BCL2	B cell leukemia/lymphoma 2	Down-regulated miR-181a/b induces multi-drug resistance in gastric and lung cancer cell lines and modulates radiosensitivity in malignant glioma cells.	[238, 239]
3	CDKN1B	cyclin-dependent kinase inhibitor 1B	Down-regulated mir-181a blocks cell cycle progression during myeloid cell differentiation.	[240]
4	CDX2	caudal type homeobox 2	High expression of miR-181 in hepatic cancer stem cells which express epithelial cell adhesion molecule induce cell proliferation and tumour initiating ability.	[241]
5	NLK	nemo-like kinase		
6	GATA6	GATA binding protein 6		
7	CYLD	cylindromatosis (turban tumor syndrome)	Up-regulated miR-181b is associated with cellular transformation.	[242]
8	VSNL1	visinin-like 1	Up-regulation of miR-181b in the temporal cortex in schizophrenia compared to control.	[243]
9	GRIA2	glutamate receptor, ionotropic, AMPA 2		
10	IL2	interleukin 2	Down-regulation of miR-181c during the process of CD4 positive T- cell activation.	[244]
11	KRAS	v-Ki-ras2 Kirsten rat sarcoma viral oncogene homolog	Down-regulated miR-181a/c is involved in tumour cell growth of gastric and oral squamous cell carcinomas.	[245, 246]
12	NOTCH4	notch 4		
13	PLAG1	pleiomorphic adenoma gene 1	Down-regulation of miR-181a/b in chronic lymphocytic leukaemia.	[247, 248]
14	TCL1A	T-cell leukemia/lymphoma 1A		
15	TIMP3	tissue inhibitor of metalloproteinase 3	Up-regulated miR-181b is associated with mitogenic growth signals in breast and hepatocellular carcinomas.	[249, 250]
16	KPNA4	karyopherin alpha 4	Expression of miR-181b down-regulates endothelial cells activation and vascular inflammation.	[251]
17	HOXA11	homeobox A11	Up-regulation of miR-181 during the process of mammalian skeletal-muscle differentiation.	[252]
18	RALA	v-ral simian leukemia viral oncogene homolog A (ras related)	Overexpression of miR-181a is associated with cell growth inhibition and apoptosis in chronic myeloid leukaemia.	[253]

Table 4.3.10 Validated targets of miR-181 family members and their biological significance.

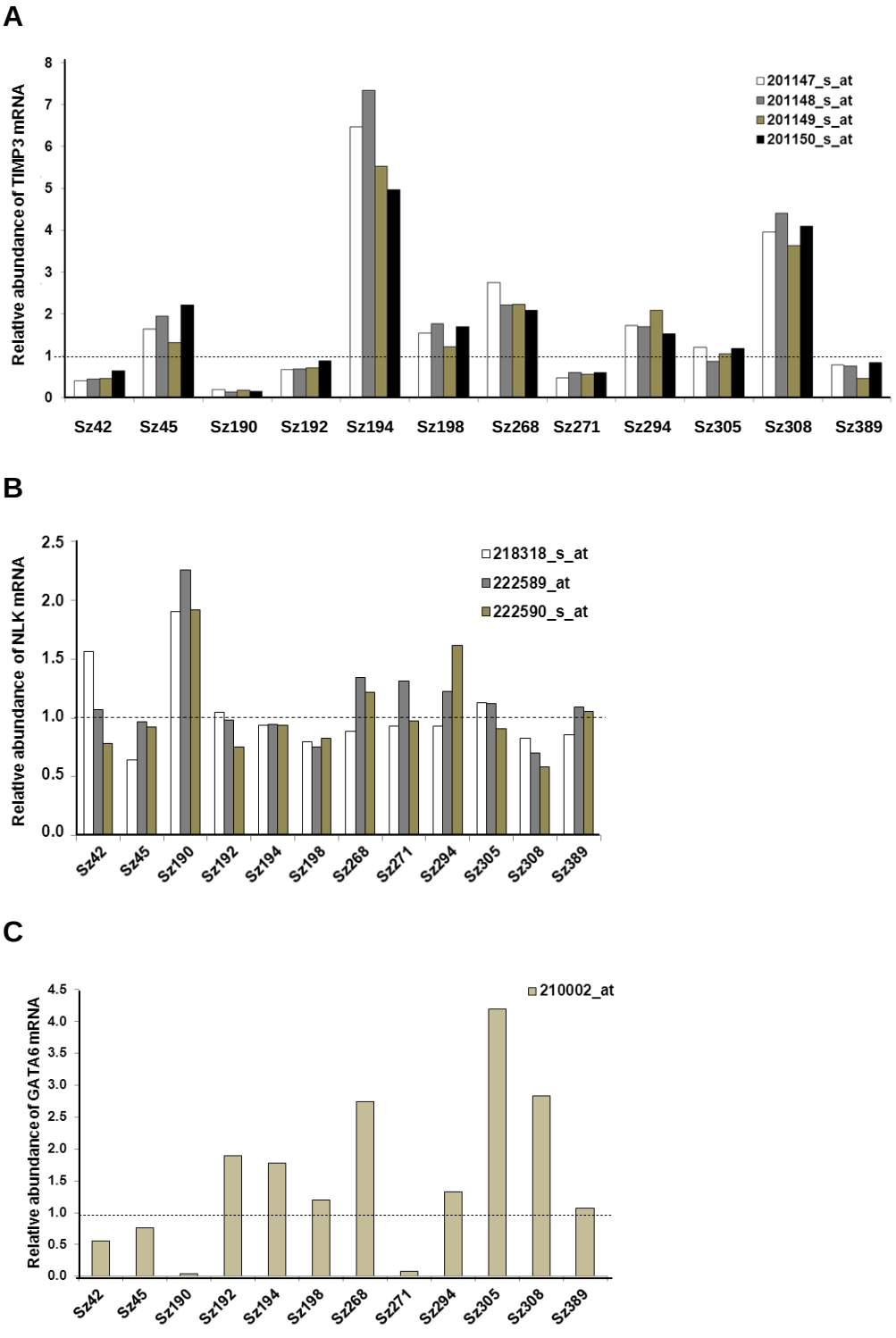

Figure 4.3.1 Microarray analysis of hsa-miR-181 targets in paired individual samples of gastric CAMs and ATMs from 12 patients. The relative mRNA abundance of (A) TIMP3, (B) NLK and (C) GATA6 in each CAM compared to corresponding ATM (abundance = 1.0). TIMP3, NLK and GATA6 were represented by 4, 3 and 1 oligonucleotides, respectively and were normalised to GAPDH.

A

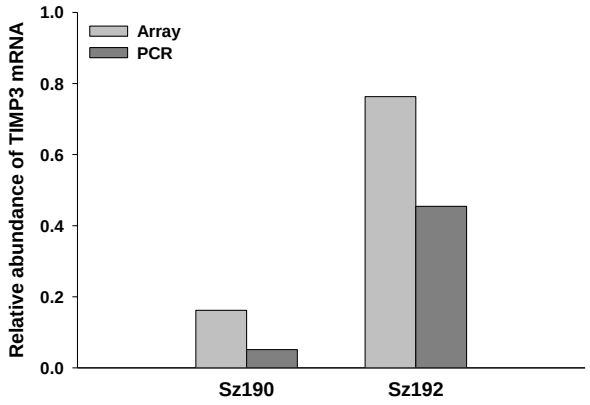

B

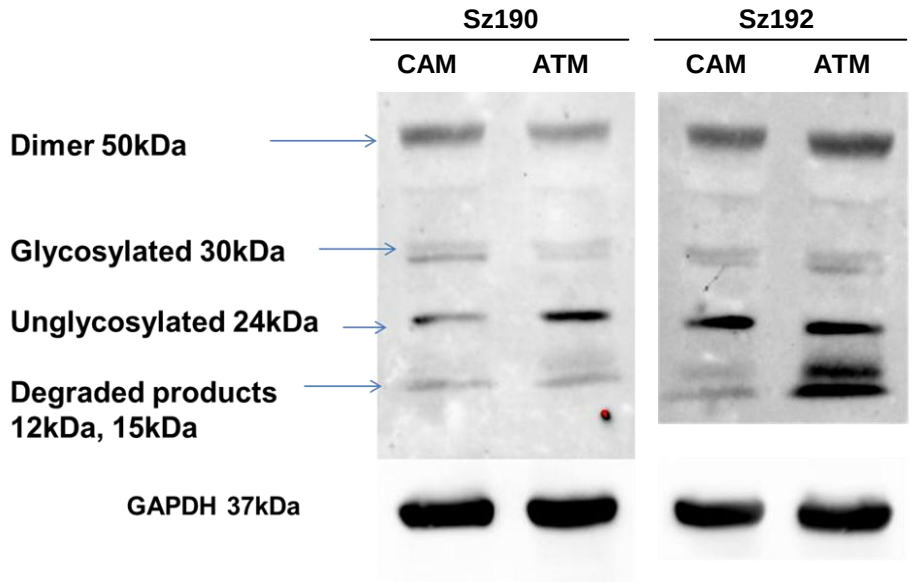

Figure 4.3.2 Decreased expression of TIMP3 in gastric CAMs of Sz190 and Sz192. (A) Relative abundance TIMP3 mRNA in CAMs compared to corresponding ATMs (abundance = 1.0) was determined by array and RT-PCR analyses. Expression of TIMP3 mRNA was normalised to GAPDH mRNA. (B) Western blot analysis of TIMP-3 in CAMs and ATMs using paired samples from Sz190 and Sz192. GAPDH was the loading control.

hsa-miR-181d that encode extracellular proteins were predicted and retrieved from TargetScan 5.1. Using gene expression data in comparisons of CAMs and corresponding ATMs from Sz190 and Sz192, those target genes that exhibited ≥ 50% decrease in mRNA abundance in CAMs compared to ATMs were analysed by MetaCore®. Significant ($p < 0.05$) enrichment of hsa-miR-181d targets in paired sample analysis of Sz190 and Sz192 are shown in Tables 4.3.11A and 4.3.11B, respectively. The most significant networks that were common in both Sz190 and Sz192 analyses were chemotaxis, connective tissue degradation, neutrophil activation and ECM remodelling. The results indicate a predicted function of hsa-miR-181d in promoting cell motility by using bioinformatics.

4.3.3 Significant networks associated with targets of differentially abundant miRNAs in gastric myofibroblasts

The identification of miRNA targets that had been validated by independent studies leads to the investigation of biological processes that are regulated by multiple miRNAs. It was because differential miRNA abundance could alter cellular processes that might distinguish between different myofibroblast populations. To do so, network enrichment analysis was performed to identify networks that were significantly enriched by potential targets of differentially abundant miRNAs in myofibroblasts.

In pairwise analysis of 12 gastric CAMs with corresponding ATMs, published and validated targets of 10 differentially abundant miRNAs were obtained from MetaCore®, and the top three enriched networks were G1-S growth factor regulation, G1-S interleukin regulation and Wnt signalling (Table 4.3.12A).

No.	Networks	p-value
1	Chemotaxis	7.98E-06
2	Cell adhesion_Leucocyte chemotaxis	8.81E-06
3	Cell adhesion_Cell-matrix interactions	4.06E-04
4	Proteolysis_Connective tissue degradation	5.45E-04
5	Inflammation_Neutrophil activation	2.40E-03
6	Proteolysis_ECM remodeling	2.77E-03
7	Immune response_Th17-derived cytokines	3.34E-03

Table 4.3.11A Significant networks enriched with hsa-miR-181d target genes that encode extracellular proteins (predicted from TargetScan5.1) in Sz190.

No.	Networks	p-value
1	**Chemotaxis**	2.35E-08
2	**Cell adhesion_Leucocyte chemotaxis**	1.99E-05
3	**Proteolysis_Connective tissue degradation**	1.23E-04
4	**Inflammation_Neutrophil activation**	5.66E-04
5	**Proteolysis_ECM remodeling**	9.30E-04
6	**Immune response_Th17-derived cytokines**	1.13E-03
7	Inflammation_Jak-STAT Pathway	3.87E-03
8	Cell adhesion_Platelet-endothelium-leucocyte	4.86E-03
9	**Cell adhesion_Cell-matrix interactions**	9.98E-03
10	Blood coagulation	1.07E-02
11	Proliferation_Positive regulation cell proliferation	1.63E-02
12	Inflammation_Protein C signaling	1.81E-02

Table 4.3.11B Significant networks enriched with hsa-miR-181d target genes that encode extracellular proteins (predicted from TargetScan5.1) in Sz192. A total of 7 networks (indicated in bold) were found in both Sz190 and Sz192.

Significant networks that were associated with cell cycle progression (G1 to S phase) were not unexpected because it is recognised that gastric CAMs exhibit an increased rate of proliferation when compared to ATMs [179]. Wnt signalling was of interest as the canonical Wnt/β-catenin signalling pathway has been shown to induce the expression of hsa-miR-181d [254]. Furthermore, some of the proteins that were annotated in Wnt signalling are already identified as validated targets of differentially abundant miRNAs; NLK and GATA6 are target genes of hsa-miR-181d while CTNNB1 and CAMK2D are target genes of hsa-miR-483-3p and hsa-miR-494, respectively (Table 4.3.1).

When potential targets of differentially abundant miRNAs in gastric CAMs compared to NTMs, and gastric ATMs compared to NTMs were analysed, the top three enriched networks were common in both analyses: a) G1-S growth factor regulation, b) G1-S interleukin regulation and c) regulation of epithelial-to-mesenchymal transition (Tables 4.3.12B, 4.3.12C). Again, cell cycle progression was not unexpected because myofibroblasts have been shown to exhibit increased proliferation when incubated in media from *H. pylori*-infected gastric epithelial cells [73], indicating *H. pylori* infection alter myofibroblast phenotype in the early stage of gastric cancer development.

All significant networks of differentially abundant miRNAs are listed in the appendices: gastric CAMs compared to ATMs (Appendix 4.3.1), gastric CAMs compared to NTMs (Appendix 4.3.2), and gastric ATMs compared to NTMs (Appendix 4.3.3).

No.	Networks	p-value
1	Cell cycle_G1-S Growth factor regulation	1.956E-14
2	Cell cycle_G1-S Interleukin regulation	3.169E-14
3	Signal transduction_WNT signalling	6.083E-11
4	Development_Hemopoiesis, Erythropoietin pathway	3.348E-09
5	Apoptosis_Anti-Apoptosis mediated by external signals via PI3K/AKT	5.769E-09
6	Development_EMT_Regulation of epithelial-to-mesenchymal transition	6.642E-09
7	Reproduction_Male sex differentiation	4.016E-08
8	Cell cycle_G0-G1	1.475E-07
9	Proliferation_Positive regulation cell proliferation	1.943E-07
10	Signal Transduction_TGF-beta, GDF and Activin signalling	2.951E-07

Table 4.3.12A Networks enriched by targets of differentially abundant miRNAs in pairwise analysis of gastric CAMs compared to ATMs.

No.	Networks	p-value
1	Cell cycle_G1-S Growth factor regulation	7.626E-11
2	Development_EMT_Regulation of epithelial-to-mesenchymal transition	1.694E-09
3	Cell cycle_G1-S Interleukin regulation	1.376E-07
4	Reproduction_FSH-beta signalling pathway	2.353E-06
5	Signal Transduction_TGF-beta, GDF and Activin signalling	3.952E-06
6	Development_Hemopoiesis, Erythropoietin pathway	6.901E-06
7	Inflammation_IL-10 anti-inflammatory response	1.572E-05
8	DNA damage_Checkpoint	2.295E-05
9	Signal transduction_Leptin signalling	2.394E-05
10	Signal transduction_WNT signalling	3.577E-05

Table 4.3.12B Networks enriched by targets of differentially abundant miRNAs in gastric CAMs compared to NTMs.

No.	Networks	p-value
1	Cell cycle_G1-S Growth factor regulation	7.361E-13
2	Cell cycle_G1-S Interleukin regulation	2.075E-10
3	Development_EMT_Regulation of epithelial-to-mesenchymal transition	2.360E-08
4	Signal Transduction_TGF-beta, GDF and Activin signalling	1.292E-07
5	Signal transduction_WNT signalling	1.620E-07
6	Development_Hemopoiesis, Erythropoietin pathway	2.342E-07
7	DNA damage_Checkpoint	9.375E-07
8	Reproduction_FSH-beta signalling pathway	7.032E-06
9	Inflammation_IL-10 anti-inflammatory response	7.076E-06
10	Signal transduction_NOTCH signalling	1.366E-05

Table 4.3.12C Networks enriched by targets of differentially abundant miRNAs in gastric ATMs compared to NTMs.

4.3.4 Significant networks associated with targets of differentially abundant miRNAs in oesophageal myofibroblasts

Using MetaCore®, potential targets of 11 differentially abundant miRNAs in oesophageal SC-CAMs compared to SC-ATMs were highly enriched for TGF-β, GDF and activin signalling, BMP and GDF signalling, and G1-S growth factor regulation (Table 4.3.13A). In the comparison between SC-CAMs and NTMs, G1-S growth factor regulation and G1-S interleukin regulation were identified as networks significantly enriched by targets of differentially abundant miRNAs (Table 4.3.13B). Additionally, the analysis of SC-ATMs compared to NTMs indicated the top three networks were: regulation of epithelial-mesenchymal transitions, TGF-β, GDF and activin signalling, and G1-S growth factor regulation (Table 4.3.13C). The results suggest that cell cycle progression, and TGF-β, GDF and activin signalling are targeted by differentially abundant miRNAs in oesophageal myofibroblasts during the development of oesophageal squamous cell carcinoma.

When network analysis was performed using potential targets of 4 differentially abundant miRNAs in oesophageal AC-CAMs compared to AC-ATMs, the top three networks were: G1-S growth factor regulation, G1-S interleukin regulation and regulation of epithelial-mesenchymal transition (Table 4.3.14A). In the comparisons between AC-CAMs and NTMs and between AC-ATMs and NTMs, the top enriched network was TGF-β, GDF and activin signalling (Table 4.3.14B), and G1-S growth factor regulation, respectively (Table 4.3.14C).

No.	Networks	p-value
1	Signal Transduction_TGF-beta, GDF and Activin signalling	2.429E-11
2	Signal Transduction_BMP and GDF signalling	3.065E-07
3	Cell cycle_G1-S Growth factor regulation	6.057E-07
4	Development_Hedgehog signalling	6.216E-07
5	Reproduction_Feeding and Neurohormone signalling	1.828E-06
6	Signal transduction_ESR1-nuclear pathway	1.963E-06
7	Cell cycle_G1-S Interleukin regulation	2.853E-06
8	Apoptosis_Anti-Apoptosis mediated by external signals via PI3K/AKT	1.026E-05
9	Development_Blood vessel morphogenesis	1.151E-05
10	Signal transduction_NOTCH signalling	1.395E-05

Table 4.3.13A Networks enriched by targets of differentially abundant miRNAs in pairwise analysis of oesophageal SC-CAMs compared to SC-ATMs.

No.	Networks	p-value
1	Cell cycle_G1-S Growth factor regulation	2.553E-12
2	Cell cycle_G0-G1	7.493E-12
3	Cell cycle_G1-S Interleukin regulation	1.352E-11
4	Cell cycle_G1-S	5.318E-10
5	Development_Hemopoiesis, Erythropoietin pathway	7.016E-10
6	Development_Hedgehog signalling	3.328E-09
7	Signal transduction_NOTCH signalling	3.772E-09
8	Development_EMT_Regulation of epithelial-to-mesenchymal transition	5.174E-09
9	Cell cycle_Core	9.081E-09
10	Apoptosis_Anti-Apoptosis mediated by external signals via PI3K/AKT	9.133E-09

Table 4.3.13B Networks enriched by targets of differentially abundant miRNAs in oesophageal SC-CAMs compared to NTMs.

No.	Networks	p-value
1	Development_EMT_Regulation of epithelial-to-mesenchymal transition	3.251E-16
2	Signal Transduction_TGF-beta, GDF and Activin signalling	3.434E-14
3	Cell cycle_G1-S Growth factor regulation	6.050E-13
4	Apoptosis_Anti-Apoptosis mediated by external signals via PI3K/AKT	1.050E-12
5	Reproduction_Feeding and Neurohormone signalling	2.405E-11
6	Signal Transduction_BMP and GDF signalling	1.799E-09
7	Inflammation_MIF signalling	3.133E-09
8	Signal transduction_Androgen receptor signaling cross-talk	3.463E-09
9	Signal transduction_WNT signalling	3.948E-09
10	Development_Cartilage development	9.792E-09

Table 4.3.13C Networks enriched by targets of differentially abundant miRNAs in oesophageal SC-ATMs compared to NTMs.

No.	Networks	p-value
1	Cell cycle_G1-S Growth factor regulation	1.026E-14
2	Cell cycle_G1-S Interleukin regulation	2.779E-10
3	Development_EMT_Regulation of epithelial-to-mesenchymal transition	2.814E-09
4	Inflammation_MIF signalling	4.128E-09
5	Reproduction_Feeding and Neurohormone signalling	6.526E-09
6	Signal Transduction_TGF-beta, GDF and Activin signalling	2.959E-08
7	DNA damage_Checkpoint	1.363E-07
8	Development_Hemopoiesis, Erythropoietin pathway	1.918E-07
9	Inflammation_IL-2 signalling	2.769E-07
10	Proliferation_Negative regulation of cell proliferation	8.930E-07

Table 4.3.14A Networks enriched by targets of differentially abundant miRNAs in pairwise analysis of oesophageal AC-CAMs compared to AC-ATMs.

No.	Networks	p-value
1	Signal Transduction_TGF-beta, GDF and Activin signalling	3.320E-04
2	Apoptosis_Anti-Apoptosis mediated by external signals by Estrogen	4.523E-04
3	Signal transduction_ESR1-membrane pathway	7.999E-04
4	Apoptosis_Anti-Apoptosis mediated by external signals via PI3K/AKT	8.117E-04
5	Proliferation_Negative regulation of cell proliferation	9.834E-04
6	Development_Regulation of angiogenesis	1.471E-03
7	Inflammation_MIF signalling	1.712E-03
8	Signal transduction_ESR1-nuclear pathway	2.107E-03
9	Signal transduction_NOTCH signalling	2.292E-03
10	Inflammation_TREM1 signalling	2.552E-03

Table 4.3.14B Networks enriched by targets of differentially abundant miRNAs in oesophageal AC-CAMs compared to NTMs.

No.	Networks	p-value
1	Cell cycle_G1-S Growth factor regulation	1.147E-11
2	Development_EMT_Regulation of epithelial-to-mesenchymal transition	1.465E-11
3	Apoptosis_Anti-Apoptosis mediated by external signals via PI3K/AKT	2.528E-10
4	Signal transduction_WNT signalling	2.860E-09
5	Reproduction_Feeding and Neurohormone signalling	7.628E-09
6	Proliferation_Negative regulation of cell proliferation	2.446E-08
7	Reproduction_Progesterone signalling	7.273E-08
8	Inflammation_MIF signalling	9.110E-08
9	Signal transduction_ESR1-membrane pathway	2.318E-07
10	Signal Transduction_TGF-beta, GDF and Activin signalling	2.858E-07

Table 4.3.14C Networks enriched by targets of differentially abundant miRNAs in oesophageal AC-ATMs compared to NTMs.

All the significant networks from the above enriched network analysis of oesophageal myofibroblasts are presented in the appendices: SC-CAMs compared to SC- ATMs (Appendix 4.3.4), SC-CAMs compared to NTMs (Appendix 4.3.5), SC-ATMs compared to NTMs (Appendix 4.3.6), AC-CAMs compared to AC-ATMs (Appendix 4.3.7), AC-CAMs compared to NTMs, (Appendix 4.3.8) and AC-ATMs compared to NTMs (Appendix 4.3.9).

4.3.5 Significant networks associated with targets of miRNAs that exhibited different abundance in 12 paired samples of gastric myofibroblasts

To determine any inter-patient variation about enriched networks that were associated with significantly different miRNAs, network analysis was performed in each paired sample of CAM and ATM. The number of miRNAs which exhibited at least 50% difference in abundance in CAMs compared to corresponding ATMs was determined in each of the 12 patients (Table 4.3.15). The potential targets of these altered miRNAs in each paired sample were obtained from MetaCore®. Network analyses showed that Wnt signalling was the only enriched network that was significant in all of the 12 patients while 4 other networks were found to be significant in all patients except Sz42 (Patient 1) (Figure 4.3.3). In total, 30 enriched networks were significant in at least 8 of the 12 patients (Appendix 4.3.10). There were a total of 7, 10 and 8 networks that were significant in 10, 9 and 8 patients, respectively. As both pairwise and individual analyses indicated Wnt signalling was deregulated by altered miRNA abundance, Wnt signalling pathways in gastric myofibroblasts were studied in the following chapter.

No.	Patient	Number of up and down-regulated miRNAs
Patient 1	Sz42	5
Patient 2	Sz45	8
Patient 3	Sz190	62
Patient 4	Sz192	54
Patient 5	Sz194	22
Patient 6	Sz198	8
Patient 7	Sz268	43
Patient 8	Sz271	42
Patient 9	Sz294	5
Patient 10	Sz305	28
Patient 11	Sz308	3
Patient 12	Sz389	31

Table 4.3.15 Numbers of miRNAs that exhibited at least 50% change in abundance in paired samples of gastric myofibroblasts (CAMs compared to ATMs) from 12 patients. Each Sz identification number is represented by a patient number for the purpose of cross-referencing.

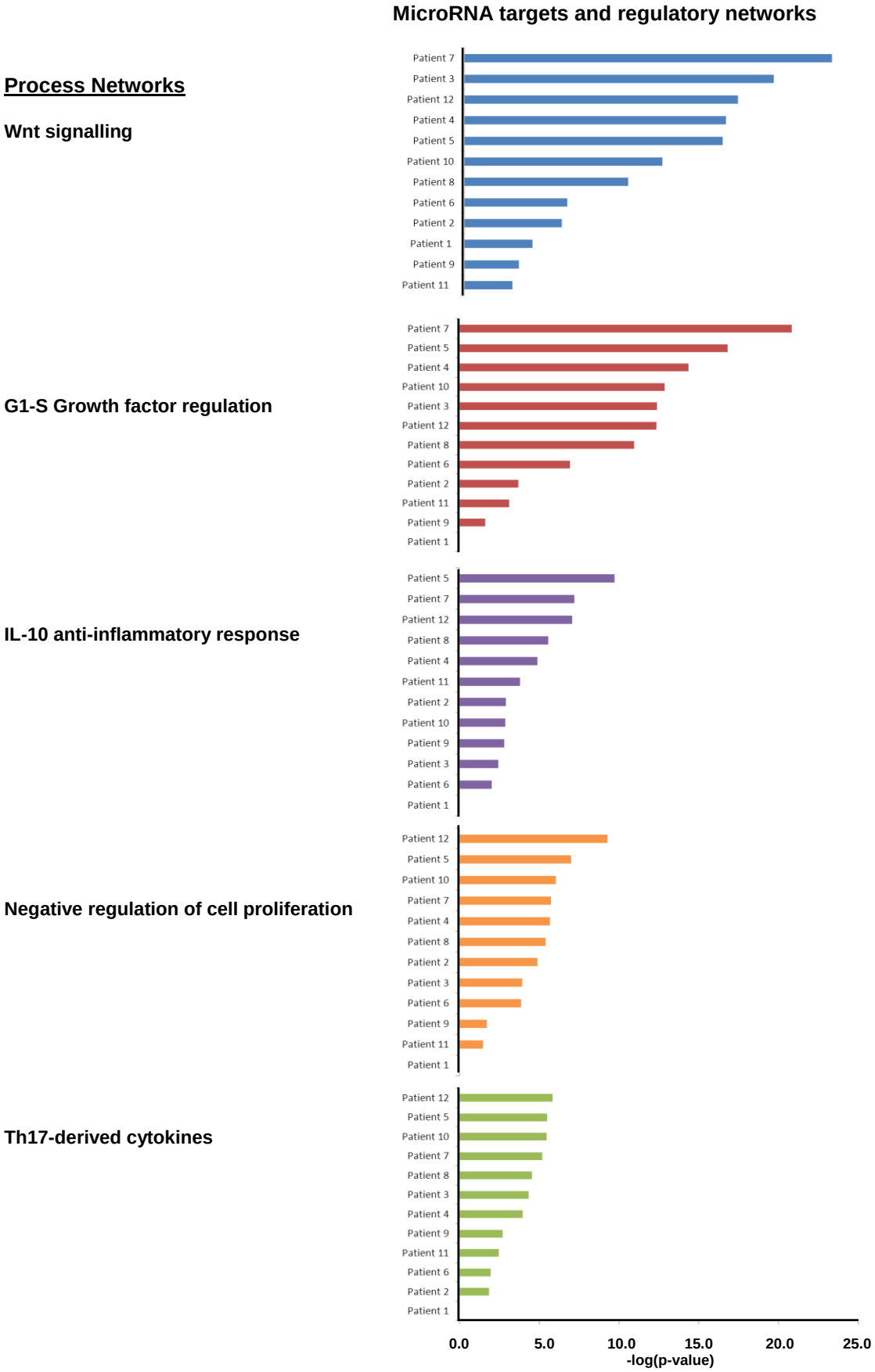

Figure 4.3.3 Top five networks that were significantly enriched by targets of miRNAs that exhibited at least 50% difference in abundance in each gastric CAM compared to corresponding ATM from 12 patients. Targets of all 12 pairs were enriched for Wnt signalling and 11 pairs were enriched for G1-S growth factor regulation, IL10 anti-inflammatory response, negative regulation of cell proliferation and Th17-derived cytokines. (Y-axis: patient number in descending magnitude of enrichment. X-axis: log p-value). Each patient number that represents a Sz identification number is indicated in Table 4.3.15.

4.3.6 Significant networks associated with targets of miRNAs that exhibited different abundance in 7 paired samples of oesophageal myofibroblasts

Network analysis was then extended to each paired sample of oesophageal myofibroblasts. The number of miRNAs that exhibited at least 50% change in abundance was determined in oesophageal SC-CAMs compared to corresponding SC-ATMs from 4 patients (Table 4.3.16). Network analysis using targets of altered miRNAs in all 4 patients identified G1-S growth factor regulation, G1-S interleukin regulation, NOTCH signalling, and TGF-β, GDF and activin signalling as highly significant networks (Figure 4.3.4). A total of 33 networks were significantly enriched in all 4 patients (Appendix 4.3.11).

In the comparison between each oesophageal AC-CAM and corresponding AC-ATM, the number of miRNAs that exhibited at least 50% difference in abundance was determined (Table 4.3.17). Networks that were significantly enriched by targets of altered miRNAs in all 3 patients, were regulation of epithelial-mesenchymal transition, TGF-β, GDF and activin signalling, Wnt signalling and G1-S growth factor regulation (Figure 4.3.5). The analysis also showed that a total of 50 networks were significantly enriched in at least 1 of the 3 patients (Appendix 4.3.12).

Patient	Number of up and down-regulated miRNAs
Sz306	23
Sz360	55
Sz373	18
Sz467	18

Table 4.3.16 Numbers of miRNAs that exhibited at least 50% change in abundance in paired samples of oesophageal myofibroblasts (SC-CAMs compared to SC-ATMs) from 4 patients.

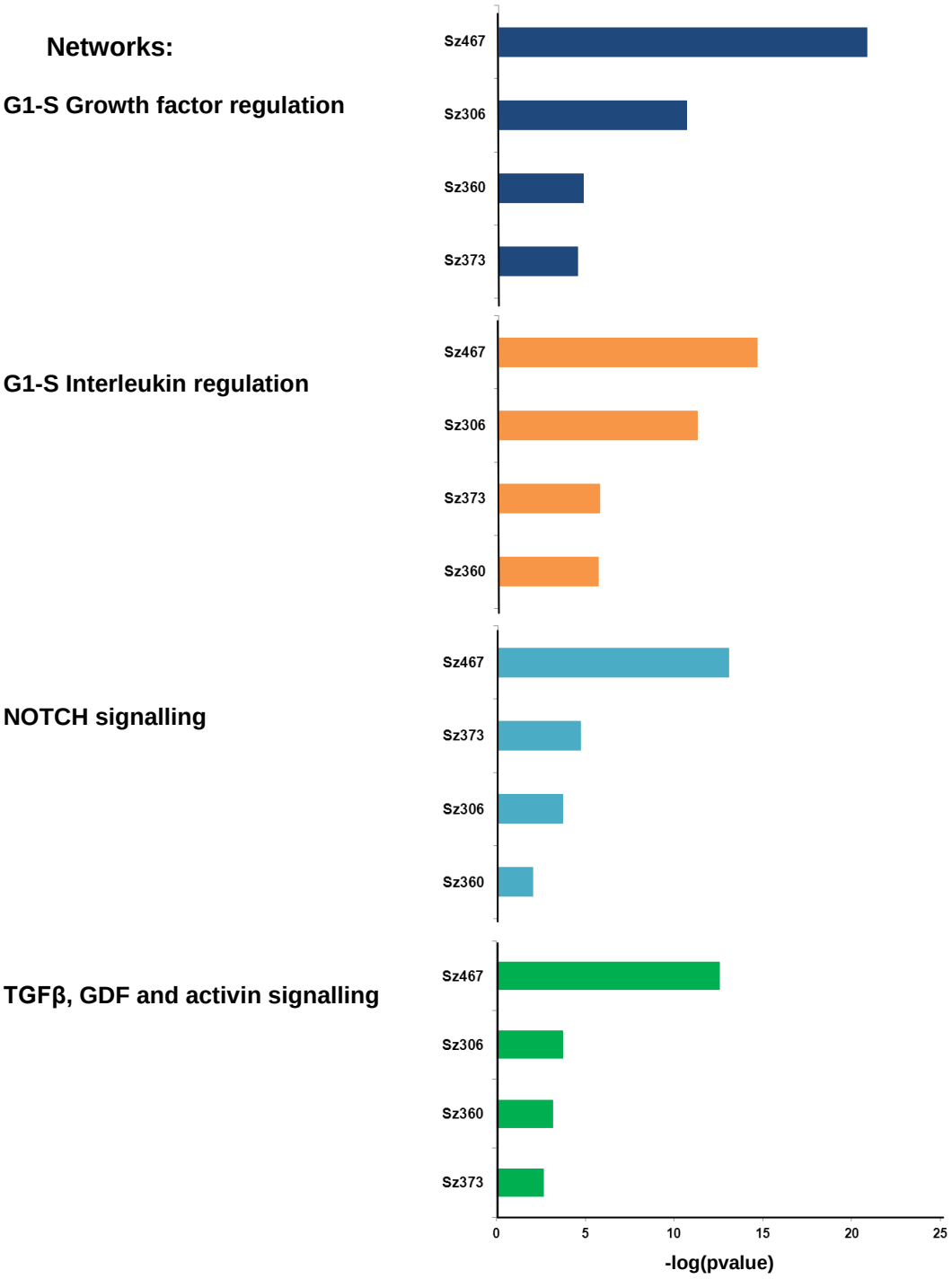

Figure 4.3.4 Top networks that were significantly enriched by targets of miRNAs that exhibited at least 50% difference in abundance in each SC-CAM compared to corresponding SC-ATM from 4 patients. Targets of all 4 pairs were enriched for G1-S growth factor regulation, G1-S interleukin regulation, NOTCH signalling and TGFβ, GDF and activin signalling. (Y-axis: patient in descending magnitude of enrichment. X-axis: log p-value).

Patient	Number of up and down-regulated miRNAs
Sz173	43
Sz193	25
Sz282	18

Table 4.3.17 Numbers of miRNAs that exhibited at least 50% change in abundance in paired samples of oesophageal myofibroblasts (AC-CAMs compared to AC-ATMs) from 3 patients.

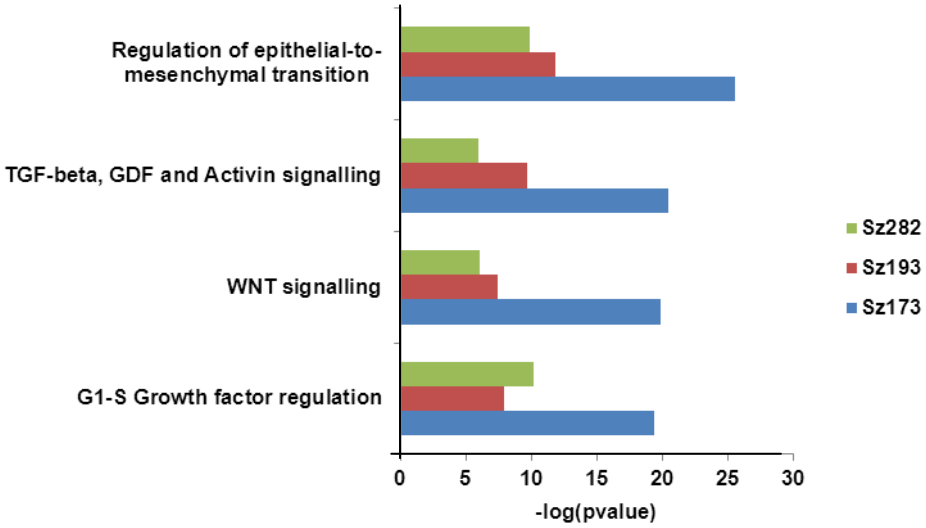

Figure 4.3.5 Top networks that were significantly enriched by targets of miRNAs that exhibited at least 50% difference in abundance in each AC-CAM compared to corresponding AC-ATM from 3 patients. Targets of all 3 pairs were enriched for regulation of epithelial-mesenchymal transition, TGFβ, GDF and activin signalling, Wnt signalling and G1-S growth factor regulation. (Y-axis: networks in descending magnitude of enrichment of Sz173. X-axis: log p-value).

4.4 Discussion

Network enrichment is a differential network analysis to identify the link between miRNA targets and interacting proteins that are involved in different biological mechanisms [255]. Network enrichment analysis was performed by using targets of miRNAs, which exhibited different abundance between myofibroblasts populations. The miRNA targets that were obtained from MetaCore® have been published and mostly experimentally validated. Validated targets of differentially abundant miRNAs that have been listed are useful to predict the functional roles of a particular miRNA. Significant networks that were associated with altered miRNA abundance in CAMs may indicate the biological processes that are deregulated in stromal cells, thus contributing to cancer initiation and progression.

Importantly, Wnt signalling was found to be highly significant in both pairwise and paired individual sample analyses of gastric CAMs and corresponding ATMs. The results suggest that the Wnt signalling pathway is altered in gastric CAMs and may contribute to the tumour-promoting properties of CAMs. In addition, TGF, GDF and activin signalling was one of the top ten networks that were significantly enriched by targets of miRNAs in pairwise and individual comparisons between oesophageal SC-CAMs and SC-ATMs, and between oesophageal AC-CAMs and AC-ATMs.

Comparisons between CAMs and NTMs were performed to identify cellular processes that may be altered in myofibroblasts during carcinogenesis. The results suggest that regulation of cell cycle progression is commonly altered in CAMs of upper gastrointestinal tract cancers, and this is consistent with the current knowledge of biology in CAMs [179]. It is also suggested that CAMs of

oesophageal adenocarcinoma exhibited properties that were found in CAMs from both gastric and oesophageal squamous cell carcinomas. Moreover, comparisons between ATMs and NTMs would be useful to identify changes in myofibroblasts that are induced by chronic inflammation (e.g. *H. pylori* infection, Barrett's metaplasia). In both gastric and oesophageal myofibroblasts, the results from network enrichment analysis identified Wnt signalling, TGF, GDF and activin signalling, and cell cycle regulation as highly significant networks.

There are some limitations of the network analysis for identifying miRNA functions. Firstly, the results may be biased because miRNA targets from MetaCore® may be associated with networks which have been studied widely while other networks are less populated with targets. Secondly, some of the significantly enriched networks may not apply to the context of myofibroblasts in the microenvironment (e.g. EMT). Thirdly, the present study used cultured myofibroblasts, which do not interact with other cell types in a tissue or tumour, so they do not accurately reflect the properties of stromal cells in the microenvironment. Lastly, there could be more functional miRNA targets that have not yet been identified and validated. As a result, enriched networks which have been identified may not truly represent the cellular functions that are influenced by miRNA regulation. Nonetheless, using current knowledge of miRNAs and cellular biology, network enrichment analysis is a time efficient approach for predicting cellular processes that are regulated by multiple miRNAs, which in turn, can be exploited for experimental work to support the findings.

Besides MetaCore®, other software, such as Ingenuity System Pathway Analysis software and DAVID (system 6.7), could be used for identifying the biological function of a set of target genes. Typically in these studies, different results may be obtained when different software is used. In addition, advances in miRNA bioinformatics have led to the development of DIANA-miRPath (v2.0), which allows the integrated analysis of miRNA targets with Kyoto Encyclopedia of Genes and Genomes (KEGG) pathway enrichment. The main advantage of using this software is that miRNA targets can be retrieved directly from TarBase or prediction algorithms. Moreover, a recent study has used co-expression meta-analysis in which miRNAs and target genes are associated by the degree of co-expression, so that the biological function of these associated targets is determined [256]. This has identified, for example, the association of miR-519d, miR-190 and miR-340 with TGF-β signalling pathway, thus demonstrated the synergy of coexpressed miRNAs in the regulation of gene expression [231, 256].

In chapter 3, hsa-miR-181d had been shown to be significantly up-regulated in gastric CAMs compared to their corresponding ATMs. The microarray data indicated higher abundance of hsa-miR-181d in 5 of the 12 pairs of gastric CAMs and ATMs (i.e. Sz190, Sz389, Sz192, Sz198 and Sz45), and validation using RT-PCR analysis was carried out using paired samples of Sz190 and Sz192. In addition, other studies have shown that miR-181 expression is regulated by nuclear factor-kappa B (NF-$_K$β) signalling [251], Wnt/β-catenin signalling [254] and TGF-β signalling [250, 257]. Taken all the data together, it seems there may be a relationship between hsa-miR-181d and Wnt signalling in gastric CAMs.

Microarray gene expression analysis of three validated targets of the miR-181 family, namely, TIMP3, GATA6 and NLK was carried out. TIMP3 was chosen because it has been shown to regulate the activity of MMPs and may contribute to ECM remodelling and wound healing [258]. Consistent with this, predicted mRNA targets of the miR-181 family that encode extracellular proteins were enriched for networks associated with ECM remodelling and connective tissue degradation. Additionally, the mRNA abundance of GATA6 and NLK was analysed as they have been shown to activate and inhibit the canonical Wnt/β-catenin signalling pathway, respectively [121, 259]. The results from gene expression analysis showed that the mRNA abundance of TIMP3 was down-regulated in gastric CAMs from paired samples of Sz190, Sz192 and Sz389. The results also indicated an inverse correlation between TIMP3 and hsa-miR-181d, compatible with the idea that TIMP3 is regulated by hsa-miR-181d in gastric CAMs. In gastric CAMs, GATA6 and NLK might be regulated by hsa-miR-181d at the translational level, but Western blot analysis still needs to be performed.

After analysing miRNA expression profiles and miRNA regulatory networks, the next chapter aimed to validate the Wnt signalling pathway that was regulated by altered miRNA abundance and to demonstrate Wnt signalling in gastric CAMs and their influence in cancer progression.

CHAPTER FIVE

Wnt signalling in gastric myofibroblasts and cancer cells

5.1 Introduction

The previous chapter aimed to identify biological processes associated with differential miRNA abundance in different populations of myofibroblasts. Using MetaCore®, enriched networks were identified using validated targets of miRNAs that exhibited difference in abundance in gastric CAMs compared to their corresponding ATMs. The results from both pairwise and individual comparisons showed that Wnt signalling was the most significantly affected network. Nevertheless, the molecular biology of deregulated Wnt signalling pathway in gastric CAMs compared to ATMs is not at all understood.

Wnt glycoproteins (e.g. Wnt-3a, Wnt-5a) are ligands for transmembrane FZD receptors, and they activate the so-called canonical or non-canonical Wnt signalling pathway [260]. The canonical Wnt/β-catenin signalling pathway has been associated with gastric carcinogenesis [261]. This may be attributable to chronic *H. pylori* infection or mutations of Wnt signalling-associated genes (e.g. APC), resulting in translocation of β-catenin into the nucleus and subsequent activation of β-catenin dependent gene transcription in gastric epithelial cells [262, 263]. Additionally, abnormal Wnt-5a expression has been found in about 30% of human gastric cancer samples and is associated with gastric cancer cell migration and invasion through the non-canonical Wnt/Ca^{2+} signalling pathway; there may also be antagonism of the canonical Wnt/β-catenin signalling pathway [264].

In normal gastric mucosa, Wnt-5a has previously been shown to be expressed in peptic/chief cells using immunocytochemistry [264]. However, the expression of WNT5A mRNA in many gastric cancer cell lines has been found to be low or

undetectable using quantitative PCR [264, 265]. It is possible that Wnt-5a is expressed by tumour stromal cells, and this is supported by evidence from other studies. Gene expression profiling has indicated increased Wnt-5a expression in microdissected stromal tissue of pancreatic carcinoma compared to stromal tissue of chronic pancreatitis, and this was validated by using immunohistochemistry [266]. In addition, ribonuclease protection analysis and *in situ* RNA hybridisation have indicated Wnt-5a transcripts to be up-regulated in macrophages during the formation of colorectal carcinoma [267]. Moreover, using microarray analysis of gene expression, it was found that Wnt-5a was up-regulated in fibroblasts from oesophageal squamous cell carcinoma compared to normal fibroblasts, and this was validated by using quantitative PCR [268]. Since little is known about Wnt signalling in gastric cancer stromal cells, the expression and function of Wnt-5a were investigated in the present study.

The aims for the work described in this chapter were:

5.1.1 To determine the expression of Wnt pathway-associated genes in 12 paired samples of gastric CAMs and ATMs from existing microarray data.

5.1.2 To study the activity of Wnt signalling pathway in gastric myofibroblasts.

5.1.3 To determine molecular and phenotypic changes in paired samples of gastric myofibroblasts, and gastric cancer cells, after incubation with recombinant Wnt-3a or Wnt-5a.

5.2 Methods

Proteins that were annotated in Wnt signalling pathways were retrieved from MetaCore®. Using GeneChip Human Genome U133 Plus 2.0 Array (Appendix 2.2), the relative abundance of transcripts selected from Wnt signalling networks was determined in each gastric CAM compared to its corresponding ATM from 12 patients. Each patient was identified by a Sz identification number and in the gene analysis, each was represented by a Patient number listed in Table 5.2.1. The abundance of WNT5A mRNA in gastric myofibroblasts was determined using quantitative RT-PCR (performed by Dr Islay Steele, Appendix 2.1). The expression of Wnt-5a in gastric myofibroblasts and cancer cell lines (AGS, MKN45) was analysed by Western blotting (Chapter 2.12). Immunocytochemistry using β-catenin mouse monoclonal antibody (Chapter 2.13) was performed in gastric myofibroblasts and MKN45 cells, and expressed as a percentage of cells containing nuclear β-catenin. A promoter reporter construct, which was associated with β-catenin-dependent TCF/LEF transcriptional activation, was transfected into gastric myofibroblasts, and the ratio of firefly luciferase is to Renilla luciferase (internal control) was determined (Chapter 2.17). Proliferation assays using EdU incorporation (Chapter 2.14) and migration assays using Boyden chambers (Chapter 2.16) were carried out after incubation with recombinant Wnt-3a or Wnt-5a.

No.	Patient
Patient 1	Sz42
Patient 2	Sz45
Patient 3	Sz190
Patient 4	Sz192
Patient 5	Sz194
Patient 6	Sz198
Patient 7	Sz268
Patient 8	Sz271
Patient 9	Sz294
Patient 10	Sz305
Patient 11	Sz308
Patient 12	Sz389

Table 5.2.1 Paired individual samples of gastric CAMs and ATMs from 12 patients. Each patient number represents a Sz identification number.

5.3 Results

5.3.1 Gene expression analysis of Wnt signalling networks

To investigate the biology of Wnt signalling pathways in gastric myofibroblasts, analysis of selected genes associated with Wnt signalling networks was performed using previously generated microarray data. In total, there are more than 150 proteins that comprise the MetaCore® Wnt signalling network. These include Wnt proteins, FZD receptors, co-receptors, putative Wnt-responsive genes and relevant intracellular signalling molecules. Initial microarray analysis showed that the transcriptomes of gastric CAMs and ATMs encoded a subset of these proteins only. For example, of all the 18 WNT genes that were represented by oligonucleotides (i.e. probes) bound to the array, WNT5A and WNT5B were found to be expressed in all samples of gastric CAMs and ATMs while the remaining genes were either undetectable or in low expression.

From gene expression data, a total of 20 transcripts were selected as they were included in Wnt signalling networks and were expressed in all samples of CAMs and ATMs. These were then classified according to their protein class, namely, receptor ligands, receptors, transcription factors, binding proteins and enzymes. In microarray analysis, there were a variable number of oligonucleotides on the array for every transcript and the signal intensity varied among oligonucleotides of a particular transcript. Thus, the mRNA abundance of each relevant oligonucleotide for selected transcripts was determined in each paired sample of gastric CAMs and ATMs from 12 patients.

The relative mRNA abundance of (A) WNT5A, (B) WNT5B and (C) TGFB2 that encode protein ligands, in each gastric CAM compared to corresponding ATM, was shown in Figure 5.3.1. Of 12 patients, a total of 10 patients, except for Sz294 and Sz305, were found to exhibit WNT5A mRNA abundance greater than 1, indicating WNT5A mRNA is up-regulated in CAMs compared to ATMs. Additionally, WNT5B mRNA abundance was found to be distinctively up-regulated in CAMs from Sz190 and Sz389. It was also found that the mRNA abundance of TGFB2 was up-regulated in paired samples from 8 of the 12 patients. When the average mRNA abundance of all relevant oligonucleotides for a transcript was determined in all CAMs and all ATMs, the results showed that the mRNA abundance of WNT5A and TGFB2 was significantly (paired t-test, $p < 0.05$) different with a fold-increase of 1.8 and 2.4, respectively, in gastric CAMs compared to ATMs (Figures 5.3.1D, 5.3.1E).

The same approach was used to analyse the abundance of other transcripts that were selected. Using 12 paired individual samples of CAMs compared to its ATMs, the relative mRNA abundance of: (A) FZD1, (B) FZD2, (C) FZD4, (D) FZD6, (E) FZD7 and (F) FZD8 that encode frizzled receptors, (G) LRP6 and (H) RYK that encode co-receptors and (I) PLAUR, which encodes uPA receptor, were determined (Figure 5.3.2). Across all 12 paired samples, FZD2 and RYK did not exhibit a great difference in mRNA abundance between CAMs and corresponding ATMs. Additionally, it was found that some individual CAMs exhibited abundance increase of more than 2-fold compared to their corresponding ATMs: FZD1 from Sz308, FZD4 from Sz190 and Sz305, FZD6 from Sz190, and FZD8 from Sz192, Sz194, Sz268 and Sz308. The mRNA abundance of PLAUR was

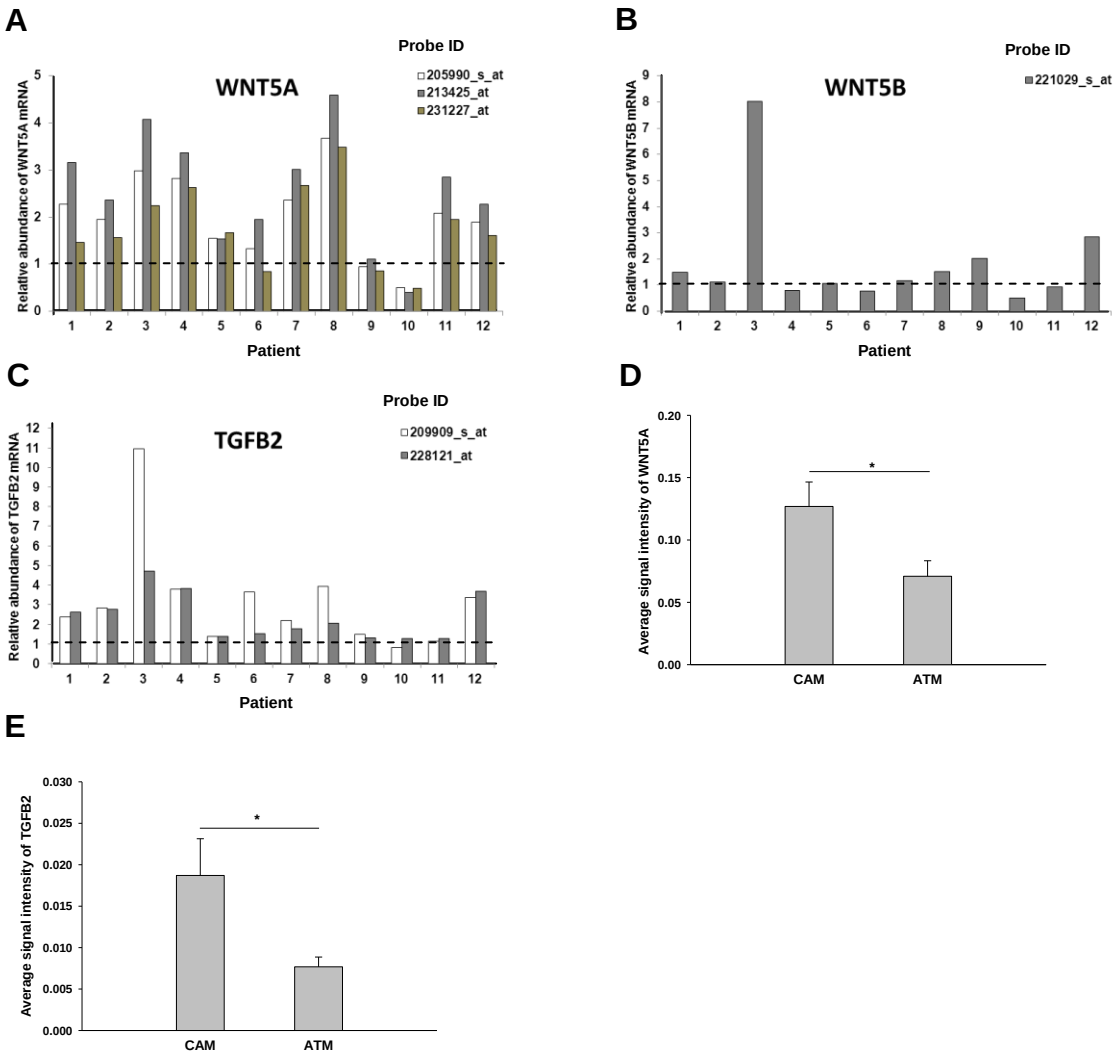

Figure 5.3.1 Microarray analysis of transcripts that encode receptor ligands in paired samples of gastric myofibroblasts from 12 patients. The abundance of (A) WNT5A which was represented by three oligonucleotides, (B) WNT5B which was represented by one oligonucleotide and (C) TGFB2 which was represented by one oligonucleotide in each gastric CAM compared to corresponding ATM (abundance = 1.0). (D) The average signal intensity of WNT5A in CAMs (n =12) and ATMs (n = 12). (E) The average signal intensity of TGFB2 in CAMs (n =12) and ATMs (n = 12). Values were normalised to GAPDH. Each patient number representing a Sz identification number is indicated in Table 5.2.1. (*$p < 0.05$)

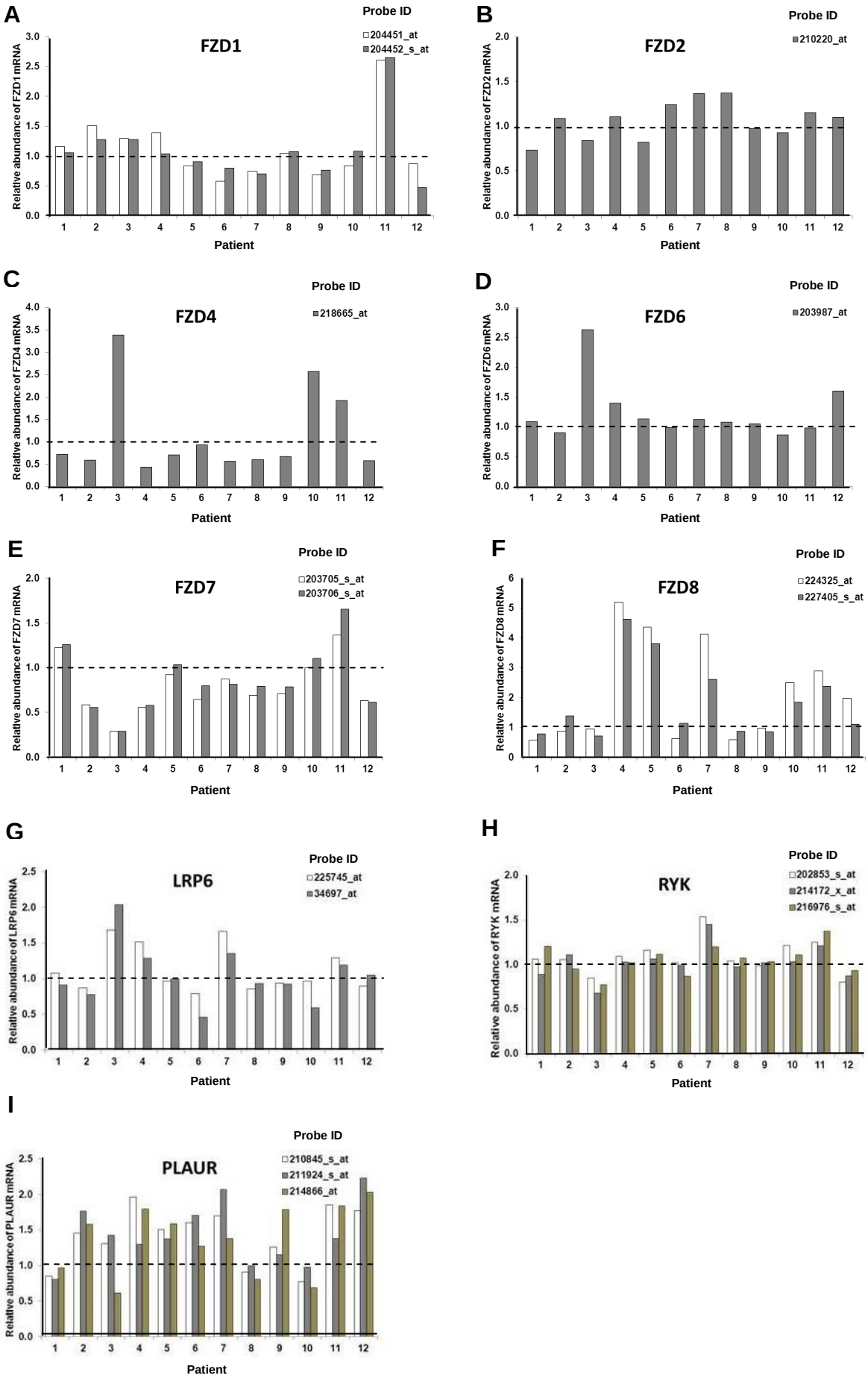
A
FZD1
Probe ID
204451_at
204452_s_at
Relative abundance of FZD1 mRNA
Patient
B
FZD2
Probe ID
210220_at
Relative abundance of FZD2 mRNA
Patient
C
FZD4
Probe ID
218665_at
Relative abundance of FZD4 mRNA
Patient
D
FZD6
Probe ID
203987_at
Relative abundance of FZD6 mRNA
Patient
E
FZD7
Probe ID
203705_s_at
203706_s_at
Relative abundance of FZD7 mRNA
Patient
F
FZD8
Probe ID
224325_at
227405_s_at
Relative abundance of FZD8 mRNA
Patient
G
LRP6
Probe ID
225745_at
34697_at
Relative abundance of LRP6 mRNA
Patient
H
RYK
Probe ID
202853_s_at
214172_x_at
216976_s_at
Relative abundance of RYK mRNA
Patient
I
PLAUR
Probe ID
210845_s_at
211924_s_at
214866_at
Relative abundance of PLAUR mRNA
Patient

Figure 5.3.2 Microarray analysis of transcripts that encode FZD and uPA receptors in paired samples of gastric myofibroblasts from 12 patients. The abundance of (A) FZD1 which was represented by two oligonucleotides, (B) FZD2 which was represented by one oligonucleotide, (C) FZD4 which was represented by one oligonucleotide, (D) FZD6 which was represented by one oligonucleotide, (E) FZD7 which was represented by two oligonucleotides, (F) FZD8 which was represented by two oligonucleotides, (G) LRP6 which was represented by two oligonucleotides, (H) RYK which was represented by three oligonucleotides and (I) PLAUR which was represented by three oligonucleotides, in each gastric CAM compared to corresponding ATM (abundance = 1.0). Values were normalised to GAPDH. Each patient number representing a Sz identification number is indicated in Table 5.2.1.

also found to be up-regulated in paired samples from 8 of the 12 patients. However, pairwise comparisons indicated no significant difference between CAMs and their corresponding ATMs in the expression of these receptors.

Subsequently, the relative mRNA abundance in CAMs compared to their corresponding ATMs was analysed for transcripts that encode transcription factors, for example, (A) JUN, (B) MYC, (C) PPARD and (D) TCF7 (Figure 5.3.3), binding proteins, for example, (A) APC and (B) CTNNB1 (Figure 5.3.4) and enzymes, for example, (A) CAMK2D and (B) MMP2 (Figure 5.3.5). In the comparison between CAMs and ATMs, the abundance difference of these transcripts was generally low and again, there was no significant difference in the expression of these transcripts that were associated with Wnt signalling.

5.3.2 Validation of Wnt-5a expression in gastric myofibroblasts by Western blotting and quantitative RT-PCR analyses

Validation was performed to demonstrate an increase in Wnt-5a expression in gastric CAMs compared to ATMs. The expression of Wnt-5a was analysed in 6 pairs of gastric CAMs and their corresponding ATMs by Western blotting (Figure 5.3.6A). Western blots showed a band at 49 kDa and the average band intensity was significantly increased (4-fold) in gastric CAMs compared to ATMs (Figure 5.3.6B). Additionally, quantitative RT-PCR analysis using paired samples from Sz190, Sz192 and Sz268 showed a significant increase (1.7-fold) in WNT5A mRNA abundance when gastric CAMs were compared to ATMs (Figure 5.3.6C).

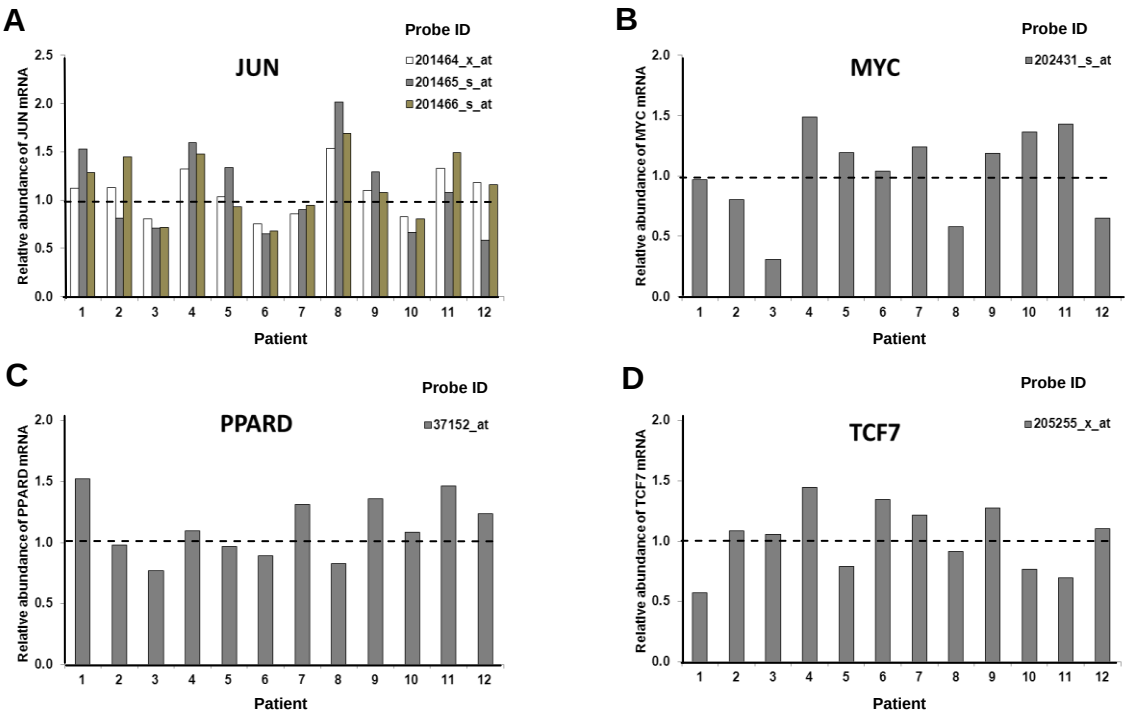

Figure 5.3.3 Microarray analysis of transcripts that encode transcription factors in paired samples of gastric myofibroblasts from 12 patients. The abundance of (A) JUN which was represented by three oligonucleotides, (B) MYC which was represented by one oligonucleotide, (C) PPARD which was represented by one oligonucleotide and (D) TCF7 which was represented by one oligonucleotide, in each gastric CAM compared to corresponding ATM (abundance = 1.0). Values were normalised to GAPDH. Each patient number representing a Sz identification number is indicated in Table 5.2.1.

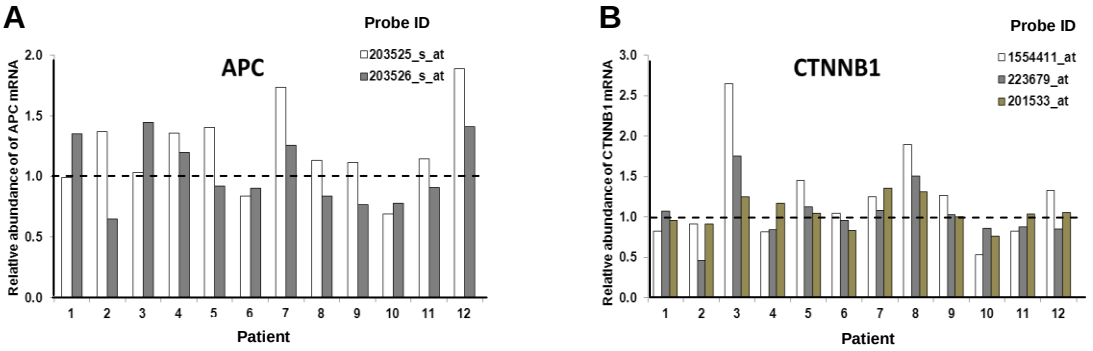

Figure 5.3.4 Microarray analysis of transcripts that encode binding proteins in paired samples of gastric myofibroblasts from 12 patients. The abundance of (A) APC which was represented by two oligonucleotides and (B) CTNNB1 which was represented by three oligonucleotides, in each gastric CAM compared to corresponding ATM (abundance = 1.0). Values were normalised to GAPDH. Each patient number representing a Sz identification number is indicated in Table 5.2.1.

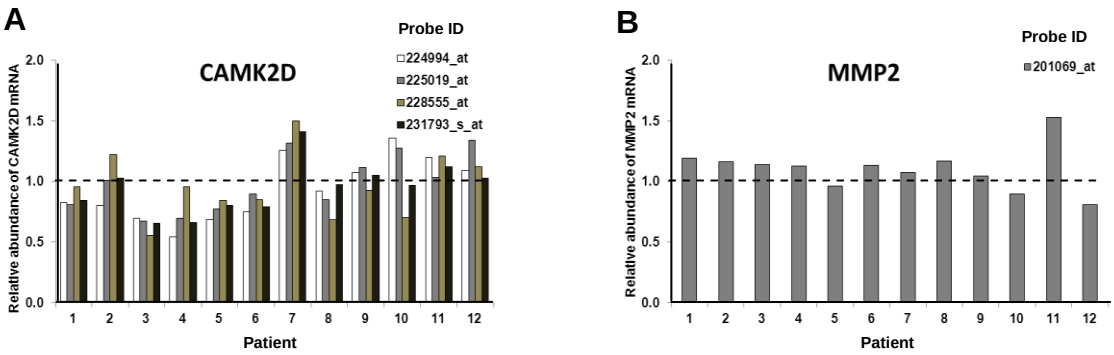

Figure 5.3.5 Microarray analysis of transcripts that encode enzymes in paired samples of gastric myofibroblasts from 12 patients. The abundance of (A) CAMK2D which was represented by four oligonucleotides and (B) MMP2 which was represented by one oligonucleotide, in each gastric CAM compared to corresponding ATM (abundance = 1.0). Values were normalised to GAPDH. Each patient number representing a Sz identification number is indicated in Table 5.2.1.

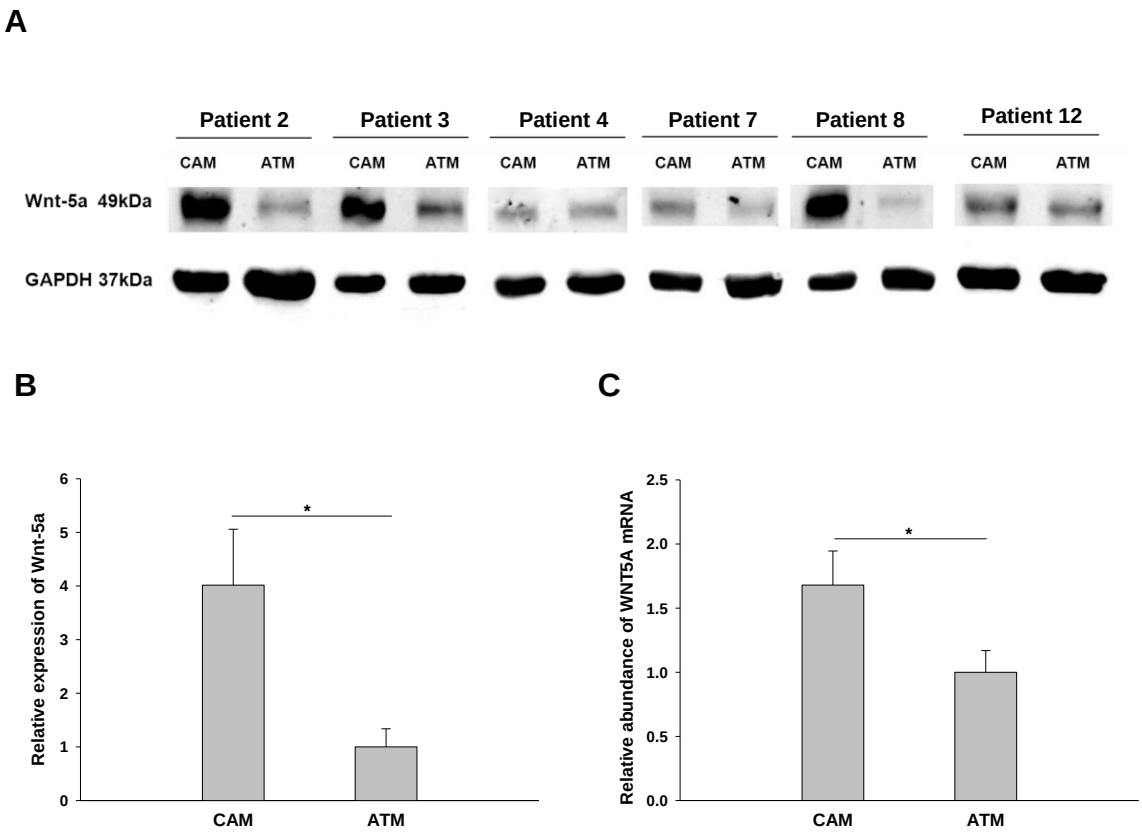

Figure 5.3.6 Increase in Wnt-5a expression in gastric CAMs. (A) Western blot analysis of Wnt-5a in 6 pairs of gastric CAMs and corresponding ATMs by using cell lysates. GAPDH was the loading control. (B) The average band intensity of Wnt-5a expression in CAMs (n = 6) and ATMs (n = 6) was determined by Western blotting. (C) The average abundance of WNT5A mRNA in CAMs (n = 3) and ATMs (n = 3) was determined by quantitative RT-PCR. Each experiment was performed in triplicate. Values were normalised to GAPDH. Each patient number representing a Sz identification number is indicated in Table 5.2.1. (*$p < 0.05$)

5.3.3 Activation of the canonical Wnt signalling pathway in gastric CAMs but to a lesser extent in their corresponding ATMs

Previously in Chapter 4, Wnt signalling was suggested to be targeted by differential miRNA abundance in gastric CAMs compared to their corresponding ATMs, but the molecular mechanism was unknown. To investigate the activity of canonical Wnt/β-catenin signalling in gastric CAMs and ATMs, immunocytochemistry using β-catenin mouse antibody was performed followed by quantification of myofibroblasts containing nuclear β-catenin.

Fluorescence images showed cytoplasmic and nuclear staining of β-catenin in paired samples of gastric CAMs and ATMs from Sz192 (Figure 5.3.7A). The cell number was determined by DAPI nuclear staining. The identification of nuclear β-catenin was generally complicated by high background when myofibroblasts were cultured in medium containing serum. Despite this, the immunocytochemistry results showed that gastric CAMs contained a higher number of myofibroblasts with nuclear localisation of β-catenin, compared to corresponding ATMs, in all 4 paired samples from Sz45, Sz190, Sz192 and Sz268, (Figure 5.3.7B).

Since an increase in nuclear β-catenin is linked to the transcriptional activity of TCF/LEF in gastric CAMs, a paired sample of gastric CAMs and ATMs from Sz192 was selected to test the hypothesis that TCF/LEF activity was increased in CAMs. It was selected because previous RT-PCR analyses validated the higher abundance of WNT5A and hsa-miR-181d in gastric CAMs compared to ATMs. Using TCF/LEF reporter assay, luciferase activity of TCF/LEF was 50% higher in CAMs than in ATMs (Figure 5.3.8). The above hypothesis was validated, thus indicating increased activity of the canonical Wnt/β-catenin pathway in CAMs.

A

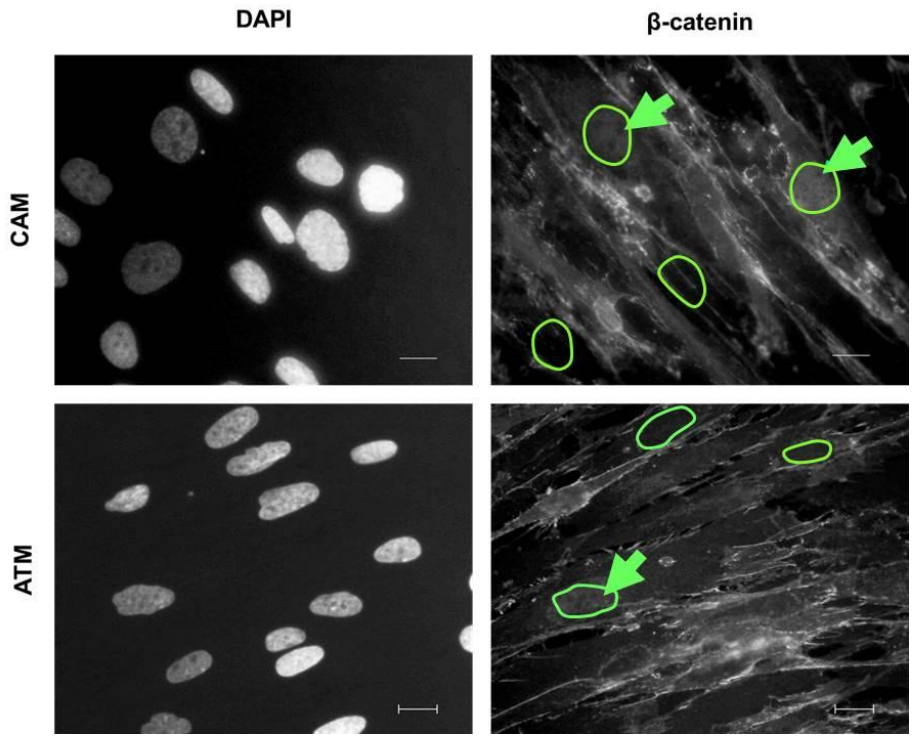

B

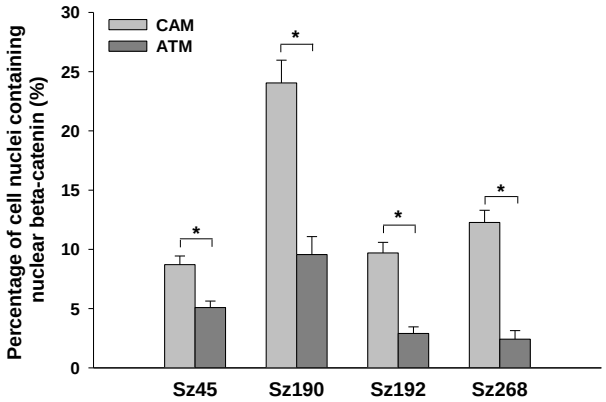

Figure 5.3.7 Increased nuclear localisation of β-catenin in gastric CAMs compared to corresponding ATMs. (A) Representative immunofluorescence images of nuclear β-catenin using a paired sample of gastric CAMs and ATMs. Scale bars 20μm. Nuclei of myofibroblasts are outlined, and arrows indicate nuclear staining of β-catenin. (B) Percentage of myofibroblasts containing nuclear β-catenin was determined using 4 paired samples of CAMs and corresponding ATMs. (*$p < 0.05$)

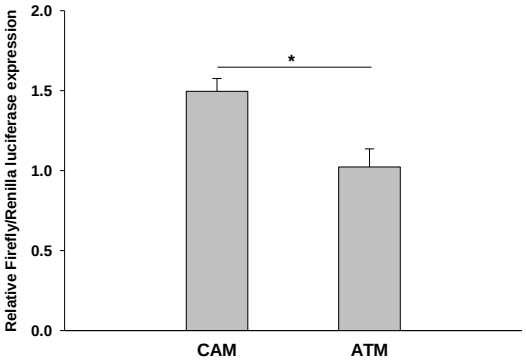

Figure 5.3.8 Gastric CAMs exhibit higher TCF/LEF activity. Using TCF/LEF reporter construct, luciferase expression was significantly increased in CAMs compared to corresponding ATMs. Each experiment was performed in triplicate. (*$p < 0.05$)

5.3.4 Increased nuclear localisation of β-catenin in MKN45 cells and gastric myofibroblasts by recombinant Wnt-3a

Wnt-3a is a well-known Wnt protein that activates the canonical Wnt/β-catenin signalling pathway, which prevents cytoplasmic degradation of β-catenin and subsequently induces nuclear translocation of β-catenin [116]. MKN45 cells were used to identify nuclear localisation of β-catenin in the presence of recombinant Wnt-3a and to determine the optimal conditions for β-catenin immunocytochemistry. Fluorescence images showed membranous and nuclear staining of β-catenin in MKN45 cells (Figure 5.3.9A). The cell number was determined by DAPI nuclear staining. There was an intense staining for β-catenin on cell membranes of MKN45 control cells, indicating a role in cell adhesion. After stimulation with 1 μg/ml Wnt-3a for 1 h, cytoplasmic and nuclear staining of β-catenin was clearly seen in MKN45 cells while staining intensity on cell membranes was decreased. The percentage of MKN45 cells containing nuclear β-catenin was significantly increased (4.4-fold) after incubation with Wnt-3a (Figure 5.3.9B).

Similarly, when a paired sample of gastric CAMs and ATMs was incubated with 1 μg/ml Wnt-3a for 1 h, localisation of β-catenin in the nuclei of myofibroblasts was observed even though there was some background staining (Figure 5.3.10A). There was cytoplasmic staining of β-catenin in control myofibroblasts. After incubation with Wnt-3a, nuclear and perinuclear staining of β-catenin was observed.

A

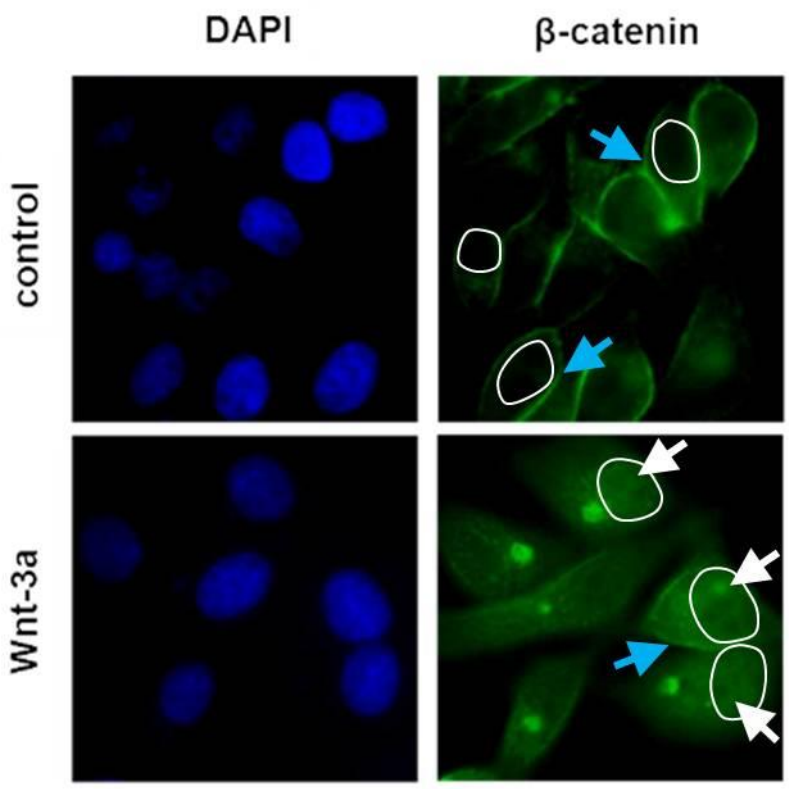

B

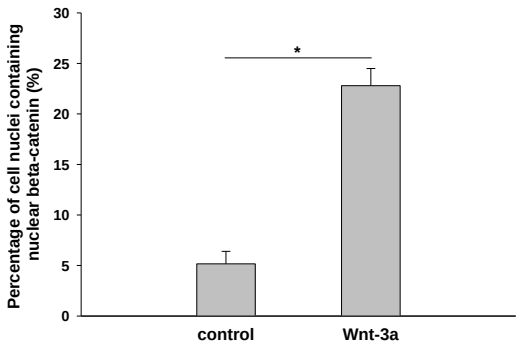

Figure 5.3.9 Increased nuclear localisation of β-catenin in MKN45 cells by recombinant Wnt-3a. (A) Representative immunofluorescence images showed localisation of β-catenin on cell membranes and in the nuclei before and after incubation with Wnt-3a (1 µg/ml, 1 h). Cell nuclei are outlined. Blue arrows indicate staining of membrane bound β-catenin and white arrows indicate nuclear staining of β-catenin. (B) Percentage of cells containing nuclear β-catenin was determined in MKN45 cells before and after incubation with Wnt-3a. Each experiment was performed in triplicate. (*$p < 0.05$)

A

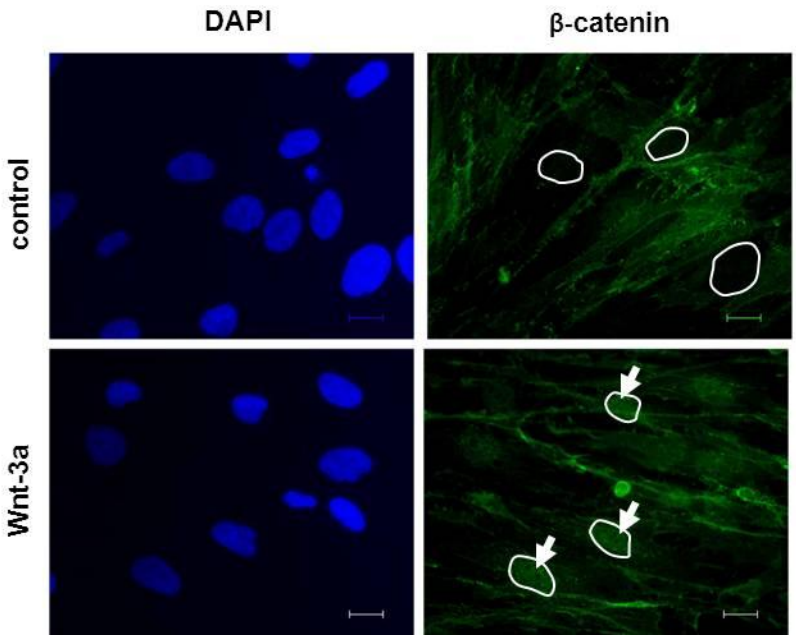

B

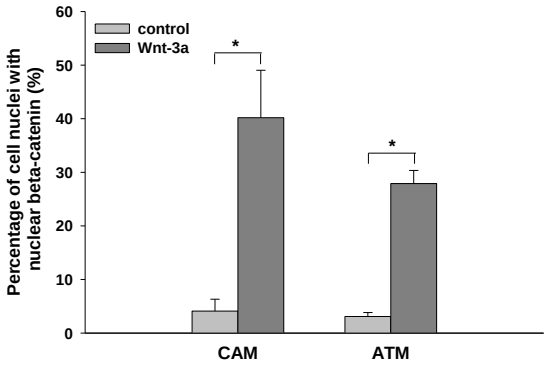

Figure 5.3.10 Increased nuclear localisation of β-catenin in gastric myofibroblasts by recombinant Wnt-3a. (A) Representative immunofluorescence images of β-catenin localisation in gastric myofibroblasts before and after incubation with Wnt-3a (1 µg/ml, 1 h). Cell nuclei are outlined and arrows indicate nuclear staining of β-catenin. Scale bars 20 µm. (B) Percentage of gastric myofibroblasts containing nuclear β-catenin was significantly increased in a paired sample of CAMs and ATMs after incubation with Wnt-3a. Each experiment was performed in triplicate. (*$p < 0.05$)

The percentage of myofibroblasts containing nuclear β-catenin was significantly increased in CAMs (10-fold) and ATMs (9-fold) after incubation with Wnt-3a (Figure 5.3.10B).

Since Wnt-5a expression was found to be increased in gastric CAMs, the biological role of Wnt-5a in gastric myofibroblasts was investigated. The same pair of CAMs and ATMs being used for the above experiment was stained with β-catenin antibody after incubation with recombinant Wnt-5a so as to determine whether Wnt-5a induced nuclear localisation of β-catenin in gastric myofibroblasts. Fluorescence images did not clearly show nuclear staining of β-catenin in gastric myofibroblasts after incubation with Wnt-5a (Figure 5.3.11A). Also, the percentage of CAMs and ATMs that contained nuclear β-catenin before and after Wnt-5a incubation was not significantly different (Figure 5.3.11B).

5.3.5 Increased TCF/LEF activity and WNT5A mRNA in gastric CAMs by recombinant Wnt-3a

In the earlier section, the activity of TCF/LEF was found to be up-regulated in CAMs compared to ATMs. Here, luciferase activity of TCF/LEF was determined in CAMs and ATMs after incubation with 1 μg/ml Wnt-3a or Wnt-5a for 8 h. The results showed that Wnt-3a, but not Wnt-5a, significantly increased (2.3-fold) luciferase activity of TCF/LEF in CAMs (Figure 5.3.12A). Luciferase activity of TCF/LEF in ATMs was significantly decreased (1.8-fold) by Wnt-5a, but no significant change was found by Wnt-3a (Figure 5.3.12B).

A

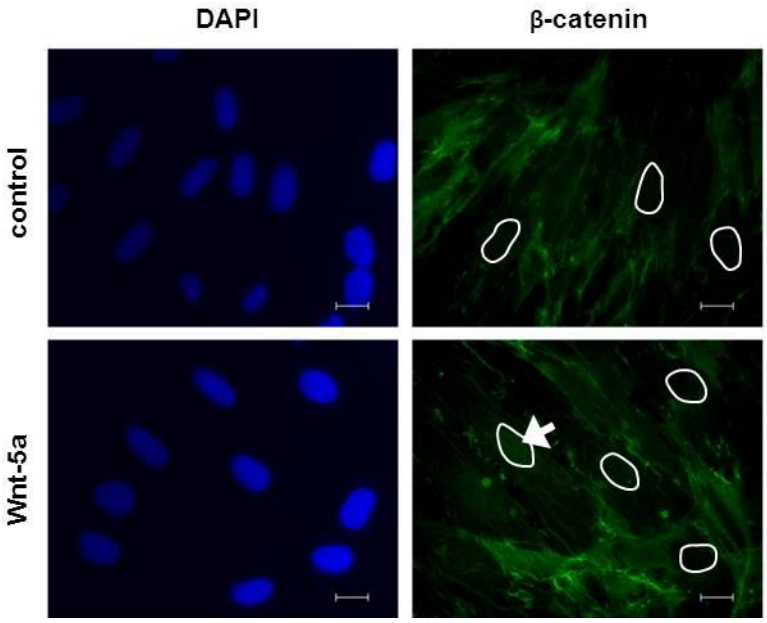

B

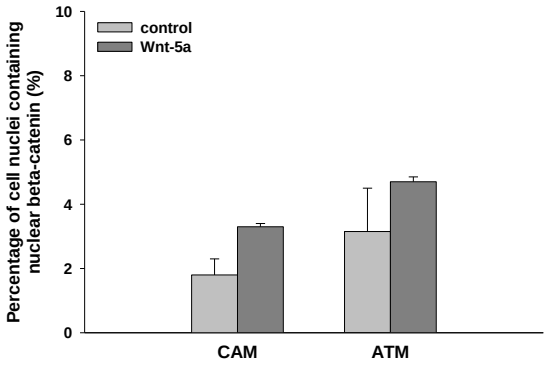

Figure 5.3.11 No significant change in nuclear localisation of β-catenin in gastric myofibroblasts by Wnt-5a. (A) Representative immunofluorescence images of β-catenin localisation in gastric myofibroblasts before and after incubation with Wnt-5a (1 µg/ml, 1 h). Cell nuclei are outlined and arrow indicates nuclear staining of β-catenin. Scale bars 20 µm. (B) Percentage of myofibroblasts containing nuclear β-catenin in a paired sample of CAMs and corresponding ATMs. Each experiment was performed in triplicate.

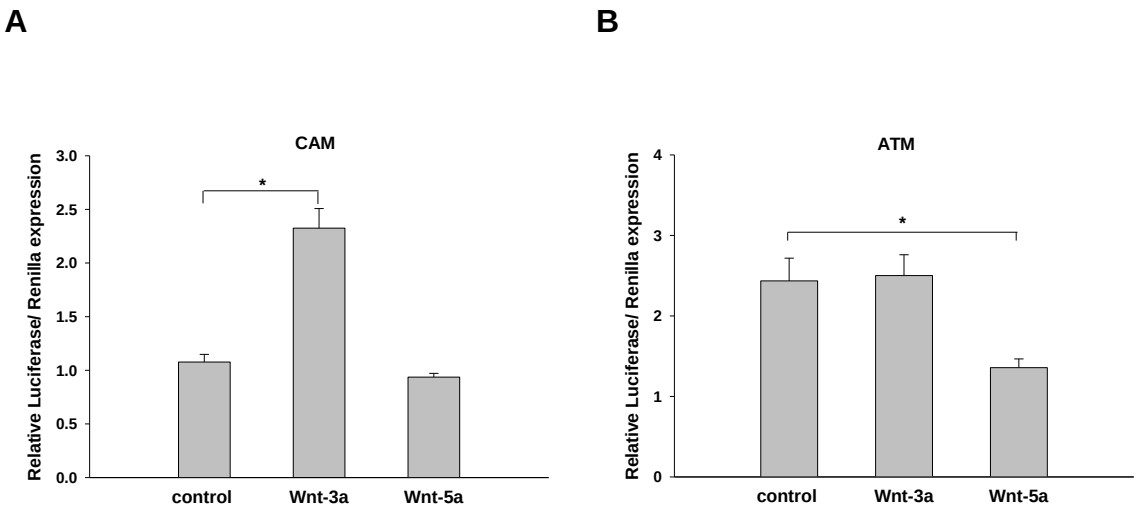

Figure 5.3.12 Wnt-3a induces TCF/LEF activity in gastric CAMs, but not in ATMs. (A) Luciferase activity of TCF/LEF reporter was significantly increased in CAMs after incubation with Wnt-3a (1 µg/ml, 8 h) but not Wnt-5a. (B) In ATMs, luciferase activity of TCF/LEF reporter was not significantly changed after incubation with Wnt-3a but a significant decrease was found after incubation with Wnt-5a (1 µg/ml, 8 h). Each experiment was performed in triplicate. (*$p < 0.05$)

Furthermore, RT-PCR analysis showed that the mRNA abundance of WNT5A was significantly increased (1.7-fold) in gastric CAMs after incubation with 1 µg/ml Wnt-3a for 24 h (Figure 5.3.13). The mRNA abundance of WNT5A was not significantly altered in CAMs when incubated with Wnt-5a. The results, therefore, suggest that Wnt-3a increases the activity of β-catenin-dependent TCF/LEF and induces the abundance of WNT5A in gastric CAMs.

5.3.6 Increased migration of gastric myofibroblasts and AGS cells by recombinant Wnt-5a

To investigate if Wnt proteins influenced migration in myofibroblasts and AGS cells, Boyden chambers were used to determine the number of cells that migrated through the membrane pores in the presence of 1 µg/ml recombinant Wnt-3a or Wnt-5a. The results showed that Wnt-3a significantly increased the migration of CAMs (2-fold), but not ATMs (Figure 5.3.14A) and that Wnt-5a significantly increased the migration of CAMs (3.5-fold) and ATMs (5.9-fold) (Figure 5.3.14B). In AGS cells, both Wnt-3a and Wnt-5a stimulated cell migration with a fold-increase of 2.7 and 3.3, respectively (Figure 5.3.14C).

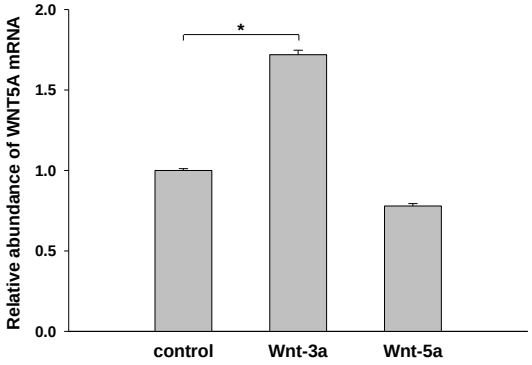

Figure 5.3.13 Wnt-5a expression in gastric CAMs is induced by Wnt-3a. The mRNA abundance of WNT5A was significantly increased in gastric CAMs after incubation with Wnt-3a (1 µg/ml, 24 h), but not Wnt-5a. Each experiment was performed in triplicate. (*$p < 0.05$)

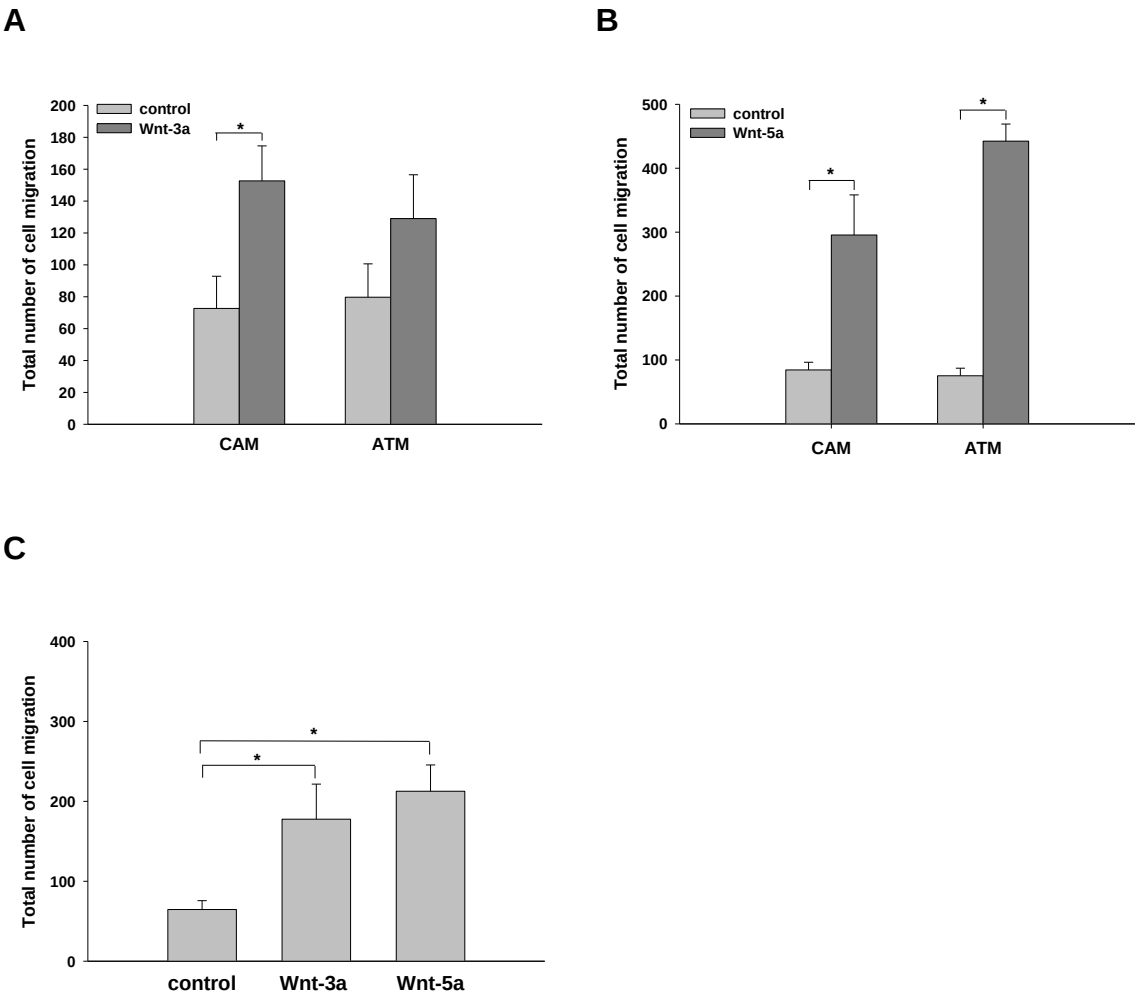

Figure 5.3.14 Increase in migration of gastric myofibroblasts and AGS cells by Wnt-5a. (A) There was a significant increase in the migration of CAMs, but not in ATMs after incubation with Wnt-3a (1 µg/ml, 16 h). (B) Incubation with Wnt-5a (1 µg/ml, 16 h) significantly increased the migration of CAMs and ATMs. (C) The migration of AGS cells was significantly increased after incubation with Wnt-3a or Wnt-5a (1 µg/ml, 16 h). Each experiment was performed in triplicate. (*$p < 0.05$)

5.3.7 Proliferation of gastric myofibroblasts is stimulated by Wnt-5a and Wnt-3a

Using EdU incorporation assay, proliferation of gastric myofibroblasts, AGS and MKN45 cells was determined after incubation with 1 µg/ml Wnt-3a or Wnt-5a. Proliferating cells that incorporated with EdU were counted, and IGF-II was used as a positive control for gastric myofibroblasts (Figure 5.3.15A). The results showed that Wnt-3a and Wnt-5a significantly increased the rate of proliferating CAMs (Figure 5.3.15B) and ATMs (Figures 5.3.15C), whereas proliferation of AGS (Figure 5.3.15D) and MKN45 cells (Figure 5.3.15E) was not significantly changed by Wnt-3a or Wnt-5a.

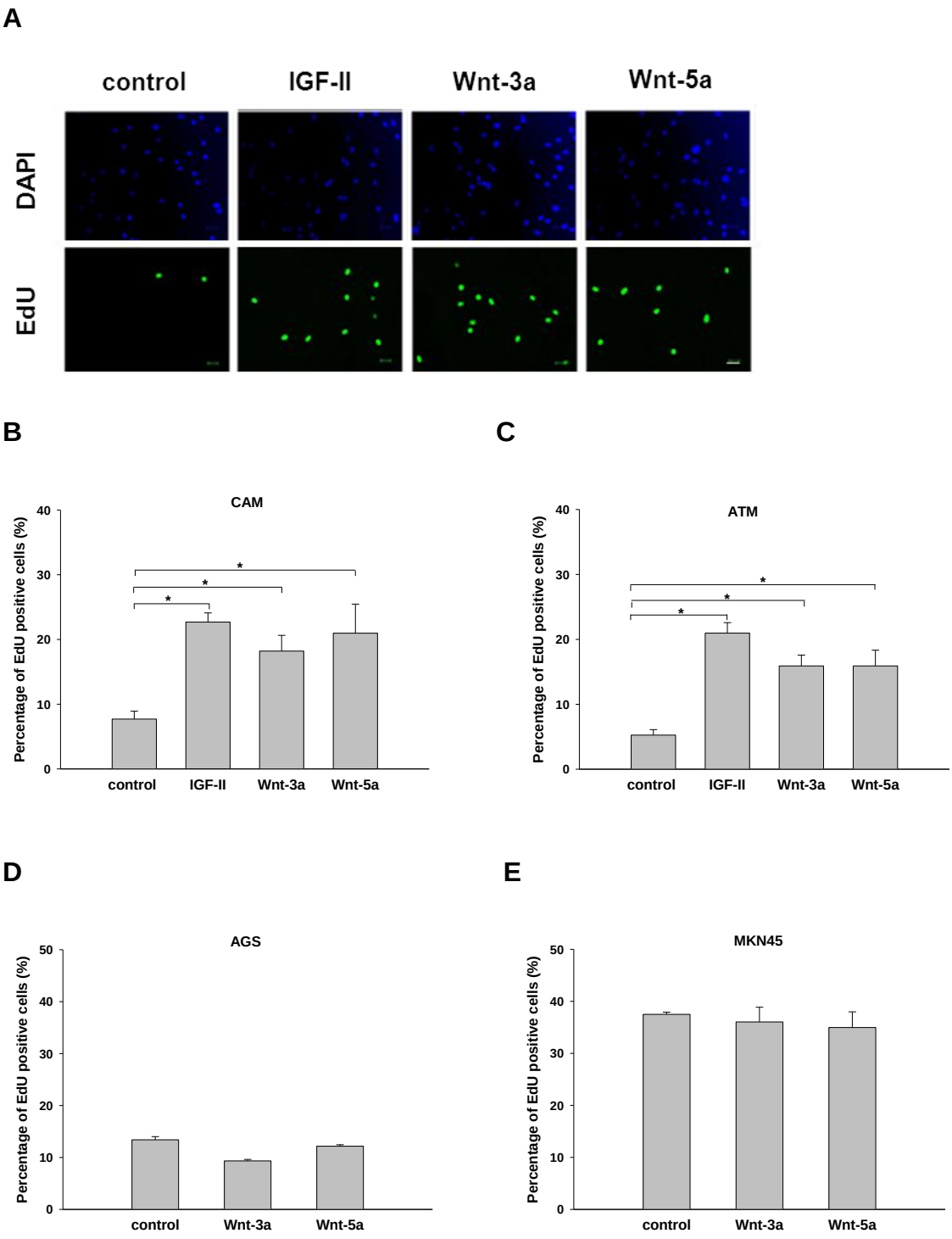

Figure 5.3.15 EdU incorporation in proliferating gastric myofibroblasts is induced by Wnt-3a and Wnt-5a. (A) Representative immunofluorescence images of proliferating cells that incorporated with EdU (green) after incubation with 1 µg/ml Wnt-3a or Wnt-5a for 24 h. IGF-II (100 ng/ml) was a positive control. Scale bars 50 µm. (B) Percentage of EdU positive cells in CAMs when incubated with Wnt-3a or Wnt-5a for 24 h. (C) Percentage of EdU positive cells in ATMs when incubated with Wnt-3a or Wnt-5a for 24 h. (D, E) No significant change in the proliferation rate of AGS and MKN45 cells after Wnt-3a or Wnt-5a incubation. Each experiment was performed in triplicate. (*$p < 0.05$)

5.4 Discussion

In the previous chapter, validated targets of significantly different miRNAs in gastric CAMs compared to their corresponding ATMs were enriched for cell cycle regulation and Wnt signalling. Furthermore, the Wnt signalling was significantly enriched with validated targets of miRNAs that were different in abundance in the comparison between each gastric CAM and its corresponding ATM from 12 patients. These findings indicate alterations of Wnt signalling pathways in gastric CAMs that could be attributable to miRNA regulation. Nevertheless, this analysis does not provide an indication of whether the Wnt signalling is up or down-regulated in CAMs or of which specific targets are affected.

In this chapter, it was shown that Wnt-5a expression is increased in gastric CAMs and that Wnt-5a induces migration and proliferation of gastric CAMs. The mechanisms are thought to involve the non-canonical Wnt signalling pathway because it was found that Wnt-5a did not induce nuclear localisation of β-catenin or increase the TCF/LEF transcriptional activity that are markers for stimulation of the canonical Wnt pathway.

To validate the bioinformatic data of miRNAs and Wnt signalling, the abundance of 20 transcripts, which were associated with Wnt signalling, was analysed in each of the 12 paired samples of gastric CAMs compared to their ATMs. Of all the 20 transcripts, the mRNA abundance of WNT5A and TGFB2 were significantly up-regulated in CAMs compared to ATMs. The link between Wnt-5a and TGFβ2 is not necessarily unexpected because the expression of Wnt-5a has been shown to be up-regulated by TGF-β signalling [269]. Additionally, gene analysis revealed that AGS and MKN45 cells did not express WNT5A mRNA. As a result, Wnt-5a

was selected for an investigation of its role in gastric CAMs and stromal-tumour interactions. Higher abundance of Wnt-5a in CAMs compared to ATMs was validated by Western blotting and quantitative PCR analyses. These analyses suggest increased abundance or activity of extracellular Wnt-5a, but future studies using conditioned medium from gastric myofibroblasts are needed to confirm this.

Wnt-5a activates mainly the non-canonical Wnt signalling pathway [120] and this was confirmed in gastric myofibroblasts by the failure of Wnt-5a to induce nuclear localisation of β-catenin and to stimulate TCF/LEF activity. The activity of canonical Wnt/β-catenin signalling pathway was also verified in gastric myofibroblasts by using immunocytochemistry of β-catenin and luciferase expression of TCF/LEF activity. The data suggest that increased activity of canonical Wnt pathway in gastric CAMs compared to ATMs, and this was increased further by Wnt-3a, but not Wnt-5a. Future studies should include nuclear extraction of gastric myofibroblasts so that the abundance of β-catenin in cell nuclei could be determined by Western blot analysis. In the future, the observation worth exploring in more detail is increased WNT5A mRNA abundance in a sample of gastric CAMs by Wnt-3a; it is known that Wnt-3a increases the transcription of TGFβ2 [270] which activates the TGF-β signalling pathway, leading to up-regulation of Wnt-5a expression [269], suggesting a possible mechanism for the present observations.

The functional roles of canonical and non-canonical Wnt signalling pathways in gastric myofibroblasts by Wnt-3a and Wnt-5a, respectively, were determined using migration and proliferation assays. Both Wnt-3a and Wnt-5a were shown to stimulate the migration and proliferation of gastric CAMs. Additionally, both Wnt-3a and Wnt-5a stimulated the proliferation of ATMs. Moreover, Wnt-5a but

not Wnt-3a stimulated the migration of ATMs. The data, therefore, suggest that Wnt-5a expression in gastric CAMs and ATMs could act in an autocrine manner and that increased abundance of Wnt-5a could play a role in regulating migration and proliferation of CAMs. Previous work using these cells has shown that CAMs exhibit a higher rate of migration and proliferation compared to corresponding ATMs [179], and it is possible that Wnt-5a is a mediator of the phenotype of CAMs.

Both Wnt-5a and Wnt-3a were found to induce the migration of AGS cancer cells. The mechanisms that might be involved include altered expression of MMPs [271, 272] and EMT [273]. Compatible with this, other studies have demonstrated that Wnt proteins from stromal cells activate Wnt signalling pathways in cancer cells, thus implicating interactions between cancer cells and the tumour microenvironment [274]. For example, Wnt-5a expression is induced in macrophages when they are co-cultured with breast cancer cells, and in turn Wnt-5a induces the invasiveness of cancer cells [275].

In conclusion, the findings suggest that Wnt-5a released from gastric CAMs influences migration and proliferation of CAMs and also contributes to cancer cell migration. Moreover, Wnt-5a expression might be regulated by β-catenin-dependent TCF/LEF activity through TGF-β signalling pathway (Figure 5.4.1). It would be useful to identify cancer cell-derived cytokines such as Wnt-3a that may act in a paracrine manner, to regulate Wnt-5a expression in CAMs. In the following chapter, the relationship between Wnt-5a and miRNAs in gastric CAMs were investigated.

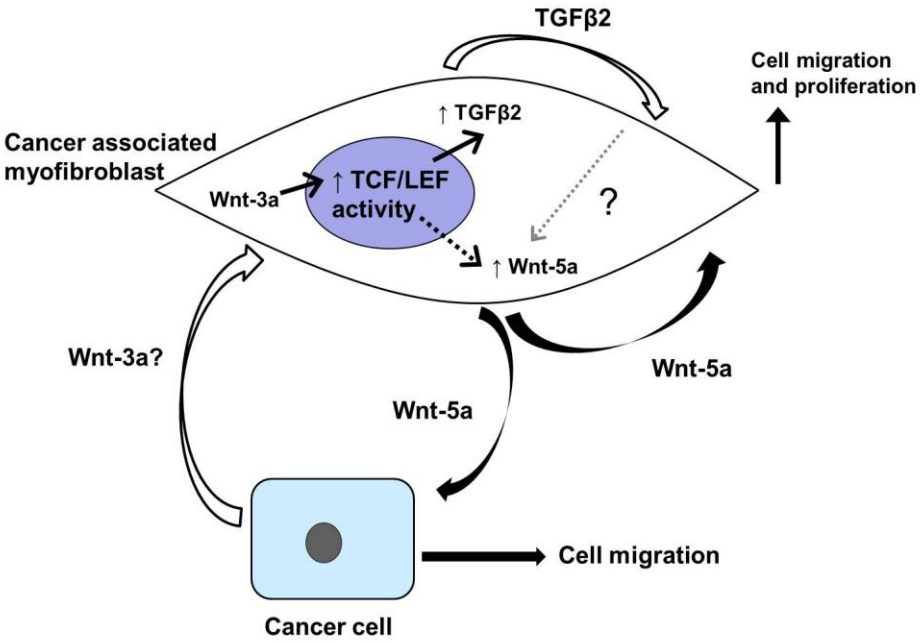

Figure 5.4.1 A schematic representation of Wnt-5a in stromal-tumour interactions. The release of Wnt-5a from CAMs stimulates the migration of cancer cells through paracrine signalling. Wnt-5a also acts in an autocrine manner to induce the migration and proliferation of CAMs. Increased Wnt-5a expression may be regulated by TCF/LEF activity in CAMs but the actual mechanism is not yet explored.

CHAPTER SIX

Role of hsa-miR-181d in gastric cancer-associated myofibroblasts

6.1 Introduction

In previous chapters, the results showed that the abundance of hsa-miR-181d and Wnt-5a was increased in gastric CAMs compared to corresponding ATMs. Wnt-5a was also found to induce migration and proliferation of gastric CAMs, and migration of AGS cells. Although increased abundance of miR-181b has been identified in cancer-associated fibroblasts from endometrial cancer [11], the functional role of hsa-miR-181d in gastric myofibroblasts is not understood. In chapter 3, paired individual sample analysis of CAMs and ATMs indicated that the mRNA and protein levels of TIMP-3 were related to hsa-miR-181d abundance. In addition, predicted targets of hsa-miR-181d that encode extracellular proteins were involved in the regulation of chemotaxis and proteolysis.

The canonical Wnt/β-catenin signalling has been shown to regulate expression of miR-181 family members in other cell types [254, 276]. Additionally, an increase in miR-181 expression has been shown to induce the motility and invasion of hepatocellular stem cells [277] and breast cancer cells [278]. Furthermore, miR-181 expression correlates with the metastatic potential of breast cancer cells [278] and is also associated with lymph-node metastasis in oral squamous cell carcinoma [279]. A study using miRNA expression profiling has identified increased expression of hsa-miR-181b and hsa-miR-181d in gastric cancer compared to normal gastric epithelium, and suggested that hsa-miR-181b associates with sensitivity to chemotherapy [280]. On the other hand, hsa-miR-181a and hsa-miR-181b could function as tumour suppressors, notably in glioma and chronic lymphocytic leukaemia [281, 282]. In view of the previously validated data that hsa-miR-181d abundance was increased and that TIMP3

transcript abundance was decreased in paired samples of gastric CAMs compared to corresponding ATMs, the hypothesis for this chapter was that hsa-miR-181d expression was regulated by Wnt signalling in CAMs and in turn, influenced cell migration by regulating ECM proteins (e.g. TIMP-3).

The specific aims for the work described in this chapter were:

6.1.1 To determine the relationship between hsa-miR-181d and Wnt-5a in gastric CAMs.

6.1.2 To investigate the functional role of hsa-miR-181d in gastric CAMs and ATMs, and its involvement in stromal-epithelial interactions.

6.2 Methods

Using quantitative RT-PCR, the relative abundance of hsa-miR-181d was determined in gastric CAMs after incubation with 1 µg/ml recombinant Wnt-3a or Wnt-5a for 24 h. Nucleofection protocol was carried out for knockdown and overexpression of hsa-miR-181d in gastric CAMs and ATMs, respectively (Chapter 2.11). After 24, 48 and 72 h post-transfection, the abundance of hsa-miR-181d and TIMP3 mRNA was determined in gastric myofibroblasts. After 48 h post-transfection, migration and EdU incorporation assays were performed in myofibroblasts in the presence or absence of 1 µg/ml recombinant Wnt-5a. Conditioned medium (CM) from transfected samples of myofibroblasts was collected to perform migration and EdU incorporation assays using AGS cells. Recombinant TIMP-3 (100 ng/ml) was used in AGS cell migration assay in the presence or absence of 1 µg/ml recombinant Wnt-5a

6.3 Results

6.3.1 An increase in hsa-miR-181d abundance in gastric CAMs by Wnt-5a

To determine whether hsa-miR-181d was regulated by Wnt signalling pathways, the abundance of hsa-miR-181d was determined in gastric CAMs after incubation with Wnt-3a or Wnt-5a. RT-PCR analysis showed that the abundance of hsa-miR-181d was significantly increased (2-fold) after incubation with Wnt-5a while no significant change was obtained after incubation with Wnt-3a (Figure 6.3.1).

6.3.2 An inverse correlation between TIMP3 mRNA and hsa-miR-181d

To investigate the role of hsa-miR-181d in gastric myofibroblasts, a strategy was adopted for hsa-miR-181d knockdown in CAMs and overexpression in ATMs, and these were carried out using nucleofection with hsa-miR-181d inhibitor and precursor plasmids, respectively. The nucleofection efficiency at 48 h post-transfection was approximately 50%, and this was obtained by determining the proportion of green fluorescent protein (GFP) positive myofibroblasts in 10 different fields and the mean was expressed as a percentage.

Since the post-transfection period that showed maximum change in hsa-miR-181d abundance was unknown, total RNA was extracted from gastric myofibroblasts after 24, 48 and 72 h post-transfection followed by the determination of hsa-miR-181d relative abundance. In hsa-miR-181d knockdown CAMs, the abundance of hsa-miR-181d was significantly decreased by approximately 30% after 48h post-

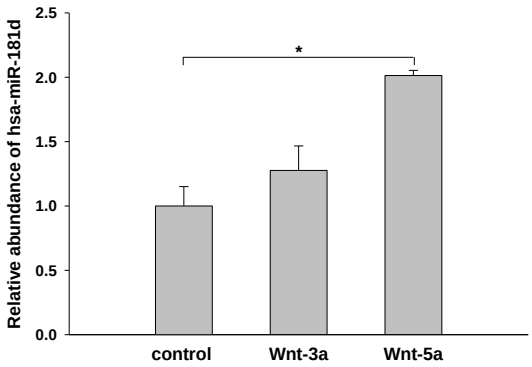

Figure 6.3.1 Abundance of hsa-miR-181d is increased in gastric CAMs by Wnt-5a. The relative abundance of hsa-miR-181d was increased significantly after gastric CAMs were incubated with 1 µg/ml Wnt-5a, but not Wnt-3a. Each experiment was performed in triplicate. (*$p < 0.05$)

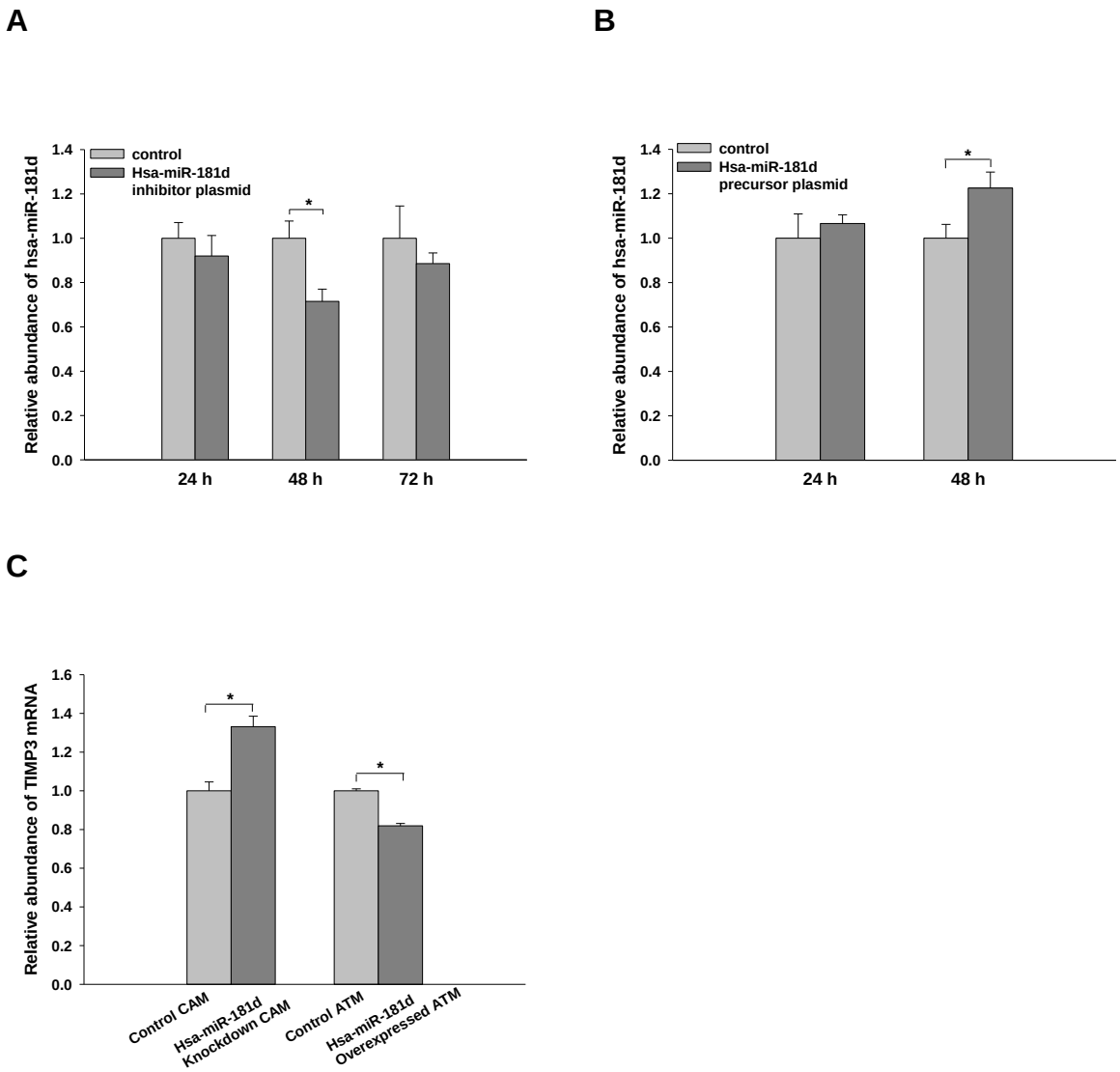

Figure 6.3.2 Abundance of TIMP3 mRNA is inversely correlated with hsa-miR-181d after hsa-miR-181d knockdown in CAMs and overexpression in ATMs. (A) The relative abundance of hsa-miR-181d in CAMs after 24, 48 and 72 h post-transfection with hsa-miR-181d inhibitor plasmid. (B) The relative abundance of hsa-miR-181d in ATMs after 24 and 48 h post-transfection with hsa-miR-181d precursor plasmid. (C) The relative mRNA abundance of TIMP3 in CAMs and ATMs after hsa-miR-181d knockdown and overexpression, respectively. Each experiment was performed in triplicate. (*$p < 0.05$)

transfection while a non-significant decrease by approximately 10% was found after 24 and 72 h post-transfection (Figure 6.3.2A). When hsa-miR-181d was overexpressed in ATMs, its abundance was significantly increased by approximately 20% after 48 h post-transfection, but no significant change was found after 24 h post-transfection (Figure 6.3.2B). The significance of hsa-miR-181d abundance difference in CAMs and ATMs was followed by analysis of TIMP3 mRNA, which is a known target of the miR-181 family. After 48 h post-transfection, the mRNA abundance of TIMP3 was significantly increased by approximately 30% in hsa-miR-181d knockdown CAMs and decreased by approximately 20% in hsa-miR-181d overexpressed ATMs (Figure 6.3.2C), indicating the abundance of TIMP3 is inversely correlated with hsa-miR-181d abundance.

6.3.3 Decreased migration and proliferation of gastric CAMs after hsa-miR-181d knockdown

Here, the role of hsa-miR-181d in the regulation of migration and proliferation in gastric CAMs was determined. After 48 h post-transfection, migration and EdU incorporation assays were carried out using hsa-miR-181d knockdown CAMs and in the presence or absence of 1 μg/ml recombinant Wnt-5a. The basal migration of gastric CAMs was significantly decreased after hsa-miR-181d knockdown (Figure 6.3.3A). In the presence of Wnt-5a, the migration of CAMs was significantly increased, and knockdown of hsa-miR-181d reduced the response. The results of EdU incorporation assays showed that the rate of proliferation was significantly

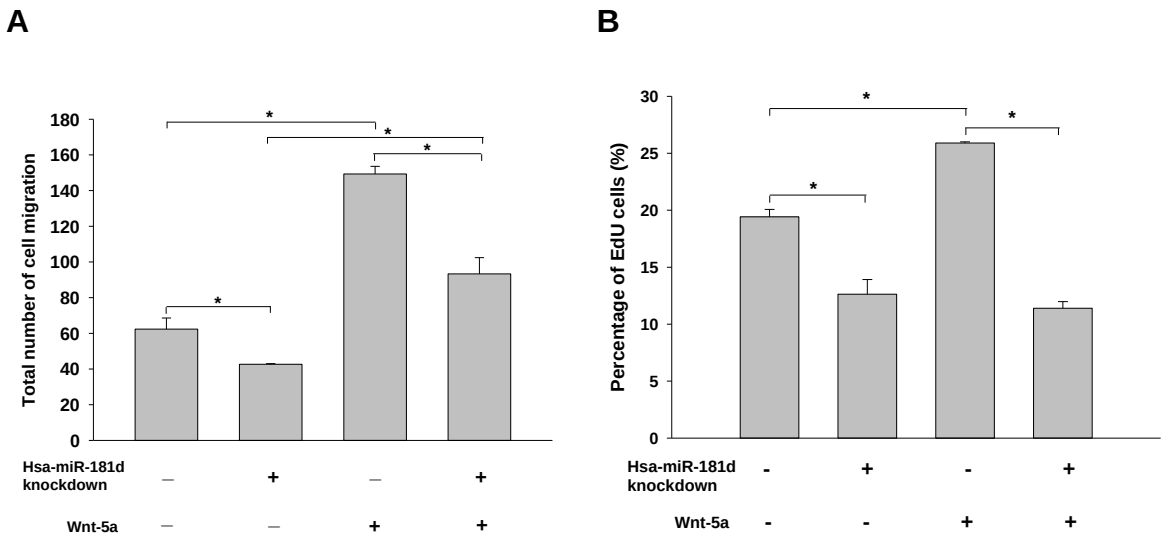

Figure 6.3.3 Decreased migration and proliferation of gastric CAMs after hsa-miR-181d knockdown. (A) The migration of hsa-miR-181d knockdown CAMs was significantly decreased when compared to control cells. Incubation with Wnt-5a (1 µg/ml, 16 h) significantly increased the migration of CAMs and hsa-miR-181d knockdown CAMs although a lower response was found in hsa-miR-181d knockdown CAMs. (B) Percentage of EdU positive cells was significantly decreased in hsa-miR-181d knockdown CAMs compared to control cells. Incubation with Wnt-5a (1 µg/ml, 24 h) significantly increased the percentage of EdU positive cells in CAMs but not after hsa-miR-181d knockdown. Each experiment was performed in triplicate. (*$p < 0.05$)

decreased in hsa-miR-181d knockdown CAMs (Figure 6.6.3B). While Wnt-5a was able to increase the proliferation rate in gastric CAMs, there was no significant change in the proliferation rate of hsa-miR-181d knockdown CAMs after incubation with Wnt-5a. .

6.3.4 Effects of AGS cell migration and proliferation when incubated in conditioned medium from CAMs and ATMs following hsa-miR-181d knockdown and overexpression, respectively

To determine whether the different hsa-miR-181d abundance in myofibroblasts regulates cancer cell migration, migration assays were performed by incubating AGS cells in CM from gastric myofibroblasts. After 48 h post-transfection, CM from hsa-miR-181d knockdown CAMs or hsa-miR-181d overexpressed ATMs was used for Boyden chamber chemotactic experiments. A significant decrease (approximately 30%) in AGS cell migration was found after incubation in CM from hsa-miR-181d knockdown CAMs compared to CM from control cells (Figure 6.3.4). On the other hand, there was no significant change in the migration of AGS cells after incubation in CM from hsa-miR-181d overexpressed ATMs and CM from control cells. Additionally, the proliferation rate of AGS cells was determined after incubation in CM from transfected samples, and the results showed there was no significant change compared to the basal control after incubation in CM from CAMs or ATMs (Figure 6.3.5).

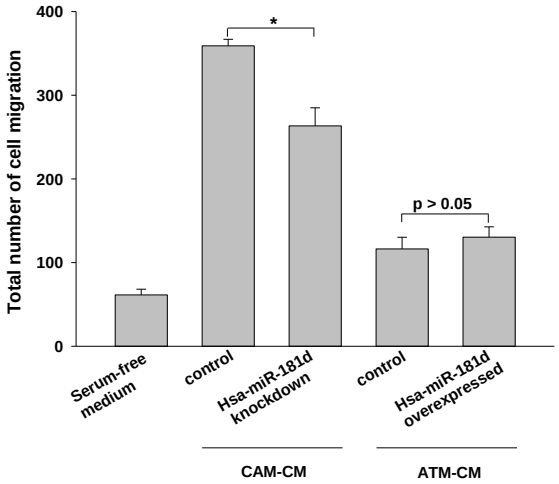

Figure 6.3.4 AGS cell migration is inhibited when incubated in CM from hsa-miR-181d knockdown CAMs. No significant change in AGS cell migration when incubated in CM from hsa-miR-181d overexpressed ATMs compared to control cells. Serum-free medium was the basal control. Each experiment was performed in triplicate. CAM-CM and ATM-CM indicate conditioned medium from CAMs and ATMs, respectively. (*$p < 0.05$)

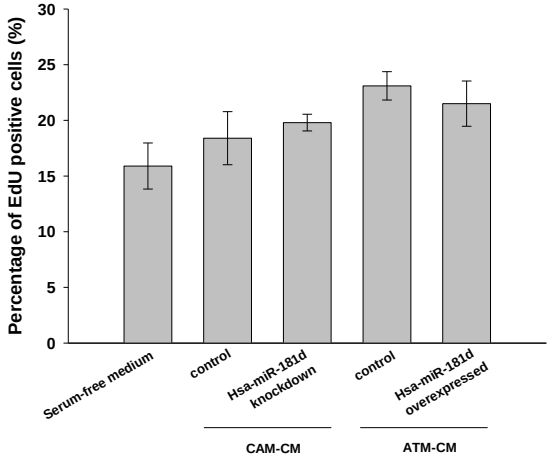

Figure 6.3.5 Proliferation rate of AGS cells was not significantly affected after incubation in CM from hsa-miR-181d knockdown CAMs and hsa-miR-181d overexpressed ATMs. Serum-free medium was the basal control. Each experiment was performed in triplicate. CAM-CM and ATM-CM indicate conditioned medium from CAMs and ATMs, respectively.

6.3.5 Inhibition of Wnt-5a-induced AGS cell migration by TIMP-3

Since TIMP3 mRNA abundance was found to be regulated by hsa-miR-181d in gastric myofibroblasts, and studies has shown that TIMP-3 inhibits the activity of MMPs, a migration assay was carried out to determine the role of TIMP-3 on migration of AGS cells. The results showed that the migration of AGS cells was unresponsive to TIMP-3 alone, but in the presence of Wnt-5a stimulation, the migration of AGS cells was significantly decreased by TIMP-3 (Figure 6.3.6).

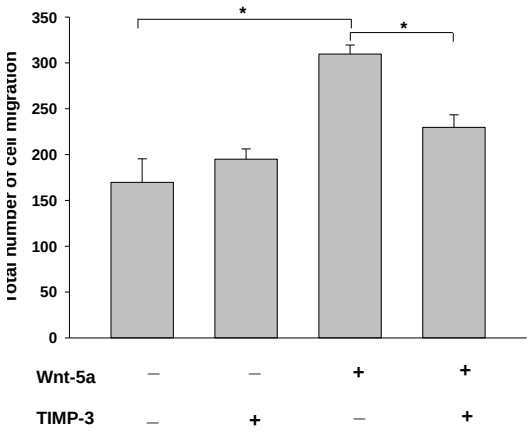

Figure 6.3.6 Wnt-5a-induced migration of AGS cells is inhibited by recombinant TIMP-3. No significant different in basal migration of AGS cells when 100 ng/ml recombinant TIMP-3 was added. 1 µg/ml Wnt-5a significantly increased the migration of AGS cells and the response was significantly decreased with the addition of TIMP-3. (*$p < 0.05$)

6.4 Discussion

This is the first study that has identified a role of hsa-miR-181d in regulating gastric CAMs and influencing cancer cell migration. The results suggest that activation of the Wnt signalling pathway by Wnt-5a regulates the abundance of hsa-miR-181d in gastric CAMs, and that hsa-miR-181d plays a role in regulating the migration and proliferation of gastric CAMs. Additionally, knockdown of hsa-miR-181d increases the expression of TIMP-3 in CAMs, and extracellular TIMP-3 could inhibit the migration of AGS cells through Wnt-5a regulatory pathway (Figure 6.4.1).

To determine the function of hsa-miR-181d in gastric myofibroblasts, nucleofection experiments with inhibitor and precursor plasmids of hsa-miR-181d were carried out using a paired sample of CAMs and ATMs. In chapter 3, RT-PCR analysis had validated an increased abundance of hsa-miR-181d in CAMs compared to corresponding ATMs. As a result, the strategy for studying hsa-miR-181d was to reduce its abundance in CAMs, termed knockdown, and to increase its abundance in ATMs, termed overexpression.

The greatest significant difference in hsa-miR-181d abundance was a decrease of 30% and was found in CAMs after 48 h post-transfection. This effect was transient as the abundance of hsa-miR-181d returned to control level after 72 h post-transfection. The nucleofection experiment demonstrated the targeting effect of TIMP3 mRNA by hsa-miR-181d following hsa-miR-181d knockdown in CAMs and hsa-miR-181d overexpression in ATMs. The transfection efficiency at 48 h post-transfection was 50% and it is considered marginally low. It might be because these myofibroblasts were primary cell lines which are hard to transfect.

To increase the transfection efficiency, non-transfected myofibroblasts should be separated from those transfected ones by using flow cytometry so that there would be a homogenous population of transfected myofibroblasts. Alternatively, myofibroblasts could be transformed into a cell line that permanently overexpresses hsa-miR-181d without losing expression when cells divide.

Previous findings in chapter 5 suggest that Wnt-5a is increased in gastric CAMs, and it may activate the non-canonical Wnt signalling pathway in gastric myofibroblasts. In this chapter, it was found that Wnt-5a stimulates the abundance of hsa-miR-181d in gastric CAMs. It would be useful to perform Wnt-5a knockdown in CAMs and then determine whether the abundance of hsa-miR-181d is down-regulated to confirm this finding. In addition, a previous study has indicated the induction of miR-181 expression in hepatocellular cancer cells by the canonical Wnt/β-catenin signalling pathway [254]. These suggest that hsa-miR-181d could be regulated by both canonical and non-canonical Wnt signalling pathways, depending on the cellular context. Since the abundance of hsa-miR-181d was previously found to be increased in CAMs compared to NTMs, it would be beneficial to investigate the regulation of hsa-miR-181d in NTMs and to determine whether this miRNA is differentially regulated in CAMs.

Functional studies of hsa-miR-181d were performed in CAMs so that the contribution of hsa-miR-181d in the tumour microenvironment could be identified. Compatible with other studies focusing on miR-181s, the results showed that the rates of migration and proliferation in gastric CAMs were inhibited when hsa-miR-181d was knockdown. Furthermore, RT-PCR analysis indicated WNT5A mRNA abundance was not significantly changed after knockdown of hsa-miR-181d in CAMs. In the presence of Wnt-5a stimulation, the

migration of hsa-miR-181d knockdown CAMs was significantly reduced when compared to control cells, indicating hsa-miR-181d is a downstream target of Wnt-5a. In contrast, the proliferation rate of hsa-miR-181d knockdown CAMs was not significantly changed after stimulation from Wnt-5a. These preliminary results suggest that Wnt-5a is a potent regulator of migrating CAMs through hsa-miR-181d while other mechanisms are involved in the regulation of cell cycle progression in CAMs.

Targets of hsa-miR-181d that encode extracellular proteins such as TIMP-3 could be involved in the regulation of AGS cell migration. The hypothesis was that Wnt-5a from CAMs induces hsa-miR-181d abundance and in turn, down-regulates the expression of ECM proteins to promote cell migration. Results obtained showed that the migration of AGS cells was partially inhibited after incubation in CM from hsa-miR-181d knockdown CAMs compared to control cells. In contrast, there was no significant difference in AGS cell migration after incubation in CM from hsa-miR-181d overexpressed ATMs and control cells. Therefore, the data suggest that targets of hsa-miR-181d in CAMs include secretory factors, which contribute to cancer cell migration. Future studies could use mass spectrometry to examine the protein abundance in CM from hsa-miR-181d knockdown CAMs so that direct and downstream targets of hsa-miR-181d could be identified. A similar approach has been used in determining the secretome of gastric myofibroblasts [179]. Moreover, migration assays have specifically indicated TIMP-3 as a putative regulator of AGS cell migration because the results showed that Wnt-5a-induced AGS cell migration was inhibited by TIMP-3, thus suggesting a common regulatory function of TIMP-3 that opposes the stimulatory effect of Wnt-5a.

In conclusion, the present study suggests that increased Wnt-5a expression in gastric CAMs may regulate the abundance of hsa-miR-181d, whose targets are associated with cell cycle and ECM proteins, thus leading to increased migration and proliferation of myofibroblast. In gastric CAMs, TIMP-3 expression is shown to be regulated by hsa-miR-181d and is involved in inhibiting Wnt-5a-stimulated migration of AGS cells, thus implicating the role of Wnt-5a and hsa-miR-181d in mediating stromal-tumour interactions to induce cell migration.

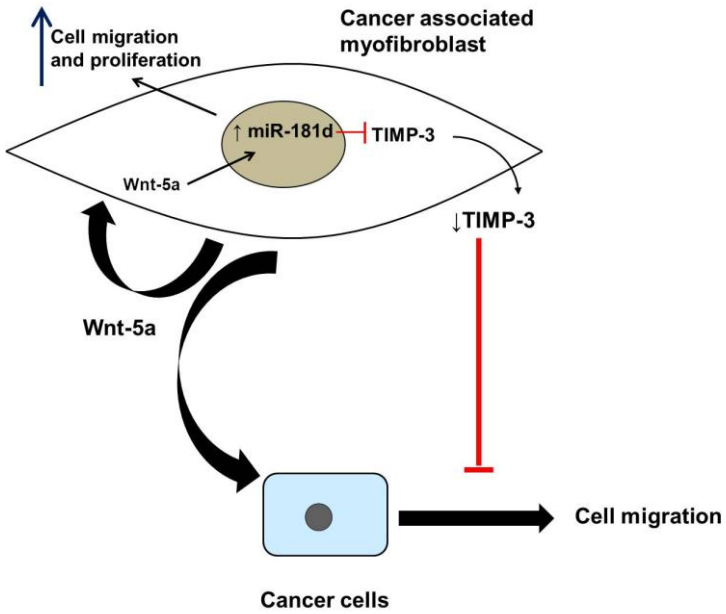

Figure 6.4.1 A schematic representation showing regulatory roles of hsa-miR-181d and Wnt-5a in CAMs and the significance for cancer cell migration. Hsa-miR-181d plays a role in the migration and proliferation of gastric CAMs. Wnt-5a stimulates the expression of hsa-miR-181d which down-regulates TIMP-3 expression, leading to an increase in cell migration.

CHAPTER SEVEN

Final discussion

7.1 Conclusions

The present thesis has characterised the miRNA expression profiles of stromal myofibroblasts from tumours, pre-neoplastic and normal stromal tissues, and has investigated the role of miRNAs in regulatory processes that might affect myofibroblast role in cancer initiation and progression. Global miRNA expression profiles of NTMs from the stomach and oesophageal tissues were clearly distinct from each other, suggesting the contribution of miRNAs in myofibroblasts that regulate the functions of different epithelia. Additionally, bone marrow derived MSCs, which are recognized as precursors of myofibroblasts, exhibited distinct global miRNA expression profiles compared to gastric and oesophageal myofibroblasts.

Network enrichment analysis was performed using validated targets of miRNAs that were different in abundance between two myofibroblast populations. The results showed that affected processes were related to the regulation of cell cycle progression and signalling pathways. Wnt signalling, in particular, was significantly influenced and was linked to different hsa-miR-181d abundance in gastric CAMs compared to ATMs.

Microarray gene expression analysis showed that WNT5A mRNA was significantly up-regulated in CAMs compared to ATMs, and the expression of Wnt-5a in paired samples of gastric myofibroblasts was validated by Western blot and RT-PCR analyses. The results from functional studies showed that Wnt-5a stimulates the migration and proliferation of gastric myofibroblasts probably by activating the non-canonical Wnt signalling pathway. In addition, the abundance of hsa-miR-181d in gastric CAMs was induced by Wnt-5a, and knockdown of

hsa-miR-181 significantly decreased the migration and proliferation of CAMs. The migration of CAMs after hsa-miR-181d knockdown, was significantly increased by Wnt-5a but a lower response was found when compared to CAMs before hsa-miR-181d knockdown. However, the proliferation rate of CAMs after hsa-miR-181d knockdown was not significantly increased in response to Wnt-5a. TIMP-3, whose expression inversely correlated with hsa-miR-181d abundance, inhibited the migration of AGS cells in the presence of Wnt-5a stimulation. These findings, therefore, suggest that Wnt-5a regulates the migration of CAMs through modulation of hsa-miR-181d, and that both Wnt-5a and hsa-miR-181d play a role in cancer cell migration through stromal-tumour interactions.

7.2 Implications of miRNA profiling

The study of miRNA expression profiles in chapter 3 showed that CAMs originated from stomach and oesophageal cancers were distinguished by their global miRNA expression. This is the first data analysis to compare miRNA expression in gastric and oesophageal CAMs. Nonetheless, the miRNA profiles could not classify gastric CAMs into their origins from different tumour subtypes such as diffuse-type and intestinal-type gastric carcinomas, suggesting gastric CAMs of different cancer subtypes exhibit a common pattern of miRNA abundance. On the other hand, the miRNA profiles of SC-CAMs and AC-CAMs might be distinct from each other. Further studies using larger sample sizes of oesophageal CAMs may help to resolve the issue of whether there are differences between oesophageal cancer subtypes. Many studies have used cancer samples for miRNA profiling, and one of the initial studies highlighted the potential of

miRNA expression for cancer-type classification [159]. This suggests miRNAs might play a role in tissue specificity and also, there might be a possibility that miRNA profiles in CAMs could determine their tumour origins in the gastrointestinal tract.

Analysis of global miRNA expression profiles showed distinct profiles of MSCs in comparison to NTMs of gastric and oesophageal origins. Studies have shown that bone marrow MSCs transform into myofibroblast phenotype during wound healing [67], but the mechanism involving miRNAs is unknown. Several miRNAs such as hsa-miR-29b and hsa-miR-34a that were significantly different in abundance have been shown to regulate differentiation of MSCs [78, 225]. Other than cells differentiation, differential miRNA abundance might play a role in phenotypic differences between MSCs and NTMs. Moreover, MSCs may contribute to myofibroblast population in the tumour stroma [193]. Therefore, to inhibit the role of MSCs in tumour growth and progression, it would be crucial to determine whether these differentially abundant miRNAs could regulate the expression of myofibroblast markers (e.g. α-SMA) or influence myofibroblast differentiation.

Using hierarchical clustering analysis of differential miRNA abundance, there were distinct clusters between CAMs and ATMs, CAMs and NTMs, and between ATMs and NTMs. Thus, mRNA abundance and protein expression that are significantly different between two different myofibroblast populations could potentially be regulated by these differentially abundant miRNAs. Furthermore, novel miRNA targets may be identified by using proteomic and gene expression data of myofibroblasts through correlation analysis and complementary binding site on 3'UTR of mRNA.

7.3 Limitations of enriched network analysis

MicroRNA research has largely focused on determining the true targets of individual miRNAs because predicted targets from computational algorithm programs show more than 30% false positives [283]. Recently, there is an increased interest in the role of co-expressed miRNAs in regulating biological processes.

In chapter 4, validated targets of differentially abundant miRNAs were used for the identification of affected processes. These processes are predictive regulation only, and the selection of processes related to myofibroblast function is needed for validation work. In addition, bioinformatic analysis does not allow the discovery of novel protein interactions or miRNA targets. Moreover, epigenetic alterations such as DNA methylation might play a prominent role in the regulation of gene expression, so that mechanisms of miRNA regulation are not responsible for specific alteration in gene expression. This was not taken into consideration in the present study, but it is highly recommended in the future. Furthermore, a recent study suggests that single-nucleotide polymorphisms (SNPs) in miRNA genes might affect their functional role, contributing to increased risk of cancer [284]. This is a research topic that needs to be explored in myofibroblast studies.

Nonetheless, bioinformatic analysis does have its advantages: a) miRNA targets that are being used are already validated so they relate to a function of a miRNA better compared to predicted targets; b) analysis of large sample sizes and comparison among different populations are efficient using the same platform and c) a better understanding of myofibroblast biology. For the latter, miRNAs that were difference in abundance in gastric CAMs compared to ATMs were involved

in the regulation of cell cycle progression. Therefore, this might result in an increased rate of proliferation in CAMs compared to ATMs, indicating the regulation of miRNAs in myofibroblast proliferation, but validation work is needed to confirm.

7.4 Implications of Wnt-5a and hsa-miR-181d

The tumour microenvironment has been implicated in malignant progression [127]. Gene expression analysis identified up-regulation of WNT5A mRNA in gastric CAMs compared to ATMs, and this occurred in 10 of the 12 pairs (83%) of gastric myofibroblasts. Since increased expression of Wnt-5a has been identified in a subset of gastric carcinoma, and has been associated with poor prognosis [264], it is suggested that increased Wnt-5a in gastric CAMs contributes to cancer progression, and that this protein might be predominantly expressed in the tumour stroma. Thus, targeting Wnt-5a signalling from stromal cells as a therapeutic strategy could inhibit tumour growth and progression. Since studies have shown that genetic alterations in stromal cells are rare, these cells, in particularly CAMs, are thought to exhibit greater genetic stability than cancer cells and less likely to acquire resistant to chemotherapy [178]. Preliminary data suggest that Wnt-3a induces Wnt-5a abundance in gastric CAMs by activating the canonical Wnt/β-catenin signalling pathway. Additionally, a recent study indicates the role of LRP6, a coreceptor of the canonical pathway, in mediating Wnt transduction, and promoting myofibroblast activation and proliferation [285]. This provides further evidence that targeting Wnt signalling is crucial to inhibit myofibroblast function in diseases.

Besides gastric cancer, Wnt-5a is implicated in malignant progression of other cancers [286], and also shown to exhibit tumour suppressive role in colorectal [287] and oesophageal squamous cell carcinomas [288]. The abnormal Wnt-5a expression in cancer might be a consequence of altered miRNA regulation even though WNT5A gene regulated by DNA methylation has been reported [287]. Unlike Wnt-3a, Wnt-5a was found to be a potent inducer of migration in gastric myofibroblasts. On the other hand, AGS cell migration, but not proliferation, was moderately increased by Wnt-5a. It would be interesting to determine changes in gene expression that are induced by Wnt-5a in CAMs, and to investigate whether these altered genes affect cancer cell behaviour through paracrine signalling or ECM remodelling. One such phenomenon is suggested in chapter 6 when it was found that Wnt-5a stimulates the abundance of hsa-miR-181d in gastric CAMs and that hsa-miR-181d down-regulates TIMP-3 expression to induce cell migration. Further studies using *in vivo* studies will be able to verify whether decreased TIMP-3 expression induce gastric cancer cell invasiveness and metastatic potential. Proteomic techniques using mass spectrometry will be useful to determine TIMP-3 activity in the ECM, and to identify novel targets of hsa-miR-181d.

Increase in hsa-miR-181d abundance was found in 5 of the 12 pairs (42%) of gastric CAMs and corresponding ATMs. This might suggest that increased Wnt-5a does not necessarily induce hsa-miR-181d abundance in CAMs. Besides Wnt signalling, regulation of miR-181c expression has been linked to DNA methylation in gastric carcinoma [245]. Since gastric CAMs have already been studied to exhibit global DNA hypomethylation [149], the association of hsa-miR-181d with epigenetics in CAMs is suggested. Furthermore, up-regulation of hsa-

miR-181d has been found in gastric carcinoma [280]. Therefore, the development of strategy targeting hsa-miR-181d in stromal and cancer cells will be important in the inhibition of cancer progression.

Currently, the first clinical trial for treating hepatitis using miRNA therapeutic approach is being carried out [289], thus raising the possibility of cancer treatment in the near future. With increasing knowledge from miRNA research and advances in miRNA treatment technique, miRNA gene therapy that regulates a number of proteins associated with the development of specific tumours is promising. Additionally, therapeutic targeting of epigenetic regulation in the tumour stroma may provide an alternative for inhibiting cancer progression, and may be more effective compared to cancer cell therapy. On the whole, the present study has identified the contribution of miRNAs in regulating cellular processes in myofibroblasts that could influence cancer progression, suggesting stromal cells as a suitable therapeutic drug target to achieve better treatment outcomes for patients with gastric and oesophageal cancers, which remain intractable to most therapies.

REFERENCES

[1] Watson JD, Crick FHC. Molecular structure of nucleic acids: A structure for deoxyribose nucleic acid. Nature. 1953;171:737-8.

[2] Crick FH. On protein synthesis. Symposia of the Society for Experimental Biology. 1958;12:138-63.

[3] Thieffry D, Sarkar S. Forty years under the central dogma. Trends in Biochemical Sciences. 1998;23:312-6.

[4] Collins FS, Lander ES, Rogers J, Waterson RH. Finishing the euchromatic sequence of the human genome. Nature. 2004;431:931-45.

[5] Lander ES, Linton LM, Birren B, Nusbaum C, Zody MC, Baldwin J, et al. Initial sequencing and analysis of the human genome. Nature. 2001;409:860-921.

[6] Zamore PD, Haley B. Ribo-gnome: the big world of small RNAs. Science (New York, NY). 2005;309:1519-24.

[7] Farazi TA, Spitzer JI, Morozov P, Tuschl T. miRNAs in human cancer. The Journal of pathology. 2011;223:102-15.

[8] Botterweck AAM, Schouten LJ, Volovics A, Dorant E, Van Den Brandt PA. Trends in incidence of adenocarcinoma of the oesophagus and gastric cardia in ten European countries. International Journal of Epidemiology. 2000;29:645-54.

[9] Ferlay J, Shin HR, Bray F, Forman D, Mathers C, Parkin DM. Estimates of worldwide burden of cancer in 2008: GLOBOCAN 2008. International journal of cancer Journal international du cancer. 2010;127:2893-917.

[10] Li H, Fan X, Houghton J. Tumor microenvironment: the role of the tumor stroma in cancer. Journal of cellular biochemistry. 2007;101:805-15.

[11] Aprelikova O, Green JE. MicroRNA regulation in cancer-associated fibroblasts. Cancer Immunology, Immunotherapy. 2012;61:231-7.

[12] Treuting PM, Valasek MA, Dintzis SM. 11 - Upper Gastrointestinal Tract. In: Piper MT, Suzanne D, Denny L, Charles W. FrevertA2 - Piper M. Treuting SDDL, Charles WF, editors. Comparative Anatomy and Histology. San Diego: Academic Press; 2012. p. 155-75.

[13] Orlando LA, Orlando RC. Esophagus, Anatomy. In: Editor-in-Chief: Leonard J, editor. Encyclopedia of Gastroenterology. New York: Elsevier; 2004. p. 763-6.

[14] Ramsay PT, Carr A. Gastric acid and digestive physiology. Surgical Clinics of North America. 2011;91:977-82.

[15] Clayburgh DR, Turner JR. Stomach, Anatomy. In: Editor-in-Chief: Leonard J, editor. Encyclopedia of Gastroenterology. New York: Elsevier; 2004. p. 458-62.

[16] Sarosiek J, McCallum RW. Mechanisms of oesophageal mucosal defence. Bailliere's Best Practice and Research in Clinical Gastroenterology. 2000;14:701-17.

[17] Mittal RK, McCallum RW. Characteristics and frequency of transient relaxations of the lower esophageal sphincter in patients with reflux esophagitis. Gastroenterology. 1988;95:593-9.

[18] Chandrasoma P. Pathological basis of gastroesophageal reflux disease. World Journal of Surgery. 2003;27:986-93.

[19] Croft J, Parry EM, Jenkins GJS, Doak SH, Baxter JN, Griffiths AP, et al. Analysis of the premalignant stages of Barrett's oesophagus through to adenocarcinoma by comparative genomic hybridization. European Journal of Gastroenterology and Hepatology. 2002;14:1179-86.

[20] Hu Y, Williams VA, Gellersen O, Jones C, Watson TJ, Peters JH. The pathogenesis of Barrett's esophagus: Secondary bile acids upregulate intestinal differentiation factor CDX2 expression in esophageal cells. Journal of Gastrointestinal Surgery. 2007;11:827-34.

[21] Toh Y, Oki E, Ohgaki K, Sakamoto Y, Ito S, Egashira A, et al. Alcohol drinking, cigarette smoking, and the development of squamous cell carcinoma of the esophagus: molecular mechanisms of carcinogenesis. International journal of clinical oncology. 2010;15:135-44.

[22] Dockray GJ. Gastrin and gastric epithelial physiology. Journal of Physiology. 1999;518:315-24.

[23] Lee ER, Leblond CP. Dynamic histology of the antral epithelium in the mouse stomach: IV. Ultrastructure and renewal of gland cells. American Journal of Anatomy. 1985;172:241-59.

[24] Modlin IM, Kidd M, Marks IN, Tang LH. The pivotal role of John S. Edkins in the discovery of gastrin. World Journal of Surgery. 1997;21:226-34.

[25] Yao X, Forte JG. Cell biology of acid secretion by the parietal cell. Annual review of physiology. 2003;65:103-31.

[26] Hakanson R, Ding XQ, Norlen P, Lindstrom E. CCK2 receptor antagonists: pharmacological tools to study the gastrin-ECL cell-parietal cell axis. Regul Pept. 1999;80:1-12.

[27] Forte JG. The gastric parietal cell: At home and abroad. European Surgery - Acta Chirurgica Austriaca. 2010;42:134-48.

[28] Allen A, Flemström G. Gastroduodenal mucus bicarbonate barrier: Protection against acid and pepsin. American Journal of Physiology - Cell Physiology. 2005;288:C1-C19.

[29] Niv Y, Fraser GM. The alkaline tide phenomenon. Journal of Clinical Gastroenterology. 2002;35:5-8.

[30] Nomura A, Stemmermann GN, Chyou PH, Perez-Perez GI, Blaser MJ. Helicobacter pylori infection and the risk for duodenal and gastric ulceration. Annals of internal medicine. 1994;120:977-81.

[31] Voutilainen M, Mantynen T, Farkkila M, Juhola M, Sipponen P. Impact of non-steroidal anti-inflammatory drug and aspirin use on the prevalence of dyspepsia and uncomplicated peptic ulcer disease. Scandinavian journal of gastroenterology. 2001;36:817-21.

[32] Kusters JG, Van Vliet AHM, Kuipers EJ. Pathogenesis of Helicobacter pylori infection. Clinical Microbiology Reviews. 2006;19:449-90.

[33] Huang JQ, Sridhar S, Hunt RH. Role of Helicobacter pylori infection and non-steroidal anti-inflammatory drugs in peptic-ulcer disease: a meta-analysis. Lancet. 2002;359:14-22.

[34] Beales IL, Calam J. Helicobacter pylori infection and tumour necrosis factor-alpha increase gastrin release from human gastric antral fragments. European journal of gastroenterology & hepatology. 1997;9:773-7.

[35] McColl KE, el-Omar EM, Gillen D. The role of H. pylori infection in the pathophysiology of duodenal ulcer disease. Journal of physiology and pharmacology : an official journal of the Polish Physiological Society. 1997;48:287-95.

[36] Murayama Y, Miyagawa JI, Higashiyama S, Kondo S, Yabu M, Isozaki K, et al. Localization of heparin-binding epidermal growth factor-like growth factor in human gastric mucosa. Gastroenterology. 1995;109:1051-9.

[37] Fukui H, Kinoshita Y, Maekawa T, Okada A, Waki S, Hassan S, et al. Regenerating gene protein may mediate gastric mucosal proliferation induced by hypergastrinemia in rats. Gastroenterology. 1998;115:1483-93.

[38] Mobley HLT, Mendz GL, Hazell SL. Helicobacter pylori [electronic book] : physiology and genetics / edited by Harry L.T. Mobley, George L. Mendz, Stuart L. Hazell: Washington, DC : ASM Press, c2001.; 2001.

[39] Shin JM, Sachs G. Pharmacology of proton pump inhibitors. Curr Gastroenterol Rep. 2008;10:528-34.

[40] El-Omar EM, Oien K, El-Nujumi A, Gillen D, Wirz A, Dahill S, et al. Helicobacter pylori infection and chronic gastric acid hyposecretion. Gastroenterology. 1997;113:15-24.

[41] Tan VPY, Wong BCY. Helicobacter pylori and gastritis: Untangling a complex relationship 27 years on. Journal of gastroenterology and hepatology. 2011;26:42-5.

[42] Uemura N, Okamoto S, Yamamoto S, Matsumura N, Yamaguchi S, Yamakido M, et al. Helicobacter pylori infection and the development of gastric cancer. New England Journal of Medicine. 2001;345:784-9.

[43] Hansson LE, Nyren O, Hsing AW, Bergstrom R, Josefsson S, Chow WH, et al. The risk of stomach cancer in patients with gastric or duodenal ulcer disease. The New England journal of medicine. 1996;335:242-9.

[44] Ghoshal UC, Chaturvedi R, Correa P. The enigma of Helicobacter pylori infection and gastric cancer. Indian journal of gastroenterology : official journal of the Indian Society of Gastroenterology. 2010;29:95-100.

[45] Chaturvedi R, Asim M, Romero-Gallo J, Barry DP, Hoge S, de Sablet T, et al. Spermine oxidase mediates the gastric cancer risk associated with Helicobacter pylori CagA. Gastroenterology. 2011;141:1696-708 e1-2.

[46] D'Elios MM, Appelmelk BJ, Amedei A, Bergman MP, Del Prete G. Gastric autoimmunity: The role of Helicobacter pylori and molecular mimicry. Trends in Molecular Medicine. 2004;10:316-23.

[47] Gueant JL, Safi A, Aimone-Gastin I, Rabesona H, Bronowicki JP, Plenat F, et al. Autoantibodies in pernicious anemia type I patients recognize sequence 251-256 in human intrinsic factor. Proceedings of the Association of American Physicians. 1997;109:462-9.

[48] Hsing AW, Hansson LE, McLaughlin JK, Nyren O, Blot WJ, Ekbom A, et al. Pernicious anemia and subsequent cancer: A population-based cohort study. Cancer. 1993;71:745-50.

[49] Brittan M, Wright NA. Gastrointestinal stem cells. The Journal of pathology. 2002;197:492-509.

[50] Mills JC, Shivdasani RA. Gastric epithelial stem cells. Gastroenterology. 2011;140:412-24.

[51] Yen TH, Wright NA. The gastrointestinal tract stem cell niche. Stem Cell Reviews. 2006;2:203-12.

[52] Shaker A, Rubin DC. Intestinal stem cells and epithelial-mesenchymal interactions in the crypt and stem cell niche. Translational Research. 2010;156:180-7.

[53] Karam SM. Lineage commitment and maturation of epithelial cells in the gut. Frontiers in bioscience : a journal and virtual library. 1999;4:D286-98.

[54] Anti M, Armuzzi A, Gasbarrini A, Gasbarrini G. Importance of changes in epithelial cell turnover during Helicobacter pylori infection in gastric carcinogenesis. Gut. 1998;43 Suppl 1:S27-32.

[55] Qiao XT, Ziel JW, McKimpson W, Madison BB, Todisco A, Merchant JL, et al. Prospective Identification of a Multilineage Progenitor in Murine Stomach Epithelium. Gastroenterology. 2007;133:1989-98.e3.

[56] Tomita H, Yamada Y, Oyama T, Hata K, Hirose Y, Hara A, et al. Development of gastric tumors in ApcMin/+ mice by the activation of the β-catenin/Tcf signaling pathway. Cancer Research. 2007;67:4079-87.

[57] Takaishi S, Okumura T, Wang TC. Gastric cancer stem cells. Journal of Clinical Oncology. 2008;26:2876-82.

[58] Chaffer CL, Brueckmann I, Scheel C, Kaestli AJ, Wiggins PA, Rodrigues LO, et al. Normal and neoplastic nonstem cells can spontaneously convert to a stem-like state. Proceedings of the National Academy of Sciences of the United States of America. 2011;108:7950-5.

[59] Alison MR, Islam S, Wright NA. Stem cells in cancer: instigators and propagators? J Cell Sci. 2010;123:2357-68.

[60] Takaishi S, Okumura T, Tu S, Wang SSW, Shibata W, Vigneshwaran R, et al. Identification of gastric cancer stem cells using the cell surface marker CD44. Stem Cells. 2009;27:1006-20.

[61] Bernardo ME, Locatelli F, Fibbe WE. Mesenchymal stromal cells. Annals of the New York Academy of Sciences. 2009;1176:101-17.

[62] Horwitz EM, Le Blanc K, Dominici M, Mueller I, Slaper-Cortenbach I, Marini FC, et al. Clarification of the nomenclature for MSC: The International Society for Cellular Therapy position statement. Cytotherapy. 2005;7:393-5.

[63] Dominici M, Le Blanc K, Mueller I, Slaper-Cortenbach I, Marini FC, Krause DS, et al. Minimal criteria for defining multipotent mesenchymal stromal cells. The International Society for Cellular Therapy position statement. Cytotherapy. 2006;8:315-7.

[64] Tse WT, Pendleton JD, Beyer WM, Egalka MC, Guinan EC. Suppression of allogeneic T-cell proliferation by human marrow stromal cells: implications in transplantation. Transplantation. 2003;75:389-97.

[65] Spaggiari GM, Capobianco A, Abdelrazik H, Becchetti F, Mingari MC, Moretta L. Mesenchymal stem cells inhibit natural killer-cell proliferation, cytotoxicity, and cytokine production: role of indoleamine 2,3-dioxygenase and prostaglandin E2. Blood. 2008;111:1327-33.

[66] Chen L, Tredget EE, Wu PY, Wu Y. Paracrine factors of mesenchymal stem cells recruit macrophages and endothelial lineage cells and enhance wound healing. PloS one. 2008;3:e1886.

[67] Desmouliere A, Chaponnier C, Gabbiani G. Tissue repair, contraction, and the myofibroblast. Wound repair and regeneration : official publication of the Wound Healing Society [and] the European Tissue Repair Society. 2005;13:7-12.

[68] Powell DW, Mifflin RC, Valentich JD, Crowe SE, Saada JI, West AB. Myofibroblasts. II. Intestinal subepithelial myofibroblasts. American Journal of Physiology - Cell Physiology. 1999;277:C183-C201.

[69] Eyden B. The myofibroblast: Phenotypic characterization as a prerequisite to understanding its functions in translational medicine: Translational Medicine. Journal of Cellular and Molecular Medicine. 2007;12:22-37.

[70] Wu KC, Jackson LM, Galvin AM, Gray T, Hawkey CJ, Mahida YR. Phenotypic and functional characterisation of myofibroblasts, macrophages, and lymphocytes migrating out of the human gastric lamina propria following the loss of epithelial cells. Gut. 1999;44:323-30.

[71] Mahida YR, Beltinger J, Makh S, Göke M, Gray T, Podolsky DK, et al. Adult human colonic subepithelial myofibroblasts express extracellular matrix proteins and cyclooxygenase-1 and -2. American Journal of Physiology - Gastrointestinal and Liver Physiology. 1997;273:G1341-G8.

[72] Cohn SM, Schloemann S, Tessner T, Seibert K, Stenson WF. Crypt stem cell survival in the mouse intestinal epithelium is regulated by prostaglandins synthesized through cyclooxygenase-1. Journal of Clinical Investigation. 1997;99:1367-79.

[73] McCaig C, Duval C, Hemers E, Steele I, Pritchard DM, Przemeck S, et al. The Role of Matrix Metalloproteinase-7 in Redefining the Gastric Microenvironment in Response to Helicobacter pylori. Gastroenterology. 2006;130:1754-63.

[74] Czepan M, Rakonczay Z, Jr., Varro A, Steele I, Dimaline R, Lertkowit N, et al. NHE1 activity contributes to migration and is necessary for proliferation of human gastric myofibroblasts. Pflugers Archiv : European journal of physiology. 2012;463:459-75.

[75] McKaig BC, Makh SS, Hawkey CJ, Podolsky DK, Mahida YR. Normal human colonic subepithelial myofibroblasts enhance epithelial migration (restitution) via TGF-β3. American Journal of Physiology - Gastrointestinal and Liver Physiology. 1999;276:G1087-G93.

[76] Beltinger J, McKaig BC, Makh S, Stack WA, Hawkey CJ, Mahida YR. Human colonic subepithelial myofibroblasts modulate transepithelial resistance and secretory response. American Journal of Physiology - Cell Physiology. 1999;277:C271-C9.

[77] Goke M, Kanai M, Podolsky DK. Intestinal fibroblasts regulate intestinal epithelial cell proliferation via hepatocyte growth factor. The American journal of physiology. 1998;274:G809-18.

[78] Visco V, Bava FA, d'Alessandro F, Cavallini M, Ziparo V, Torrisi MR. Human colon fibroblasts induce differentiation and proliferation of intestinal epithelial cells through the direct paracrine action of keratinocyte growth factor. Journal of cellular physiology. 2009;220:204-13.

[79] Otte JM, Rosenberg IM, Podolsky DK. Intestinal myofibroblasts in innate immune responses of the intestine. Gastroenterology. 2003;124:1866-78.

[80] Saada JI, Pinchuk IV, Barrera CA, Adegboyega PA, Suarez G, Mifflin RC, et al. Subepithelial myofibroblasts are novel nonprofessional APCs in the human colonic mucosa. Journal of immunology (Baltimore, Md : 1950). 2006;177:5968-79.

[81] Fan D, Takawale A, Lee J, Kassiri Z. Cardiac fibroblasts, fibrosis and extracellular matrix remodeling in heart disease. Fibrogenesis & tissue repair. 2012;5:15.

[82] Stamenkovic I. Extracellular matrix remodelling: The role of matrix metalloproteinases. Journal of Pathology. 2003;200:448-64.

[83] Powell DW, Adegboyega PA, Di Mari JF, Mifflin RC. Epithelial cells and their neighbors I. Role of intestinal myofibroblasts in development, repair, and cancer. American journal of physiology Gastrointestinal and liver physiology. 2005;289:G2-7.

[84] van Hinsbergh VW, Engelse MA, Quax PH. Pericellular proteases in angiogenesis and vasculogenesis. Arteriosclerosis, thrombosis, and vascular biology. 2006;26:716-28.

[85] Łukaszewicz-Zajac M, Mroczko B, Szmitkowski M. Gastric cancer - The role of matrix metalloproteinases in tumor progression. Clinica Chimica Acta. 2011;412:1725-30.

[86] Groblewska M, Siewko M, Mroczko B, Szmitkowski M. The role of matrix metalloproteinases (MMPs) and their inhibitors (TIMPs) in the development of esophageal cancer. Folia Histochemica et Cytobiologica. 2012;50:12-9.

[87] Sternlicht MD, Werb Z. How matrix metalloproteinases regulate cell behavior. 2001. p. 463-516.

[88] Bamba S, Andoh A, Yasui H, Araki Y, Bamba T, Fujiyama Y. Matrix metalloproteinase-3 secretion from human colonic subepithelial myofibroblasts: role of interleukin-17. Journal of gastroenterology. 2003;38:548-54.

[89] Okuno T, Andoh A, Bamba S, Araki Y, Fujiyama Y, Fujiyama M, et al. Interleukin-1beta and tumor necrosis factor-alpha induce chemokine and matrix metalloproteinase gene expression in human colonic subepithelial myofibroblasts. Scandinavian journal of gastroenterology. 2002;37:317-24.

[90] McKaig BC, McWilliams D, Watson SA, Mahida YR. Expression and regulation of tissue inhibitor of metalloproteinase-1 and matrix metalloproteinases by intestinal myofibroblasts in inflammatory bowel disease. The American journal of pathology. 2003;162:1355-60.

[91] McCawley LJ, Matrisian LM. Matrix metalloproteinases: they're not just for matrix anymore! Current opinion in cell biology. 2001;13:534-40.

[92] Hemers E, Duval C, McCaig C, Handley M, Dockray GJ, Varro A. Insulin-like growth factor binding protein-5 is a target of matrix metalloproteinase-7: Implications for epithelial-mesenchymal signaling. Cancer Research. 2005;65:7363-9.

[93] Murphy G. Tissue inhibitors of metalloproteinases. Genome Biology. 2011;12.

[94] Leco KJ, Khokha R, Pavloff N, Hawkes SP, Edwards DR. Tissue inhibitor of metalloproteinases-3 (TIMP-3) is an extracellular matrix-associated protein with a distinctive pattern of expression in mouse cells and tissues. The Journal of biological chemistry. 1994;269:9352-60.

[95] Leco KJ, Apte SS, Taniguchi GT, Hawkes SP, Khokha R, Schultz GA, et al. Murine tissue inhibitor of metalloproteinases-4 (Timp-4): cDNA isolation and expression in adult mouse tissues. FEBS letters. 1997;401:213-7.

[96] Bodger K, Ahmed S, Pazmany L, Pritchard DM, Micheal A, Khan AL, et al. Altered gastric corpus expression of tissue inhibitors of metalloproteinases in human and murine Helicobacter infection. Journal of clinical pathology. 2008;61:72-8.

[97] Andreasen PA, Kjoller L, Christensen L, Duffy MJ. The urokinase-type plasminogen activator system in cancer metastasis: a review. International journal of cancer Journal international du cancer. 1997;72:1-22.

[98] Kenny S, Duval C, Sammut SJ, Steele I, Pritchard DM, Atherton JC, et al. Increased expression of the urokinase plasminogen activator system by Helicobacter pylori in gastric epithelial cells. American journal of physiology Gastrointestinal and liver physiology. 2008;295:G431-41.

[99] Powell DW, Mifflin RC, Valentich JD, Crowe SE, Saada JI, West AB. Myofibroblasts. I. Paracrine cells important in health and disease. American Journal of Physiology - Cell Physiology. 1999;277:C1-C19.

[100] Yeung TM, Chia LA, Kosinski CM, Kuo CJ. Regulation of self-renewal and differentiation by the intestinal stem cell niche. Cellular and Molecular Life Sciences. 2011;68:2513-23.

[101] Miyazono K. Positive and negative regulation of TGF-beta signaling. J Cell Sci. 2000;113 (Pt 7):1101-9.

[102] Naef M, Ishiwata T, Friess H, Büchler MW, Gold LI, Korc M. Differential localization of transforming growth factor-β isoforms in human gastric mucosa and overexpression in gastric carcinoma. International Journal of Cancer. 1997;71:131-7.

[103] Shinto O, Yashiro M, Toyokawa T, Nishii T, Kaizaki R, Matsuzaki T, et al. Phosphorylated Smad2 in Advanced Stage Gastric Carcinoma. BMC Cancer. 2010;10.

[104] Lees C, Howie S, Sartor RB, Satsangi J. The hedgehog signalling pathway in the gastrointestinal tract: Implications for development, homeostasis, and disease. Gastroenterology. 2005;129:1696-710.

[105] Zacharias WJ, Li X, Madison BB, Kretovich K, Kao JY, Merchant JL, et al. Hedgehog is an anti-inflammatory epithelial signal for the intestinal lamina propria. Gastroenterology. 2010;138:2368-77, 77 e1-4.

[106] Van Den Brink GR. Hedgehog signaling in development and homeostasis of the gastrointestinal tract. Physiological Reviews. 2007;87:1343-75.

[107] Carpenter D, Stone DM, Brush J, Ryan A, Armanini M, Frantz G, et al. Characterization of two patched receptors for the vertebrate hedgehog protein family. Proceedings of the National Academy of Sciences of the United States of America. 1998;95:13630-4.

[108] Fuccillo M, Joyner AL, Fishell G. Morphogen to mitogen: the multiple roles of hedgehog signalling in vertebrate neural development. Nature reviews Neuroscience. 2006;7:772-83.

[109] van den Brink GR, Hardwick JC, Tytgat GN, Brink MA, Ten Kate FJ, Van Deventer SJ, et al. Sonic hedgehog regulates gastric gland morphogenesis in man and mouse. Gastroenterology. 2001;121:317-28.

[110] Dimmler A, Brabletz T, Hlubek F, Häfner M, Rau T, Kirchner T, et al. Transcription of Sonic Hedgehog, a Potential Factor for Gastric Morphogenesis and Gastric Mucosa Maintenance, Is Up-regulated in Acidic Conditions. Laboratory Investigation. 2003;83:1829-37.

[111] Merchant JL. Hedgehog signalling in gut development, physiology and cancer. Journal of Physiology. 2012;590:421-32.

[112] Katoh M, Katoh M. Notch signaling in gastrointestinal tract (review). International journal of oncology. 2007;30:247-51.

[113] Kim TH, Shivdasani RA. Notch signaling in stomach epithelial stem cell homeostasis. J Exp Med. 2011;208:677-88.

[114] Aster JC, Blacklow SC. Targeting the Notch pathway: twists and turns on the road to rational therapeutics. Journal of clinical oncology : official journal of the American Society of Clinical Oncology. 2012;30:2418-20.

[115] Clevers H. Wnt/β-Catenin Signaling in Development and Disease. Cell. 2006;127:469-80.

[116] Katoh M, Katoh M. WNT signaling pathway and stem cell signaling network. Clinical cancer research : an official journal of the American Association for Cancer Research. 2007;13:4042-5.

[117] Schulte G, Bryja V. The Frizzled family of unconventional G-protein-coupled receptors. Trends in pharmacological sciences. 2007;28:518-25.

[118] Nelson WJ, Nusse R. Convergence of Wnt, β-Catenin, and Cadherin pathways. Science (New York, NY). 2004;303:1483-7.

[119] Clevers H, Nusse R. Wnt/beta-catenin signaling and disease. Cell. 2012;149:1192-205.

[120] Mikels AJ, Nusse R. Purified Wnt5a protein activates or inhibits beta-catenin-TCF signaling depending on receptor context. PLoS biology. 2006;4.

[121] Ishitani T, Kishida S, Hyodo-Miura J, Ueno N, Yasuda J, Waterman M, et al. The TAK1-NLK mitogen-activated protein kinase cascade functions in the Wnt-5a/Ca2+ pathway to antagonize Wnt/β-catenin signaling. Molecular and Cellular Biology. 2003;23:131-9.

[122] Huelsken J, Behrens J. The Wnt signalling pathway. Journal of cell science. 2002;115:3977-8.

[123] Andoh A, Bamba S, Fujiyama Y, Brittan M, Wright NA. Colonic subepithelial myofibroblasts in mucosal inflammation and repair: Contribution of bone marrow-derived stem cells to the gut regenerative response. Journal of Gastroenterology. 2005;40:1089-99.

[124] Hughes KR, Sablitzky F, Mahida YR. Expression profiling of Wnt family of genes in normal and inflammatory bowel disease primary human intestinal myofibroblasts and normal human colonic crypt epithelial cells. Inflammatory Bowel Diseases. 2011;17:213-20.

[125] Gregorieff A, Pinto D, Begthel H, Destrée O, Kielman M, Clevers H. Expression pattern of Wnt signaling components in the adult intestine. Gastroenterology. 2005;129:626-38.

[126] Wu WK, Cho CH, Lee CW, Fan D, Wu K, Yu J, et al. Dysregulation of cellular signaling in gastric cancer. Cancer letters. 2010;295:144-53.

[127] Hanahan D, Weinberg RA. Hallmarks of cancer: The next generation. Cell. 2011;144:646-74.

[128] Langley RR, Fidler IJ. The seed and soil hypothesis revisited--the role of tumor-stroma interactions in metastasis to different organs. International journal of cancer Journal international du cancer. 2011;128:2527-35.

[129] Paget S. THE DISTRIBUTION OF SECONDARY GROWTHS IN CANCER OF THE BREAST. The Lancet. 1889;133:571-3.

[130] Ribatti D. The contribution of Harold F. Dvorak to the study of tumor angiogenesis and stroma generation mechanisms. Endothelium : journal of endothelial cell research. 2007;14:131-5.

[131] Chiba T, Marusawa H, Ushijima T. Inflammation-associated cancer development in digestive organs: mechanisms and roles for genetic and epigenetic modulation. Gastroenterology. 2012;143:550-63.

[132] Hanahan D, Weinberg RA. The hallmarks of cancer. Cell. 2000;100:57-70.

[133] Hsu PP, Sabatini DM. Cancer cell metabolism: Warburg and beyond. Cell. 2008;134:703-7.

[134] Bhowmick NA, Neilson EG, Moses HL. Stromal fibroblasts in cancer initiation and progression. Nature. 2004;432:332-7.

[135] Futreal PA, Coin L, Marshall M, Down T, Hubbard T, Wooster R, et al. A census of human cancer genes. Nature Reviews Cancer. 2004;4:177-83.

[136] Knudson AG. Two genetic hits (more or less) to cancer. Nature Reviews Cancer. 2001;1:157-62.

[137] Knudson AG, Jr. Mutation and cancer: statistical study of retinoblastoma. Proc Natl Acad Sci U S A. 1971;68:820-3.

[138] Oda T, Kanai Y, Oyama T, Yoshiura K, Shimoyama Y, Birchmeier W, et al. E-cadherin gene mutations in human gastric carcinoma cell lines. Proceedings of the National Academy of Sciences of the United States of America. 1994;91:1858-62.

[139] Fearon ER, Vogelstein B. A genetic model for colorectal tumorigenesis. Cell. 1990;61:759-67.

[140] Hudler P. Genetic aspects of gastric cancer instability. TheScientificWorldJournal. 2012;2012:761909.

[141] Weiss MM, Kuipers EJ, Postma C, Snijders AM, Pinkel D, Meuwissen SGM, et al. Genomic alterations in primary gastric adenocarcinomas correlate with clinicopathological characteristics and survival. Cellular Oncology. 2004;26:307-17.

[142] Ottini L, Falchetti M, Lupi R, Rizzolo P, Agnese V, Colucci G, et al. Patterns of genomic instability in gastric cancer: clinical implications and perspectives. Annals of oncology : official journal of the European Society for Medical Oncology / ESMO. 2006;17 Suppl 7:vii97-102.

[143] Selcuklu SD, Spillane C. Translational epigenetics: clinical approaches to epigenome therapeutics for cancer. Epigenetics : official journal of the DNA Methylation Society. 2008;3:107-12.

[144] Smith LT, Otterson GA, Plass C. Unraveling the epigenetic code of cancer for therapy. Trends in Genetics. 2007;23:449-56.

[145] Fearon ER. Molecular genetics of colorectal cancer. 2011. p. 479-507.

[146] Tamura G, Yin J, Wang S, Fleisher AS, Zou T, Abraham JM, et al. E-cadherin gene promoter hypermethylation in primary human gastric carcinomas. Journal of the National Cancer Institute. 2000;92:569-73.

[147] Maekita T, Nakazawa K, Mihara M, Nakajima T, Yanaoka K, Iguchi M, et al. High levels of aberrant DNA methylation in Helicobacter pylori-infected gastric mucosae and its possible association with gastric cancer risk. Clinical cancer research : an official journal of the American Association for Cancer Research. 2006;12:989-95.

[148] Gonda TA, Kim YI, Salas MC, Gamble MV, Shibata W, Muthupalani S, et al. Folic acid increases global DNA methylation and reduces inflammation to prevent Helicobacter-associated gastric cancer in mice. Gastroenterology. 2012;142:824-33 e7.

[149] Jiang L, Gonda TA, Gamble MV, Salas M, Seshan V, Tu S, et al. Global hypomethylation of genomic DNA in cancer-associated myofibroblasts. Cancer Research. 2008;68:9900-8.

[150] Tazawa H, Kagawa S, Fujiwara T. MicroRNAs as potential target gene in cancer gene therapy of gastrointestinal tumors. Expert opinion on biological therapy. 2011;11:145-55.

[151] McKenna LB, Schug J, Vourekas A, McKenna JB, Bramswig NC, Friedman JR, et al. MicroRNAs control intestinal epithelial differentiation, architecture, and barrier function. Gastroenterology. 2010;139:1654-64.e1.

[152] Noto JM, Peek RM. The Role of microRNAs in Helicobacter pylori Pathogenesis and Gastric Carcinogenesis. Frontiers in cellular and infection microbiology. 2011;1:21.

[153] Song JH, Meltzer SJ. MicroRNAs in pathogenesis, diagnosis, and treatment of gastroesophageal cancers. Gastroenterology. 2012;143:35-47 e2.

[154] Saito Y, Suzuki H, Hibi T. The role of microRNAs in gastrointestinal cancers. Journal of gastroenterology. 2009;44 Suppl 19:18-22.

[155] Calin GA, Sevignani C, Dumitru CD, Hyslop T, Noch E, Yendamuri S, et al. Human microRNA genes are frequently located at fragile sites and genomic regions involved in cancers. Proc Natl Acad Sci U S A. 2004;101:2999-3004.

[156] Lewis BP, Burge CB, Bartel DP. Conserved seed pairing, often flanked by adenosines, indicates that thousands of human genes are microRNA targets. Cell. 2005;120:15-20.

[157] Zhang B, Pan X, Cobb GP, Anderson TA. microRNAs as oncogenes and tumor suppressors. Developmental biology. 2007;302:1-12.

[158] Garzon R, Fabbri M, Cimmino A, Calin GA, Croce CM. MicroRNA expression and function in cancer. Trends in molecular medicine. 2006;12:580-7.

[159] Lu J, Getz G, Miska EA, Alvarez-Saavedra E, Lamb J, Peck D, et al. MicroRNA expression profiles classify human cancers. Nature. 2005;435:834-8.

[160] Mathe EA, Nguyen GH, Bowman ED, Zhao Y, Budhu A, Schetter AJ, et al. MicroRNA expression in squamous cell carcinoma and adenocarcinoma of the esophagus: associations with survival. Clinical cancer research : an official journal of the American Association for Cancer Research. 2009;15:6192-200.

[161] Zhang BG, Li JF, Yu BQ, Zhu ZG, Liu BY, Yan M. microRNA-21 promotes tumor proliferation and invasion in gastric cancer by targeting PTEN. Oncology reports. 2012;27:1019-26.

[162] Takagi T, Iio A, Nakagawa Y, Naoe T, Tanigawa N, Akao Y. Decreased expression of microRNA-143 and -145 in human gastric cancers. Oncology. 2009;77:12-21.

[163] Jin Z, Selaru FM, Cheng Y, Kan T, Agarwal R, Mori Y, et al. MicroRNA-192 and -215 are upregulated in human gastric cancer in vivo and suppress ALCAM expression in vitro. Oncogene. 2011;30:1577-85.

[164] Braun CJ, Zhang X, Savelyeva I, Wolff S, Moll UM, Schepeler T, et al. p53-Responsive micrornas 192 and 215 are capable of inducing cell cycle arrest. Cancer research. 2008;68:10094-104.

[165] Lujambio A, Calin GA, Villanueva A, Ropero S, Sánchez-Céspedes M, Blanco D, et al. A microRNA DNA methylation signature for human cancer metastasis. Proceedings of the National Academy of Sciences of the United States of America. 2008;105:13556-61.

[166] Lujambio A, Esteller M. CpG island hypermethylation of tumor suppressor microRNAs in human cancer. Cell cycle (Georgetown, Tex). 2007;6:1455-9.

[167] Han L, Witmer PD, Casey E, Valle D, Sukumar S. DNA methylation regulates MicroRNA expression. Cancer biology & therapy. 2007;6:1284-8.

[168] Hayashi Y, Tsujii M, Wang J, Kondo J, Akasaka T, Jin Y, et al. CagA mediates epigenetic regulation to attenuate let-7 expression in Helicobacter pylori-related carcinogenesis. Gut. 2012.

[169] Fabbri M, Calin GA. Epigenetics and miRNAs in human cancer. Advances in genetics. 2010;70:87-99.

[170] Orimo A, Weinberg RA. Stromal fibroblasts in cancer: A novel tumor-promoting cell type. Cell Cycle. 2006;5:1597-601.

[171] Quante M, Wang TC. Inflammation and stem cells in gastrointestinal carcinogenesis. Physiology (Bethesda, Md). 2008;23:350-9.

[172] Zhi K, Shen X, Zhang H, Bi J. Cancer-associated fibroblasts are positively correlated with metastatic potential of human gastric cancers. Journal of experimental & clinical cancer research : CR. 2010;29:66.

[173] Balkwill F, Mantovani A. Inflammation and cancer: back to Virchow? Lancet. 2001;357:539-45.

[174] Raza A, Franklin MJ, Dudek AZ. Pericytes and vessel maturation during tumor angiogenesis and metastasis. American Journal of Hematology. 2010;85:593-8.

[175] Sugiyama Y, Farrow B, Murillo C, Li J, Watanabe H, Sugiyama K, et al. Analysis of differential gene expression patterns in colon cancer and cancer stroma using microdissected tissues. Gastroenterology. 2005;128:480-6.

[176] Niu HT, Yang CM, Jiang G, Xu T, Cao YW, Zhao J, et al. Cancer stroma proteome expression profile of superficial bladder transitional cell carcinoma and biomarker discovery. Journal of cancer research and clinical oncology. 2011;137:1273-82.

[177] Hill R, Song Y, Cardiff RD, Van Dyke T. Selective evolution of stromal mesenchyme with p53 loss in response to epithelial tumorigenesis. Cell. 2005;123:1001-11.

[178] Gonda TA, Varro A, Wang TC, Tycko B. Molecular biology of cancer-associated fibroblasts: can these cells be targeted in anti-cancer therapy? Seminars in cell & developmental biology. 2010;21:2-10.

[179] Holmberg C, Quante M, Steele I, Kumar JD, Balabanova S, Duval C, et al. Release of TGFβig-h3 by gastric myofibroblasts slows tumor growth and is decreased with cancer progression. Carcinogenesis. 2012;33:1553-62.

[180] Fuyuhiro Y, Yashiro M, Noda S, Matsuoka J, Hasegawa T, Kato Y, et al. Cancer-associated orthotopic myofibroblasts stimulates the motility of gastric carcinoma cells. Cancer science. 2012;103:797-805.

[181] Grugan KD, Miller CG, Yao Y, Michaylira CZ, Ohashi S, Klein-Szanto AJ, et al. Fibroblast-secreted hepatocyte growth factor plays a functional role in esophageal squamous cell carcinoma invasion. Proceedings of the National Academy of Sciences of the United States of America. 2010;107:11026-31.

[182] Noma K, Smalley KSM, Lioni M, Naomoto Y, Tanaka N, El-Deiry W, et al. The Essential Role of Fibroblasts in Esophageal Squamous Cell Carcinoma-Induced Angiogenesis. Gastroenterology. 2008;134:1981-93.

[183] Anderberg C, Pietras K. On the origin of cancer-associated fibroblasts. Cell Cycle. 2009;8:1461-2.

[184] Cho JA, Park H, Lim EH, Kim KH, Choi JS, Lee JH, et al. Exosomes from ovarian cancer cells induce adipose tissue-derived mesenchymal stem cells to acquire the physical and functional characteristics of tumor-supporting myofibroblasts. Gynecol Oncol. 2011;123:379-86.

[185] Aprelikova O, Palla J, Hibler B, Yu X, Greer YE, Yi M, et al. Silencing of miR-148a in cancer-associated fibroblasts results in WNT10B-mediated stimulation of tumor cell motility. Oncogene. 2012.

[186] Aprelikova O, Yu X, Palla J, Wei BR, John S, Yi M, et al. The role of miR-31 and its target gene SATB2 in cancer-associated fibroblasts. Cell cycle (Georgetown, Tex). 2010;9:4387-98.

[187] Bronisz A, Godlewski J, Wallace JA, Merchant AS, Nowicki MO, Mathsyaraja H, et al. Reprogramming of the tumour microenvironment by stromal PTEN-regulated miR-320. Nat Cell Biol. 2012;14:159-67.

[188] Zhao L, Sun Y, Hou Y, Peng Q, Wang L, Luo H, et al. MiRNA expression analysis of cancer-associated fibroblasts and normal fibroblasts in breast cancer. The international journal of biochemistry & cell biology. 2012;44:2051-9.

[189] Enkelmann A, Heinzelmann J, Von Eggeling F, Walter M, Berndt A, Wunderlich H, et al. Specific protein and miRNA patterns characterise tumour-associated fibroblasts in bladder cancer. Journal of cancer research and clinical oncology. 2011;137:751-9.

[190] Ishii G, Sangai T, Oda T, Aoyagi Y, Hasebe T, Kanomata N, et al. Bone-marrow-derived myofibroblasts contribute to the cancer-induced stromal reaction. Biochemical and Biophysical Research Communications. 2003;309:232-40.

[191] Mishra PJ, Mishra PJ, Humeniuk R, Medina DJ, Alexe G, Mesirov JP, et al. Carcinoma-associated fibroblast-like differentiation of human mesenchymal stem cells. Cancer Research. 2008;68:4331-9.

[192] Direkze NC, Hodivala-Dilke K, Jeffery R, Hunt T, Poulsom R, Oukrif D, et al. Bone marrow contribution to tumor-associated myofibroblasts and fibroblasts. Cancer Research. 2004;64:8492-5.

[193] Quante M, Tu SP, Tomita H, Gonda T, Wang SSW, Takashi S, et al. Bone Marrow-Derived Myofibroblasts Contribute to the Mesenchymal Stem Cell Niche and Promote Tumor Growth. Cancer Cell. 2011;19:257-72.

[194] Peters BA, Diaz Jr LA, Polyak K, Meszler L, Romans K, Guinan EC, et al. Contribution of bone marrow-derived endothelial cells to human tumor vasculature. Nature Medicine. 2005;11:261-2.

[195] Bellows CF, Zhang Y, Chen J, Frazier ML, Kolonin MG. Circulation of progenitor cells in obese and lean colorectal cancer patients. Cancer Epidemiology Biomarkers and Prevention. 2011;20:2461-8.

[196] Mishra PJ, Mishra PJ, Glod JW, Banerjee D. Mesenchymal stem cells: Flip side of the coin. Cancer Research. 2009;69:1255-8.

[197] Polyak K, Haviv I, Campbell IG. Co-evolution of tumor cells and their microenvironment. Trends in Genetics. 2009;25:30-8.

[198] Guo X, Oshima H, Kitmura T, Taketo MM, Oshima M. Stromal fibroblasts activated by tumor cells promote angiogenesis in mouse gastric cancer. The Journal of biological chemistry. 2008;283:19864-71.

[199] Ritchie ME, Silver J, Oshlack A, Holmes M, Diyagama D, Holloway A, et al. A comparison of background correction methods for two-colour microarrays. Bioinformatics. 2007;23:2700-7.

[200] Griffiths-Jones S, Saini HK, Van Dongen S, Enright AJ. miRBase: Tools for microRNA genomics. Nucleic acids research. 2008;36:D154-D8.

[201] Li C, Hung Wong W. Model-based analysis of oligonucleotide arrays: model validation, design issues and standard error application. Genome Biology. 2001;2.

[202] Vergoulis T, Vlachos IS, Alexiou P, Georgakilas G, Maragkakis M, Reczko M, et al. TarBase 6.0: Capturing the exponential growth of miRNA targets with experimental support. Nucleic acids research. 2012;40:D222-D9.

[203] Xiao F, Zuo Z, Cai G, Kang S, Gao X, Li T. miRecords: An integrated resource for microRNA-target interactions. Nucleic acids research. 2009;37:D105-D10.

[204] Friedman RC, Farh KKH, Burge CB, Bartel DP. Most mammalian mRNAs are conserved targets of microRNAs. Genome Research. 2009;19:92-105.

[205] Chen HC, Chen GH, Chen YH, Liao WL, Liu CY, Chang KP, et al. MicroRNA deregulation and pathway alterations in nasopharyngeal carcinoma. Br J Cancer. 2009;100:1002-11.

[206] Pfaffl MW. A new mathematical model for relative quantification in real-time RT-PCR. Nucleic acids research. 2001;29.

[207] Nishida N, Nagahara M, Sato T, Mimori K, Sudo T, Tanaka F, et al. Microarray analysis of colorectal cancer stromal tissue reveals upregulation of two oncogenic miRNA clusters. Clinical Cancer Research. 2012;18:3054-70.

[208] Mraz M, Malinova K, Mayer J, Pospisilova S. MicroRNA isolation and stability in stored RNA samples. Biochemical and Biophysical Research Communications. 2009;390:1-4.

[209] Callari M, Dugo M, Musella V, Marchesi E, Chiorino G, Grand MM, et al. Comparison of microarray platforms for measuring differential microRNA expression in paired normal/cancer colon tissues. PloS one. 2012;7:e45105.

[210] Válóczi A, Hornyik C, Varga N, Burgyán J, Kauppinen S, Havelda Z. Sensitive and specific detection of microRNAs by northern blot analysis using LNA-modified oligonucleotide probes. Nucleic acids research. 2004;32.

[211] Wienholds E, Kloosterman WP, Miska E, Alvarez-Saavedra E, Berezikov E, De Bruijn E, et al. Cell biology: MicroRNA expression in zebrafish embryonic development. Science. 2005;309:310-1.

[212] Castoldi M, Schmidt S, Benes V, Noerholm M, Kulozik AE, Hentze MW, et al. A sensitive array for microRNA expression profiling (miChip) based on locked nucleic acids (LNA). RNA. 2006;12:913-20.

[213] Rossing M, Borup R, Henao R, Winther O, Vikesaa J, Niazi O, et al. Down-regulation of microRNAs controlling tumourigenic factors in follicular thyroid carcinoma. Journal of Molecular Endocrinology. 2012;48:11-23.

[214] Willenbrock H, Salomon J, Søkilde R, Barken KB, Hansen TN, Nielsen FC, et al. Quantitative miRNA expression analysis: Comparing microarrays with next-generation sequencing. RNA. 2009;15:2028-34.

[215] Kim NH, Kim HS, Kim NG, Lee I, Choi HS, Li XY, et al. p53 and microRNA-34 are suppressors of canonical Wnt signaling. Science Signaling. 2011;4.

[216] Ren XP, Wu J, Wang X, Sartor MA, Qian J, Jones K, et al. MicroRNA-320 is involved in the regulation of cardiac ischemia/reperfusion injury by targeting heat-shock protein 20. Circulation. 2009;119:2357-66.

[217] Mycko MP, Cichalewska M, Machlanska A, Cwiklinska H, Mariasiewicz M, Selmaj KW. MicroRNA-301a regulation of a T-helper 17 immune response controls autoimmune demyelination. Proceedings of the National Academy of Sciences of the United States of America. 2012;109:E1248-E57.

[218] Zhu QY, Liu Q, Chen JX, Lan K, Ge BX. MicroRNA-101 targets MAPK phosphatase-1 to regulate the activation of MAPKs in macrophages. Journal of immunology (Baltimore, Md : 1950). 2010;185:7435-42.

[219] Walker JL, Zhai N, Zhang L, Bleaken BM, Wolff I, Gerhart J, et al. Unique precursors for the mesenchymal cells involved in injury response and fibrosis. Proceedings of the National Academy of Sciences of the United States of America. 2010;107:13730-5.

[220] Kapinas K, Kessler C, Ricks T, Gronowicz G, Delany AM. miR-29 modulates Wnt signaling in human osteoblasts through a positive feedback loop. Journal of Biological Chemistry. 2010;285:25221-31.

[221] Yang J, Qin S, Yi C, Ma G, Zhu H, Zhou W, et al. MiR-140 is co-expressed with Wwp2-C transcript and activated by Sox9 to target Sp1 in maintaining the chondrocyte proliferation. FEBS letters. 2011;585:2992-7.

[222] Bousquet M, Nguyen D, Chen C, Shields L, Lodish HF. MicroRNA-125b transforms myeloid cell lines by repressing multiple mRNA. Haematologica. 2012;97:1713-21.

[223] Wang J, Cao N, Yuan M, Cui H, Tang Y, Qin L, et al. MicroRNA-125b/Lin28 Pathway Contributes to the Mesendodermal Fate Decision of Embryonic Stem Cells. Stem cells and development. 2012;21:1524-37.

[224] Aranha MM, Santos DM, Solá S, Steer CJ, Rodrigues CM. miR-34a regulates mouse neural stem cell differentiation. PloS one. 2011;6.

[225] Chang SJ, Weng SL, Hsieh JY, Wang TY, Chang MD, Wang HW. MicroRNA-34a modulates genes involved in cellular motility and oxidative phosphorylation in neural precursors derived from human umbilical cord mesenchymal stem cells. BMC medical genomics. 2011;4:65.

[226] Li N, Kaur S, Greshock J, Lassus H, Zhong X, Wang Y, et al. A combined array-based comparative genomic hybridization and functional library screening approach identifies mir-30d as an oncomir in cancer. Cancer research. 2012;72:154-64.

[227] Nakano H, Miyazawa T, Kinoshita K, Yamada Y, Yoshida T. Functional screening identifies a microRNA, miR-491 that induces apoptosis by targeting Bcl-X(L) in colorectal cancer cells. International journal of cancer Journal international du cancer. 2010;127:1072-80.

[228] Lewis BP, Shih IH, Jones-Rhoades MW, Bartel DP, Burge CB. Prediction of Mammalian MicroRNA Targets. Cell. 2003;115:787-98.

[229] Meng F, Glaser SS, Francis H, Demorrow S, Han Y, Passarini JD, et al. Functional analysis of microRNAs in human hepatocellular cancer stem cells. Journal of cellular and molecular medicine. 2012;16:160-73.

[230] Li QJ, Chau J, Ebert PJ, Sylvester G, Min H, Liu G, et al. miR-181a is an intrinsic modulator of T cell sensitivity and selection. Cell. 2007;129:147-61.

[231] Gusev Y, Schmittgen TD, Lerner M, Postier R, Brackett D. Computational analysis of biological functions and pathways collectively targeted by co-expressed microRNAs in cancer. BMC Bioinformatics. 2007;8.

[232] Wu S, Huang S, Ding J, Zhao Y, Liang L, Liu T, et al. Multiple microRNAs modulate p21Cip1/Waf1 expression by directly targeting its 3′ untranslated region. Oncogene. 2010;29:2302-8.

[233] Thomson DW, Bracken CP, Goodall GJ. Experimental strategies for microRNA target identification. Nucleic Acids Research. 2011;39:6845-53.

[234] Krek A, Grün D, Poy MN, Wolf R, Rosenberg L, Epstein EJ, et al. Combinatorial microRNA target predictions. Nature Genetics. 2005;37:495-500.

[235] Van Der Auwera I, Limame R, Van Dam P, Vermeulen PB, Dirix LY, Van Laere SJ. Integrated miRNA and mRNA expression profiling of the inflammatory breast cancer subtype. British Journal of Cancer. 2010;103:532-41.

[236] Musumeci M, Coppola V, Addario A, Patrizii M, Maugeri-Saccá M, Memeo L, et al. Control of tumor and microenvironment cross-talk by miR-15a and miR-16 in prostate cancer. Oncogene. 2011;30:4231-42.

[237] De Yébenes VG, Belver L, Pisano DG, González S, Villasante A, Croce C, et al. miR-181b negatively regulates activation-induced cytidine deaminase in B cells. Journal of Experimental Medicine. 2008;205:2199-206.

[238] Zhu W, Shan X, Wang T, Shu Y, Liu P. MiR-181b modulates multidrug resistance by targeting BCL2 in human cancer cell lines. International Journal of Cancer. 2010;127:2520-9.

[239] Chen G, Zhu W, Shi D, Lv L, Zhang C, Liu P, et al. MicroRNA-181a sensitizes human malignant glioma U87MG cells to radiation by targeting Bcl-2. Oncology reports. 2010;23:997-1003.

[240] Cuesta R, Martínez-Sánchez A, Gebauer F. miR-181a regulates cap-dependent translation of p27kip1 mRNA in myeloid cells. Molecular and Cellular Biology. 2009;29:2841-51.

[241] Ji J, Yamashita T, Budhu A, Forgues M, Jia HL, Li C, et al. Identification of microRNA-181 by genome-wide screening as a critical player in EpCAM-positive hepatic cancer stem cells. Hepatology. 2009;50:472-80.

[242] Iliopoulos D, Jaeger SA, Hirsch HA, Bulyk ML, Struhl K. STAT3 activation of miR-21 and miR-181b-1 via PTEN and CYLD are part of the epigenetic switch linking inflammation to cancer. Mol Cell. 2010;39:493-506.

[243] Beveridge NJ, Tooney PA, Carroll AP, Gardiner E, Bowden N, Scott RJ, et al. Dysregulation of miRNA 181b in the temporal cortex in schizophrenia. Human Molecular Genetics. 2008;17:1156-68.

[244] Xue Q, Guo ZY, Li W, Wen WH, Meng YL, Jia LT, et al. Human activated CD4(+) T lymphocytes increase IL-2 expression by downregulating microRNA-181c. Molecular immunology. 2011;48:592-9.

[245] Hashimoto Y, Akiyama Y, Otsubo T, Shimada S, Yuasa Y. Involvement of epigenetically silenced microRNA-181c in gastric carcinogenesis. Carcinogenesis. 2010;31:777-84.

[246] Shin KH, Bae SD, Hong HS, Kim RH, Kang MK, Park NH. miR-181a shows tumor suppressive effect against oral squamous cell carcinoma cells by downregulating K-ras. Biochem Biophys Res Commun. 2011;404:896-902.

[247] Pallasch CP, Patz M, Yoon JP, Hagist S, Eggle D, Claus R, et al. miRNA deregulation by epigenetic silencing disrupts suppression of the oncogene PLAG1 in chronic lymphocytic leukemia. Blood. 2009;114:3255-64.

[248] Pekarsky Y, Santanam U, Cimmino A, Palamarchuk A, Efanov A, Maximov V, et al. Tcl1 expression in chronic lymphocytic leukemia is regulated by miR-29 and miR-181. Cancer Res. 2006;66:11590-3.

[249] Lu Y, Roy S, Nuovo G, Ramaswamy B, Miller T, Shapiro C, et al. Anti-microRNA-222 (anti-miR-222) and -181B suppress growth of tamoxifen-resistant xenografts in mouse by targeting TIMP3 protein and modulating mitogenic signal. The Journal of biological chemistry. 2011;286:42292-302.

[250] Wang B, Hsu SH, Majumder S, Kutay H, Huang W, Jacob ST, et al. TGFbeta-mediated upregulation of hepatic miR-181b promotes hepatocarcinogenesis by targeting TIMP3. Oncogene. 2010;29:1787-97.

[251] Sun X, Icli B, Wara AK, Belkin N, He S, Kobzik L, et al. MicroRNA-181b regulates NF-kappaB-mediated vascular inflammation. The Journal of clinical investigation. 2012;122:1973-90.

[252] Naguibneva I, Ameyar-Zazoua M, Polesskaya A, Ait-Si-Ali S, Groisman R, Souidi M, et al. The microRNA miR-181 targets the homeobox protein Hox-A11 during mammalian myoblast differentiation. Nature Cell Biology. 2006;8:278-84.

[253] Fei J, Li Y, Zhu X, Luo X. miR-181a post-transcriptionally downregulates oncogenic RalA and contributes to growth inhibition and apoptosis in chronic myelogenous leukemia (CML). PloS one. 2012;7:e32834.

[254] Ji J, Yamashita T, Wang XW. Wnt/beta-catenin signaling activates microRNA-181 expression in hepatocellular carcinoma. Cell and Bioscience. 2011;1.

[255] Alexeyenko A, Lee W, Pernemalm M, Guegan J, Dessen P, Lazar V, et al. Network enrichment analysis: extension of gene-set enrichment analysis to gene networks. BMC bioinformatics. 2012;13:226.

[256] Gennarino VA, D'Angelo G, Dharmalingam G, Fernandez S, Russolillo G, Sanges R, et al. Identification of microRNA-regulated gene networks by expression analysis of target genes. Genome Research. 2012;22:1163-72.

[257] Wang Y, Yu Y, Tsuyada A, Ren X, Wu X, Stubblefield K, et al. Transforming growth factor-beta regulates the sphere-initiating stem cell-like feature in breast cancer through miRNA-181 and ATM. Oncogene. 2011;30:1470-80.

[258] Rutnam ZJ, Wight TN, Yang BB. miRNAs regulate expression and function of extracellular matrix molecules. Matrix biology : journal of the International Society for Matrix Biology. 2012.

[259] Zhong Y, Wang Z, Fu B, Pan F, Yachida S, Dhara M, et al. GATA6 activates Wnt signaling in pancreatic cancer by negatively regulating the Wnt antagonist Dickkopf-1. PloS one. 2011;6:e22129.

[260] Angers S, Moon RT. Proximal events in Wnt signal transduction. Nature Reviews Molecular Cell Biology. 2009;10:468-77.

[261] Oshima H, Oshima M. Mouse models of gastric tumors: Wnt activation and PGE2 induction. Pathology International. 2010;60:599-607.

[262] Clements WM, Wang J, Sarnaik A, Kim OJ, MacDonald J, Fenoglio-Preiser C, et al. β-catenin mutation is a frequent cause of Wnt pathway activation in gastric cancer. Cancer research. 2002;62:3503-6.

[263] Franco AT, Israel DA, Washington MK, Krishna U, Fox JG, Rogers AB, et al. Activation of β-catenin by carcinogenic Helicobacter pylori. Proceedings of the National Academy of Sciences of the United States of America. 2005;102:10646-51.

[264] Kurayoshi M, Oue N, Yamamoto H, Kishida M, Inoue A, Asahara T, et al. Expression of Wnt-5a is correlated with aggressiveness of gastric cancer by stimulating cell migration and invasion. Cancer Research. 2006;66:10439-48.

[265] Saitoh T, Mine T, Katoh M. Frequent up-regulation of WNT5A mRNA in primary gastric cancer. International journal of molecular medicine. 2002;9:515-9.

[266] Pilarsky C, Ammerpohl O, Sipos B, Dahl E, Hartmann A, Wellmann A, et al. Activation of Wnt signalling in stroma from pancreatic cancer identified by gene expression profiling. Journal of Cellular and Molecular Medicine. 2008;12:2823-35.

[267] Smith K, Bui TD, Poulsom R, Kaklamanis L, Williams G, Harris AL. Up-regulation of macrophage wnt gene expression in adenoma-carcinoma progression of human colorectal cancer. British journal of cancer. 1999;81:496-502.

[268] Zhang C, Fu L, Fu J, Hu L, Yang H, Rong TH, et al. Fibroblast growth factor receptor 2-positive fibroblasts provide a suitable microenvironment for tumor development and progression in esophageal carcinoma. Clinical cancer research : an official journal of the American Association for Cancer Research. 2009;15:4017-27.

[269] Katoh M, Katoh M. Transcriptional mechanisms of WNT5A based on NF-κB, Hedgehog, TGFβ, and Notch signaling cascades. International Journal of Molecular Medicine. 2009;23:763-9.

[270] Chen S, McLean S, Carter DE, Leask A. The gene expression profile induced by Wnt 3a in NIH 3T3 fibroblasts. Journal of cell communication and signaling. 2007;1:175-83.

[271] Takahashi M, Tsunoda T, Seiki M, Nakamura Y, Furukawa Y. Identification of membrane-type matrix metalloproteinase-1 as a target of the β-catenin/Tcf4 complex in human colorectal cancers. Oncogene. 2002;21:5861-7.

[272] Yamamoto H, Oue N, Sato A, Hasegawa Y, Yamamoto H, Matsubara A, et al. Wnt5a signaling is involved in the aggressiveness of prostate cancer and expression of metalloproteinase. Oncogene. 2010;29:2036-46.

[273] Han R, Xiong J, Xiao R, Altaf E, Wang J, Liu Y, et al. Activation of beta-catenin signaling is critical for doxorubicin-induced epithelial-mesenchymal transition in BGC-823 gastric cancer cell line. Tumour biology : the journal of the International Society for Oncodevelopmental Biology and Medicine. 2013;34:277-84.

[274] Macheda ML, Stacker SA. Importance of Wnt signaling in the tumor stroma microenvironment. Current cancer drug targets. 2008;8:454-65.

[275] Pukrop T, Klemm F, Hagemann T, Gradl D, Schulz M, Siemes S, et al. Wnt 5a signaling is critical for macrophage-induced invasion of breast cancer cell lines. Proceedings of the National Academy of Sciences of the United States of America. 2006;103:5454-9.

[276] Qin L, Chen Y, Niu Y, Chen W, Wang Q, Xiao S, et al. A deep investigation into the adipogenesis mechanism: profile of microRNAs regulating adipogenesis by modulating the canonical Wnt/beta-catenin signaling pathway. BMC genomics. 2010;11:320.

[277] Meng F, Glaser SS, Francis H, DeMorrow S, Han Y, Passarini JD, et al. Functional analysis of microRNAs in human hepatocellular cancer stem cells. Journal of cellular and molecular medicine. 2012;16:160-73.

[278] Taylor MA, Sossey-Alaoui K, Thompson CL, Danielpour D, Schiemann WP. TGF-beta upregulates miR-181a expression to promote breast cancer metastasis. The Journal of clinical investigation. 2013;123:150-63.

[279] Yang CC, Hung PS, Wang PW, Liu CJ, Chu TH, Cheng HW, et al. miR-181 as a putative biomarker for lymph-node metastasis of oral squamous cell carcinoma. Journal of oral pathology & medicine : official publication of the International Association of Oral Pathologists and the American Academy of Oral Pathology. 2011;40:397-404.

[280] Kim CH, Kim HK, Rettig RL, Kim J, Lee ET, Aprelikova O, et al. miRNA signature associated with outcome of gastric cancer patients following chemotherapy. BMC medical genomics. 2011;4:79.

[281] Efanov A, Zanesi N, Nazaryan N, Santanam U, Palamarchuk A, Croce CM, et al. CD5+CD23+ leukemic cell populations in TCL1 transgenic mice show significantly increased proliferation and Akt phosphorylation. Leukemia. 2010;24:970-5.

[282] Shi L, Cheng Z, Zhang J, Li R, Zhao P, Fu Z, et al. hsa-mir-181a and hsa-mir-181b function as tumor suppressors in human glioma cells. Brain Research. 2008;1236:185-93.

[283] Gusev Y, Brackett DJ. MicroRNA expression profiling in cancer from a bioinformatics prospective. Expert Review of Molecular Diagnostics. 2007;7:787-92.

[284] Yang Q, Jie Z, Ye S, Li Z, Han Z, Wu J, et al. Genetic variations in miR-27a gene decrease mature miR-27a level and reduce gastric cancer susceptibility. Oncogene. 2012.

[285] Ren S, Johnson BG, Kida Y, Ip C, Davidson KC, Lin SL, et al. LRP-6 is a coreceptor for multiple fibrogenic signaling pathways in pericytes and myofibroblasts that are inhibited by DKK-1. Proc Natl Acad Sci U S A. 2013;110:1440-5.

[286] McDonald SL, Silver A. The opposing roles of Wnt-5a in cancer. British journal of cancer. 2009;101:209-14.

[287] Ying Y, Tao Q. Epigenetic disruption of the WNT/beta-catenin signaling pathway in human cancers. Epigenetics : official journal of the DNA Methylation Society. 2009;4:307-12.

[288] Li J, Ying J, Fan Y, Wu L, Ying Y, Chan AT, et al. WNT5A antagonizes WNT/beta-catenin signaling and is frequently silenced by promoter CpG methylation in esophageal squamous cell carcinoma. Cancer biology & therapy. 2010;10:617-24.

[289] Lindow M, Kauppinen S. Discovering the first microrna-targeted drug. Journal of Cell Biology. 2012;199:407-12.

APPENDICES

Appendix 2.1

Real-time quantitative RT-PCR analysis

All cDNAs were prepared using 2 µg of RNA which was reverse transcribed with AMV reverse transcriptase (Promega, Southampton, UK) and oligoDT (Promega). Real-time PCR was carried out in an ABI7500 thermocycler (Applied Biosystems, Warrington, UK) using Precision 2x real time PCR master mix (Primer Design, Southampton, UK) and either 5'-FAM, 3'-TAMRA double dye probes (Eurogentec, Southampton, UK) or SYBR green chemistry. Primers used for PCR analyses were GAPDH, TIMP3 and WNT5A (Appendix Table 2.1). Standard curves were developed using serial dilutions of cDNA template corresponding to the relevant gene amplicon ligated into pGEM-T Easy (Promega). This work was done by Dr Islay Steele.

Primer/Probe	Sequence
hGAPDH probe	CGT CGC CAG CCG AGC CAC A
hGAPDH forward	GCT CCT CCT GTT CGA CAG TCA
hGAPDH reverse	ACC TTC CCC ATG GTG TCT GA
hTIMP 3 forward	CCA GGA CGC CTT CTG CAA
hTIMP 3 reverse	CCC CTC CTT TAC CAG CTT CTT C
hWnt5A probe	TTT CTT TTC TGC CTC ACC CCT TTG TCT CCA
hWnt5A forward	GAA ATG CGT GTT GGG TTG AAG
hWnt5A reverse	AAG TAA TGC CCT CTC CAC AAA G

Appendix Table 2.1 PCR primer and probe sequences of GAPDH, TIMP3 and WNT5A.

Appendix 2.2

Gene expression arrays

Myofibroblasts were cultured at 80% confluency and RNA was extracted using the RNeasy kit (Qiagen, Crawley, UK) according to the manufacturer's instructions. Samples were analysed using GeneChip©Human Genome U133 Plus 2.0 arrays (Affymetrix, Santa Clara, CA, USA) according to the manufacturer's instructions at the Liverpool Genome Facility and using a GeneChip® Scanner 3000 (Affymetrix) to generate images. Further analysis was performed to identify the corresponding gene products by using MetaCore™, a data-mining tool developed by GeneGo (www.genego.com); and to annotate the gene products by cellular component using Gene Ontology database (www.geneontology.org). Quality control was performed using Microarray Suite 5.0 QC Metrics (Affymetrix) to ensure the uniformity of the arrays. Gene array data was analysed using GeneSpring GX v.10 (Agilent Technologies, Wokingham, UK). Experiments were normalised by using the MAS5 algorithm and filtered using the present (P), marginal (M) and absent (A) calls generated by MAS5. In each comparison being performed, the gene must be flagged as P at least 1 of the experimental groups. Statistical analysis was performed using unpaired t-tests within GeneSpring as indicated.

No.	Sample	Number of passages	ID number	A_{260}/A_{280} ratio	A_{260}/A_{230} ratio	RNA concentration (µg/µl)	Cell number ($\times 10^6$)	RNA integrity number (RIN)
1	Sz173/4	7	AV203	1.97	1.24	0.292	0.78	9.9
2	Sz282/4	6	AV204	2	2.05	0.867	1.78	10
3	Sz198/4	7	AV205	2.03	1.04	0.472	1.92	10
4	Sz294/4	6	AV206	2	1.78	0.674	0.75	10
5	Sz308/4	11	AV207	1.99	1.51	0.683	1	10
6	Sz389/4	5	AV208	1.99	1.63	0.724	1	10
7	Sz305/4	10	AV209	2.01	0.85	0.152	0.28	9.7
8	L429/2 (replicate 1)	8	AV210	2.02	1.74	0.819	1.58	-
9	L429/2 (replicate 2)	8	AV211	2.04	1.54	0.661	1.78	-
10	L429/2 (replicate 3)	8	AV212	2.03	1.94	0.728	1.4	-
11	L429/2 (replicate 4)	8	AV213	2.04	2.08	1.01	1.85	-
12	L429/2 (replicate 5)	8	AV214	2.05	1.82	0.809	1.85	-
13	L429/2 (replicate 6)	8	AV215	2.03	1.56	0.673	2.25	-
14	L395/2	10	AV218	2.05	1.46	0.716	1.23	9.7
15	L7641/22	5	AV219	2.05	1.78	1.36	3.63	9.7
16	L7642/9	4	AV220	2.03	1.55	0.52	1.03	9.8
17	Sz190/1	7	AV221	2.02	1.67	0.613	1.73	9.8
18	Sz190/2	7	AV222	2.01	1.95	0.577	1.43	9.9
19	Sz192/1	8	AV223	2.03	1.97	1.34	1.45	10
20	Sz192/2	6	AV224	2.02	1.51	0.952	1.85	9.8
21	Sz294/1	6	AV225	2.04	1.71	0.979	1.6	9.9
22	Sz294/2	6	AV226	2.04	2.04	0.836	1.85	9.7
23	Sz305/1	6	AV227	2.02	0.81	0.564	1.6	10
24	Sz305/22	5	AV228	2.04	1.95	0.929	1.78	9.7
25	Sz271/1	7	AV229	2.01	1.23	0.745	1.45	9.9
26	Sz271/2	8	AV230	2.02	1.44	0.919	1.28	9.8
27	HMSC7F3914	5	AV232	2.03	2	0.96	1.5	9.7
28	Sz42/9	5	AV233	2.03	1.73	0.955	0.95	9.4
29	Sz173/9	6	AV234	2.01	1.79	0.747	1.48	9.9
30	Sz45/1	6	AV235	2.04	1.82	0.935	2.88	9.8
31	Sz45/9	6	AV236	2.03	1.25	0.306	1.08	9.6
32	HMSC7F3674	5	AV237	2.01	1.69	0.63	1.5	9.7
33	HMSC7F3753	5	AV238	2.02	1.53	0.591	1.5	9.7
34	Sz268/2	9	AV239	2.01	1.64	0.81	0.68	9.7
35	Sz306/2	10	AV240	2.04	1.66	0.378	0.83	9.5
36	Sz194/2	6	AV241	2.06	0.91	0.36	0.73	9.6
37	Sz279/6	6	AV242	2.05	1.9	0.908	2.3	9.6
38	Sz306/1	7	AV243	2.05	1.4	0.588	1.25	9.6
39	Sz467/2	8	AV244	2.05	1.99	1.02	3.7	9.7
40	Sz173/1	9	AV245	2.05	1.38	0.435	1.05	9.5
41	Sz173/2	8	AV246	2.01	1.79	0.81	2.13	9.5
42	Sz282/2	7	AV247	2.03	1.63	1.03	1.28	9.6
43	Sz373/2	8	AV248	2.03	1.87	1.2	2.6	9.7
44	HMSCGF4393	7	AV249	2.04	1.42	0.702	1.5	9.7
45	HMSC7F3458	5	AV250	2.02	1.82	0.541	1.5	9.2

46	HMSC PromoCell	5	AV251	2.03	1.99	0.9362	1.5	9.5
47	Sz194/1	6	AV252	2.03	1.54	0.977	1.03	9.6
48	Sz268/22	7	AV253	2.05	2.1	1.21	1.1	9.7
49	Sz282/1	7	AV254	2.04	1.96	1.15	1.83	9.7
50	Sz308/1	7	AV255	2.02	2.05	0.884	1	9.3
51	Sz308/22	7	AV256	2.03	1.54	0.585	1	9.8
52	Sz45/2	6	AV257	2.04	1.34	0.624	1.85	9.8
53	Sz45/22	8	AV258	2.01	1.49	0.809	1.18	9.7
54	Sz187/1	8	AV259	2.04	1.97	1.23	2.58	9.6
55	Sz193/2	6	AV260	2.03	1.77	0.818	1.18	9.5
56	Sz193/1	6	AV261	2.03	1.9	1.05	2.7	9.7
57	Sz198/1	7	AV262	2.04	1.74	1.35	3.08	9.9
58	Sz198/2	7	AV263	2.01	1.9	0.914	1.15	9.8
59	Sz197/1	6	AV264	2.02	1.54	0.758	2.75	9.7
60	Sz173/22	9	AV265	2.04	1.83	0.695	1.5	9.6
61	Sz268/1	7	AV266	2.03	1.94	0.963	1.78	9.7
62	Sz241/6	7	AV267	2.03	1.74	0.608	1.25	9.6
63	Sz261/6	5	AV268	2.02	1.99	0.735	1.58	9.6
64	Sz360/1	6	AV269	2.05	1.04	0.506	1.6	9.3
65	Sz389/1	6	AV270	2.04	1.89	0.714	1.6	9.8
66	Sz389/2	6	AV271	2.04	1.89	0.906	1.3	9.6
67	L1212/22	4	AV272	2.07	1.12	1.19	4	9.5
68	Sz246/22	6	AV273	2.06	2.01	1.08	1.9	9.9
69	Sz279/22	4	AV274	2.04	1.8	1.04	4	9.9
70	Sz334/2	5	AV275	2.05	1.77	0.592	2.1	9.9
71	Sz360/2	6	AV276	2.07	0.88	0.384	0.9	9.6
72	Sz246/2	6	AV277	2.03	1.56	0.582	1.1	9.3
73	Sz246/6	5	AV278	2.03	1.49	0.879	1.5	9.4
74	Sz261/2	6	AV279	2.05	1.76	0.669	2.6	9.7
75	Sz334/22	5	AV280	2.06	1.12	0.374	2.2	9.6
76	Sz241/2	6	AV281	1.99	1.26	0.485	1.8	9.1
77	Sz261/22	6	AV282	2	1.99	0.71	1.9	9.7
78	Sz351/2	5	AV283	2.01	1.83	0.865	1.9	9.6
79	Sz351/6	5	AV284	2.02	1.05	0.733	1.6	9.6
80	Sz42/2	7	AV285	2.02	1.58	0.968	2	9.3
81	Sz196/2	5	AV286	2.03	1.95	0.489	1.9	9.7
82	Sz334/6	5	AV287	2.02	1.93	1.15	2.3	10
83	L355/22	5	AV288	2.03	1.56	1.05	2.1	9.3
84	Sz241/22	6	AV289	2.04	1.47	0.56	1.8	9.7
85	Sz351/22	5	AV290	2.04	1.63	0.441	1.3	9.2
86	Sz373/1	7	AV291	2.04	2.05	0.802	1.48	9.4
87	Sz467/1	7	AV292	2.05	0.61	0.239	1.03	9.6
88	Sz42/1	5	AV293	2.02	1.38	1.07	6	8.4
89	Sz294/22	5	AV294	2.04	1.52	1.01	1.93	9.7
90	L429/2	6	AV295	2.02	1.61	0.613	1.6	9.7

Appendix 3.2.1 RNA purity, RNA concentration and RIN were determined in human myofibroblasts and MSCs. Myofibroblast sample is represented by Sz or L, followed by patient number and tissue origin. Legend: HMSC; human mesenchymal stromal cells, Sz; patient tissue from Szeged, L; patient tissue from Liverpool. Tissue origins: 1 (cancer tissue), 2 (adjacent non-tumour tissue or gastric corpus), 4 (lymph node), 6 (squamous oesophagus), 9 (omentum) and 22 (gastric antrum).

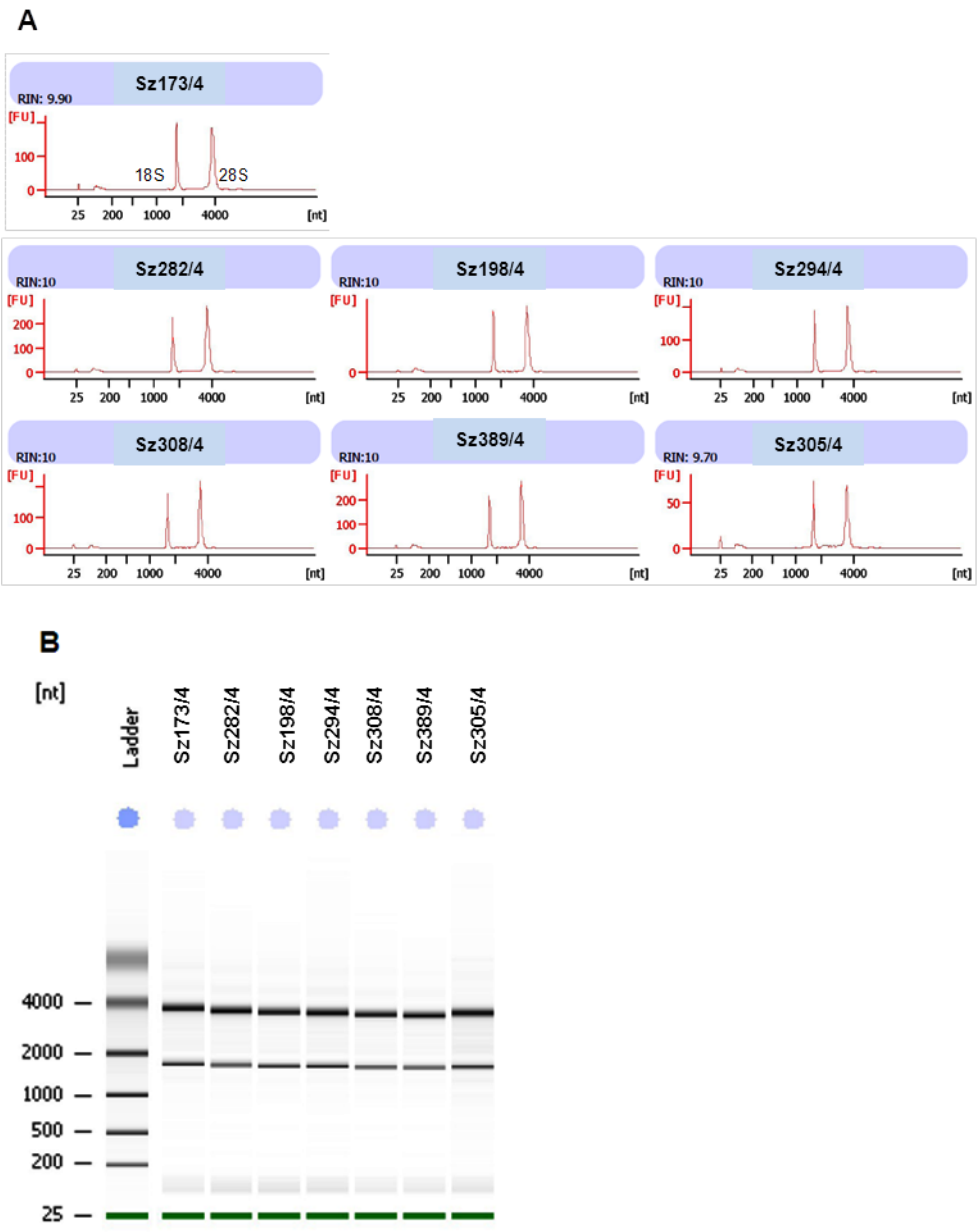

Appendix 3.2.2 Good RNA quality and no DNA contamination in total RNA sample of myofibroblasts of lymph node origin. (A) Each electropherogram showed two resolving peaks at approximately 4000 and 2000 nt representing rRNA 28S and 18S respectively. RIN of more than 9.5 was obtained. (B) Electrophoresis assay showed two distinct bands, namely, rRNA 28S and 18S, at 4000 and 2000 nt respectively. nt represents nucleotides.

Sample	miRNA concentration (pg/µl) (Input: 100ng/µl Total RNA)	Proportion of miRNAs in total RNA (%)	Small RNA concentration (pg/µl)	Proportion of miRNAs in small RNA (%)
Sz282/4	341.5	0.342	13150	2.57
Sz294/4	153.8	0.154	12849	1.20
Sz308/4	378.0	0.378	12008	3.15
Sz389/4	412.3	0.412	11742	3.51

Appendix 3.2.3 Concentration of miRNAs (10 to 40 nt) and small RNAs (<200 nt) in total RNA samples from lymph node derived myofibroblasts. The proportion of miRNAs in total RNA sample and small RNA fraction were determined.

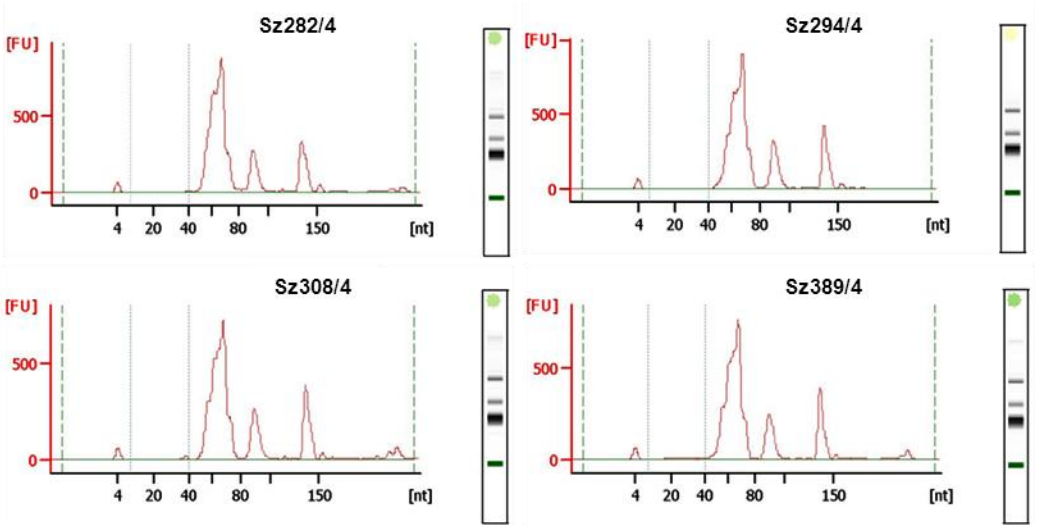

Appendix 3.2.4 Small RNA assay using total RNA samples of lymph node derived myofibroblasts. Three resolving peaks between 4 and 150 nt indicates the integrity of small RNAs.

Sample	ID number	miRNA concentration (pg/µl)	Small RNA concentration (pg/µl)	Proportion of miRNAs in 100ng total RNA (%)	Proportion of miRNAs in small RNAs (%)
Sz294/1	AV142*	392.5	4232	0.393	9
	AV225	414.6	11007	0.415	4
Sz294/2	AV143*	358.5	1927	0.359	19
	AV226	352.5	12576	0.353	3
Sz190/1	AV152*	868.5	4131	0.869	21
	AV221	216.2	10654	0.216	2
Sz190/2	AV153*	299.2	2918	0.299	10
	AV222	313.1	6735	0.313	5

Appendix 3.2.5 Small RNA concentration increased after six months storage at -80^{o}C whereas miRNA concentration was not greatly affected. Asterisk indicates storage of sample for more than six months at -80^{o}C.

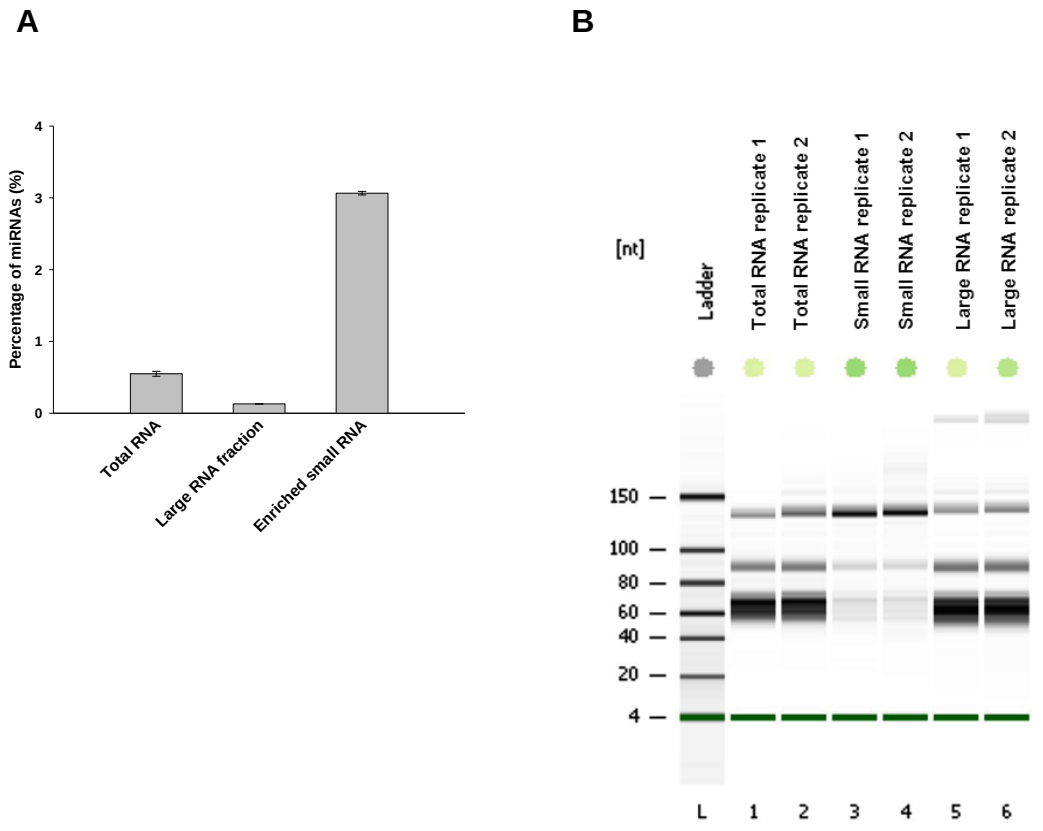

Appendix 3.2.6 Concentration of miRNAs increases six-fold in enriched small RNA sample compared to total RNA sample. (A) The percentage of miRNAs increased from 0.5% to 3% after enrichment procedure. 0.1% miRNAs was detected in large RNA fraction. (B) Electrophoresis assay showed bands intensity in total RNA, large RNA fraction and enriched small RNA fraction.

A

	Slide #					
Hy3	1	2	3	4	5	6
1	-					
2	0.99	-				
3	1.00	0.98	-			
4	1.00	0.99	1.00	-		
5	1.00	0.99	1.00	1.00	-	
6	0.99	0.97	1.00	0.99	1.00	-

B

	Slide #					
Hy5	1	2	3	4	5	6
1	-					
2	1.00	-				
3	1.00	1.00	-			
4	1.00	1.00	1.00	-		
5	1.00	1.00	1.00	1.00	-	
6	1.00	1.00	1.00	1.00	1.00	-

Appendix 3.2.7 Correlation between spike-in controls for (A) Hy3 and (B) Hy5 channels on different array slides of MSCs (n = 6). Pearson correlation coefficient of about 1 was obtained.

A

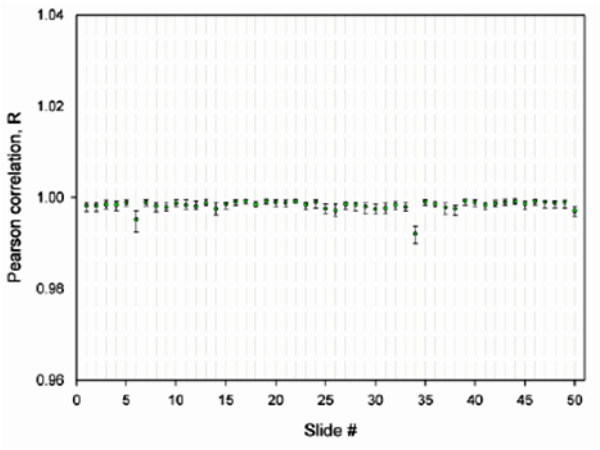

B

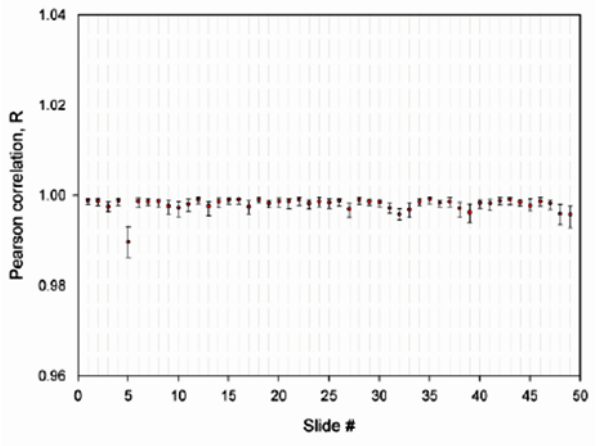

Appendix 3.2.8 Correlation between spike-in controls for (A) Hy3 and (B) Hy5 channels on different array slides of gastric myofibroblasts (n = 49). Pearson correlation coefficient of about 1 was obtained.

A

	Slide #																				
Hy3	1	2	3	4	5	6	7	8	9	10	11	12	13	14	15	16	17	18	19	20	21	22
1	-																					
2	0.999	-																				
3	0.995	0.997	-																			
4	0.993	0.994	0.996	-																		
5	0.997	0.996	0.989	0.992	-																	
6	0.992	0.986	0.977	0.979	0.993	-																
7	0.996	0.992	0.987	0.987	0.994	0.998	-															
8	0.998	0.997	0.994	0.995	0.996	0.993	0.998	-														
9	0.970	0.975	0.988	0.986	0.960	0.938	0.957	0.971	-													
10	0.974	0.977	0.989	0.989	0.985	0.947	0.965	0.977	0.999	-												
11	0.989	0.983	0.971	0.971	0.990	0.999	0.995	0.989	0.927	0.936	-											
12	0.997	0.996	0.998	0.995	0.990	0.985	0.994	0.998	0.981	0.986	0.980	-										
13	0.996	0.992	0.985	0.987	0.995	0.998	1.000	0.998	0.954	0.962	0.996	0.993	-									
14	0.998	0.996	0.991	0.991	0.996	0.996	0.999	0.999	0.964	0.970	0.993	0.996	0.999	-								
15	0.997	0.993	0.987	0.986	0.994	0.997	0.999	0.998	0.956	0.963	0.995	0.994	0.999	0.999	-							
16	0.997	0.994	0.988	0.988	0.995	0.997	1.000	0.998	0.958	0.965	0.995	0.995	1.000	1.000	1.000	-						
17	0.996	0.992	0.989	0.987	0.992	0.995	0.999	0.998	0.961	0.968	0.993	0.996	0.999	0.999	1.000	0.999	-					
18	0.997	0.995	0.995	0.993	0.991	0.988	0.996	0.999	0.976	0.981	0.984	0.999	0.995	0.998	0.997	0.997	0.998	-				
19	0.991	0.985	0.976	0.977	0.991	1.000	0.998	0.992	0.936	0.946	0.999	0.985	0.998	0.996	0.998	0.997	0.996	0.989	-			
20	0.989	0.983	0.973	0.974	0.989	0.999	0.997	0.991	0.933	0.944	0.999	0.984	0.998	0.994	0.997	0.996	0.995	0.988	1.000	-		
21	0.974	0.965	0.950	0.952	0.977	0.994	0.987	0.975	0.898	0.910	0.997	0.964	0.988	0.982	0.986	0.985	0.983	0.970	0.995	0.996	-	
22	0.985	0.978	0.965	0.966	0.986	0.998	0.993	0.985	0.919	0.929	1.000	0.976	0.994	0.990	0.993	0.992	0.990	0.980	0.999	0.999	0.999	-

B

	Slide #																					
Hy5	1	2	3	4	5	6	7	8	9	10	11	12	13	14	15	16	17	18	19	20	21	22
1	-																					
2	0.995	-																				
3	0.997	1.000	-																			
4	0.994	0.996	0.998	-																		
5	0.994	0.997	0.998	1.000	-																	
6	0.998	0.990	0.993	0.993	0.993	-																
7	0.997	0.986	0.990	0.991	0.990	1.000	-															
8	0.999	0.996	0.998	0.997	0.997	0.998	0.997	-														
9	0.994	0.995	0.997	1.000	1.000	0.994	0.992	0.997	-													
10	0.991	0.985	0.989	0.995	0.994	0.994	0.995	0.994	0.997	-												
11	0.997	0.985	0.989	0.989	0.988	0.999	1.000	0.995	0.990	0.992	-											
12	0.997	0.987	0.991	0.991	0.991	1.000	1.000	0.997	0.993	0.995	1.000	-										
13	0.996	0.985	0.989	0.990	0.989	0.999	1.000	0.996	0.991	0.994	0.999	1.000	-									
14	0.998	0.991	0.994	0.994	0.994	1.000	0.999	0.999	0.995	0.994	0.998	0.999	0.999	-								
15	0.999	0.991	0.994	0.994	0.994	1.000	0.999	0.999	0.994	0.994	0.998	0.999	0.999	1.000	-							
16	0.998	0.989	0.992	0.992	0.992	1.000	0.999	0.998	0.993	0.994	0.998	0.999	0.999	1.000	1.000	-						
17	0.994	0.981	0.986	0.986	0.986	0.998	0.999	0.994	0.988	0.992	0.999	0.999	1.000	0.998	0.998	0.999	-					
18	0.997	0.989	0.992	0.992	0.992	1.000	1.000	0.998	0.993	0.994	0.999	1.000	1.000	1.000	1.000	1.000	0.999	-				
19	0.994	0.980	0.985	0.984	0.984	0.998	0.999	0.993	0.986	0.990	0.999	0.999	0.999	0.997	0.997	0.998	1.000	0.998	-			
20	0.990	0.971	0.977	0.977	0.976	0.995	0.997	0.988	0.979	0.986	0.997	0.996	0.997	0.993	0.994	0.995	0.998	0.995	0.999	-		
21	0.985	0.963	0.969	0.970	0.968	0.991	0.994	0.982	0.972	0.981	0.995	0.993	0.994	0.989	0.989	0.991	0.996	0.991	0.997	0.999	-	
22	0.990	0.971	0.977	0.976	0.975	0.994	0.996	0.987	0.977	0.984	0.997	0.996	0.996	0.993	0.993	0.994	0.998	0.995	0.999	1.000	0.999	-

Appendix 3.2.9 Correlation between spike-in controls for (A) Hy3 and (B) Hy5 channels on different array slides of oesophageal myofibroblasts (n = 22). Pearson correlation coefficient of about 1 was obtained.

No.	Probe Id	Annotation	Number of samples
1	146011	hsa-let-7a	6
2	42530	hsa-let-7a-2*	6
3	17749	hsa-let-7b	6
4	42769	hsa-let-7b*	6
5	145820	hsa-let-7c	6
6	145968	hsa-let-7d	6
7	145846	hsa-let-7e	6
8	17752	hsa-let-7f	6
9	145840	hsa-let-7f-1*	6
10	46438	hsa-let-7g	6
11	9938	hsa-let-7i	6
12	145746	hsa-let-7i*	6
13	145943	hsa-miR-100	6
14	31026	hsa-miR-101	6
15	10919	hsa-miR-103	6
16	46801	hsa-miR-106a	6
17	19582	hsa-miR-106b	6
18	10923	hsa-miR-107	6
19	13485	hsa-miR-10a	6
20	10925	hsa-miR-10b	6
21	46258	hsa-miR-1184	6
22	46712	hsa-miR-1201	6
23	46345	hsa-miR-1207-3p	6
24	46806	hsa-miR-1227	6
25	46514	hsa-miR-1246	6
26	145977	hsa-miR-1247	6
27	46427	hsa-miR-1248	6
28	46210	hsa-miR-1249	6
29	46380	hsa-miR-1255a	6
30	46923	hsa-miR-1259	6
31	10928	hsa-miR-125a-5p	6
32	30787	hsa-miR-125b	6
33	145838	hsa-miR-125b-1*	6
34	145975	hsa-miR-1260	6
35	46248	hsa-miR-1261	6
36	46732	hsa-miR-1264	6
37	46737	hsa-miR-1265	6
38	42829	hsa-miR-127-3p	6
39	46292	hsa-miR-1274a	6
40	46328	hsa-miR-1274b	6
41	46620	hsa-miR-1275	6
42	42692	hsa-miR-127-5p	6
43	46698	hsa-miR-1280	6
44	46634	hsa-miR-1281	6
45	145981	hsa-miR-1285	6
46	46921	hsa-miR-1290	6
47	42467	hsa-miR-129-5p	6
48	46944	hsa-miR-1297	6
49	46739	hsa-miR-1308	6
50	10138	hsa-miR-130a	6
51	10936	hsa-miR-130b	6
52	145760	hsa-miR-136	6
53	42512	hsa-miR-136*	6
54	145749	hsa-miR-137	6
55	13140	hsa-miR-138	6
56	42872	hsa-miR-138-1*	6
57	42630	hsa-miR-140-3p	6
58	4700	hsa-miR-140-5p	6
59	46467	hsa-miR-143*	6
60	42641	hsa-miR-145	6
61	31867	hsa-miR-145*	6
62	146072	hsa-miR-1469	6
63	10306	hsa-miR-146b-5p	6

64	10955	hsa-miR-148a	6
65	19585	hsa-miR-148b	6
66	42486	hsa-miR-149*	6
67	145678	hsa-miR-150	6
68	17463	hsa-miR-151-3p	6
69	11260	hsa-miR-151-5p	6
70	17676	hsa-miR-152	6
71	145857	hsa-miR-154	6
72	10964	hsa-miR-155	6
73	27720	hsa-miR-15a	6
74	17280	hsa-miR-15b	6
75	10967	hsa-miR-16	6
76	42650	hsa-miR-17	6
77	42865	hsa-miR-181a	6
78	10972	hsa-miR-181b	6
79	145636	hsa-miR-181d	6
80	46810	hsa-miR-1827	6
81	10977	hsa-miR-183	6
82	17953	hsa-miR-183*	6
83	145801	hsa-miR-184	6
84	42902	hsa-miR-185	6
85	17904	hsa-miR-185*	6
86	18739	hsa-miR-186	6
87	42588	hsa-miR-18a	6
88	27536	hsa-miR-190	6
89	28431	hsa-miR-1908	6
90	10985	hsa-miR-191	6
91	146103	hsa-miR-1913	6
92	146091	hsa-miR-1914	6
93	10986	hsa-miR-193a-3p	6
94	46443	hsa-miR-193a-5p	6
95	10987	hsa-miR-193b	6
96	13148	hsa-miR-195	6
97	10990	hsa-miR-196a	6
98	145889	hsa-miR-196b	6
99	146165	hsa-miR-1973	6
100	146200	hsa-miR-1974	6
101	146140	hsa-miR-1976	6
102	146001	hsa-miR-1977	6
103	146016	hsa-miR-1978	6
104	146167	hsa-miR-1979	6
105	10995	hsa-miR-199a-3p/hsa-miR-199b-3p	6
106	29562	hsa-miR-199a-5p	6
107	19591	hsa-miR-199b-5p	6
108	10997	hsa-miR-19a	6
109	10998	hsa-miR-19b	6
110	42968	hsa-miR-202	6
111	145996	hsa-miR-205*	6
112	145845	hsa-miR-20a	6
113	5740	hsa-miR-21	6
114	42524	hsa-miR-21*	6
115	145852	hsa-miR-210	6
116	146161	hsa-miR-2115*	6
117	146010	hsa-miR-2116	6
118	11014	hsa-miR-214	6
119	145822	hsa-miR-214*	6
120	11020	hsa-miR-22	6
121	42532	hsa-miR-22*	6
122	11022	hsa-miR-221	6
123	42475	hsa-miR-221*	6
124	11023	hsa-miR-222	6
125	17918	hsa-miR-222*	6
126	11024	hsa-miR-223	6
127	42566	hsa-miR-224	6

128	146163	hsa-miR-224*	6
129	42744	hsa-miR-23a	6
130	145841	hsa-miR-23b	6
131	17506	hsa-miR-24	6
132	146043	hsa-miR-24-1*	6
133	42950	hsa-miR-24-2*	6
134	42682	hsa-miR-25	6
135	42929	hsa-miR-25*	6
136	11030	hsa-miR-26a	6
137	146008	hsa-miR-26b	6
138	46483	hsa-miR-27a	6
139	145944	hsa-miR-27b	6
140	146100	hsa-miR-296-5p	6
141	11038	hsa-miR-299-5p	6
142	11039	hsa-miR-29a	6
143	145638	hsa-miR-29a*	6
144	11040	hsa-miR-29b	6
145	17810	hsa-miR-29b-1*	6
146	11041	hsa-miR-29c	6
147	42513	hsa-miR-300	6
148	13143	hsa-miR-301a	6
149	146086	hsa-miR-30a	6
150	146112	hsa-miR-30b	6
151	42923	hsa-miR-30c	6
152	19596	hsa-miR-30d	6
153	28191	hsa-miR-30e	6
154	145676	hsa-miR-30e*	6
155	11052	hsa-miR-31	6
156	46320	hsa-miR-31*	6
157	11053	hsa-miR-32	6
158	29575	hsa-miR-32*	6
159	27533	hsa-miR-320a	6
160	46324	hsa-miR-320b	6
161	46228	hsa-miR-320c	6
162	46870	hsa-miR-320d	6
163	42887	hsa-miR-331-3p	6
164	11065	hsa-miR-335	6
165	145745	hsa-miR-335*	6
166	42673	hsa-miR-337-3p	6
167	17944	hsa-miR-337-5p	6
168	42739	hsa-miR-339-5p	6
169	29872	hsa-miR-340	6
170	32884	hsa-miR-342-3p	6
171	27217	hsa-miR-34a	6
172	42724	hsa-miR-34b	6
173	11074	hsa-miR-34c-5p	6
174	145865	hsa-miR-361-3p	6
175	14301	hsa-miR-361-5p	6
176	27544	hsa-miR-363*	6
177	11078	hsa-miR-365	6
178	29529	hsa-miR-369-3p	6
179	145844	hsa-miR-374a	6
180	14302	hsa-miR-374b	6
181	146009	hsa-miR-376a	6
182	42885	hsa-miR-376a*	6
183	145642	hsa-miR-376b	6
184	42629	hsa-miR-376c	6
185	11091	hsa-miR-377	6
186	11093	hsa-miR-379	6
187	145832	hsa-miR-381	6
188	145643	hsa-miR-382	6
189	145644	hsa-miR-409-3p	6
190	11102	hsa-miR-410	6
191	17482	hsa-miR-411	6

192	42784	hsa-miR-411*	6
193	42730	hsa-miR-423-3p	6
194	27565	hsa-miR-423-5p	6
195	42965	hsa-miR-424	6
196	17608	hsa-miR-425	6
197	18847	hsa-miR-450a	6
198	29379	hsa-miR-452	6
199	146076	hsa-miR-483-3p	6
200	145753	hsa-miR-484	6
201	42694	hsa-miR-485-3p	6
202	14285	hsa-miR-487b	6
203	17927	hsa-miR-491-3p	6
204	42661	hsa-miR-492	6
205	11125	hsa-miR-493*	6
206	145901	hsa-miR-494	6
207	42676	hsa-miR-495	6
208	42442	hsa-miR-498	6
209	42581	hsa-miR-513a-5p	6
210	42550	hsa-miR-516a-5p	6
211	145725	hsa-miR-518b	6
212	13137	hsa-miR-518e*/hsa-miR-519a*/hsa-miR-519b-5p/ hsa-miR-519c-5p/hsa-miR-522*/hsa-miR-523*	6
213	46221	hsa-miR-519d	6
214	13132	hsa-miR-519e*	6
215	11175	hsa-miR-525-5p	6
216	14272	hsa-miR-542-3p	6
217	42917	hsa-miR-551b	6
218	28966	hsa-miR-574-3p	6
219	27740	hsa-miR-574-5p	6
220	17295	hsa-miR-583	6
221	145647	hsa-miR-584	6
222	42531	hsa-miR-602	6
223	27672	hsa-miR-615-3p	6
224	32825	hsa-miR-620	6
225	145740	hsa-miR-625*	6
226	42958	hsa-miR-628-3p	6
227	17566	hsa-miR-629*	6
228	17354	hsa-miR-637	6
229	42832	hsa-miR-638	6
230	42679	hsa-miR-642	6
231	21498	hsa-miR-654-3p	6
232	29736	hsa-miR-656	6
233	145973	hsa-miR-664	6
234	145768	hsa-miR-665	6
235	29490	hsa-miR-7	6
236	29190	hsa-miR-708	6
237	146196	hsa-miR-711	6
238	146064	hsa-miR-718	6
239	42751	hsa-miR-720	6
240	27568	hsa-miR-744	6
241	145805	hsa-miR-765	6
242	42808	hsa-miR-874	6
243	46259	hsa-miR-885-5p	6
244	42806	hsa-miR-886-3p	6
245	17885	hsa-miR-886-5p	6
246	42825	hsa-miR-888*	6
247	145693	hsa-miR-92a	6
248	30687	hsa-miR-93	6
249	42539	hsa-miR-933	6
250	42776	hsa-miR-938	6
251	42608	hsa-miR-942	6
252	11182	hsa-miR-98	6
253	42708	hsa-miR-99a	6
254	11184	hsa-miR-99b	6

255	28302	hsa-miRPlus-A1015	6
256	42780	hsa-miRPlus-A1065	6
257	42793	hsa-miRPlus-A1072	6
258	17858	hsa-miRPlus-A1073	6
259	17848	hsa-miRPlus-A1087	6
260	28534	hsa-miRPlus-D1058	6
261	46649	hsa-miRPlus-E1012	6
262	46466	hsa-miRPlus-E1016	6
263	21526	hsa-miRPlus-E1031	6
264	46749	hsa-miRPlus-E1033	6
265	46537	hsa-miRPlus-E1038	6
266	46352	hsa-miRPlus-E1082	6
267	46512	hsa-miRPlus-E1088	6
268	46330	hsa-miRPlus-E1097	6
269	46861	hsa-miRPlus-E1098	6
270	46382	hsa-miRPlus-E1104	6
271	145983	hsa-miRPlus-E1114	6
272	46733	hsa-miRPlus-E1117	6
273	46662	hsa-miRPlus-E1146	6
274	145938	hsa-miRPlus-E1151	6
275	46555	hsa-miRPlus-E1153	6
276	46561	hsa-miRPlus-E1168	6
277	46817	hsa-miRPlus-E1172	6
278	46506	hsa-miRPlus-E1186	6
279	45587	hsa-miRPlus-E1200	6
280	46883	hsa-miRPlus-E1209	6
281	46343	hsa-miRPlus-E1212	6
282	46885	hsa-miRPlus-E1225	6
283	145935	hsa-miRPlus-E1232	6
284	46557	hsa-miRPlus-E1233	6
285	46247	hsa-miRPlus-E1234	6
286	46256	hsa-miRPlus-E1238	6
287	46711	hsa-miRPlus-E1245	6
288	46445	hsa-miRPlus-E1247	6
289	145978	hsa-miRPlus-E1258	6
290	45891	hsa-miRPlus-E1285	6
291	46756	hsa-miRPlus-F1001	6
292	46635	hsa-miRPlus-F1004	6
293	46731	hsa-miRPlus-F1017	6
294	46933	hsa-miRPlus-F1026	6
295	46297	hsa-miRPlus-F1041	6
296	46519	hsa-miRPlus-F1042	6
297	46417	hsa-miRPlus-F1058	6
298	46334	hsa-miRPlus-F1059	6
299	46630	hsa-miRPlus-F1064	6
300	46871	hsa-miRPlus-F1066	6
301	46386	hsa-miRPlus-F1074	6
302	46498	hsa-miRPlus-F1099	6
303	46241	hsa-miRPlus-F1130	6
304	46353	hsa-miRPlus-F1147	6
305	46590	hsa-miRPlus-F1154	6
306	45614	hsa-miRPlus-F1155	6
307	46474	hsa-miRPlus-F1158	6
308	46601	hsa-miRPlus-F1163	6
309	46298	hsa-miRPlus-F1180	6
310	46602	hsa-miRPlus-F1194	6
311	46882	hsa-miRPlus-F1195	6
312	46655	hsa-miRPlus-F1215	6
313	46632	hsa-miRPlus-F1222	6
314	46599	hsa-miRPlus-F1225	6
315	46359	hsa-miRPlus-F1231	6
316	146113	hsa-miRPlus-G1246-3p	6
317	146158	hsa-miRPlus-G1316-5p	6
318	17854	hsa-miR-106b*	5

319	46624	hsa-miR-1236	5
320	42571	hsa-miR-129*	5
321	42783	hsa-miR-197	5
322	5730	hsa-miR-208a	5
323	11037	hsa-miR-299-3p	5
324	11045	hsa-miR-302c*	5
325	17893	hsa-miR-362-3p	5
326	14270	hsa-miR-493	5
327	11164	hsa-miR-519e	5
328	17546	hsa-miR-585	5
329	42818	hsa-miR-597	5
330	42749	hsa-miR-659	5
331	145701	hsa-miR-668	5
332	30033	hsa-miR-877	5
333	42771	hsa-miR-877*	5
334	17718	hsa-miR-92b	5
335	46580	hsa-miRPlus-E1077	5
336	46379	hsa-miRPlus-E1093	5
337	145940	hsa-miRPlus-E1110	5
338	46473	hsa-miRPlus-E1112	5
339	46529	hsa-miRPlus-F1023	5
340	46570	hsa-miRPlus-F1080	5
341	46273	hsa-miRPlus-F1166	5
342	46412	hsa-miRPlus-F1206	5

Appendix 3.3.1 MicroRNAs that were expressed in at least 80% of MSCs (n = 6).

No.	Probe Id	Annotation	Number of samples
1	146011	hsa-let-7a	6
2	42530	hsa-let-7a-2*	6
3	17749	hsa-let-7b	6
4	145820	hsa-let-7c	6
5	145968	hsa-let-7d	6
6	145846	hsa-let-7e	6
7	17752	hsa-let-7f	6
8	46438	hsa-let-7g	6
9	9938	hsa-let-7i	6
10	145943	hsa-miR-100	6
11	31026	hsa-miR-101	6
12	10919	hsa-miR-103	6
13	46801	hsa-miR-106a	6
14	19582	hsa-miR-106b	6
15	10923	hsa-miR-107	6
16	13485	hsa-miR-10a	6
17	46258	hsa-miR-1184	6
18	46712	hsa-miR-1201	6
19	46345	hsa-miR-1207-3p	6
20	46514	hsa-miR-1246	6
21	145977	hsa-miR-1247	6
22	46210	hsa-miR-1249	6
23	46380	hsa-miR-1255a	6
24	46923	hsa-miR-1259	6
25	10928	hsa-miR-125a-5p	6
26	30787	hsa-miR-125b	6
27	145975	hsa-miR-1260	6
28	46248	hsa-miR-1261	6
29	46732	hsa-miR-1264	6
30	46737	hsa-miR-1265	6
31	42829	hsa-miR-127-3p	6
32	46292	hsa-miR-1274a	6
33	46328	hsa-miR-1274b	6
34	46620	hsa-miR-1275	6
35	46698	hsa-miR-1280	6
36	145981	hsa-miR-1285	6
37	42571	hsa-miR-129*	6
38	46921	hsa-miR-1290	6
39	42467	hsa-miR-129-5p	6
40	46944	hsa-miR-1297	6
41	46739	hsa-miR-1308	6
42	10138	hsa-miR-130a	6
43	10936	hsa-miR-130b	6
44	145760	hsa-miR-136	6
45	42512	hsa-miR-136*	6
46	13140	hsa-miR-138	6
47	42872	hsa-miR-138-1*	6
48	42630	hsa-miR-140-3p	6
49	42641	hsa-miR-145	6
50	146072	hsa-miR-1469	6
51	19585	hsa-miR-148b	6
52	42486	hsa-miR-149*	6
53	145678	hsa-miR-150	6
54	17463	hsa-miR-151-3p	6
55	11260	hsa-miR-151-5p	6
56	17676	hsa-miR-152	6
57	27720	hsa-miR-15a	6
58	17280	hsa-miR-15b	6
59	10967	hsa-miR-16	6
60	42650	hsa-miR-17	6
61	42865	hsa-miR-181a	6
62	145636	hsa-miR-181d	6
63	46810	hsa-miR-1827	6

64	10977	hsa-miR-183	6
65	17953	hsa-miR-183*	6
66	145801	hsa-miR-184	6
67	42902	hsa-miR-185	6
68	17904	hsa-miR-185*	6
69	18739	hsa-miR-186	6
70	27536	hsa-miR-190	6
71	28431	hsa-miR-1908	6
72	10985	hsa-miR-191	6
73	146091	hsa-miR-1914	6
74	10986	hsa-miR-193a-3p	6
75	46443	hsa-miR-193a-5p	6
76	10987	hsa-miR-193b	6
77	13148	hsa-miR-195	6
78	42538	hsa-miR-196a*	6
79	42783	hsa-miR-197	6
80	146165	hsa-miR-1973	6
81	146200	hsa-miR-1974	6
82	146001	hsa-miR-1977	6
83	146016	hsa-miR-1978	6
84	146167	hsa-miR-1979	6
85	10995	hsa-miR-199a-3p/hsa-miR-199b-3p	6
86	29562	hsa-miR-199a-5p	6
87	19591	hsa-miR-199b-5p	6
88	10997	hsa-miR-19a	6
89	10998	hsa-miR-19b	6
90	42968	hsa-miR-202	6
91	145996	hsa-miR-205*	6
92	145845	hsa-miR-20a	6
93	5740	hsa-miR-21	6
94	42524	hsa-miR-21*	6
95	145852	hsa-miR-210	6
96	146161	hsa-miR-2115*	6
97	146010	hsa-miR-2116	6
98	11014	hsa-miR-214	6
99	11020	hsa-miR-22	6
100	42532	hsa-miR-22*	6
101	11022	hsa-miR-221	6
102	42475	hsa-miR-221*	6
103	11023	hsa-miR-222	6
104	42566	hsa-miR-224	6
105	146163	hsa-miR-224*	6
106	42744	hsa-miR-23a	6
107	145841	hsa-miR-23b	6
108	17506	hsa-miR-24	6
109	146043	hsa-miR-24-1*	6
110	42950	hsa-miR-24-2*	6
111	42682	hsa-miR-25	6
112	42929	hsa-miR-25*	6
113	11030	hsa-miR-26a	6
114	146008	hsa-miR-26b	6
115	46483	hsa-miR-27a	6
116	145944	hsa-miR-27b	6
117	11038	hsa-miR-299-5p	6
118	11039	hsa-miR-29a	6
119	145638	hsa-miR-29a*	6
120	11040	hsa-miR-29b	6
121	11041	hsa-miR-29c	6
122	42513	hsa-miR-300	6
123	13143	hsa-miR-301a	6
124	146086	hsa-miR-30a	6
125	146112	hsa-miR-30b	6
126	42923	hsa-miR-30c	6
127	19596	hsa-miR-30d	6

128	28191	hsa-miR-30e	6
129	145676	hsa-miR-30e*	6
130	11052	hsa-miR-31	6
131	46320	hsa-miR-31*	6
132	11053	hsa-miR-32	6
133	29575	hsa-miR-32*	6
134	27533	hsa-miR-320a	6
135	46324	hsa-miR-320b	6
136	46228	hsa-miR-320c	6
137	46870	hsa-miR-320d	6
138	42957	hsa-miR-323-3p	6
139	42887	hsa-miR-331-3p	6
140	11065	hsa-miR-335	6
141	145745	hsa-miR-335*	6
142	42673	hsa-miR-337-3p	6
143	17944	hsa-miR-337-5p	6
144	42739	hsa-miR-339-5p	6
145	145859	hsa-miR-33a	6
146	145950	hsa-miR-33b	6
147	29872	hsa-miR-340	6
148	27217	hsa-miR-34a	6
149	42724	hsa-miR-34b	6
150	145865	hsa-miR-361-3p	6
151	14301	hsa-miR-361-5p	6
152	11078	hsa-miR-365	6
153	29529	hsa-miR-369-3p	6
154	145844	hsa-miR-374a	6
155	14302	hsa-miR-374b	6
156	146009	hsa-miR-376a	6
157	42885	hsa-miR-376a*	6
158	145642	hsa-miR-376b	6
159	42629	hsa-miR-376c	6
160	11091	hsa-miR-377	6
161	11093	hsa-miR-379	6
162	145832	hsa-miR-381	6
163	145644	hsa-miR-409-3p	6
164	17482	hsa-miR-411	6
165	42784	hsa-miR-411*	6
166	42730	hsa-miR-423-3p	6
167	27565	hsa-miR-423-5p	6
168	42965	hsa-miR-424	6
169	18847	hsa-miR-450a	6
170	29379	hsa-miR-452	6
171	146076	hsa-miR-483-3p	6
172	42480	hsa-miR-485-5p	6
173	14285	hsa-miR-487b	6
174	42703	hsa-miR-490-3p	6
175	17822	hsa-miR-490-5p	6
176	17927	hsa-miR-491-3p	6
177	42661	hsa-miR-492	6
178	11125	hsa-miR-493*	6
179	145901	hsa-miR-494	6
180	42442	hsa-miR-498	6
181	42581	hsa-miR-513a-5p	6
182	42550	hsa-miR-516a-5p	6
183	145725	hsa-miR-518b	6
184	13137	hsa-miR-518e*/hsa-miR-519a*/hsa-miR-519b-5p/ hsa-miR-519c-5p/hsa-miR-522*/hsa-miR-523*	6
185	46221	hsa-miR-519d	6
186	13132	hsa-miR-519e*	6
187	11175	hsa-miR-525-5p	6
188	14272	hsa-miR-542-3p	6
189	42917	hsa-miR-551b	6
190	28966	hsa-miR-574-3p	6

191	27740	hsa-miR-574-5p	6
192	17295	hsa-miR-583	6
193	145647	hsa-miR-584	6
194	42531	hsa-miR-602	6
195	27672	hsa-miR-615-3p	6
196	32825	hsa-miR-620	6
197	145740	hsa-miR-625*	6
198	42958	hsa-miR-628-3p	6
199	17566	hsa-miR-629*	6
200	17354	hsa-miR-637	6
201	42832	hsa-miR-638	6
202	42679	hsa-miR-642	6
203	21498	hsa-miR-654-3p	6
204	145973	hsa-miR-664	6
205	145768	hsa-miR-665	6
206	29490	hsa-miR-7	6
207	146196	hsa-miR-711	6
208	42751	hsa-miR-720	6
209	27568	hsa-miR-744	6
210	145805	hsa-miR-765	6
211	42808	hsa-miR-874	6
212	46259	hsa-miR-885-5p	6
213	42806	hsa-miR-886-3p	6
214	17885	hsa-miR-886-5p	6
215	42825	hsa-miR-888*	6
216	145693	hsa-miR-92a	6
217	30687	hsa-miR-93	6
218	42539	hsa-miR-933	6
219	11182	hsa-miR-98	6
220	42708	hsa-miR-99a	6
221	11184	hsa-miR-99b	6
222	28302	hsa-miRPlus-A1015	6
223	42780	hsa-miRPlus-A1065	6
224	42793	hsa-miRPlus-A1072	6
225	17858	hsa-miRPlus-A1073	6
226	17848	hsa-miRPlus-A1087	6
227	28534	hsa-miRPlus-D1058	6
228	46649	hsa-miRPlus-E1012	6
229	46466	hsa-miRPlus-E1016	6
230	21526	hsa-miRPlus-E1031	6
231	46749	hsa-miRPlus-E1033	6
232	46537	hsa-miRPlus-E1038	6
233	46580	hsa-miRPlus-E1077	6
234	46352	hsa-miRPlus-E1082	6
235	46512	hsa-miRPlus-E1088	6
236	46330	hsa-miRPlus-E1097	6
237	46861	hsa-miRPlus-E1098	6
238	46382	hsa-miRPlus-E1104	6
239	145983	hsa-miRPlus-E1114	6
240	46733	hsa-miRPlus-E1117	6
241	46662	hsa-miRPlus-E1146	6
242	145938	hsa-miRPlus-E1151	6
243	46555	hsa-miRPlus-E1153	6
244	46561	hsa-miRPlus-E1168	6
245	46817	hsa-miRPlus-E1172	6
246	46506	hsa-miRPlus-E1186	6
247	46883	hsa-miRPlus-E1209	6
248	46343	hsa-miRPlus-E1212	6
249	46885	hsa-miRPlus-E1225	6
250	145935	hsa-miRPlus-E1232	6
251	46247	hsa-miRPlus-E1234	6
252	46256	hsa-miRPlus-E1238	6
253	46445	hsa-miRPlus-E1247	6
254	145978	hsa-miRPlus-E1258	6

255	45891	hsa-miRPlus-E1285	6
256	46731	hsa-miRPlus-F1017	6
257	46933	hsa-miRPlus-F1026	6
258	46519	hsa-miRPlus-F1042	6
259	46334	hsa-miRPlus-F1059	6
260	46630	hsa-miRPlus-F1064	6
261	46871	hsa-miRPlus-F1066	6
262	46386	hsa-miRPlus-F1074	6
263	46498	hsa-miRPlus-F1099	6
264	46241	hsa-miRPlus-F1130	6
265	46353	hsa-miRPlus-F1147	6
266	46590	hsa-miRPlus-F1154	6
267	45614	hsa-miRPlus-F1155	6
268	46273	hsa-miRPlus-F1166	6
269	46298	hsa-miRPlus-F1180	6
270	46786	hsa-miRPlus-F1193	6
271	46602	hsa-miRPlus-F1194	6
272	46882	hsa-miRPlus-F1195	6
273	46655	hsa-miRPlus-F1215	6
274	46632	hsa-miRPlus-F1222	6
275	46599	hsa-miRPlus-F1225	6
276	46359	hsa-miRPlus-F1231	6
277	146113	hsa-miRPlus-G1246-3p	6
278	146158	hsa-miRPlus-G1316-5p	6
279	145840	hsa-let-7f-1*	5
280	46624	hsa-miR-1236	5
281	46634	hsa-miR-1281	5
282	10306	hsa-miR-146b-5p	5
283	10964	hsa-miR-155	5
284	10972	hsa-miR-181b	5
285	146103	hsa-miR-1913	5
286	32884	hsa-miR-342-3p	5
287	145643	hsa-miR-382	5
288	17608	hsa-miR-425	5
289	42676	hsa-miR-495	5
290	46829	hsa-miR-664*	5
291	42761	hsa-miR-675	5
292	29190	hsa-miR-708	5
293	42776	hsa-miR-938	5
294	145940	hsa-miRPlus-E1110	5
295	46711	hsa-miRPlus-E1245	5
296	46756	hsa-miRPlus-F1001	5
297	46570	hsa-miRPlus-F1080	5
298	46474	hsa-miRPlus-F1158	5

Appendix 3.3.2a MicroRNAs that were expressed in at least 80% of gastric NTMs (n = 6) from corpus.

No.	Probe Id	Annotation	Number of samples
1	146011	hsa-let-7a	6
2	42530	hsa-let-7a-2*	6
3	17749	hsa-let-7b	6
4	145820	hsa-let-7c	6
5	145968	hsa-let-7d	6
6	145846	hsa-let-7e	6
7	17752	hsa-let-7f	6
8	145840	hsa-let-7f-1*	6
9	46438	hsa-let-7g	6
10	9938	hsa-let-7i	6
11	145943	hsa-miR-100	6
12	31026	hsa-miR-101	6
13	10919	hsa-miR-103	6
14	46801	hsa-miR-106a	6
15	19582	hsa-miR-106b	6
16	10923	hsa-miR-107	6
17	13485	hsa-miR-10a	6
18	46258	hsa-miR-1184	6
19	46712	hsa-miR-1201	6
20	46514	hsa-miR-1246	6
21	145977	hsa-miR-1247	6
22	46210	hsa-miR-1249	6
23	46380	hsa-miR-1255a	6
24	46923	hsa-miR-1259	6
25	10928	hsa-miR-125a-5p	6
26	30787	hsa-miR-125b	6
27	145975	hsa-miR-1260	6
28	46248	hsa-miR-1261	6
29	46732	hsa-miR-1264	6
30	46737	hsa-miR-1265	6
31	42829	hsa-miR-127-3p	6
32	46292	hsa-miR-1274a	6
33	46328	hsa-miR-1274b	6
34	46620	hsa-miR-1275	6
35	46698	hsa-miR-1280	6
36	145981	hsa-miR-1285	6
37	42571	hsa-miR-129*	6
38	46921	hsa-miR-1290	6
39	42467	hsa-miR-129-5p	6
40	46944	hsa-miR-1297	6
41	46739	hsa-miR-1308	6
42	10138	hsa-miR-130a	6
43	10936	hsa-miR-130b	6
44	145760	hsa-miR-136	6
45	42512	hsa-miR-136*	6
46	13140	hsa-miR-138	6
47	42872	hsa-miR-138-1*	6
48	42630	hsa-miR-140-3p	6
49	42641	hsa-miR-145	6
50	146072	hsa-miR-1469	6
51	19585	hsa-miR-148b	6
52	42486	hsa-miR-149*	6
53	145678	hsa-miR-150	6
54	17463	hsa-miR-151-3p	6
55	11260	hsa-miR-151-5p	6
56	17676	hsa-miR-152	6
57	10964	hsa-miR-155	6
58	27720	hsa-miR-15a	6
59	17280	hsa-miR-15b	6
60	10967	hsa-miR-16	6
61	42650	hsa-miR-17	6
62	42865	hsa-miR-181a	6
63	10972	hsa-miR-181b	6

64	145636	hsa-miR-181d	6
65	46810	hsa-miR-1827	6
66	10977	hsa-miR-183	6
67	17953	hsa-miR-183*	6
68	145801	hsa-miR-184	6
69	42902	hsa-miR-185	6
70	17904	hsa-miR-185*	6
71	18739	hsa-miR-186	6
72	42588	hsa-miR-18a	6
73	27536	hsa-miR-190	6
74	28431	hsa-miR-1908	6
75	10985	hsa-miR-191	6
76	146103	hsa-miR-1913	6
77	146091	hsa-miR-1914	6
78	10986	hsa-miR-193a-3p	6
79	46443	hsa-miR-193a-5p	6
80	10987	hsa-miR-193b	6
81	13148	hsa-miR-195	6
82	42538	hsa-miR-196a*	6
83	42783	hsa-miR-197	6
84	146165	hsa-miR-1973	6
85	146200	hsa-miR-1974	6
86	146001	hsa-miR-1977	6
87	146016	hsa-miR-1978	6
88	146167	hsa-miR-1979	6
89	10995	hsa-miR-199a-3p/hsa-miR-199b-3p	6
90	29562	hsa-miR-199a-5p	6
91	19591	hsa-miR-199b-5p	6
92	10997	hsa-miR-19a	6
93	10998	hsa-miR-19b	6
94	42968	hsa-miR-202	6
95	145996	hsa-miR-205*	6
96	145845	hsa-miR-20a	6
97	5740	hsa-miR-21	6
98	42524	hsa-miR-21*	6
99	145852	hsa-miR-210	6
100	146161	hsa-miR-2115*	6
101	146010	hsa-miR-2116	6
102	11014	hsa-miR-214	6
103	11020	hsa-miR-22	6
104	42532	hsa-miR-22*	6
105	11022	hsa-miR-221	6
106	42475	hsa-miR-221*	6
107	11023	hsa-miR-222	6
108	42566	hsa-miR-224	6
109	146163	hsa-miR-224*	6
110	42744	hsa-miR-23a	6
111	145841	hsa-miR-23b	6
112	17506	hsa-miR-24	6
113	146043	hsa-miR-24-1*	6
114	42950	hsa-miR-24-2*	6
115	42682	hsa-miR-25	6
116	42929	hsa-miR-25*	6
117	11030	hsa-miR-26a	6
118	146008	hsa-miR-26b	6
119	46483	hsa-miR-27a	6
120	145944	hsa-miR-27b	6
121	146049	hsa-miR-28-5p	6
122	11038	hsa-miR-299-5p	6
123	11039	hsa-miR-29a	6
124	145638	hsa-miR-29a*	6
125	11040	hsa-miR-29b	6
126	11041	hsa-miR-29c	6
127	42513	hsa-miR-300	6

128	13143	hsa-miR-301a	6
129	146086	hsa-miR-30a	6
130	146112	hsa-miR-30b	6
131	42923	hsa-miR-30c	6
132	19596	hsa-miR-30d	6
133	28191	hsa-miR-30e	6
134	145676	hsa-miR-30e*	6
135	11052	hsa-miR-31	6
136	46320	hsa-miR-31*	6
137	11053	hsa-miR-32	6
138	29575	hsa-miR-32*	6
139	27533	hsa-miR-320a	6
140	46324	hsa-miR-320b	6
141	46228	hsa-miR-320c	6
142	46870	hsa-miR-320d	6
143	42957	hsa-miR-323-3p	6
144	42887	hsa-miR-331-3p	6
145	11065	hsa-miR-335	6
146	145745	hsa-miR-335*	6
147	42673	hsa-miR-337-3p	6
148	17944	hsa-miR-337-5p	6
149	42739	hsa-miR-339-5p	6
150	145859	hsa-miR-33a	6
151	145950	hsa-miR-33b	6
152	29872	hsa-miR-340	6
153	32884	hsa-miR-342-3p	6
154	27217	hsa-miR-34a	6
155	42724	hsa-miR-34b	6
156	145865	hsa-miR-361-3p	6
157	14301	hsa-miR-361-5p	6
158	11078	hsa-miR-365	6
159	29529	hsa-miR-369-3p	6
160	145844	hsa-miR-374a	6
161	14302	hsa-miR-374b	6
162	146009	hsa-miR-376a	6
163	42885	hsa-miR-376a*	6
164	145642	hsa-miR-376b	6
165	42629	hsa-miR-376c	6
166	11091	hsa-miR-377	6
167	11093	hsa-miR-379	6
168	145832	hsa-miR-381	6
169	145643	hsa-miR-382	6
170	145644	hsa-miR-409-3p	6
171	17482	hsa-miR-411	6
172	42784	hsa-miR-411*	6
173	42730	hsa-miR-423-3p	6
174	27565	hsa-miR-423-5p	6
175	42965	hsa-miR-424	6
176	17608	hsa-miR-425	6
177	18847	hsa-miR-450a	6
178	29379	hsa-miR-452	6
179	146076	hsa-miR-483-3p	6
180	42480	hsa-miR-485-5p	6
181	14285	hsa-miR-487b	6
182	42703	hsa-miR-490-3p	6
183	17822	hsa-miR-490-5p	6
184	17927	hsa-miR-491-3p	6
185	42661	hsa-miR-492	6
186	11125	hsa-miR-493*	6
187	145901	hsa-miR-494	6
188	42676	hsa-miR-495	6
189	42442	hsa-miR-498	6
190	42581	hsa-miR-513a-5p	6
191	42550	hsa-miR-516a-5p	6

192	145725	hsa-miR-518b	6
193	13137	hsa-miR-518e*/hsa-miR-519a*/hsa-miR-519b-5p/ hsa-miR-519c-5p/hsa-miR-522*/hsa-miR-523*	6
194	46221	hsa-miR-519d	6
195	13132	hsa-miR-519e*	6
196	11175	hsa-miR-525-5p	6
197	14272	hsa-miR-542-3p	6
198	42917	hsa-miR-551b	6
199	28966	hsa-miR-574-3p	6
200	27740	hsa-miR-574-5p	6
201	17295	hsa-miR-583	6
202	145647	hsa-miR-584	6
203	42531	hsa-miR-602	6
204	27672	hsa-miR-615-3p	6
205	32825	hsa-miR-620	6
206	145740	hsa-miR-625*	6
207	42958	hsa-miR-628-3p	6
208	17566	hsa-miR-629*	6
209	17354	hsa-miR-637	6
210	42832	hsa-miR-638	6
211	42679	hsa-miR-642	6
212	21498	hsa-miR-654-3p	6
213	145973	hsa-miR-664	6
214	145768	hsa-miR-665	6
215	145701	hsa-miR-668	6
216	42761	hsa-miR-675	6
217	29490	hsa-miR-7	6
218	146196	hsa-miR-711	6
219	42751	hsa-miR-720	6
220	27568	hsa-miR-744	6
221	145805	hsa-miR-765	6
222	42808	hsa-miR-874	6
223	30033	hsa-miR-877	6
224	46259	hsa-miR-885-5p	6
225	42806	hsa-miR-886-3p	6
226	17885	hsa-miR-886-5p	6
227	42825	hsa-miR-888*	6
228	145693	hsa-miR-92a	6
229	30687	hsa-miR-93	6
230	42539	hsa-miR-933	6
231	11182	hsa-miR-98	6
232	42708	hsa-miR-99a	6
233	11184	hsa-miR-99b	6
234	28302	hsa-miRPlus-A1015	6
235	42780	hsa-miRPlus-A1065	6
236	42793	hsa-miRPlus-A1072	6
237	17858	hsa-miRPlus-A1073	6
238	17848	hsa-miRPlus-A1087	6
239	28534	hsa-miRPlus-D1058	6
240	46649	hsa-miRPlus-E1012	6
241	46466	hsa-miRPlus-E1016	6
242	21526	hsa-miRPlus-E1031	6
243	46749	hsa-miRPlus-E1033	6
244	46537	hsa-miRPlus-E1038	6
245	46580	hsa-miRPlus-E1077	6
246	46352	hsa-miRPlus-E1082	6
247	46512	hsa-miRPlus-E1088	6
248	46330	hsa-miRPlus-E1097	6
249	46861	hsa-miRPlus-E1098	6
250	46382	hsa-miRPlus-E1104	6
251	145940	hsa-miRPlus-E1110	6
252	145983	hsa-miRPlus-E1114	6
253	46733	hsa-miRPlus-E1117	6
254	46662	hsa-miRPlus-E1146	6

255	145938	hsa-miRPlus-E1151	6
256	46555	hsa-miRPlus-E1153	6
257	46561	hsa-miRPlus-E1168	6
258	46817	hsa-miRPlus-E1172	6
259	46506	hsa-miRPlus-E1186	6
260	46883	hsa-miRPlus-E1209	6
261	46343	hsa-miRPlus-E1212	6
262	46885	hsa-miRPlus-E1225	6
263	145935	hsa-miRPlus-E1232	6
264	46247	hsa-miRPlus-E1234	6
265	46256	hsa-miRPlus-E1238	6
266	46711	hsa-miRPlus-E1245	6
267	46445	hsa-miRPlus-E1247	6
268	145978	hsa-miRPlus-E1258	6
269	45891	hsa-miRPlus-E1285	6
270	46731	hsa-miRPlus-F1017	6
271	46933	hsa-miRPlus-F1026	6
272	46519	hsa-miRPlus-F1042	6
273	46334	hsa-miRPlus-F1059	6
274	46630	hsa-miRPlus-F1064	6
275	46871	hsa-miRPlus-F1066	6
276	46386	hsa-miRPlus-F1074	6
277	46498	hsa-miRPlus-F1099	6
278	46241	hsa-miRPlus-F1130	6
279	46353	hsa-miRPlus-F1147	6
280	46590	hsa-miRPlus-F1154	6
281	45614	hsa-miRPlus-F1155	6
282	46273	hsa-miRPlus-F1166	6
283	46786	hsa-miRPlus-F1193	6
284	46602	hsa-miRPlus-F1194	6
285	46882	hsa-miRPlus-F1195	6
286	46655	hsa-miRPlus-F1215	6
287	46632	hsa-miRPlus-F1222	6
288	46599	hsa-miRPlus-F1225	6
289	46359	hsa-miRPlus-F1231	6
290	146113	hsa-miRPlus-G1246-3p	6
291	146158	hsa-miRPlus-G1316-5p	6
292	46345	hsa-miR-1207-3p	5
293	46427	hsa-miR-1248	5
294	46634	hsa-miR-1281	5
295	10306	hsa-miR-146b-5p	5
296	27544	hsa-miR-363*	5
297	42694	hsa-miR-485-3p	5
298	42818	hsa-miR-597	5
299	146064	hsa-miR-718	5
300	46297	hsa-miRPlus-F1041	5
301	46298	hsa-miRPlus-F1180	5

Appendix 3.3.2b MicroRNAs that were expressed in at least 80% of gastric NTMs (n = 6) from antrum.

No.	Probe Id	Annotation	Number of samples
1	146011	hsa-let-7a	6
2	42530	hsa-let-7a-2*	6
3	17749	hsa-let-7b	6
4	42769	hsa-let-7b*	6
5	145820	hsa-let-7c	6
6	145968	hsa-let-7d	6
7	145846	hsa-let-7e	6
8	17752	hsa-let-7f	6
9	145840	hsa-let-7f-1*	6
10	46438	hsa-let-7g	6
11	9938	hsa-let-7i	6
12	145943	hsa-miR-100	6
13	31026	hsa-miR-101	6
14	10919	hsa-miR-103	6
15	46801	hsa-miR-106a	6
16	19582	hsa-miR-106b	6
17	10923	hsa-miR-107	6
18	13485	hsa-miR-10a	6
19	46258	hsa-miR-1184	6
20	46712	hsa-miR-1201	6
21	46345	hsa-miR-1207-3p	6
22	46806	hsa-miR-1227	6
23	46624	hsa-miR-1236	6
24	46514	hsa-miR-1246	6
25	145977	hsa-miR-1247	6
26	46427	hsa-miR-1248	6
27	46210	hsa-miR-1249	6
28	46380	hsa-miR-1255a	6
29	46923	hsa-miR-1259	6
30	10928	hsa-miR-125a-5p	6
31	30787	hsa-miR-125b	6
32	145975	hsa-miR-1260	6
33	46248	hsa-miR-1261	6
34	46732	hsa-miR-1264	6
35	46737	hsa-miR-1265	6
36	42829	hsa-miR-127-3p	6
37	46292	hsa-miR-1274a	6
38	46328	hsa-miR-1274b	6
39	46620	hsa-miR-1275	6
40	46698	hsa-miR-1280	6
41	46634	hsa-miR-1281	6
42	145981	hsa-miR-1285	6
43	42571	hsa-miR-129*	6
44	46921	hsa-miR-1290	6
45	42467	hsa-miR-129-5p	6
46	46944	hsa-miR-1297	6
47	46739	hsa-miR-1308	6
48	10138	hsa-miR-130a	6
49	10936	hsa-miR-130b	6
50	145760	hsa-miR-136	6
51	42512	hsa-miR-136*	6
52	13140	hsa-miR-138	6
53	42872	hsa-miR-138-1*	6
54	42630	hsa-miR-140-3p	6
55	42641	hsa-miR-145	6
56	31867	hsa-miR-145*	6
57	146072	hsa-miR-1469	6
58	10306	hsa-miR-146b-5p	6
59	19585	hsa-miR-148b	6
60	42486	hsa-miR-149*	6
61	145678	hsa-miR-150	6
62	17463	hsa-miR-151-3p	6
63	11260	hsa-miR-151-5p	6

64	17676	hsa-miR-152	6
65	10964	hsa-miR-155	6
66	27720	hsa-miR-15a	6
67	17280	hsa-miR-15b	6
68	10967	hsa-miR-16	6
69	42650	hsa-miR-17	6
70	42865	hsa-miR-181a	6
71	10972	hsa-miR-181b	6
72	145636	hsa-miR-181d	6
73	46810	hsa-miR-1827	6
74	10977	hsa-miR-183	6
75	17953	hsa-miR-183*	6
76	145801	hsa-miR-184	6
77	42902	hsa-miR-185	6
78	17904	hsa-miR-185*	6
79	18739	hsa-miR-186	6
80	42588	hsa-miR-18a	6
81	27536	hsa-miR-190	6
82	28431	hsa-miR-1908	6
83	10985	hsa-miR-191	6
84	146103	hsa-miR-1913	6
85	146091	hsa-miR-1914	6
86	10986	hsa-miR-193a-3p	6
87	46443	hsa-miR-193a-5p	6
88	10987	hsa-miR-193b	6
89	13148	hsa-miR-195	6
90	42783	hsa-miR-197	6
91	146165	hsa-miR-1973	6
92	146200	hsa-miR-1974	6
93	146001	hsa-miR-1977	6
94	146016	hsa-miR-1978	6
95	146167	hsa-miR-1979	6
96	10995	hsa-miR-199a-3p/hsa-miR-199b-3p	6
97	29562	hsa-miR-199a-5p	6
98	19591	hsa-miR-199b-5p	6
99	10997	hsa-miR-19a	6
100	10998	hsa-miR-19b	6
101	42968	hsa-miR-202	6
102	145996	hsa-miR-205*	6
103	145845	hsa-miR-20a	6
104	5740	hsa-miR-21	6
105	42524	hsa-miR-21*	6
106	145852	hsa-miR-210	6
107	146161	hsa-miR-2115*	6
108	146010	hsa-miR-2116	6
109	11014	hsa-miR-214	6
110	11020	hsa-miR-22	6
111	42532	hsa-miR-22*	6
112	11022	hsa-miR-221	6
113	42475	hsa-miR-221*	6
114	11023	hsa-miR-222	6
115	42566	hsa-miR-224	6
116	146163	hsa-miR-224*	6
117	42744	hsa-miR-23a	6
118	145841	hsa-miR-23b	6
119	17506	hsa-miR-24	6
120	146043	hsa-miR-24-1*	6
121	42950	hsa-miR-24-2*	6
122	42682	hsa-miR-25	6
123	42929	hsa-miR-25*	6
124	11030	hsa-miR-26a	6
125	146008	hsa-miR-26b	6
126	46483	hsa-miR-27a	6
127	145944	hsa-miR-27b	6

128	11037	hsa-miR-299-3p	6
129	11038	hsa-miR-299-5p	6
130	11039	hsa-miR-29a	6
131	145638	hsa-miR-29a*	6
132	11040	hsa-miR-29b	6
133	17810	hsa-miR-29b-1*	6
134	11041	hsa-miR-29c	6
135	42513	hsa-miR-300	6
136	13143	hsa-miR-301a	6
137	146086	hsa-miR-30a	6
138	146112	hsa-miR-30b	6
139	42923	hsa-miR-30c	6
140	19596	hsa-miR-30d	6
141	28191	hsa-miR-30e	6
142	145676	hsa-miR-30e*	6
143	11052	hsa-miR-31	6
144	46320	hsa-miR-31*	6
145	11053	hsa-miR-32	6
146	29575	hsa-miR-32*	6
147	27533	hsa-miR-320a	6
148	46324	hsa-miR-320b	6
149	46228	hsa-miR-320c	6
150	46870	hsa-miR-320d	6
151	42887	hsa-miR-331-3p	6
152	11065	hsa-miR-335	6
153	145745	hsa-miR-335*	6
154	42673	hsa-miR-337-3p	6
155	17944	hsa-miR-337-5p	6
156	42739	hsa-miR-339-5p	6
157	29872	hsa-miR-340	6
158	32884	hsa-miR-342-3p	6
159	27217	hsa-miR-34a	6
160	42724	hsa-miR-34b	6
161	145865	hsa-miR-361-3p	6
162	14301	hsa-miR-361-5p	6
163	11078	hsa-miR-365	6
164	29529	hsa-miR-369-3p	6
165	145844	hsa-miR-374a	6
166	14302	hsa-miR-374b	6
167	146009	hsa-miR-376a	6
168	42885	hsa-miR-376a*	6
169	145642	hsa-miR-376b	6
170	42629	hsa-miR-376c	6
171	11091	hsa-miR-377	6
172	11093	hsa-miR-379	6
173	145832	hsa-miR-381	6
174	145643	hsa-miR-382	6
175	145644	hsa-miR-409-3p	6
176	11102	hsa-miR-410	6
177	17482	hsa-miR-411	6
178	42784	hsa-miR-411*	6
179	42730	hsa-miR-423-3p	6
180	27565	hsa-miR-423-5p	6
181	42965	hsa-miR-424	6
182	17608	hsa-miR-425	6
183	18847	hsa-miR-450a	6
184	29379	hsa-miR-452	6
185	146076	hsa-miR-483-3p	6
186	145753	hsa-miR-484	6
187	14285	hsa-miR-487b	6
188	42703	hsa-miR-490-3p	6
189	17822	hsa-miR-490-5p	6
190	17927	hsa-miR-491-3p	6
191	42661	hsa-miR-492	6

192	11125	hsa-miR-493*	6
193	145901	hsa-miR-494	6
194	42676	hsa-miR-495	6
195	42442	hsa-miR-498	6
196	42581	hsa-miR-513a-5p	6
197	42550	hsa-miR-516a-5p	6
198	145725	hsa-miR-518b	6
199	13137	hsa-miR-518e*/hsa-miR-519a*/hsa-miR-519b-5p/ hsa-miR-519c-5p/hsa-miR-522*/hsa-miR-523*	6
200	46221	hsa-miR-519d	6
201	13132	hsa-miR-519e*	6
202	11175	hsa-miR-525-5p	6
203	14272	hsa-miR-542-3p	6
204	42917	hsa-miR-551b	6
205	28966	hsa-miR-574-3p	6
206	27740	hsa-miR-574-5p	6
207	17295	hsa-miR-583	6
208	145647	hsa-miR-584	6
209	17546	hsa-miR-585	6
210	42531	hsa-miR-602	6
211	27672	hsa-miR-615-3p	6
212	32825	hsa-miR-620	6
213	145740	hsa-miR-625*	6
214	42958	hsa-miR-628-3p	6
215	17566	hsa-miR-629*	6
216	17354	hsa-miR-637	6
217	42832	hsa-miR-638	6
218	42679	hsa-miR-642	6
219	21498	hsa-miR-654-3p	6
220	29736	hsa-miR-656	6
221	145973	hsa-miR-664	6
222	145768	hsa-miR-665	6
223	29490	hsa-miR-7	6
224	146196	hsa-miR-711	6
225	146064	hsa-miR-718	6
226	42751	hsa-miR-720	6
227	27568	hsa-miR-744	6
228	145805	hsa-miR-765	6
229	42808	hsa-miR-874	6
230	30033	hsa-miR-877	6
231	46259	hsa-miR-885-5p	6
232	42806	hsa-miR-886-3p	6
233	17885	hsa-miR-886-5p	6
234	42825	hsa-miR-888*	6
235	145693	hsa-miR-92a	6
236	30687	hsa-miR-93	6
237	42539	hsa-miR-933	6
238	11182	hsa-miR-98	6
239	42708	hsa-miR-99a	6
240	11184	hsa-miR-99b	6
241	28302	hsa-miRPlus-A1015	6
242	42780	hsa-miRPlus-A1065	6
243	42793	hsa-miRPlus-A1072	6
244	17858	hsa-miRPlus-A1073	6
245	17848	hsa-miRPlus-A1087	6
246	28534	hsa-miRPlus-D1058	6
247	46649	hsa-miRPlus-E1012	6
248	46466	hsa-miRPlus-E1016	6
249	21526	hsa-miRPlus-E1031	6
250	46749	hsa-miRPlus-E1033	6
251	46537	hsa-miRPlus-E1038	6
252	46580	hsa-miRPlus-E1077	6
253	46512	hsa-miRPlus-E1088	6
254	46330	hsa-miRPlus-E1097	6

255	46861	hsa-miRPlus-E1098	6
256	46382	hsa-miRPlus-E1104	6
257	145940	hsa-miRPlus-E1110	6
258	145983	hsa-miRPlus-E1114	6
259	46733	hsa-miRPlus-E1117	6
260	46662	hsa-miRPlus-E1146	6
261	145938	hsa-miRPlus-E1151	6
262	46555	hsa-miRPlus-E1153	6
263	46561	hsa-miRPlus-E1168	6
264	46817	hsa-miRPlus-E1172	6
265	46506	hsa-miRPlus-E1186	6
266	46883	hsa-miRPlus-E1209	6
267	46343	hsa-miRPlus-E1212	6
268	46885	hsa-miRPlus-E1225	6
269	145935	hsa-miRPlus-E1232	6
270	46557	hsa-miRPlus-E1233	6
271	46256	hsa-miRPlus-E1238	6
272	46445	hsa-miRPlus-E1247	6
273	145978	hsa-miRPlus-E1258	6
274	45891	hsa-miRPlus-E1285	6
275	46756	hsa-miRPlus-F1001	6
276	46635	hsa-miRPlus-F1004	6
277	46731	hsa-miRPlus-F1017	6
278	46933	hsa-miRPlus-F1026	6
279	46297	hsa-miRPlus-F1041	6
280	46519	hsa-miRPlus-F1042	6
281	46334	hsa-miRPlus-F1059	6
282	46630	hsa-miRPlus-F1064	6
283	46871	hsa-miRPlus-F1066	6
284	46386	hsa-miRPlus-F1074	6
285	46498	hsa-miRPlus-F1099	6
286	46241	hsa-miRPlus-F1130	6
287	46353	hsa-miRPlus-F1147	6
288	46590	hsa-miRPlus-F1154	6
289	45614	hsa-miRPlus-F1155	6
290	46601	hsa-miRPlus-F1163	6
291	46273	hsa-miRPlus-F1166	6
292	46298	hsa-miRPlus-F1180	6
293	46602	hsa-miRPlus-F1194	6
294	46882	hsa-miRPlus-F1195	6
295	46655	hsa-miRPlus-F1215	6
296	46632	hsa-miRPlus-F1222	6
297	46599	hsa-miRPlus-F1225	6
298	46359	hsa-miRPlus-F1231	6
299	146113	hsa-miRPlus-G1246-3p	6
300	146158	hsa-miRPlus-G1316-5p	6
301	145746	hsa-let-7i*	5
302	145857	hsa-miR-154	5
303	42538	hsa-miR-196a*	5
304	146140	hsa-miR-1976	5
305	146049	hsa-miR-28-5p	5
306	11061	hsa-miR-329	5
307	145859	hsa-miR-33a	5
308	145950	hsa-miR-33b	5
309	27544	hsa-miR-363*	5
310	145705	hsa-miR-431	5
311	11111	hsa-miR-432	5
312	42694	hsa-miR-485-3p	5
313	145701	hsa-miR-668	5
314	29190	hsa-miR-708	5
315	46742	hsa-miRPlus-E1067	5
316	46352	hsa-miRPlus-E1082	5
317	46296	hsa-miRPlus-F1036	5
318	46570	hsa-miRPlus-F1080	5

319	46503	hsa-miRPlus-F1104	5
320	46702	hsa-miRPlus-F1190	5

Appendix 3.3.3 MicroRNAs that were expressed in at least 80% of oesophageal NTMs (n = 6).

No.	Probe Id	Annotation	Relative abundance	p-value
1	145975	hsa-miR-1260	-1.46	8.95E-04
2	42751	hsa-miR-720	-1.46	2.98E-04
3	46512	hsa-miRPlus-E1088	-1.43	4.17E-05
4	46382	hsa-miRPlus-E1104	1.35	4.50E-05
5	46324	hsa-miR-320b	1.36	5.68E-04
6	145805	hsa-miR-765	1.37	1.17E-04
7	42829	hsa-miR-127-3p	1.37	1.63E-04
8	28966	hsa-miR-574-3p	1.38	4.43E-07
9	46712	hsa-miR-1201	1.38	2.04E-06
10	17295	hsa-miR-583	1.38	6.68E-06
11	146086	hsa-miR-30a	1.39	3.63E-04
12	46228	hsa-miR-320c	1.42	1.60E-04
13	17749	hsa-let-7b	1.44	6.18E-04
14	27533	hsa-miR-320a	1.46	1.33E-04
15	19596	hsa-miR-30d	1.46	1.83E-06
16	31026	hsa-miR-101	1.57	5.50E-04
17	13143	hsa-miR-301a	1.59	9.77E-05
18	46870	hsa-miR-320d	1.59	1.34E-06
19	42872	hsa-miR-138-1*	1.67	1.30E-04

Appendix 3.3.4 Relative abundance of significantly different miRNAs in gastric NTMs compared to oesophageal NTMs, at $p < 0.001$.

No.	Probe Id	Annotation	Relative abundance	p-value
1	46749	hsa-miRPlus-E1033	-2.78	7.98E-07
2	11041	hsa-miR-29c	-2.5	2.43E-07
3	146076	hsa-miR-483-3p	-2.44	2.65E-05
4	42965	hsa-miR-424	-2.44	9.12E-06
5	42679	hsa-miR-642	-2.43	4.87E-06
6	31026	hsa-miR-101	-2.31	2.16E-06
7	13143	hsa-miR-301a	-2.26	2.43E-08
8	28302	hsa-miRPlus-A1015	-2.14	4.50E-06
9	11040	hsa-miR-29b	-1.91	3.94E-04
10	146112	hsa-miR-30b	-1.82	5.64E-06
11	19596	hsa-miR-30d	-1.8	2.65E-09
12	46630	hsa-miRPlus-F1064	-1.8	1.73E-05
13	145844	hsa-miR-374a	-1.78	9.70E-08
14	46882	hsa-miRPlus-F1195	-1.76	7.70E-06
15	46555	hsa-miRPlus-E1153	-1.76	3.81E-05
16	27217	hsa-miR-34a	-1.74	2.19E-04
17	42887	hsa-miR-331-3p	-1.73	1.80E-06
18	46382	hsa-miRPlus-E1104	-1.71	1.29E-08
19	27568	hsa-miR-744	-1.69	3.21E-11
20	145678	hsa-miR-150	-1.67	5.63E-05
21	10919	hsa-miR-103	-1.62	1.12E-06
22	145805	hsa-miR-765	-1.59	1.37E-06
23	10138	hsa-miR-130a	-1.58	7.62E-06
24	42513	hsa-miR-300	-1.57	8.19E-04
25	42872	hsa-miR-138-1*	-1.57	7.22E-04
26	10923	hsa-miR-107	-1.57	4.99E-08
27	42917	hsa-miR-551b	-1.56	1.52E-06
28	17904	hsa-miR-185*	-1.54	5.42E-05
29	42885	hsa-miR-376a*	-1.5	7.07E-07
30	28966	hsa-miR-574-3p	-1.49	5.58E-08
31	46870	hsa-miR-320d	-1.46	4.81E-05
32	17295	hsa-miR-583	-1.45	9.12E-07
33	11260	hsa-miR-151-5p	-1.43	3.23E-05
34	14272	hsa-miR-542-3p	-1.41	2.43E-04
35	145935	hsa-miRPlus-E1232	-1.4	4.05E-04
36	19585	hsa-miR-148b	-1.39	6.14E-05
37	146113	hsa-miRPlus-G1246-3p	-1.39	2.53E-04
38	145938	hsa-miRPlus-E1151	-1.39	1.83E-06
39	45614	hsa-miRPlus-F1155	-1.38	3.48E-04
40	10985	hsa-miR-191	-1.37	6.73E-05
41	46228	hsa-miR-320c	-1.36	4.25E-04
42	27565	hsa-miR-423-5p	-1.35	4.42E-04
43	11039	hsa-miR-29a	-1.35	9.24E-04
44	42475	hsa-miR-221*	1.43	1.59E-05
45	42630	hsa-miR-140-3p	1.49	3.78E-05
46	27720	hsa-miR-15a	1.71	1.10E-05
47	42751	hsa-miR-720	1.76	9.83E-05
48	30787	hsa-miR-125b	1.93	1.68E-04

Appendix 3.3.5 Relative abundance of significantly different miRNAs in MSCs compared to gastric NTMs, at $p < 0.001$.

No.	Probe Id	Annotation	Relative abundance	p-value
1	46749	hsa-miRPlus-E1033	-2.43	1.23E-04
2	11041	hsa-miR-29c	-1.88	5.43E-05
3	27217	hsa-miR-34a	-1.79	4.92E-05
4	11014	hsa-miR-214	1.39	3.80E-04
5	11022	hsa-miR-221	1.6	5.44E-05
6	11023	hsa-miR-222	1.77	8.99E-04
7	42630	hsa-miR-140-3p	1.85	1.23E-06
8	27720	hsa-miR-15a	1.91	5.02E-05
9	42641	hsa-miR-145	2.12	8.24E-04

Appendix 3.3.6 Relative abundance of significantly different miRNAs in MSCs compared to oesophageal NTMs, at $p < 0.001$.

No.	Probe Id	Annotation	Relative abundance	p-value
1	46871	hsa-miRPlus-F1066	1.23	1.30E-04
2	46933	hsa-miRPlus-F1026	1.33	3.42E-05
3	45614	hsa-miRPlus-F1155	1.35	2.49E-04
4	145745	hsa-miR-335*	1.36	1.39E-04
5	42730	hsa-miR-423-3p	1.36	9.61E-05
6	46221	hsa-miR-519d	1.38	2.38E-05
7	10985	hsa-miR-191	1.40	1.39E-04
8	145935	hsa-miRPlus-E1232	1.42	5.17E-04
9	11184	hsa-miR-99b	1.43	5.28E-06
10	146167	hsa-miR-1979	1.44	2.98E-04
11	145938	hsa-miRPlus-E1151	1.45	1.01E-07
12	145805	hsa-miR-765	1.50	3.38E-06
13	46662	hsa-miRPlus-E1146	1.54	3.25E-05
14	19596	hsa-miR-30d	1.55	2.98E-04
15	14285	hsa-miR-487b	1.56	3.09E-04
16	46801	hsa-miR-106a	1.58	6.95E-04
17	146008	hsa-miR-26b	1.59	3.67E-05
18	46353	hsa-miRPlus-F1147	1.60	6.96E-04
19	42917	hsa-miR-551b	1.61	2.41E-04
20	42524	hsa-miR-21*	1.61	4.01E-04
21	145693	hsa-miR-92a	1.62	1.83E-04
22	145844	hsa-miR-374a	1.68	3.05E-06
23	10997	hsa-miR-19a	1.70	4.58E-05
24	42486	hsa-miR-149*	1.72	1.96E-04
25	42825	hsa-miR-888*	1.73	3.32E-06
26	42929	hsa-miR-25*	1.73	7.57E-04
27	46731	hsa-miRPlus-F1017	1.74	1.49E-04
28	46698	hsa-miR-1280	1.81	6.94E-07
29	145820	hsa-let-7c	1.83	5.86E-04
30	145996	hsa-miR-205*	1.83	1.27E-05
31	46328	hsa-miR-1274b	1.86	2.23E-06
32	42724	hsa-miR-34b	1.86	2.53E-06
33	31026	hsa-miR-101	1.93	6.21E-06
34	145801	hsa-miR-184	1.95	9.35E-04
35	42539	hsa-miR-933	1.98	8.53E-07
36	28302	hsa-miRPlus-A1015	1.98	2.41E-05
37	10998	hsa-miR-19b	2.03	9.05E-06
38	17927	hsa-miR-491-3p	2.28	1.71E-08

Appendix 3.3.7 Relative abundance of significantly different miRNAs in gastric CAMs compared to SC-CAMs, at $p < 0.001$.

No.	Probe Id	Annotation	Relative abundance	p-value
1	46861	hsa-miRPlus-E1098	1.25	7.67E-04
2	145938	hsa-miRPlus-E1151	1.32	3.56E-06
3	10985	hsa-miR-191	1.37	3.86E-04
4	145844	hsa-miR-374a	1.40	8.18E-04
5	145805	hsa-miR-765	1.47	2.67E-05
6	145983	hsa-miRPlus-E1114	1.49	3.62E-05
7	42539	hsa-miR-933	1.53	2.51E-04
8	17927	hsa-miR-491-3p	1.54	8.79E-04
9	42917	hsa-miR-551b	1.56	9.01E-04
10	46882	hsa-miRPlus-F1195	1.56	8.41E-04
11	19596	hsa-miR-30d	1.60	4.22E-04
12	28302	hsa-miRPlus-A1015	1.66	7.78E-04
13	42872	hsa-miR-138-1*	1.78	8.81E-04

Appendix 3.3.8 Relative abundance of significantly different miRNAs in gastric CAMs compared to AC-CAMs, at $p < 0.001$.

Patient	hsa-miR-494
Sz192	-1.72
Sz190	-1.5
Sz294	-1.29
Sz268	-1.29
Sz308	-1.22
Sz305	-1.2
Sz194	-1.15
Sz389	-1.14
Sz42	-1.1
Sz198	1.03
Sz45	1.15
Sz271	1.2
Patient	**hsa-miR-106b**
Sz268	1.69
Sz192	1.51
Sz190	1.4
Sz305	1.38
Sz194	1.35
Sz271	1.19
Sz42	1.1
Sz308	1
Sz198	-1.03
Sz294	-1.06
Sz389	-1.08
Sz45	-1.1
Patient	**hsa-miR-130b**
Sz190	1.94
Sz192	1.93
Sz305	1.34
Sz268	1.28
Sz389	1.22
Sz198	1.1
Sz308	1.08
Sz294	1.04
Sz271	1.02
Sz194	-1.03
Sz45	-1.07
Sz42	-1.11
Patient	**hsa-miR-301a**
Sz190	2.35
Sz192	1.61
Sz305	1.41
Sz268	1.31
Sz389	1.27
Sz42	1.08
Sz308	1.08
Sz194	1.03
Sz198	-1.03
Sz271	-1.06
Sz45	-1.1
Sz294	-1.41

Patient	hsa-miR-483-3p
Sz192	-1.8
Sz268	-1.58
Sz389	-1.37
Sz194	-1.2
Sz305	-1.19
Sz308	-1.11
Sz45	-1.09
Sz190	-1.07
Sz294	-1.03
Sz42	-1.01
Sz198	1.09
Sz271	1.11
Patient	**hsa-miR-93**
Sz268	1.71
Sz192	1.54
Sz190	1.54
Sz305	1.45
Sz194	1.23
Sz271	1.18
Sz389	1.05
Sz308	1.04
Sz294	-1.01
Sz42	-1.03
Sz198	-1.08
Sz45	-1.18
Patient	**hsa-miR-32**
Sz190	1.96
Sz268	1.43
Sz192	1.41
Sz45	1.19
Sz389	1.17
Sz305	1.16
Sz198	1.14
Sz271	1.14
Sz194	1.04
Sz42	1.03
Sz294	1.03
Sz308	1
Patient	**hsa-miR-15a**
Sz268	2.26
Sz194	1.58
Sz271	1.41
Sz190	1.38
Sz192	1.37
Sz198	1.11
Sz305	1.09
Sz42	-1.01
Sz45	-1.01
Sz308	-1.03
Sz389	-1.07
Sz294	-1.23

Patient	hsa-miR-181d
Sz190	2.47
Sz389	1.62
Sz192	1.5
Sz198	1.36
Sz45	1.31
Sz271	1.17
Sz194	1.15
Sz268	1.09
Sz305	1.03
Sz294	-1.02
Sz42	-1.05
Sz308	-1.17
Patient	**hsa-miR-15b**
Sz268	2.19
Sz305	1.58
Sz192	1.57
Sz194	1.49
Sz190	1.15
Sz45	1.14
Sz198	1.11
Sz308	1.11
Sz271	1.1
Sz42	-1.01
Sz294	-1.01
Sz389	-1.2

Appendix 3.3.9 Relative abundance of 10 miRNAs in paired individual samples of gastric CAMs compared to corresponding ATMs from 12 patients.

No.	Probe Id	Annotation	Relative abundance	p-value
1	146016	hsa-miR-1978	-1.96	7.78E-04
2	42965	hsa-miR-424	-1.67	6.02E-04
3	42641	hsa-miR-145	-1.59	1.48E-02
4	11014	hsa-miR-214	-1.47	5.82E-04
5	145725	hsa-miR-518b	-1.47	3.98E-03
6	11030	hsa-miR-26a	-1.37	1.03E-03
7	42679	hsa-miR-642	-1.37	3.38E-03
8	46883	hsa-miRPlus-E1209	-1.37	3.52E-04
9	42513	hsa-miR-300	-1.35	5.46E-04
10	21526	hsa-miRPlus-E1031	1.36	2.64E-02
11	46506	hsa-miRPlus-E1186	1.37	2.00E-03
12	46732	hsa-miR-1264	1.38	6.95E-05
13	46698	hsa-miR-1280	1.40	2.38E-05
14	42825	hsa-miR-888*	1.42	2.79E-05
15	145978	hsa-miRPlus-E1258	1.42	4.95E-04
16	46292	hsa-miR-1274a	1.61	1.94E-04

Appendix 3.3.10 Relative abundance of significantly different miRNAs in gastric ATMs compared to NTMs, at $p < 0.05$.

No.	Probe Id	Annotation	Relative abundance	p-value
1	46258	hsa-miR-1184	-1.45	2.37E-02
2	46883	hsa-miRPlus-E1209	-1.33	1.27E-02
3	145801	hsa-miR-184	-1.20	3.20E-02
4	17482	hsa-miR-411	1.16	1.66E-02
5	11038	hsa-miR-299-5p	1.19	2.24E-02
6	42532	hsa-miR-22*	1.20	1.56E-02
7	11182	hsa-miR-98	1.22	8.20E-03
8	145820	hsa-let-7c	1.27	3.45E-02
9	146011	hsa-let-7a	1.29	8.99E-04
10	17944	hsa-miR-337-5p	1.30	2.68E-02
11	10987	hsa-miR-193b	1.37	5.92E-03
12	42744	hsa-miR-23a	1.40	2.56E-02
13	46483	hsa-miR-27a	1.40	2.38E-02
14	145944	hsa-miR-27b	1.42	4.81E-02
15	11052	hsa-miR-31	1.62	4.48E-03
16	11065	hsa-miR-335	2.87	3.68E-03

Appendix 3.3.11 Relative abundance of significantly different miRNAs in pairwise analysis of SC-CAMs compared to SC-ATMs, at $p < 0.05$ (paired t-test).

Patient	hsa-miR-1184
Sz360	-1.78
Sz467	-1.58
Sz306	-1.29
Sz373	-1.23

Patient	hsa-miR-184
Sz373	-1.35
Sz360	-1.23
Sz306	-1.17
Sz467	-1.07

Patient	hsa-miR-411
Sz306	1.23
Sz373	1.21
Sz467	1.15
Sz360	1.07

Patient	hsa-miR-299-5p
Sz467	1.25
Sz360	1.25
Sz373	1.23
Sz306	1.06

Patient	hsa-miR-98
Sz373	1.32
Sz467	1.22
Sz306	1.17
Sz360	1.15

Patient	hsa-let-7c
Sz360	1.54
Sz467	1.24
Sz306	1.19
Sz373	1.15

Patient	hsa-let-7a
Sz373	1.33
Sz467	1.31
Sz360	1.29
Sz306	1.22

Patient	hsa-miR-337-5p
Sz373	1.46
Sz467	1.41
Sz306	1.29
Sz360	1.09

Patient	hsa-miR-193b
Sz467	1.52
Sz373	1.43
Sz360	1.31
Sz306	1.24

Patient	hsa-miR-27a
Sz467	1.7
Sz373	1.5
Sz360	1.28
Sz306	1.19

Patient	hsa-miR-23a
Sz467	1.72
Sz373	1.49
Sz360	1.28
Sz306	1.19

Patient	hsa-miR-27b
Sz467	1.87
Sz373	1.5
Sz306	1.21
Sz360	1.18

Patient	hsa-miR-31
Sz306	1.9
Sz360	1.68
Sz467	1.55
Sz373	1.41

Patient	hsa-miR-335
Sz373	3.87
Sz306	3.18
Sz360	2.53
Sz467	2.17

Appendix 3.3.12 Relative abundance of 14 miRNAs in paired individual samples of SC-CAMs compared to corresponding SC-ATMs from 4 patients.

No.	Probe Id	Annotation	Relative abundance	p-value
1	10998	hsa-miR-19b	-1.61	2.25E-04
2	31026	hsa-miR-101	-1.59	8.03E-03
3	145693	hsa-miR-92a	-1.56	3.60E-04
4	10997	hsa-miR-19a	-1.49	3.28E-04
5	42703	hsa-miR-490-3p	-1.45	1.02E-02
6	42708	hsa-miR-99a	-1.45	3.97E-02
7	145845	hsa-miR-20a	-1.41	3.74E-03
8	46801	hsa-miR-106a	-1.39	1.31E-02
9	17927	hsa-miR-491-3p	-1.39	8.91E-04
10	32884	hsa-miR-342-3p	-1.35	5.75E-03
11	17566	hsa-miR-629*	-1.35	3.46E-03
12	11023	hsa-miR-222	1.46	4.01E-03
13	17506	hsa-miR-24	1.47	4.53E-03
14	146086	hsa-miR-30a	1.51	4.72E-02
15	11022	hsa-miR-221	1.54	9.86E-04
16	145852	hsa-miR-210	1.60	2.67E-02
17	13140	hsa-miR-138	1.62	1.88E-02
18	145981	hsa-miR-1285	1.93	5.40E-03

Appendix 3.3.13 Relative abundance of significantly different miRNAs in oesophageal SC-CAMs compared to oesophageal NTMs, at $p < 0.05$.

No.	Probe Id	Annotation	Relative abundance	p-value
1	42965	hsa-miR-424	-1.72	2.18E-02
2	42708	hsa-miR-99a	-1.67	2.98E-02
3	145820	hsa-let-7c	-1.64	2.32E-03
4	10306	hsa-miR-146b-5p	-1.61	1.55E-02
5	31026	hsa-miR-101	-1.59	2.54E-02
6	10987	hsa-miR-193b	-1.54	5.03E-04
7	11052	hsa-miR-31	-1.52	1.82E-02
8	46320	hsa-miR-31*	-1.52	1.54E-02
9	11030	hsa-miR-26a	-1.49	3.46E-02
10	17749	hsa-let-7b	-1.47	7.93E-03
11	46561	hsa-miRPlus-E1168	-1.47	4.16E-02
12	5740	hsa-miR-21	-1.43	3.52E-02
13	30787	hsa-miR-125b	-1.41	2.24E-02
14	10998	hsa-miR-19b	-1.41	3.23E-02
15	145647	hsa-miR-584	-1.39	2.76E-02
16	146011	hsa-let-7a	-1.37	5.91E-03
17	145832	hsa-miR-381	-1.35	5.69E-03
18	29379	hsa-miR-452	-1.35	3.75E-02
19	146001	hsa-miR-1977	1.36	2.17E-02
20	11039	hsa-miR-29a	1.36	2.68E-03
21	11022	hsa-miR-221	1.41	7.99E-04
22	11041	hsa-miR-29c	1.44	3.16E-02
23	11023	hsa-miR-222	1.50	3.09E-03
24	146165	hsa-miR-1973	1.65	7.62E-03
25	46620	hsa-miR-1275	1.70	3.15E-03
26	11040	hsa-miR-29b	1.87	1.30E-03

Appendix 3.3.14 Relative abundance of significantly different miRNAs in oesophageal SC-ATMs compared to oesophageal NTMs, at $p < 0.05$.

No.	Probe	Annotation	Relative abundance	p-value
1	27533	hsa-miR-320a	1.15	2.29E-02
2	46324	hsa-miR-320b	1.16	2.73E-02
3	10967	hsa-miR-16	1.19	7.88E-03
4	31867	hsa-miR-145*	1.34	3.59E-02
5	42641	hsa-miR-145	1.82	1.90E-02

Appendix 3.3.15 Relative abundance of significantly different miRNAs in pairwise analysis of AC-CAMs compared to AC-ATMs, at $p < 0.05$ (paired t-test).

	Sz173	Sz193	Sz282
hsa-miR-16	1.21	1.16	1.22
hsa-miR-145	2.04	1.91	1.54
hsa-miR-320a	1.18	1.10	1.16
hsa-miR-320b	1.22	1.12	1.15

Appendix 3.3.16 Relative abundance of miRNAs in paired individual samples of AC-CAMs compared to corresponding AC-ATMs from 3 patients.

No.	Probe Id	Annotation	Relative abundance	p-value
1	10306	hsa-miR-146b-5p	-1.85	8.18E-03
2	29379	hsa-miR-452	-1.39	2.39E-02
3	146113	hsa-miRPlus-G1246-3p	-1.33	4.41E-04
4	46923	hsa-miR-1259	-1.32	3.46E-03
5	46466	hsa-miRPlus-E1016	-1.32	7.02E-03
6	17944	hsa-miR-337-5p	-1.15	3.95E-02
7	11175	hsa-miR-525-5p	1.16	3.62E-02
8	45891	hsa-miRPlus-E1285	1.19	3.16E-02
9	145981	hsa-miR-1285	1.44	2.31E-02

Appendix 3.3.17 Relative abundance of significantly different miRNAs in oesophageal AC-CAMs compared to oesophageal NTMs, at $p < 0.05$.

No.	Probe Id	Annotation	Relative abundance	p-value
1	42965	hsa-miR-424	-1.69	2.18E-02
2	11030	hsa-miR-26a	-1.52	8.78E-03
3	31026	hsa-miR-101	-1.47	7.17E-03
4	42708	hsa-miR-99a	-1.47	4.44E-02
5	10306	hsa-miR-146b-5p	-1.45	2.87E-02
6	30787	hsa-miR-125b	-1.43	6.62E-03
7	27217	hsa-miR-34a	-1.35	1.21E-02
8	146200	hsa-miR-1974	1.35	2.14E-02
9	11040	hsa-miR-29b	1.38	3.73E-02
10	46292	hsa-miR-1274a	1.50	4.33E-02

Appendix 3.3.18 Relative abundance of significantly different miRNAs in oesophageal AC-ATMs compared to oesophageal NTMs, at $p < 0.05$.

No.	Networks	p-value
1	Cell cycle_G1-S Growth factor regulation	1.956E-14
2	Cell cycle_G1-S Interleukin regulation	3.169E-14
3	Signal transduction_WNT signalling	6.083E-11
4	Development_Hemopoiesis, Erythropoietin pathway	3.348E-09
5	Apoptosis_Anti-Apoptosis mediated by external signals via PI3K/AKT	5.769E-09
6	Development_EMT_Regulation of epithelial-to-mesenchymal transition	6.642E-09
7	Reproduction_Male sex differentiation	4.016E-08
8	Cell cycle_G0-G1	1.475E-07
9	Proliferation_Positive regulation cell proliferation	1.943E-07
10	Signal Transduction_TGF-beta, GDF and Activin signalling	2.951E-07
11	Cell cycle_Core	3.402E-07
12	DNA damage_Checkpoint	1.483E-06
13	Reproduction_Feeding and Neurohormone signalling	1.761E-06
14	Development_Hedgehog signalling	3.903E-06
15	Development_Regulation of telomere length	4.668E-06
16	Cell cycle_G1-S	6.524E-06
17	Inflammation_IL-2 signalling	1.400E-05
18	Inflammation_IL-10 anti-inflammatory response	1.653E-05
19	Signal transduction_Leptin signalling	2.653E-05
20	Cardiac development_BMP_TGF_beta_signalling	2.711E-05
21	Inflammation_MIF signalling	3.075E-05
22	Reproduction_FSH-beta signalling pathway	4.991E-05
23	Signal transduction_NOTCH signalling	5.538E-05
24	Development_Regulation of angiogenesis	6.641E-05
25	Immune response_TCR signalling	6.981E-05
26	Reproduction_Progesterone signalling	7.596E-05
27	Proliferation_Negative regulation of cell proliferation	9.736E-05
28	Signal transduction_Androgen receptor nuclear signalling	1.168E-04
29	Development_Ossification and bone remodelling	1.183E-04
30	Apoptosis_Anti-Apoptosis mediated by external signals via MAPK and JAK/STAT	1.276E-04
31	Cardiac development_Role of NADPH oxidase and ROS	1.443E-04
32	Inflammation_IL-6 signalling	1.640E-04
33	Signal transduction_ESR1-nuclear pathway	2.376E-04
34	Development_Blood vessel morphogenesis	2.900E-04
35	Inflammation_IFN-gamma signalling	5.347E-04
36	Signal Transduction_BMP and GDF signalling	5.945E-04
37	Signal transduction_Androgen receptor signalling cross-talk	6.191E-04
38	Cell cycle_G2-M	7.777E-04
39	Apoptosis_Apoptosis stimulation by external signals	8.402E-04
40	Immune response_Th17-derived cytokines	1.006E-03
41	Development_Keratinocyte differentiation	1.063E-03
42	Signal Transduction_Cholecystokinin signalling	1.401E-03
43	Reproduction_Spermatogenesis, motility and copulation	1.459E-03
44	Proliferation_Lymphocyte proliferation	1.566E-03
45	Apoptosis_Anti-apoptosis mediated by external signals via NF-kB	1.906E-03
46	Inflammation_Jak-STAT Pathway	1.969E-03
47	Signal transduction_ERBB-family signalling	2.353E-03
48	Inflammation_IL-4 signalling	3.038E-03
49	Inflammation_Kallikrein-kinin system	3.610E-03
50	Inflammation_Interferon signalling	3.610E-03

Appendix 4.3.1 Networks enriched by targets of differentially abundant miRNAs in pairwise analysis of gastric CAMs compared to ATMs.

No.	Networks	p-value
1	Cell cycle_G1-S Growth factor regulation	7.626E-11
2	Development_EMT_Regulation of epithelial-to-mesenchymal transition	1.694E-09
3	Cell cycle_G1-S Interleukin regulation	1.376E-07
4	Reproduction_FSH-beta signalling pathway	2.353E-06
5	Signal Transduction_TGF-beta, GDF and Activin signalling	3.952E-06
6	Development_Hemopoiesis, Erythropoietin pathway	6.901E-06
7	Inflammation_IL-10 anti-inflammatory response	1.572E-05
8	DNA damage_Checkpoint	2.295E-05
9	Signal transduction_Leptin signalling	2.394E-05
10	Signal transduction_WNT signalling	3.577E-05
11	Signal transduction_NOTCH signalling	4.388E-05
12	Proliferation_Positive regulation cell proliferation	4.607E-05
13	Reproduction_Male sex differentiation	3.119E-04
14	Development_Regulation of angiogenesis	3.959E-04
15	Development_Ossification and bone remodelling	4.260E-04
16	Development_Hedgehog signalling	5.265E-04
17	Development_Blood vessel morphogenesis	5.672E-04
18	Proliferation_Negative regulation of cell proliferation	8.177E-04
19	Signal transduction_Androgen receptor signalling cross-talk	9.207E-04
20	Signal transduction_ESR1-nuclear pathway	1.039E-03
21	Cell cycle_G1-S	1.216E-03
22	Cell cycle_Core	2.515E-03
23	Signal transduction_Nitric oxide signalling	4.472E-03
24	Signal transduction_ERBB-family signalling	4.472E-03
25	Cardiac development_BMP_TGF_beta_signalling	5.830E-03
26	Cell adhesion_Cadherins	7.056E-03
27	Apoptosis_Anti-Apoptosis mediated by external signals via MAPK and JAK/STAT	7.416E-03
28	Cell adhesion_Glycoconjugates	9.577E-03
29	Cell cycle_G0-G1	9.577E-03
30	Reproduction_GnRH signalling pathway	1.031E-02

Appendix 4.3.2 Networks enriched by targets of differentially abundant miRNAs in gastric CAMs compared to NTMs.

No.	Networks	p-value
1	Cell cycle_G1-S Growth factor regulation	7.361E-13
2	Cell cycle_G1-S Interleukin regulation	2.075E-10
3	Development_EMT_Regulation of epithelial-to-mesenchymal transition	2.360E-08
4	Signal Transduction_TGF-beta, GDF and Activin signalling	1.292E-07
5	Signal transduction_WNT signalling	1.620E-07
6	Development_Hemopoiesis, Erythropoietin pathway	2.342E-07
7	DNA damage_Checkpoint	9.375E-07
8	Reproduction_FSH-beta signalling pathway	7.032E-06
9	Inflammation_IL-10 anti-inflammatory response	7.076E-06
10	Signal transduction_NOTCH signalling	1.366E-05
11	Signal transduction_Androgen receptor signalling cross-talk	4.972E-05
12	Inflammation_MIF signalling	6.923E-05
13	Cell cycle_G1-S	9.537E-05
14	Proliferation_Positive regulation cell proliferation	1.018E-04
15	Reproduction_Male sex differentiation	1.232E-04
16	Cell cycle_Core	2.024E-04
17	Reproduction_Feeding and Neurohormone signalling	2.485E-04
18	Signal transduction_ERBB-family signalling	2.955E-04
19	Proliferation_Negative regulation of cell proliferation	3.622E-04
20	Signal transduction_ESR1-membrane pathway	4.770E-04
21	Development_Hedgehog signalling	1.082E-03
22	Development_Ossification and bone remodelling	1.360E-03
23	Cardiac development_Role of NADPH oxidase and ROS	1.553E-03
24	Inflammation_IL-4 signalling	2.115E-03
25	Proliferation_Lymphocyte proliferation	2.687E-03
26	Signal transduction_Nitric oxide signalling	2.912E-03
27	Apoptosis_Anti-Apoptosis mediated by external signals via PI3K/AKT	3.541E-03
28	Cell adhesion_Cadherins	3.933E-03
29	Immune response_Innate immune response to RNA viral infection	4.211E-03
30	Cell adhesion_Glycoconjugates	6.324E-03
31	Cell cycle_G0-G1	6.324E-03
32	Immune response_Th17-derived cytokines	6.324E-03
33	Development_Blood vessel morphogenesis	6.697E-03
34	Cell adhesion_Platelet-endothelium-leucocyte interactions	7.642E-03
35	Reproduction_Progesterone signalling	7.650E-03
36	Immune response_T helper cell differentiation	7.881E-03
37	Signal transduction_Leptin signalling	7.881E-03
38	Signal transduction_ESR1-nuclear pathway	7.995E-03
39	Translation_Regulation of initiation	1.376E-02
40	Development_Keratinocyte differentiation	1.391E-02
41	Signal Transduction_BMP and GDF signalling	1.400E-02
42	Development_Regulation of angiogenesis	1.553E-02

Appendix 4.3.3 Networks enriched by targets of differentially abundant miRNAs in gastric ATMs compared to NTMs.

No.	Networks	p-value
1	Signal Transduction_TGF-beta, GDF and Activin signalling	2.429E-11
2	Signal Transduction_BMP and GDF signalling	3.065E-07
3	Cell cycle_G1-S Growth factor regulation	6.057E-07
4	Development_Hedgehog signalling	6.216E-07
5	Reproduction_Feeding and Neurohormone signalling	1.828E-06
6	Signal transduction_ESR1-nuclear pathway	1.963E-06
7	Cell cycle_G1-S Interleukin regulation	2.853E-06
8	Apoptosis_Anti-Apoptosis mediated by external signals via PI3K/AKT	1.026E-05
9	Development_Blood vessel morphogenesis	1.151E-05
10	Signal transduction_NOTCH signalling	1.395E-05
11	Development_Hemopoiesis, Erythropoietin pathway	1.594E-05
12	Proliferation_Negative regulation of cell proliferation	2.550E-05
13	Proliferation_Positive regulation cell proliferation	5.401E-05
14	Cell cycle_G1-S	6.556E-05
15	Signal transduction_ESR1-membrane pathway	1.145E-04
16	Transcription_Nuclear receptors transcriptional regulation	2.216E-04
17	Cardiac development_Role of NADPH oxidase and ROS	2.274E-04
18	Reproduction_Progesterone signalling	2.376E-04
19	Signal transduction_Androgen receptor signaling cross-talk	2.782E-04
20	Apoptosis_Anti-Apoptosis mediated by external signals by Estrogen	2.782E-04
21	Reproduction_Male sex differentiation	3.343E-04
22	Apoptosis_Apoptosis stimulation by external signals	3.441E-04
23	Development_EMT_Regulation of epithelial-to-mesenchymal transition	4.244E-04
24	Cell cycle_G0-G1	4.569E-04
25	Inflammation_TREM1 signalling	4.606E-04
26	Signal transduction_WNT signalling	5.121E-04
27	Development_Regulation of telomere length	7.711E-04
28	Development_Neurogenesis in general	7.826E-04
29	Inflammation_IL-10 anti-inflammatory response	7.980E-04
30	Immune response_Th17-derived cytokines	7.980E-04
31	Development_Skeletal muscle development	8.164E-04
32	Inflammation_Jak-STAT Pathway	9.515E-04
33	Inflammation_IL-6 signalling	1.017E-03
34	Cardiac development_Wnt_beta-catenin, Notch, VEGF, IP3 and integrin	1.026E-03
35	Apoptosis_Anti-apoptosis mediated by external signals via NF-kB	1.315E-03
36	Development_Ossification and bone remodelling	1.802E-03
37	Reproduction_Spermatogenesis, motility and copulation	1.932E-03
38	Reproduction_FSH-beta signalling pathway	2.056E-03
39	Inflammation_MIF signalling	3.356E-03
40	Response to hypoxia and oxidative stress	3.853E-03
41	Development_Keratinocyte differentiation	3.919E-03
42	Proteolysis_ECM remodelling	7.368E-03
43	Cardiac development_BMP_TGF_beta_signalling	8.193E-03
44	Development_Regulation of angiogenesis	8.401E-03
45	Cell cycle_G2-M	1.083E-02
46	Apoptosis_Anti-Apoptosis mediated by external signals via MAPK and	1.128E-02
47	Cardiac development_FGF_ErbB signalling	1.165E-02
48	Development_Cartilage development	1.200E-02
49	Cell adhesion_Integrin-mediated cell-matrix adhesion	1.202E-02
50	Inflammation_IFN-gamma signalling	1.278E-02

Appendix 4.3.4 Networks enriched by targets of differentially abundant miRNAs in pairwise analysis of oesophageal SC-CAMs compared to SC-ATMs.

No.	Networks	p-value
1	Cell cycle_G1-S Growth factor regulation	2.553E-12
2	Cell cycle_G0-G1	7.493E-12
3	Cell cycle_G1-S Interleukin regulation	1.352E-11
4	Cell cycle_G1-S	5.318E-10
5	Development_Hemopoiesis, Erythropoietin pathway	7.016E-10
6	Development_Hedgehog signalling	3.328E-09
7	Signal transduction_NOTCH signalling	3.772E-09
8	Development_EMT_Regulation of epithelial-to-mesenchymal transition	5.174E-09
9	Cell cycle_Core	9.081E-09
10	Apoptosis_Anti-Apoptosis mediated by external signals via PI3K/AKT	9.133E-09
11	Signal Transduction_TGF-beta, GDF and Activin signalling	2.708E-08
12	Development_Regulation of telomere length	4.526E-08
13	Proliferation_Positive regulation cell proliferation	1.399E-07
14	Proliferation_Negative regulation of cell proliferation	1.939E-07
15	Immune response_Th17-derived cytokines	2.851E-07
16	Signal transduction_WNT signalling	4.613E-07
17	Inflammation_MIF signalling	9.048E-07
18	Cardiac development_Role of NADPH oxidase and ROS	1.028E-06
19	DNA damage_Checkpoint	1.028E-06
20	Reproduction_Progesterone signalling	1.362E-06
21	Signal transduction_Androgen receptor signalling cross-talk	2.397E-06
22	Development_Blood vessel morphogenesis	9.009E-06
23	Apoptosis_Anti-Apoptosis mediated by external signals by Estrogen	1.732E-05
24	Cardiac development_Wnt_beta-catenin, Notch, VEGF, IP3 and integrin signalling	2.469E-05
25	Signal transduction_ESR1-nuclear pathway	3.755E-05
26	Inflammation_Interferon signalling	5.716E-05
27	Reproduction_Feeding and Neurohormone signalling	6.527E-05
28	Inflammation_IL-10 anti-inflammatory response	8.036E-05
29	Cardiac development_BMP_TGF_beta_signalling	1.496E-04
30	Cell adhesion_Amyloid proteins	1.503E-04
31	Apoptosis_Anti-Apoptosis mediated by external signals via MAPK and JAK/STAT	1.668E-04
32	Apoptosis_Apoptosis stimulation by external signals	1.799E-04
33	Signal transduction_Androgen receptor nuclear signalling	1.987E-04
34	Apoptosis_Apoptotic mitochondria	2.161E-04
35	Inflammation_IL-2 signalling	4.203E-04
36	Signal Transduction_BMP and GDF signalling	5.077E-04
37	Inflammation_Amphoterin signalling	6.345E-04
38	Apoptosis_Endoplasmic reticulum stress pathway	6.975E-04
39	Apoptosis_Apoptotic nucleus	7.614E-04
40	Immune response_TCR signalling	8.972E-04
41	Signal transduction_ERBB-family signalling	1.063E-03
42	Cardiac development_FGF_ErbB signalling	1.078E-03
43	Autophagy_Autophagy	1.595E-03
44	Signal transduction_ESR1-membrane pathway	1.729E-03
45	DNA damage_Core	2.217E-03
46	Inflammation_IL-4 signalling	2.514E-03
47	Apoptosis_Anti-apoptosis mediated by external signals via NF-kB	3.304E-03
48	Development_Regulation of angiogenesis	3.529E-03
49	Signal Transduction_Cholecystokinin signalling	4.023E-03
50	Development_Keratinocyte differentiation	4.661E-03

Appendix 4.3.5 Networks enriched by targets of differentially abundant miRNAs in oesophageal SC-CAMs compared to oesophageal NTMs.

No.	Networks	p-value
1	Development_EMT_Regulation of epithelial-to-mesenchymal transition	3.251E-16
2	Signal Transduction_TGF-beta, GDF and Activin signalling	3.434E-14
3	Cell cycle_G1-S Growth factor regulation	6.050E-13
4	Apoptosis_Anti-Apoptosis mediated by external signals via PI3K/AKT	1.050E-12
5	Reproduction_Feeding and Neurohormone signalling	2.405E-11
6	Signal Transduction_BMP and GDF signalling	1.799E-09
7	Inflammation_MIF signalling	3.133E-09
8	Signal transduction_Androgen receptor signalling cross-talk	3.463E-09
9	Signal transduction_WNT signalling	3.948E-09
10	Development_Cartilage development	9.792E-09
11	Reproduction_FSH-beta signalling pathway	3.808E-08
12	Immune response_Th17-derived cytokines	6.182E-08
13	Proliferation_Negative regulation of cell proliferation	8.582E-08
14	Cell cycle_G1-S Interleukin regulation	8.994E-08
15	Cell adhesion_Cell-matrix interactions	1.686E-07
16	Apoptosis_Apoptosis stimulation by external signals	3.012E-07
17	Development_Hemopoiesis, Erythropoietin pathway	3.557E-07
18	Development_Regulation of angiogenesis	4.285E-07
19	Signal transduction_ESR1-nuclear pathway	8.043E-07
20	Proliferation_Positive regulation cell proliferation	1.292E-06
21	Signal transduction_NOTCH signalling	1.691E-06
22	Development_Ossification and bone remodelling	2.110E-06
23	Signal transduction_Nitric oxide signalling	3.657E-06
24	Signal transduction_ERBB-family signalling	3.722E-06
25	Reproduction_Progesterone signalling	4.083E-06
26	Inflammation_TREM1 signalling	6.987E-06
27	Apoptosis_Anti-Apoptosis mediated by external signals by Estrogen	7.915E-06
28	Cell adhesion_Platelet-endothelium-leucocyte interactions	9.622E-06
29	Reproduction_Male sex differentiation	9.853E-06
30	Apoptosis_Endoplasmic reticulum stress pathway	2.654E-05
31	Apoptosis_Apoptotic nucleus	3.019E-05
32	Apoptosis_Anti-Apoptosis mediated by external signals via MAPK and JAK/STAT	3.324E-05
33	DNA damage_Checkpoint	3.378E-05
34	Development_Hedgehog signalling	4.008E-05
35	Signal transduction_ESR1-membrane pathway	4.619E-05
36	Proteolysis_ECM remodelling	4.668E-05
37	Apoptosis_Apoptotic mitochondria	4.668E-05
38	Immune response_TCR signalling	5.122E-05
39	Cell adhesion_Amyloid proteins	5.210E-05
40	Inflammation_Amphoterin signalling	5.322E-05
41	Cell cycle_G1-S	5.426E-05
42	Inflammation_IL-10 anti-inflammatory response	5.616E-05
43	Cell adhesion_Integrin-mediated cell-matrix adhesion	6.794E-05
44	Cell cycle_G0-G1	9.793E-05
45	Cardiac development_BMP_TGF_beta_signalling	1.038E-04
46	Signal transduction_Leptin signalling	1.188E-04
47	Cell cycle_Core	1.577E-04
48	Cardiac development_FGF_ErbB signaling	2.345E-04
49	Cardiac development_Role of NADPH oxidase and ROS	3.860E-04
50	Cell adhesion_Glycoconjugates	4.195E-04

Appendix 4.3.6 Networks enriched by targets of differentially abundant miRNAs in oesophageal SC-ATMs compared to oesophageal NTMs.

No.	Networks	p-value
1	Cell cycle_G1-S Growth factor regulation	1.026E-14
2	Cell cycle_G1-S Interleukin regulation	2.779E-10
3	Development_EMT_Regulation of epithelial-to-mesenchymal transition	2.814E-09
4	Inflammation_MIF signalling	4.128E-09
5	Reproduction_Feeding and Neurohormone signalling	6.526E-09
6	Signal Transduction_TGF-beta, GDF and Activin signalling	2.959E-08
7	DNA damage_Checkpoint	1.363E-07
8	Development_Hemopoiesis, Erythropoietin pathway	1.918E-07
9	Inflammation_IL-2 signalling	2.769E-07
10	Proliferation_Negative regulation of cell proliferation	8.930E-07
11	Signal transduction_ESR1-nuclear pathway	1.597E-06
12	Reproduction_FSH-beta signalling pathway	2.522E-06
13	Proliferation_Positive regulation cell proliferation	2.639E-06
14	Apoptosis_Anti-Apoptosis mediated by external signals via PI3K/AKT	3.358E-06
15	Cell cycle_G0-G1	3.917E-06
16	Cell cycle_G1-S	4.581E-06
17	Reproduction_Male sex differentiation	4.976E-06
18	Inflammation_IL-10 anti-inflammatory response	5.196E-06
19	Signal transduction_ESR1-membrane pathway	5.957E-06
20	Reproduction_Progesterone signalling	2.378E-05
21	Cell cycle_Core	2.828E-05
22	Signal transduction_WNT signalling	6.335E-05
23	Signal transduction_Androgen receptor signaling cross-talk	2.294E-04
24	Signal transduction_CREM pathway	2.856E-04
25	Immune response_Th17-derived cytokines	3.898E-04
26	Development_Regulation of angiogenesis	4.206E-04
27	Cell adhesion_Platelet-endothelium-leucocyte interactions	8.719E-04
28	Apoptosis_Anti-apoptosis mediated by external signals via NF-kB	8.872E-04
29	Signal transduction_Nitric oxide signalling	1.243E-03
30	Development_Blood vessel morphogenesis	1.336E-03
31	Apoptosis_Anti-Apoptosis mediated by external signals by Estrogen	1.372E-03
32	Inflammation_IL-4 signalling	1.425E-03
33	Inflammation_IFN-gamma signalling	1.773E-03
34	Inflammation_Amphoterin signalling	1.902E-03
35	Immune response_BCR pathway	2.039E-03
36	Cell cycle_G2-M	2.277E-03
37	Signal transduction_Leptin signalling	2.361E-03
38	Development_Hedgehog signalling	2.914E-03
39	Signal transduction_NOTCH signalling	3.976E-03
40	Inflammation_Jak-STAT Pathway	6.634E-03
41	Inflammation_IL-13 signalling pathway	7.474E-03
42	Cytoskeleton_Macropinocytosis and its regulation	9.432E-03
43	Inflammation_IL-6 signalling	1.047E-02
44	Signal transduction_ERBB-family signalling	1.252E-02
45	Apoptosis_Anti-Apoptosis mediated by external signals via MAPK and JAK/STAT	1.269E-02
46	Reproduction_Spermatogenesis, motility and copulation	1.430E-02
47	Inflammation_Interferon signalling	1.430E-02
48	Inflammation_TREM1 signalling	1.733E-02

Appendix 4.3.7 Networks enriched by targets of differentially abundant miRNAs in pairwise analysis of oesophageal AC-CAMs compared to AC-ATMs.

No.	Networks	p-value
1	Signal Transduction_TGF-beta, GDF and Activin signalling	3.320E-04
2	Apoptosis_Anti-Apoptosis mediated by external signals by Estrogen	4.523E-04
3	Signal transduction_ESR1-membrane pathway	7.999E-04
4	Apoptosis_Anti-Apoptosis mediated by external signals via PI3K/AKT	8.117E-04
5	Proliferation_Negative regulation of cell proliferation	9.834E-04
6	Development_Regulation of angiogenesis	1.471E-03
7	Inflammation_MIF signalling	1.712E-03
8	Signal transduction_ESR1-nuclear pathway	2.107E-03
9	Signal transduction_NOTCH signalling	2.292E-03
10	Inflammation_TREM1 signalling	2.552E-03
11	Apoptosis_Apoptosis stimulation by external signals	4.286E-03
12	Reproduction_FSH-beta signalling pathway	5.035E-03
13	Cell adhesion_Platelet-endothelium-leucocyte interactions	5.859E-03
14	Signal transduction_WNT signalling	7.571E-03

Appendix 4.3.8 Networks enriched by targets of differentially abundant miRNAs in oesophageal AC-CAMs compared to oesophageal NTMs.

No.	Networks	p-value
1	Cell cycle_G1-S Growth factor regulation	1.147E-11
2	Development_EMT_Regulation of epithelial-to-mesenchymal transition	1.465E-11
3	Apoptosis_Anti-Apoptosis mediated by external signals via PI3K/AKT	2.528E-10
4	Signal transduction_WNT signalling	2.860E-09
5	Reproduction_Feeding and Neurohormone signalling	7.628E-09
6	Proliferation_Negative regulation of cell proliferation	2.446E-08
7	Reproduction_Progesterone signalling	7.273E-08
8	Inflammation_MIF signalling	9.110E-08
9	Signal transduction_ESR1-membrane pathway	2.318E-07
10	Signal Transduction_TGF-beta, GDF and Activin signalling	2.858E-07
11	Signal transduction_Androgen receptor signalling cross-talk	4.710E-07
12	DNA damage_Checkpoint	7.495E-07
13	Signal transduction_ESR1-nuclear pathway	7.712E-07
14	Cell cycle_G1-S Interleukin regulation	9.904E-07
15	Signal transduction_NOTCH signalling	4.617E-06
16	Signal transduction_ERBB-family signalling	4.899E-06
17	Development_Cartilage development	4.899E-06
18	Immune response_Th17-derived cytokines	1.000E-05
19	Reproduction_FSH-beta signalling pathway	1.049E-05
20	Reproduction_Male sex differentiation	2.428E-05
21	Apoptosis_Apoptosis stimulation by external signals	2.654E-05
22	Cardiac development_FGF_ErbB signalling	3.890E-05
23	Proliferation_Positive regulation cell proliferation	4.507E-05
24	Apoptosis_Anti-Apoptosis mediated by external signals via MAPK and JAK/STAT	5.425E-05
25	Cell cycle_G0-G1	5.833E-05
26	Development_Hemopoiesis, Erythropoietin pathway	8.825E-05
27	Signal Transduction_BMP and GDF signalling	1.127E-04
28	Development_Hedgehog signalling	1.286E-04
29	Apoptosis_Anti-Apoptosis mediated by external signals by Estrogen	1.307E-04
30	Development_Ossification and bone remodelling	1.763E-04
31	Development_Regulation of angiogenesis	1.907E-04
32	Muscle contraction_Relaxin signalling	2.474E-04
33	Cell cycle_G2-M	2.891E-04
34	Inflammation_IL-10 anti-inflammatory response	4.579E-04
35	Cell adhesion_Cell-matrix interactions	5.161E-04
36	Signal transduction_Nitric oxide signalling	7.083E-04
37	Cell cycle_Core	7.858E-04
38	Apoptosis_Endoplasmic reticulum stress pathway	9.205E-04
39	DNA damage_Core	9.742E-04
40	Apoptosis_Apoptotic mitochondria	1.025E-03
41	Cell adhesion_Platelet-endothelium-leucocyte interactions	1.295E-03
42	Apoptosis_Apoptotic nucleus	1.416E-03
43	Immune response_IL-5 signalling	1.429E-03
44	Inflammation_IL-2 signalling	1.679E-03
45	Cell cycle_G1-S	1.947E-03
46	Cardiac development_BMP_TGF_beta_signalling	2.035E-03
47	Cell adhesion_Amyloid proteins	2.247E-03
48	Reproduction_Gonadotropin regulation	2.584E-03
49	Apoptosis_Anti-apoptosis mediated by external signals via NF-kB	4.987E-03
50	Reproduction_GnRH signalling pathway	7.544E-03

Appendix 4.3.9 Networks enriched by targets of differentially abundant miRNAs in oesophageal AC-ATMs compared to oesophageal NTMs.

No.	Networks	Patient no.	p-value	Minimum p-value	Count (out of 12)
1	Cell cycle_G1-S Growth factor regulation	Patient 2	1.98E-04	1.42E-21	11
		Patient 3	4.04E-13		
		Patient 4	4.39E-15		
		Patient 5	1.60E-17		
		Patient 6	1.15E-07		
		Patient 7	1.42E-21		
		Patient 8	1.14E-11		
		Patient 9	2.34E-02		
		Patient 10	1.37E-13		
		Patient 11	7.67E-04		
		Patient 12	4.38E-13		
2	Cell cycle_G1-S Interleukin regulation	Patient 2	1.79E-06	1.54E-21	10
		Patient 3	2.17E-09		
		Patient 4	9.23E-14		
		Patient 5	8.28E-17		
		Patient 6	1.51E-05		
		Patient 7	1.54E-21		
		Patient 8	3.39E-07		
		Patient 10	1.71E-13		
		Patient 11	1.01E-05		
		Patient 12	3.40E-11		
3	Signal Transduction_TGF-beta, GDF and Activin signaling	Patient 3	3.84E-17	3.84E-17	10
		Patient 4	2.36E-08		
		Patient 5	2.21E-07		
		Patient 6	6.55E-09		
		Patient 7	3.37E-09		
		Patient 8	3.85E-15		
		Patient 9	1.26E-02		
		Patient 10	1.15E-07		
		Patient 11	2.71E-03		
		Patient 12	2.43E-14		
4	Development_EMT_Regulation of epithelial-to-mesenchymal transition	Patient 2	7.16E-04	6.72E-17	10
		Patient 3	6.72E-17		
		Patient 4	7.03E-11		
		Patient 5	2.22E-11		
		Patient 6	1.36E-06		
		Patient 7	9.45E-14		
		Patient 8	1.56E-13		
		Patient 9	4.01E-02		
		Patient 10	3.14E-08		
		Patient 12	5.84E-12		
5	Signal transduction_NOTCH signaling	Patient 2	4.66E-03	1.24E-11	9
		Patient 3	1.24E-11		
		Patient 4	9.78E-13		
		Patient 5	4.14E-08		
		Patient 6	5.53E-03		
		Patient 7	3.82E-14		
		Patient 8	6.87E-08		
		Patient 10	2.40E-11		
		Patient 12	1.22E-07		
6	Signal transduction_WNT signaling	Patient 1	4.65E-03	2.25E-11	12
		Patient 2	4.42E-04		
		Patient 3	2.25E-11		
		Patient 4	9.85E-10		
		Patient 5	1.27E-09		
		Patient 6	2.89E-04		
		Patient 7	2.19E-13		
		Patient 8	2.34E-06		
		Patient 9	1.33E-02		
		Patient 10	1.52E-07		
		Patient 11	2.26E-02		
		Patient 12	3.82E-10		

7	Apoptosis_Anti-Apoptosis mediated by external signals via PI3K/AKT	Patient 3	1.50E-10	1.50E-10	8
		Patient 4	9.42E-07		
		Patient 5	5.29E-08		
		Patient 7	5.04E-09		
		Patient 8	2.34E-06		
		Patient 9	1.39E-03		
		Patient 10	6.80E-06		
		Patient 12	3.37E-05		
8	Reproduction_FSH-beta signaling pathway	Patient 3	1.74E-10	1.74E-10	9
		Patient 4	2.78E-07		
		Patient 5	1.51E-05		
		Patient 6	3.14E-06		
		Patient 7	4.99E-08		
		Patient 8	1.38E-07		
		Patient 10	5.29E-04		
		Patient 11	2.20E-03		
		Patient 12	5.71E-08		
9	Inflammation_IL-10 anti-inflammatory response	Patient 2	1.51E-03	3.85E-10	11
		Patient 3	4.39E-03		
		Patient 4	1.88E-05		
		Patient 5	3.85E-10		
		Patient 6	1.06E-02		
		Patient 7	1.07E-07		
		Patient 8	3.97E-06		
		Patient 9	1.90E-03		
		Patient 10	1.58E-03		
		Patient 11	2.10E-04		
		Patient 12	1.47E-07		
10	Proliferation_Negative regulation of cell proliferation	Patient 2	1.89E-05	1.05E-09	11
		Patient 3	1.52E-04		
		Patient 4	3.19E-06		
		Patient 5	1.69E-07		
		Patient 6	1.82E-04		
		Patient 7	2.66E-06		
		Patient 8	5.73E-06		
		Patient 9	2.13E-02		
		Patient 10	1.40E-06		
		Patient 11	3.55E-02		
		Patient 12	1.05E-09		
11	Proliferation_Positive regulation cell proliferation	Patient 2	1.69E-03	1.48E-09	9
		Patient 3	1.48E-09		
		Patient 4	5.88E-09		
		Patient 5	1.17E-05		
		Patient 7	1.81E-08		
		Patient 8	1.66E-05		
		Patient 9	2.61E-02		
		Patient 10	1.89E-05		
		Patient 12	2.25E-05		
12	Inflammation_TREM1 signaling	Patient 3	6.20E-03	3.56E-09	8
		Patient 4	9.24E-04		
		Patient 5	3.56E-09		
		Patient 7	1.17E-08		
		Patient 8	9.76E-04		
		Patient 9	6.15E-03		
		Patient 10	1.75E-05		
		Patient 12	7.00E-03		
13	Reproduction_Progesterone signaling	Patient 3	1.21E-04	1.60E-08	9
		Patient 4	1.39E-04		
		Patient 5	3.09E-06		
		Patient 7	1.60E-08		
		Patient 8	2.25E-02		
		Patient 9	2.03E-02		
		Patient 10	3.48E-05		
		Patient 11	3.39E-02		
		Patient 12	6.55E-04		

14	Cell cycle_G0-G1	Patient 1	4.76E-03	2.87E-08	10
		Patient 2	8.46E-06		
		Patient 3	1.12E-06		
		Patient 4	1.88E-05		
		Patient 5	3.83E-07		
		Patient 6	1.06E-02		
		Patient 7	1.07E-07		
		Patient 8	2.74E-05		
		Patient 10	2.87E-08		
		Patient 12	1.45E-06		
15	Development_Hedgehog signaling	Patient 3	3.20E-07	3.03E-08	8
		Patient 4	4.01E-06		
		Patient 5	7.75E-07		
		Patient 6	3.78E-02		
		Patient 7	3.03E-08		
		Patient 8	1.19E-06		
		Patient 10	1.32E-05		
		Patient 12	3.03E-04		
16	Development_Regulation of angiogenesis	Patient 2	1.27E-02	4.09E-08	10
		Patient 3	4.09E-08		
		Patient 4	1.13E-04		
		Patient 5	2.09E-06		
		Patient 6	5.93E-04		
		Patient 7	1.64E-06		
		Patient 8	3.21E-08		
		Patient 9	5.20E-04		
		Patient 10	7.76E-04		
		Patient 12	1.27E-05		
17	Cell cycle_Core	Patient 2	1.34E-06	6.51E-08	9
		Patient 3	5.88E-06		
		Patient 4	4.07E-05		
		Patient 5	1.36E-07		
		Patient 6	5.56E-04		
		Patient 7	6.51E-08		
		Patient 8	2.24E-03		
		Patient 10	1.03E-06		
		Patient 12	8.28E-07		
18	Signal transduction_ERBB-family signaling	Patient 3	1.06E-03	6.61E-08	9
		Patient 4	5.86E-04		
		Patient 5	1.62E-04		
		Patient 6	4.99E-03		
		Patient 7	6.61E-08		
		Patient 8	2.82E-05		
		Patient 10	5.96E-06		
		Patient 11	2.52E-02		
		Patient 12	1.13E-03		
19	Reproduction_Feeding and Neurohormone signaling	Patient 3	8.44E-05	2.74E-07	8
		Patient 4	1.56E-06		
		Patient 5	4.20E-07		
		Patient 6	4.72E-02		
		Patient 7	2.74E-07		
		Patient 8	7.06E-03		
		Patient 10	7.91E-07		
		Patient 12	2.67E-05		
20	Apoptosis_Apoptosis stimulation by external signals	Patient 3	1.76E-06	2.83E-07	8
		Patient 4	8.49E-03		
		Patient 5	3.18E-05		
		Patient 6	1.64E-02		
		Patient 7	7.15E-05		
		Patient 8	2.83E-07		
		Patient 10	3.09E-04		
		Patient 12	9.68E-04		

21	Cell adhesion_Platelet-endothelium-leucocyte interactions	Patient 1	1.92E-02	7.10E-07	9
		Patient 3	4.93E-06		
		Patient 4	2.04E-03		
		Patient 5	4.00E-06		
		Patient 7	9.88E-06		
		Patient 8	2.77E-05		
		Patient 9	2.18E-06		
		Patient 10	5.07E-03		
		Patient 12	7.10E-07		
22	Signal transduction_ESR1-nuclear pathway	Patient 2	1.95E-02	1.43E-06	8
		Patient 3	1.43E-06		
		Patient 4	4.00E-06		
		Patient 5	3.66E-03		
		Patient 7	1.11E-04		
		Patient 8	4.19E-06		
		Patient 10	1.76E-02		
		Patient 12	6.37E-03		
23	Immune response_Th17-derived cytokines	Patient 2	1.38E-02	1.45E-06	11
		Patient 3	4.37E-05		
		Patient 4	1.09E-04		
		Patient 5	3.07E-06		
		Patient 6	1.06E-02		
		Patient 7	6.50E-06		
		Patient 8	2.74E-05		
		Patient 9	1.90E-03		
		Patient 10	3.49E-06		
		Patient 11	3.34E-03		
		Patient 12	1.45E-06		
24	Cardiac development_BMP_TGF_beta_signaling	Patient 2	3.25E-02	2.07E-06	9
		Patient 3	2.07E-06		
		Patient 4	1.67E-03		
		Patient 5	2.07E-02		
		Patient 6	6.64E-03		
		Patient 7	9.78E-03		
		Patient 8	1.96E-05		
		Patient 10	8.18E-03		
		Patient 12	9.47E-04		
25	Translation_Regulation of initiation	Patient 3	4.43E-03	2.52E-06	8
		Patient 4	6.41E-04		
		Patient 5	1.45E-02		
		Patient 6	2.48E-02		
		Patient 7	2.52E-06		
		Patient 8	1.70E-02		
		Patient 10	2.92E-03		
		Patient 12	7.49E-03		
26	Cell adhesion_Glycoconjugates	Patient 1	4.68E-02	3.07E-06	10
		Patient 3	4.39E-03		
		Patient 4	3.32E-02		
		Patient 5	3.07E-06		
		Patient 6	1.06E-02		
		Patient 7	4.25E-05		
		Patient 8	2.74E-05		
		Patient 9	2.61E-02		
		Patient 11	3.74E-02		
		Patient 12	9.54E-05		
27	Reproduction_Male sex differentiation	Patient 2	1.99E-03	6.45E-06	9
		Patient 3	1.75E-05		
		Patient 4	4.84E-03		
		Patient 5	1.82E-05		
		Patient 7	1.32E-05		
		Patient 8	6.45E-06		
		Patient 10	1.24E-04		
		Patient 11	8.12E-03		
		Patient 12	1.39E-04		

28	Inflammation_IL-4 signaling	Patient 3	1.53E-03	6.42E-05	9
		Patient 4	7.68E-04		
		Patient 5	1.69E-04		
		Patient 6	4.38E-03		
		Patient 7	6.42E-05		
		Patient 8	4.01E-03		
		Patient 9	3.98E-02		
		Patient 10	1.00E-03		
		Patient 12	8.41E-05		
29	Signal transduction_Nitric oxide signaling	Patient 3	4.84E-03	1.95E-04	10
		Patient 4	1.25E-02		
		Patient 5	2.23E-02		
		Patient 6	3.25E-02		
		Patient 7	2.76E-04		
		Patient 8	1.95E-04		
		Patient 9	1.75E-02		
		Patient 10	4.96E-04		
		Patient 11	2.52E-02		
		Patient 12	6.64E-03		
30	Proteolysis_ECM remodeling	Patient 3	2.87E-03	2.42E-03	8
		Patient 4	6.85E-03		
		Patient 5	2.42E-03		
		Patient 6	8.44E-03		
		Patient 7	1.51E-02		
		Patient 8	2.81E-03		
		Patient 9	2.31E-02		
		Patient 12	2.46E-03		

Appendix 4.3.10 Networks significantly enriched by targets of miRNAs that exhibit at least 50% difference in abundance in each gastric CAM compared to corresponding ATM from 12 patients.

No.	Networks	Patient	p-value
1	Cell cycle_G1-S Growth factor regulation	Sz306	3.67E-11
		Sz360	2.01E-05
		Sz373	4.17E-05
		Sz467	3.91E-21
2	Cell cycle_G1-S Interleukin regulation	Sz306	9.83E-12
		Sz360	3.06E-06
		Sz373	2.53E-06
		Sz467	4.87E-15
3	Signal transduction_NOTCH signaling	Sz306	2.51E-04
		Sz360	1.22E-02
		Sz373	2.63E-05
		Sz467	1.61E-13
4	Signal Transduction_TGF-beta, GDF and Activin signaling	Sz306	1.88E-04
		Sz360	7.02E-04
		Sz373	2.19E-03
		Sz467	2.65E-13
5	Development_EMT_Regulation of epithelial-to-mesenchymal transition	Sz306	1.54E-10
		Sz360	9.78E-05
		Sz373	1.27E-05
		Sz467	4.17E-13
6	Apoptosis_Anti-Apoptosis mediated by external signals via PI3K/AKT	Sz306	6.31E-05
		Sz360	4.02E-02
		Sz373	8.61E-03
		Sz467	6.53E-12
7	Development_Hemopoiesis, Erythropoietin pathway	Sz306	4.88E-06
		Sz360	1.31E-03
		Sz373	5.61E-04
		Sz467	7.51E-11
8	Signal transduction_WNT signaling	Sz306	7.09E-06
		Sz360	3.69E-04
		Sz373	2.93E-06
		Sz467	1.95E-10
9	Apoptosis_Apoptosis stimulation by external signals	Sz306	2.64E-03
		Sz360	2.97E-03
		Sz373	3.43E-04
		Sz467	5.75E-10
10	Cell cycle_G1-S	Sz306	3.71E-06
		Sz360	1.24E-04
		Sz373	1.43E-06
		Sz467	8.83E-09
11	Development_Hedgehog signaling	Sz306	2.27E-02
		Sz360	3.71E-02
		Sz373	2.31E-05
		Sz467	1.34E-08
12	Apoptosis_Anti-Apoptosis mediated by external signals by Estrogen	Sz306	1.53E-05
		Sz360	5.53E-05
		Sz373	8.60E-06
		Sz467	2.95E-08
13	Cell cycle_Core	Sz306	6.83E-06
		Sz360	3.22E-05
		Sz373	1.31E-04
		Sz467	2.98E-08
14	Immune response_Th17-derived cytokines	Sz306	1.15E-02
		Sz360	1.25E-03
		Sz373	3.11E-05
		Sz467	6.63E-08
15	Proliferation_Positive regulation cell proliferation	Sz306	6.12E-05
		Sz360	2.85E-04
		Sz373	1.90E-03
		Sz467	1.14E-07
16	Apoptosis_Anti-Apoptosis mediated by external signals via MAPK and JAK/STAT	Sz306	7.12E-05
		Sz360	2.27E-02
		Sz373	8.32E-04
		Sz467	1.81E-07
17	Immune response_TCR signaling	Sz306	2.82E-04
		Sz360	9.30E-03
		Sz373	3.75E-03

		Sz467	2.21E-07
18	Reproduction_Progesterone signaling	Sz306	7.31E-05
		Sz360	5.86E-04
		Sz373	6.96E-04
		Sz467	3.45E-07
19	Inflammation_TREM1 signaling	Sz306	1.02E-03
		Sz360	7.73E-03
		Sz373	1.10E-04
		Sz467	4.69E-07
20	Cell cycle_G0-G1	Sz306	2.16E-04
		Sz360	8.28E-04
		Sz373	1.57E-05
		Sz467	6.68E-07
21	DNA damage_Checkpoint	Sz306	8.94E-05
		Sz360	4.92E-02
		Sz373	1.24E-03
		Sz467	6.88E-07
22	Development_Regulation of angiogenesis	Sz306	1.24E-02
		Sz360	2.41E-02
		Sz373	3.48E-05
		Sz467	7.11E-07
23	Signal transduction_ESR1-nuclear pathway	Sz306	4.72E-02
		Sz360	9.62E-03
		Sz373	7.03E-05
		Sz467	8.88E-07
24	Development_Regulation of telomere length	Sz306	4.02E-04
		Sz360	2.77E-04
		Sz373	2.82E-05
		Sz467	1.22E-06
25	Signal transduction_ESR1-membrane pathway	Sz306	5.83E-06
		Sz360	1.31E-04
		Sz373	3.54E-02
		Sz467	1.86E-06
26	Inflammation_IL-10 anti-inflammatory response	Sz306	5.46E-05
		Sz360	1.25E-03
		Sz373	3.54E-06
		Sz467	2.36E-06
27	Inflammation_IL-2 signaling	Sz306	1.15E-02
		Sz360	1.25E-03
		Sz373	8.35E-03
		Sz467	2.36E-06
28	Signal Transduction_BMP and GDF signaling	Sz306	6.75E-03
		Sz360	4.80E-04
		Sz373	4.62E-03
		Sz467	9.27E-06
29	Cell cycle_G2-M	Sz306	4.87E-03
		Sz360	1.91E-03
		Sz373	4.53E-05
		Sz467	3.55E-05
30	Inflammation_Amphoterin signaling	Sz306	1.68E-03
		Sz360	3.70E-03
		Sz373	5.29E-03
		Sz467	5.62E-05
31	Cell adhesion_Glycoconjugates	Sz306	8.64E-05
		Sz360	2.49E-02
		Sz373	2.87E-02
		Sz467	1.19E-02
32	Development_Skeletal muscle development	Sz306	2.32E-02
		Sz360	1.02E-02
		Sz373	9.43E-04
		Sz467	2.81E-04
33	Immune response_BCR pathway	Sz306	4.01E-02
		Sz360	2.60E-02
		Sz373	3.01E-02
		Sz467	1.30E-02

Appendix 4.3.11 Networks significantly enriched by targets of miRNAs that exhibit at least 50% difference in abundance in each SC-CAM compared to corresponding SC-ATM from 4 patients.

No.	Networks	p-value		
		Sz173	Sz193	Sz282
1	Development_EMT_Regulation of epithelial-to-mesenchymal	3.257e-26	1.503e-12	1.372e-10
2	Signal Transduction_TGF-beta, GDF and Activin signaling	3.405e-21	2.281e-10	1.238e-6
3	Signal transduction_WNT signaling	1.528e-20	3.601e-8	9.044e-7
4	Cell cycle_G1-S Growth factor regulation	4.815e-20	1.217e-8	7.032e-11
5	Signal transduction_NOTCH signaling	1.259e-19	1.572e-4	4.708e-13
6	Cell cycle_G1-S Interleukin regulation	4.346e-15	4.167e-7	9.610e-12
7	Apoptosis_Apoptosis stimulation by external signals	4.063e-13	2.376e-3	1.566e-3
8	Development_Hedgehog signaling	1.134e-12	2.466e-4	1.996e-11
9	Development_Blood vessel morphogenesis	1.833e-12		3.877e-5
10	Development_Keratinocyte differentiation	1.101e-11		4.539e-4
11	Apoptosis_Anti-Apoptosis mediated by external signals via PI3K/AKT	1.643e-11	2.821e-8	2.539e-2
12	Apoptosis_Anti-Apoptosis mediated by external signals by Estrogen	6.969e-11	5.314e-3	1.215e-4
13	Reproduction_FSH-beta signaling pathway	7.259e-11	1.095e-4	7.348e-5
14	Development_Hemopoiesis, Erythropoietin pathway	7.330e-11	4.981e-6	9.597e-6
15	Cell cycle_Core	1.034e-10		7.966e-4
16	Signal transduction_ESR1-nuclear pathway	1.874e-10	2.388e-3	4.990e-6
17	Signal transduction_Androgen receptor signaling cross-talk	2.155e-9	2.377e-7	1.444e-3
18	Reproduction_Feeding and Neurohormone signaling	4.019e-9	1.910e-6	3.434e-4
19	Proliferation_Negative regulation of cell proliferation	5.919e-9	2.016e-5	5.599e-4
20	Reproduction_Male sex differentiation	7.352e-9	4.644e-6	2.741e-6
21	Cardiac development_Role of NADPH oxidase and ROS	8.151e-9	5.293e-6	2.636e-5
22	Reproduction_Progesterone signaling	8.877e-9	4.623e-4	8.326e-5
23	Cell cycle_G0-G1	9.687e-9	1.446e-4	2.659e-4
24	Signal Transduction_BMP and GDF signaling	1.304e-8	3.658e-6	7.141e-3
25	Proliferation_Positive regulation cell proliferation	2.020e-8	2.401e-4	8.875e-6
26	Signal transduction_ERBB-family signaling	2.272e-8	2.090e-3	1.930e-4
27	DNA damage_Checkpoint	2.633e-8	1.640e-2	3.986e-5
28	Apoptosis_Anti-Apoptosis mediated by external signals via MAPK and	4.301e-8	2.823e-2	
29	Immune response_Th17-derived cytokines	8.734e-8	5.271e-6	1.362e-2
30	Apoptosis_Apoptotic nucleus	2.702e-7	1.085e-3	2.458e-2
31	Signal transduction_Leptin signaling	2.804e-7	3.415e-2	2.396e-4
32	Inflammation_IL-10 anti-inflammatory response	6.818e-7	1.983e-4	3.670e-5
33	Cell cycle_G2-M	8.074e-7		1.489e-5
34	Immune response_TCR signaling	8.345e-7	2.087e-2	1.696e-2
35	Inflammation_MIF signaling	4.248e-5	9.264e-7	8.009e-3
36	Development_Ossification and bone remodeling	1.472e-6	1.069e-3	3.320e-2
37	Inflammation_TREM1 signaling	1.507e-6	5.405e-3	2.971e-3
38	Cardiac development_BMP_TGF_beta_signaling	1.852e-6	1.327e-4	3.151e-3
39	Development_Cartilage development	1.105e-4	2.248e-6	
40	Inflammation_Amphoterin signaling	2.581e-6	2.612e-5	2.230e-4
41	Cell adhesion_Cell-matrix interactions		3.084e-6	
42	Development_Regulation of angiogenesis	3.272e-6	8.141e-4	1.216e-3
43	Translation_Regulation of initiation	1.427e-5	3.423e-2	4.193e-6
44	Cardiac development_FGF_ErbB signaling	4.918e-6	2.890e-3	1.852e-2
45	Cell adhesion_Platelet-endothelium-leucocyte interactions	5.783e-6	6.803e-4	
46	Signal transduction_Nitric oxide signaling	6.509e-6	4.703e-3	7.309e-3
47	Signal transduction_ESR1-membrane pathway	3.676e-4	7.828e-6	4.127e-5
48	Inflammation_IL-2 signaling	8.251e-6	2.687e-3	1.880e-3
49	Development_Regulation of telomere length	8.464e-6	1.056e-2	3.163e-2
50	Reproduction_Gonadotropin regulation	1.273e-5		3.742e-3

Appendix 4.3.12 Networks significantly enriched by targets of miRNAs that exhibit at least 50% difference in abundance in each AC-CAM compared to corresponding AC-ATM from 3 patients. Networks with $p > 0.05$ were indicated by shading in grey.